



# Binary (r)evolution: from binaries to gravitational waves

**S Chaty** (APC, Université Paris Cité)  
X, LLR, 28 mars 2022

E. Chassande-Mottin, E. Porter, F. Fortin, J. Marchioro (APC)

T. Foglizzo, J. Guilet, A. Petiteau (CEA)

F. García, A. Simaz Bunzel (IAR)



Labex

**UnivEarthS**



Université  
Paris Cité

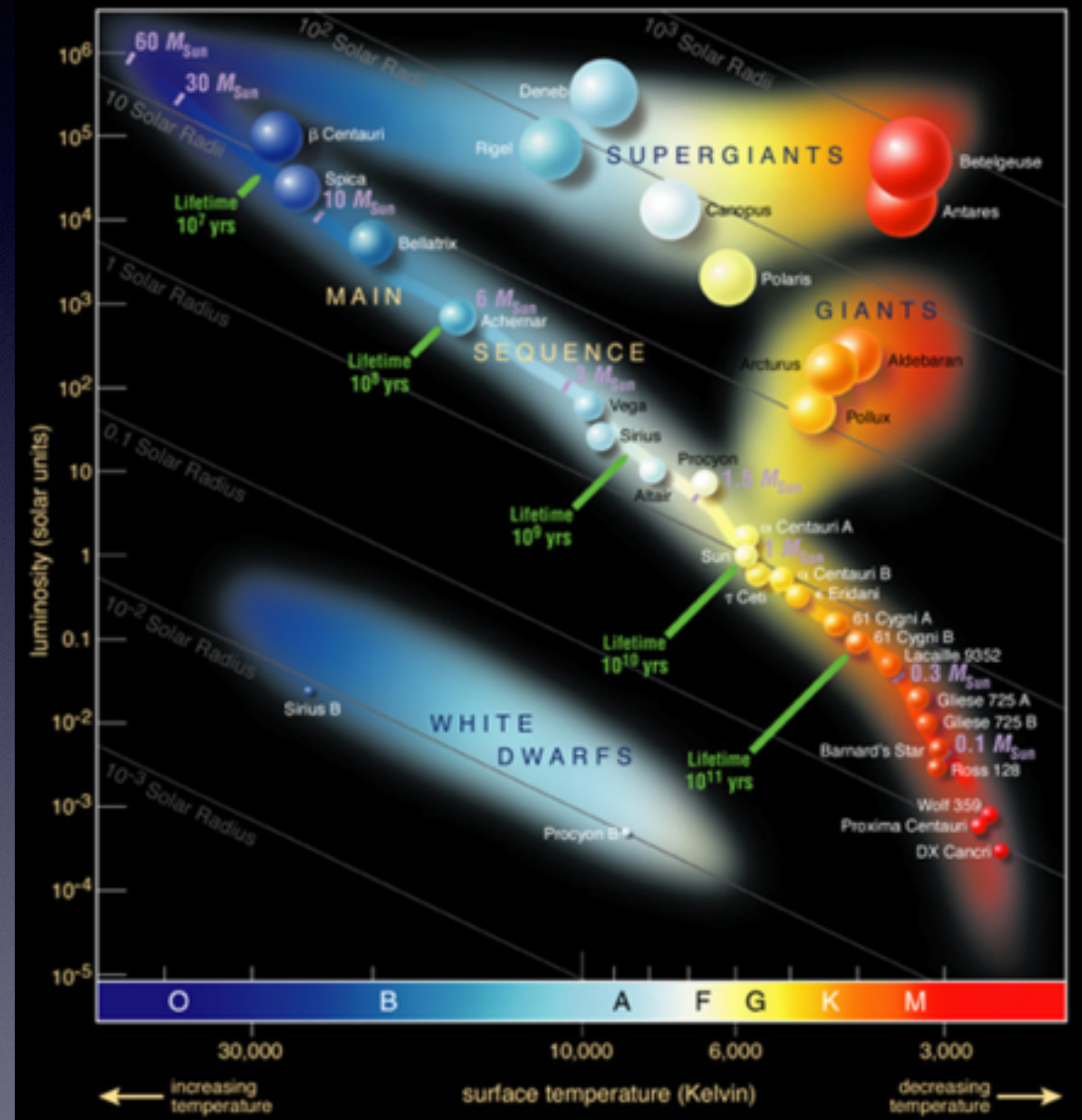


# Stellar evolution



# Stellar evolution

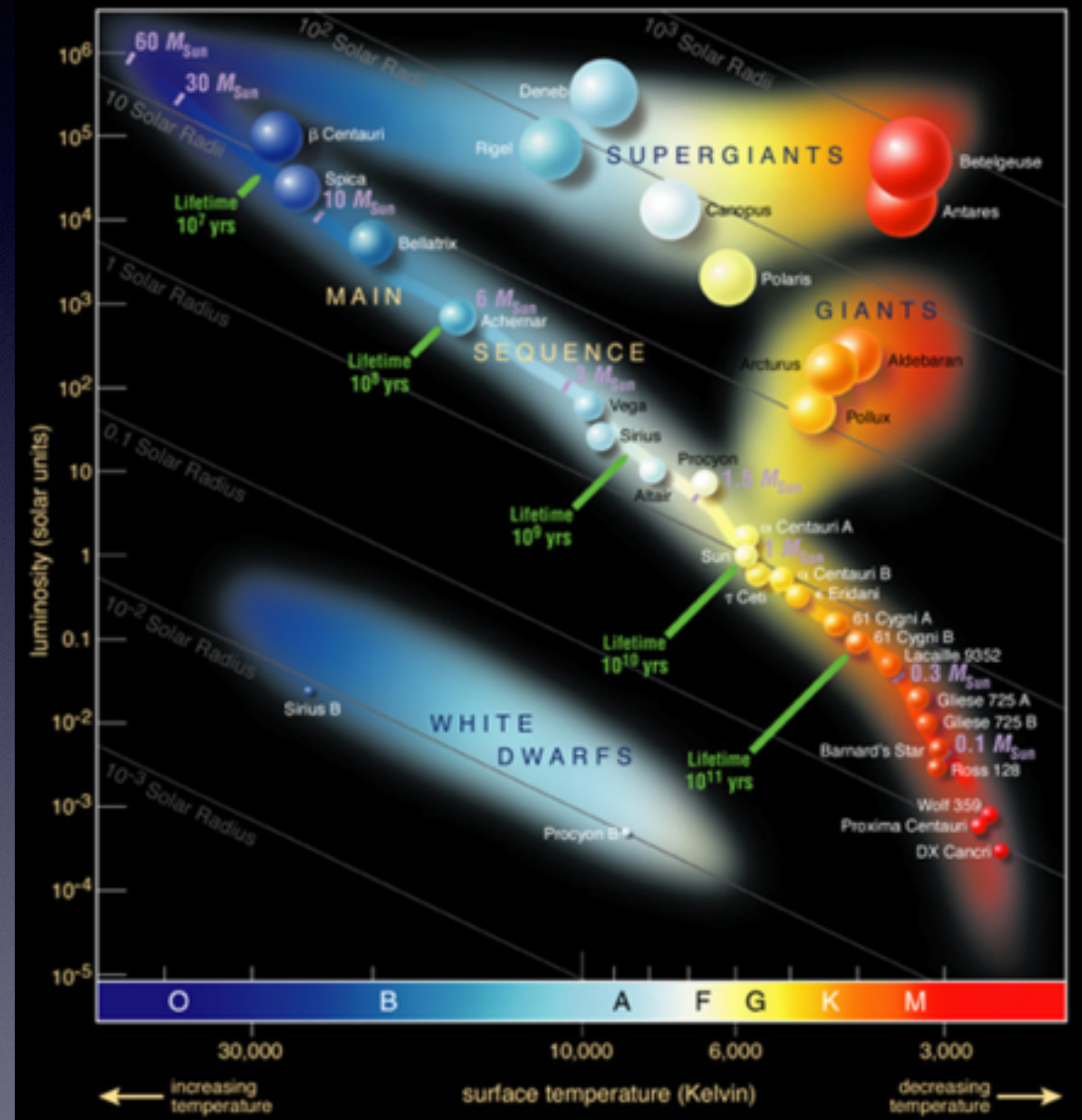
- HR diagram describes the evolution of a single and isolated star...





# Stellar evolution

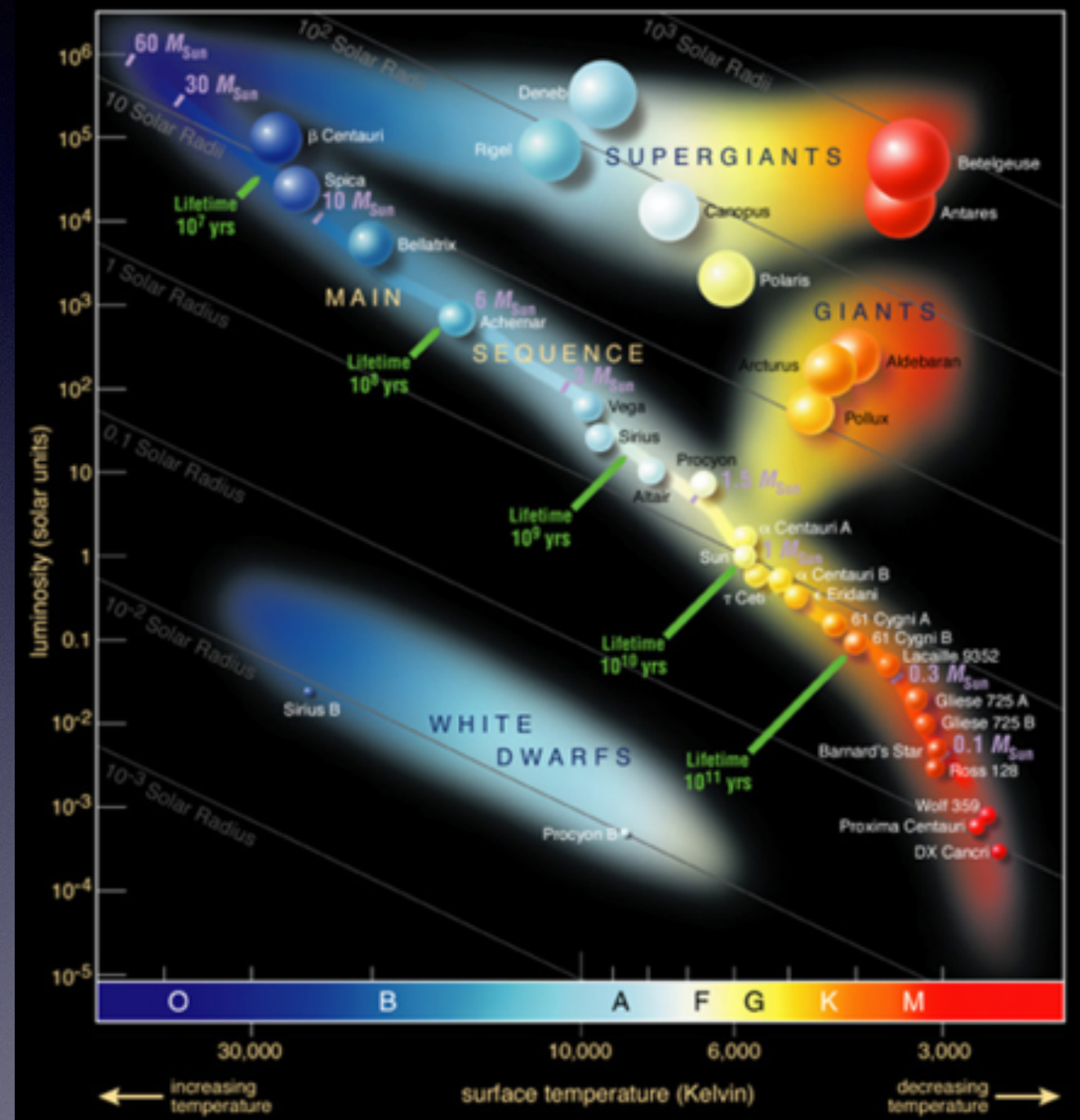
- HR diagram describes the evolution of a single and isolated star...
- ...however, most stars belong to multiple systems: +70% of massive stars experience a binary interaction during their evolution (Sana+2012)





# Stellar evolution

- HR diagram describes the evolution of a single and isolated star...
- ...however, most stars belong to multiple systems: +70% of massive stars experience a binary interaction during their evolution (Sana+2012)
- Transfer of matter/angular momentum strongly influences binary evolution



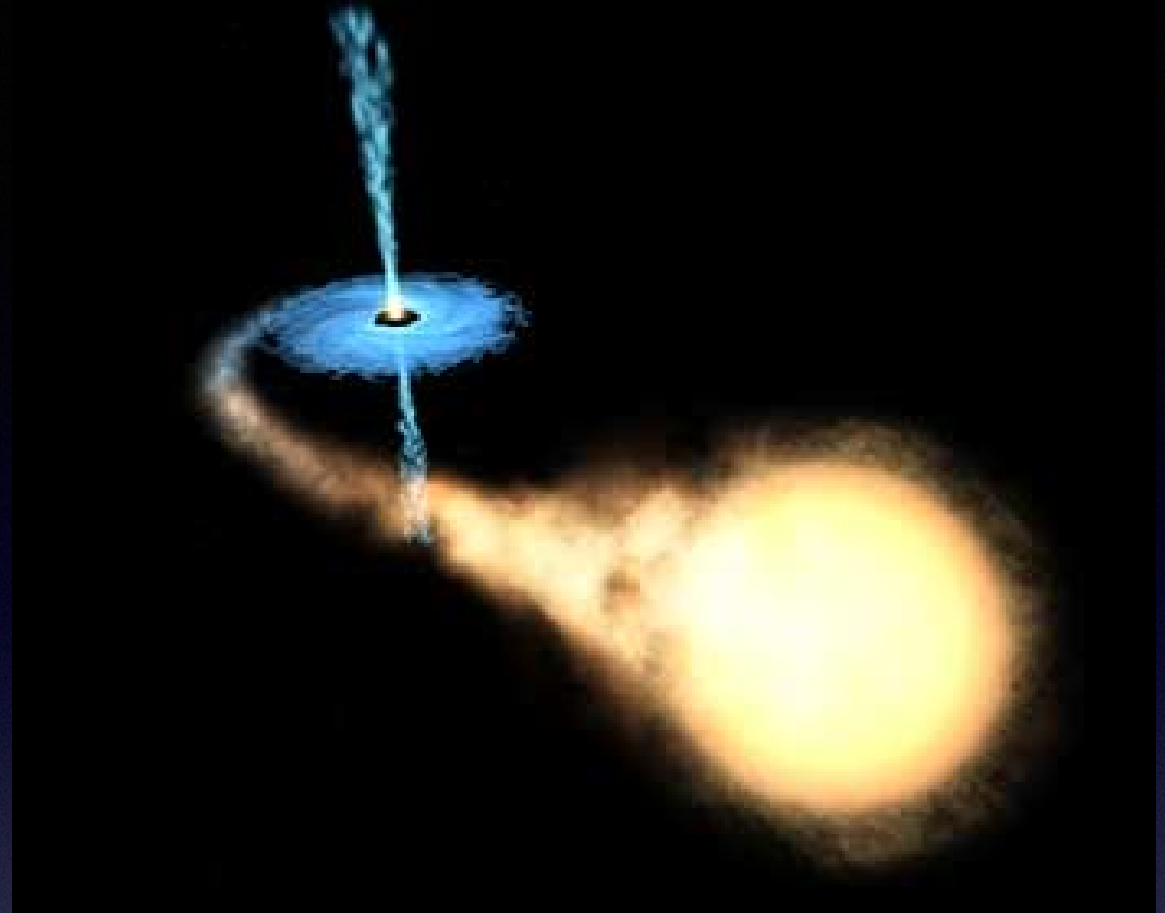


# Accreting binaries



# Accreting binaries

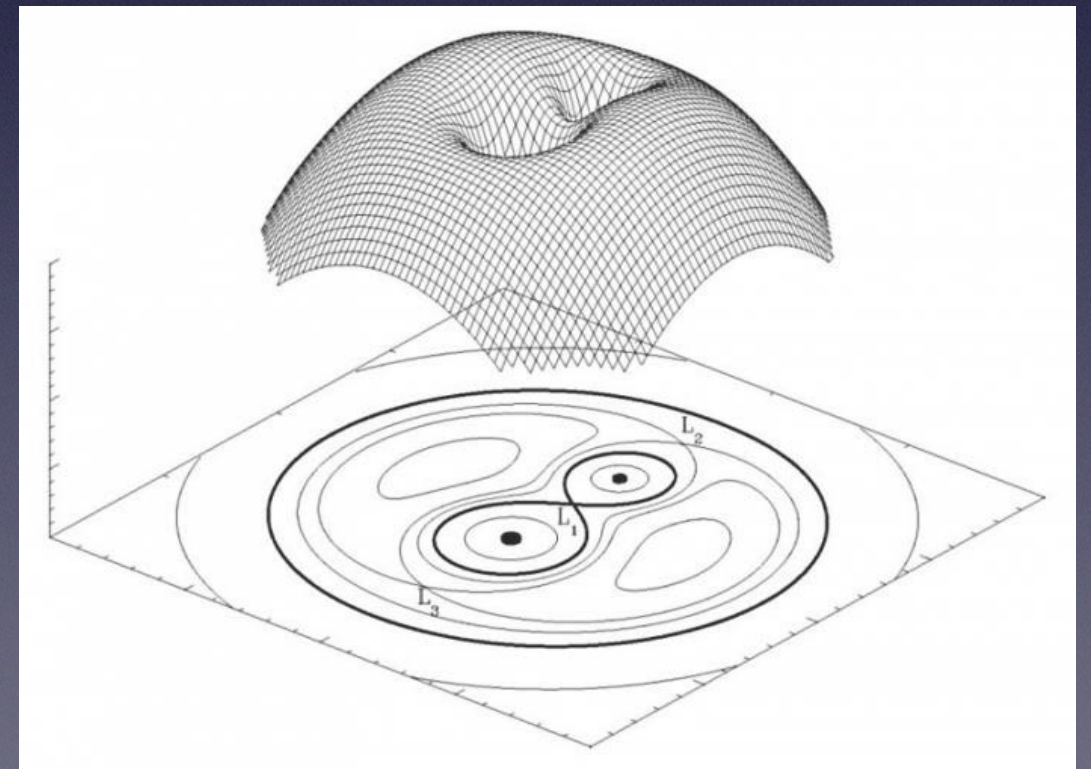
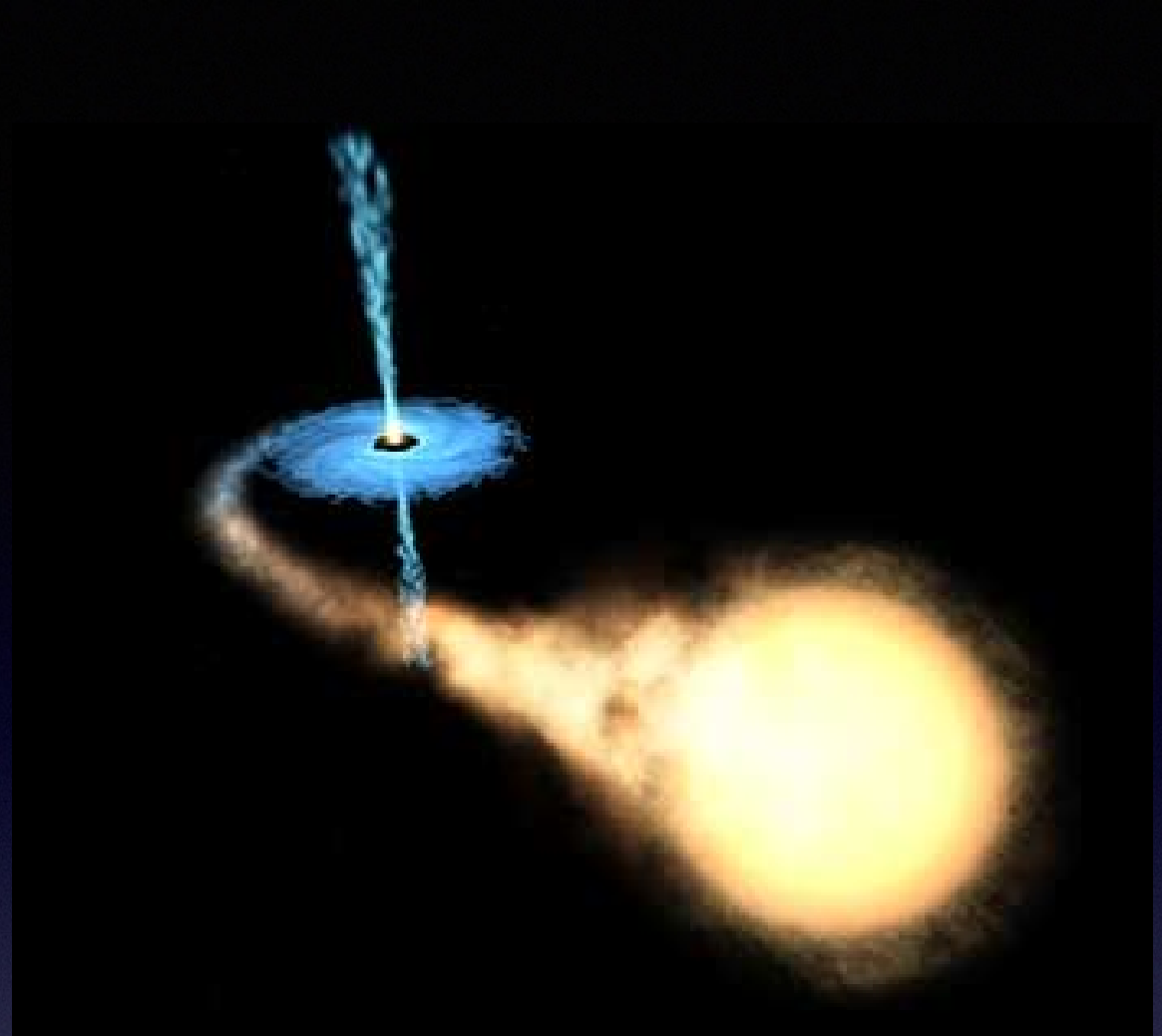
- Discovery of X-ray binaries in 1960s: compact object accreting from companion star (Nobel prize in Physics: Giacconi 2002)





# Accreting binaries

- Discovery of X-ray binaries in 1960s: compact object accreting from companion star (Nobel prize in Physics: Giacconi 2002)
- Roche lobe geometry

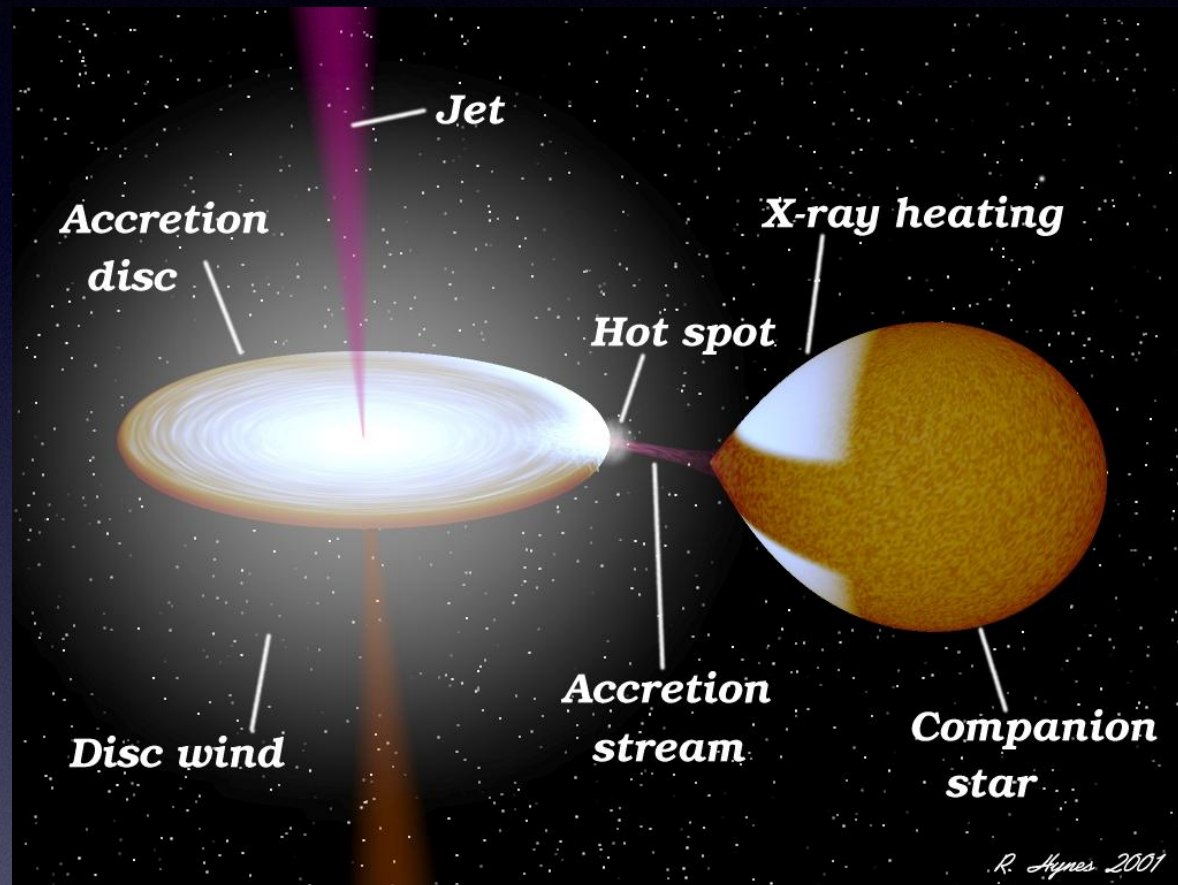




# Accreting binaries



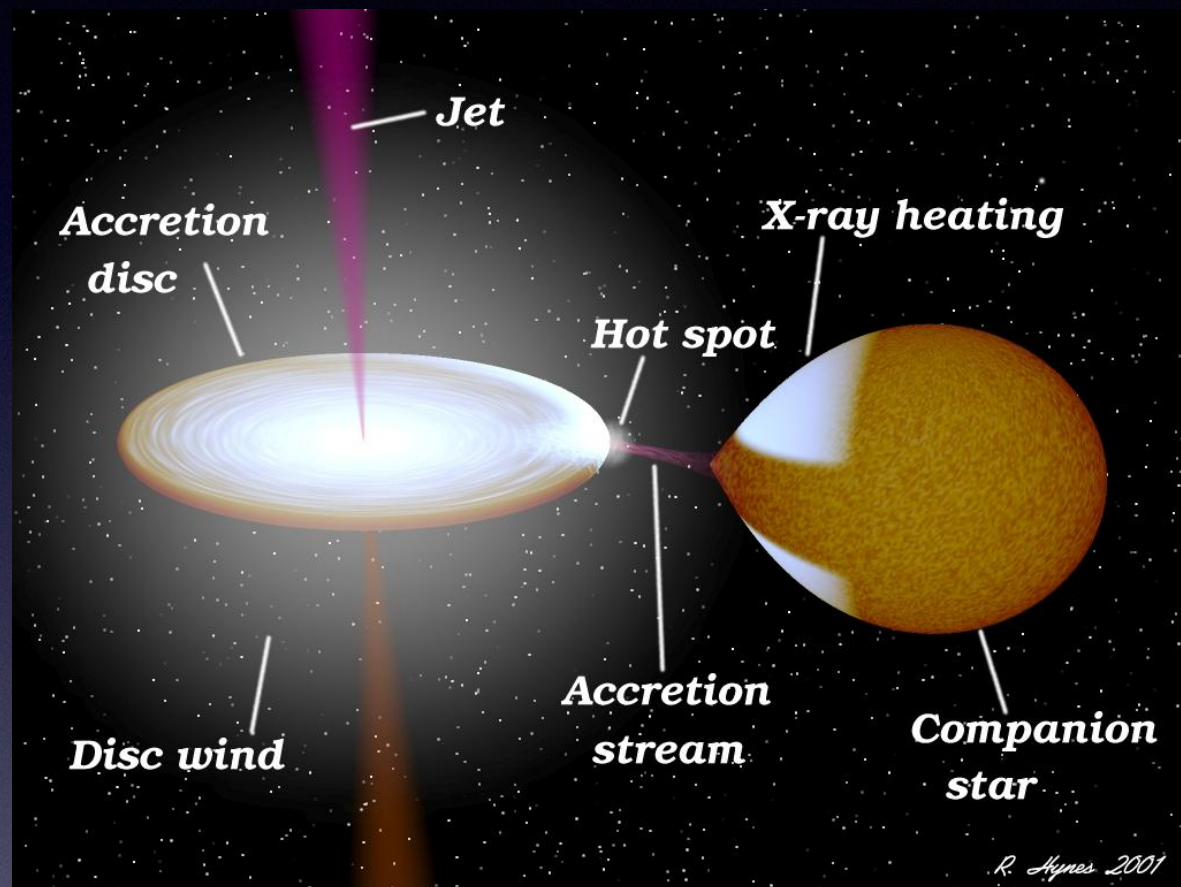
# Accreting binaries



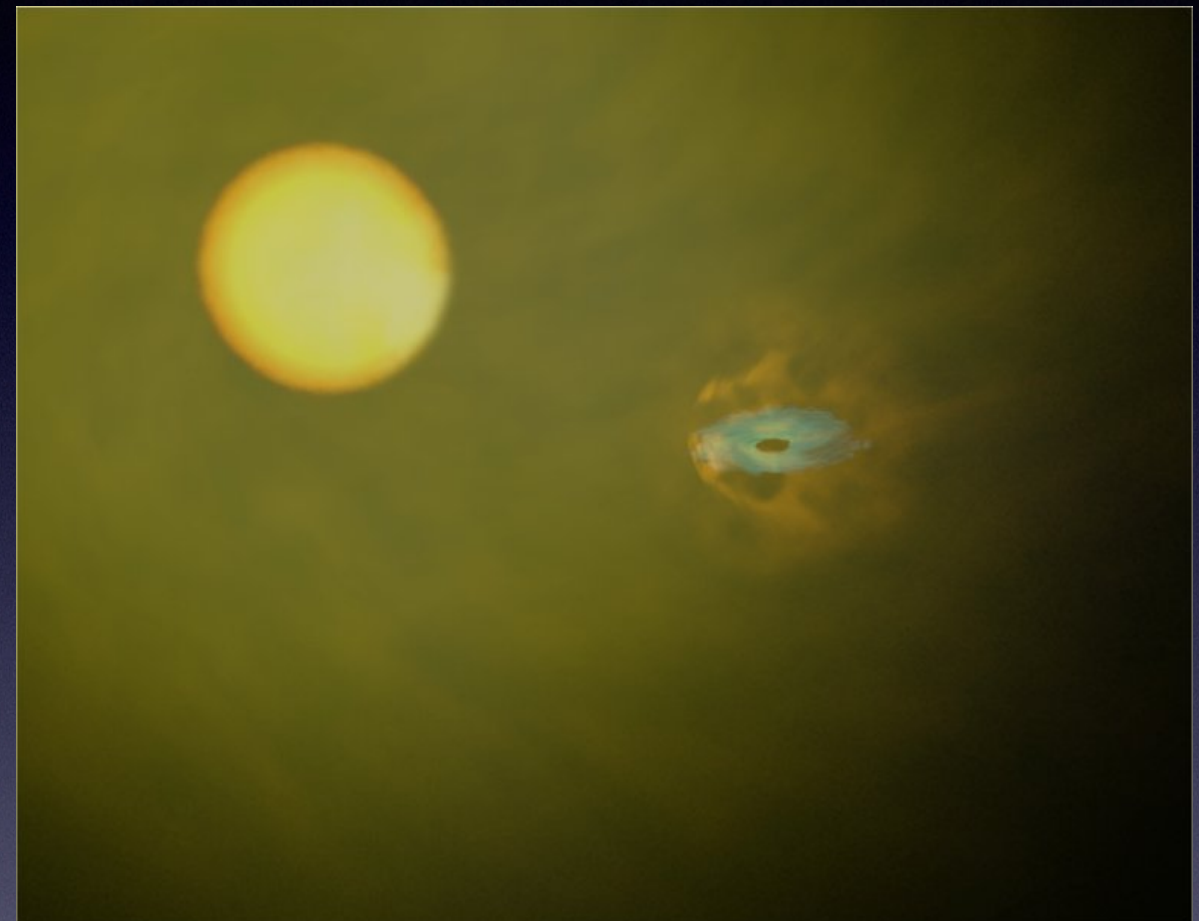
Low-mass X-ray Binaries  
(~250 LMXB):  
Roche lobe overflow



# Accreting binaries



Low-mass X-ray Binaries  
(~250 LMXB):  
Roche lobe overflow



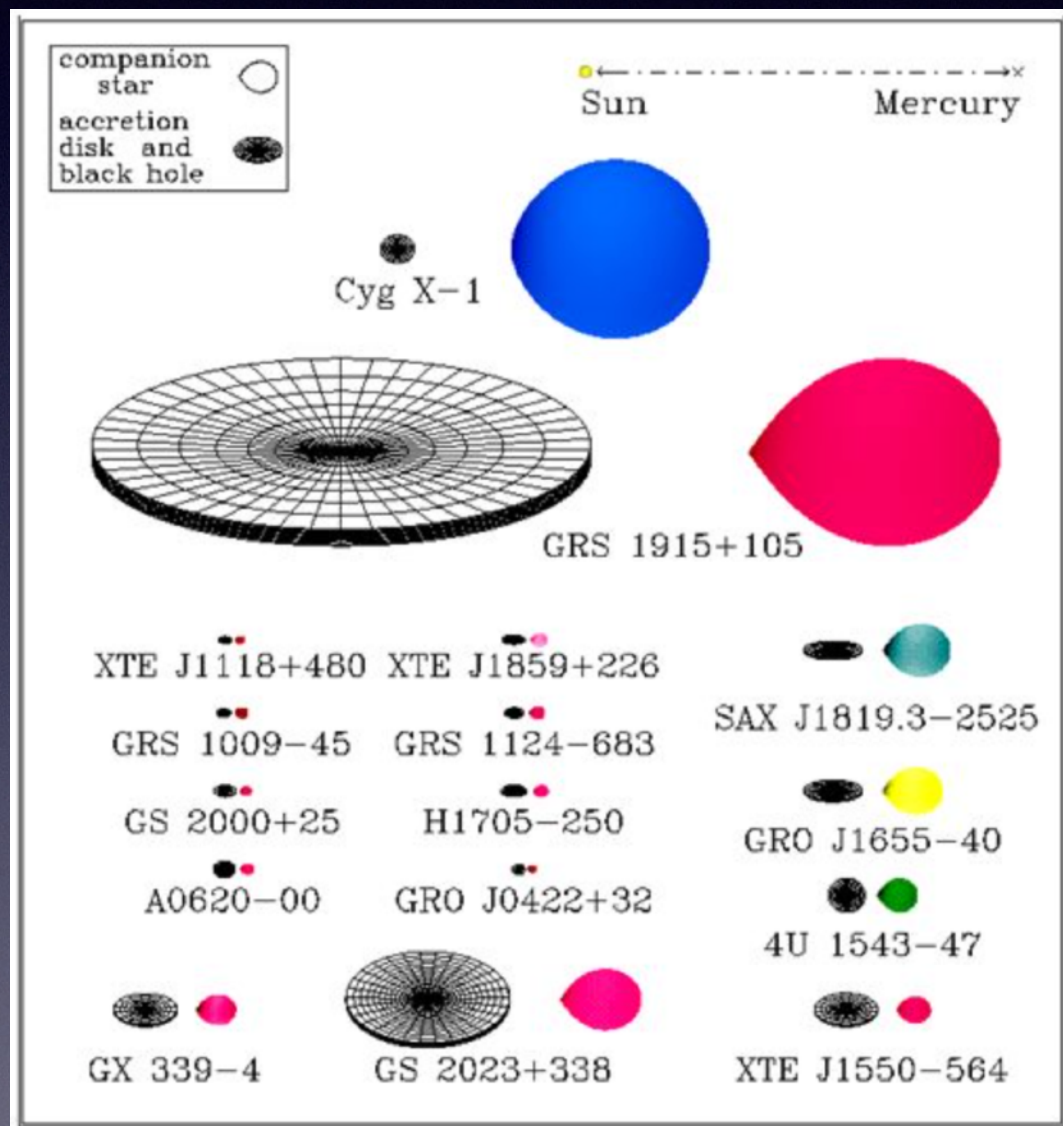
High-mass X-ray Binaries  
(~167 HMXB):  
Stellar wind accretion



# Accreting binaries



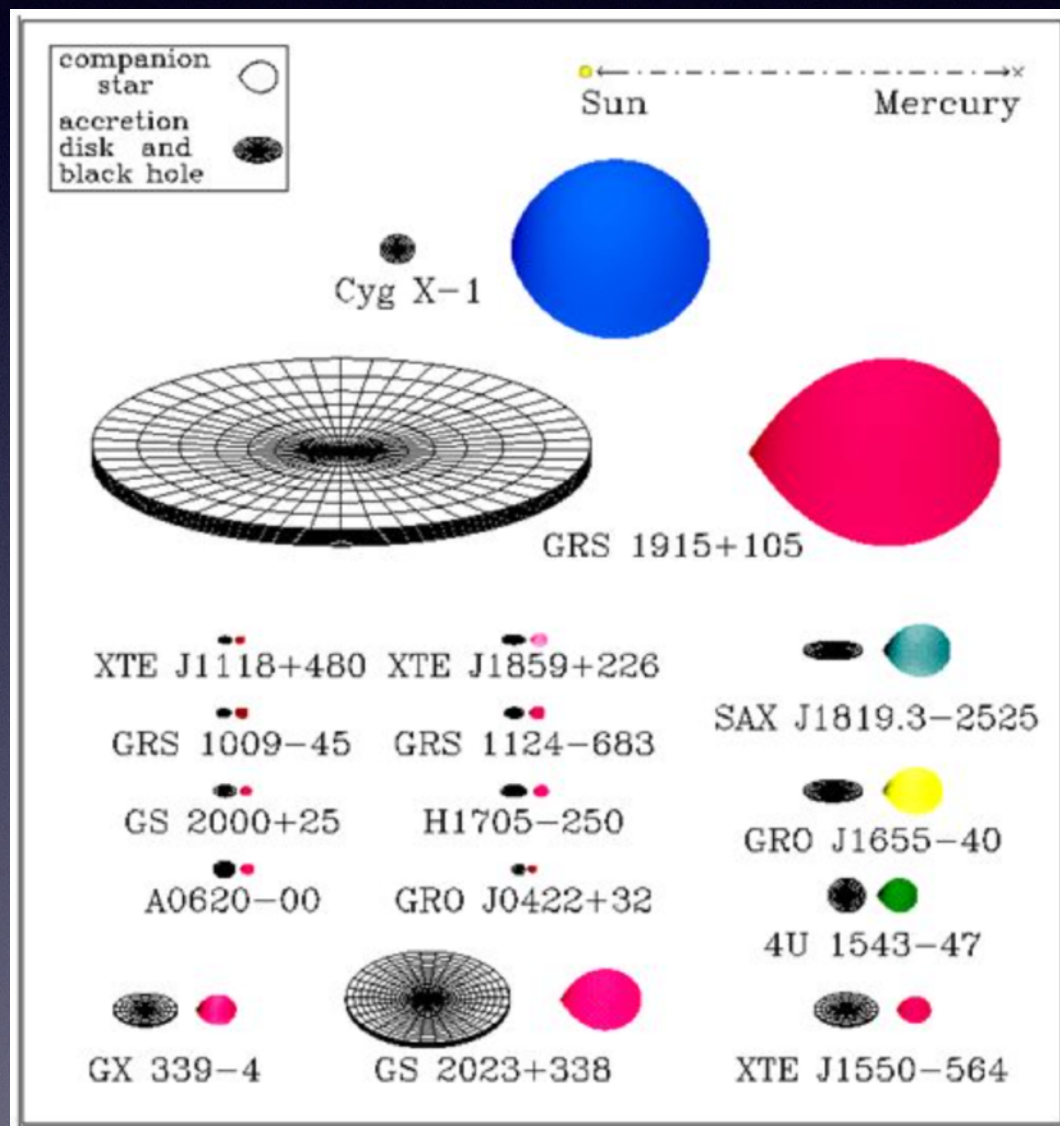
# Accreting binaries



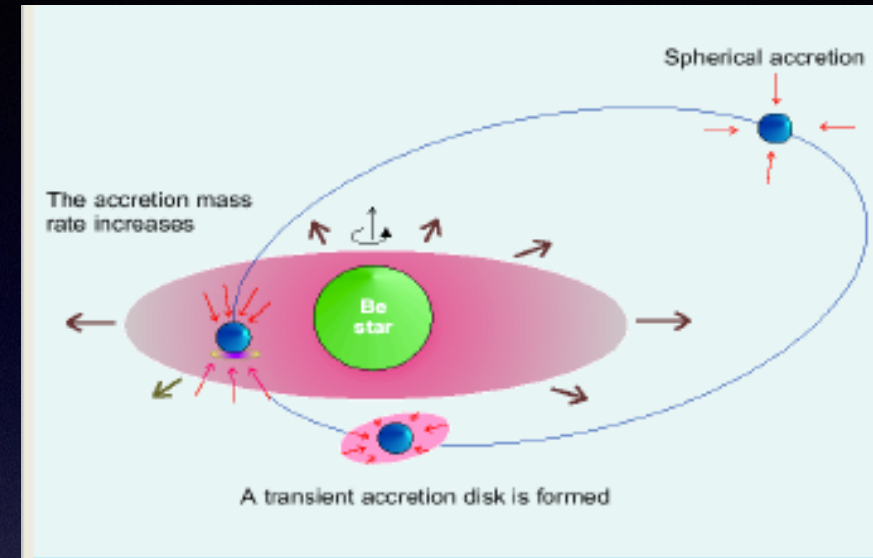
**LMXB**



# Accreting binaries



**LMXB**

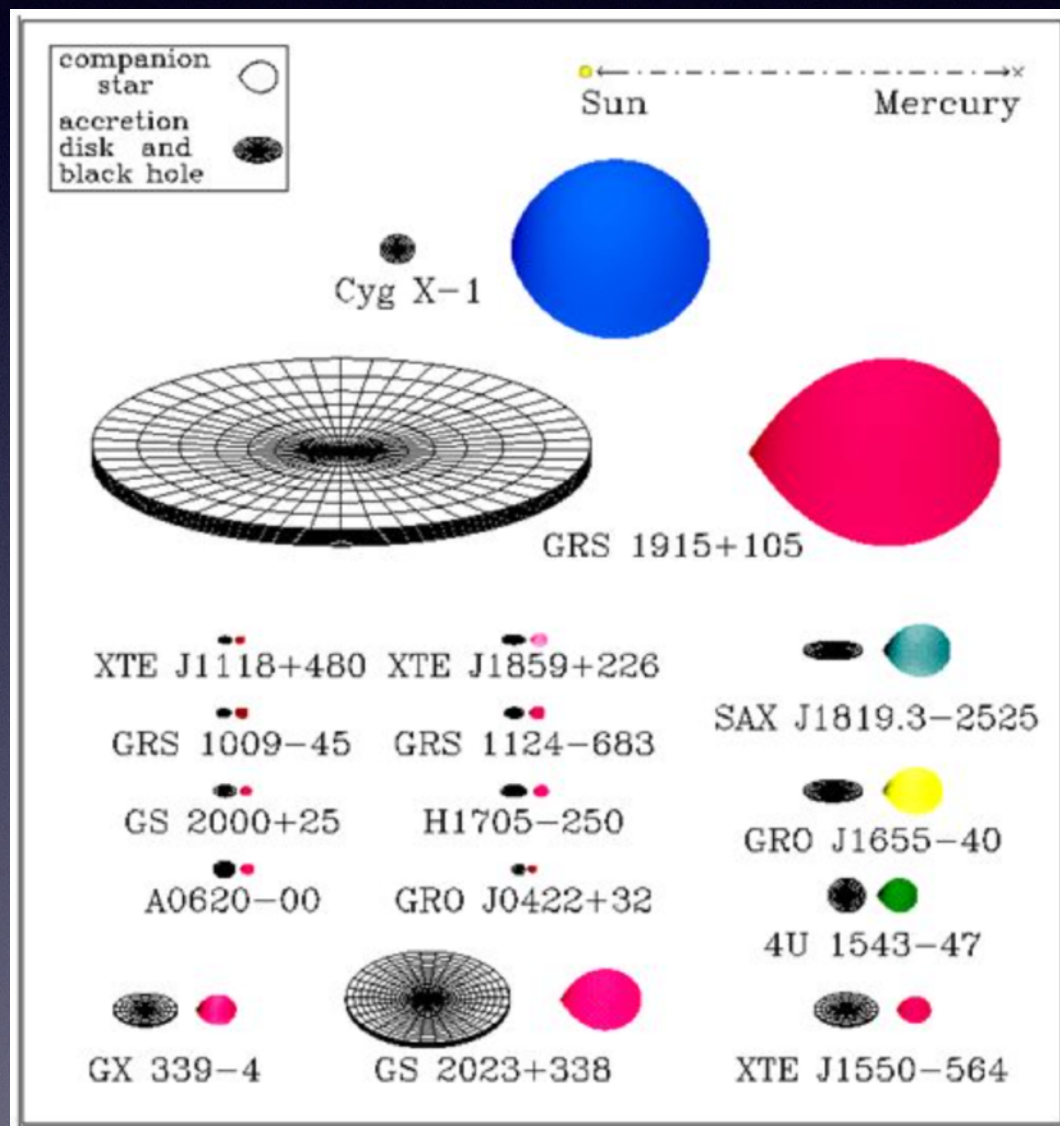


**BeHMXB**

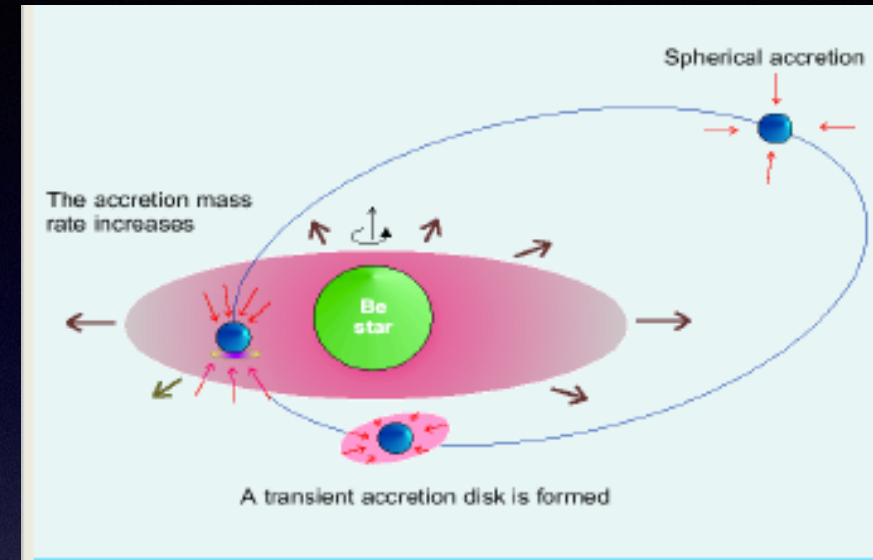
**HMXB**



# Accreting binaries

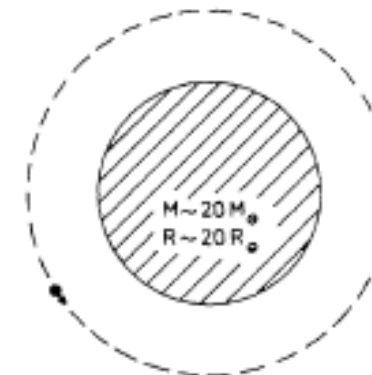


**LMXB**



**BeHMXB**

## STANDARD MASSIVE X-RAY BINARY



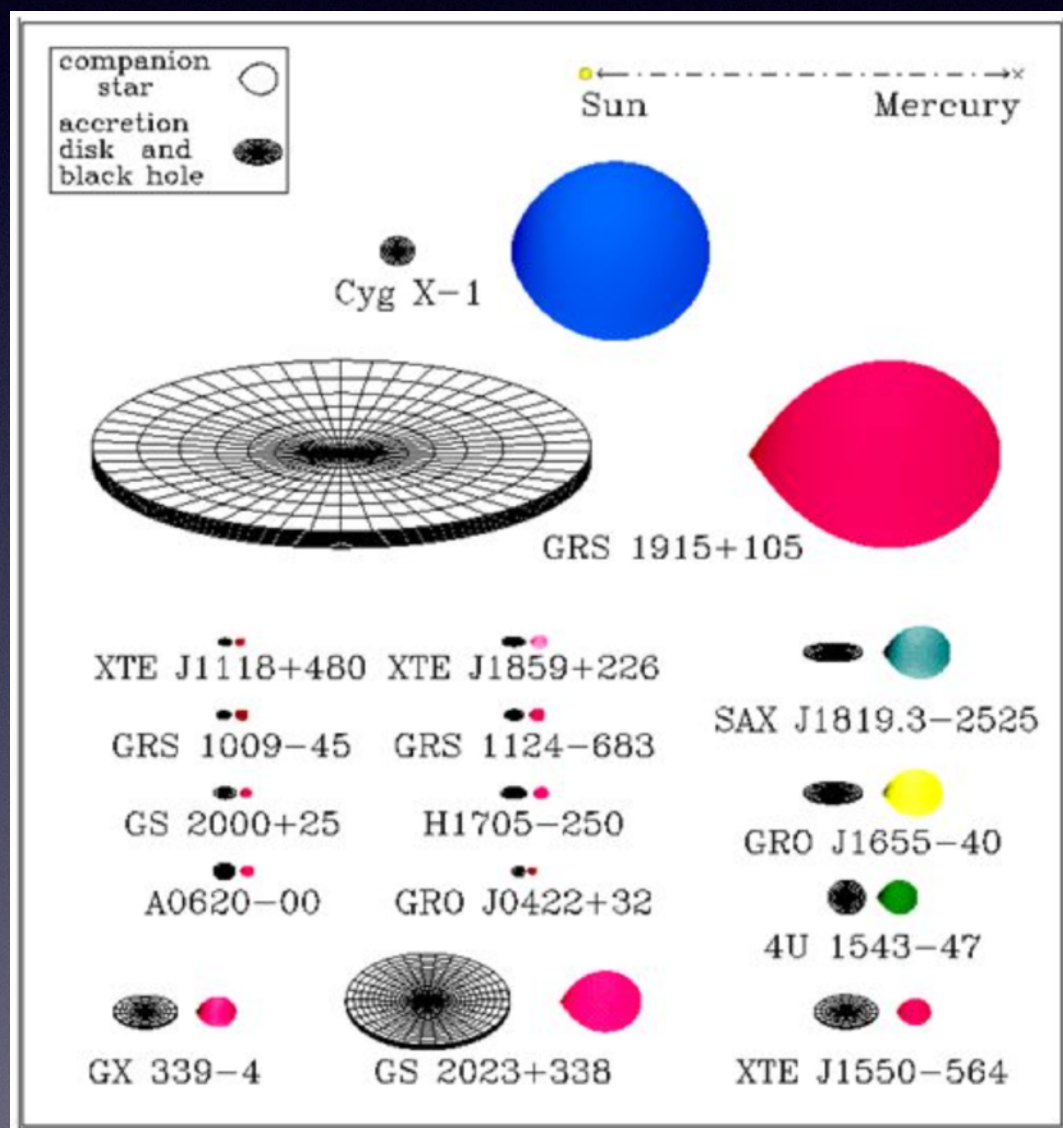
- Companion evolved to fill critical potential lobe
- $Z^d \lesssim P_{orb} \lesssim 10^d$
- Circular Orbit
- Eclipses likely
- "Steady" X-ray emission
- Mass transfer ( $10^{-10} - 10^{-8} M_{\odot} \text{ yr}^{-1}$ ) by Roche lobe overflow, stellar wind or both

**sgHMXB**

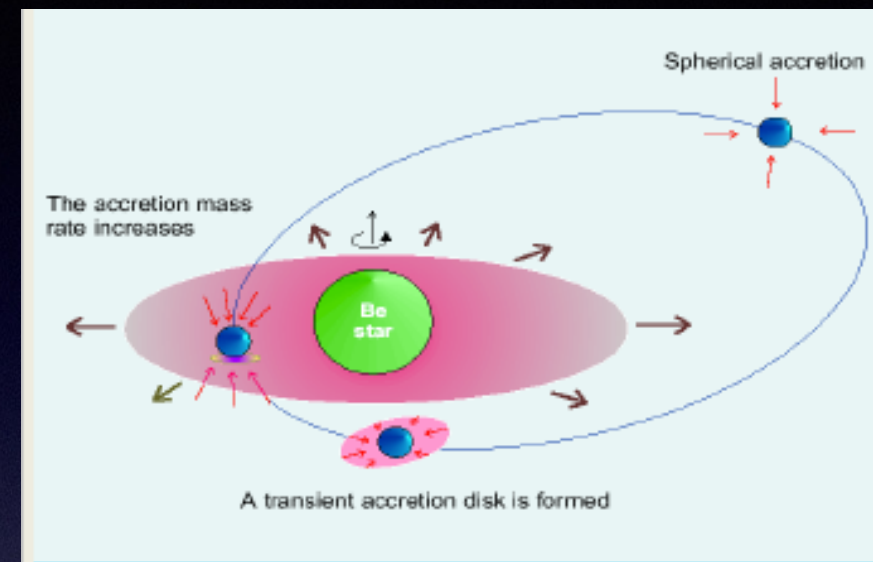
**HMXB**



# Accreting binaries

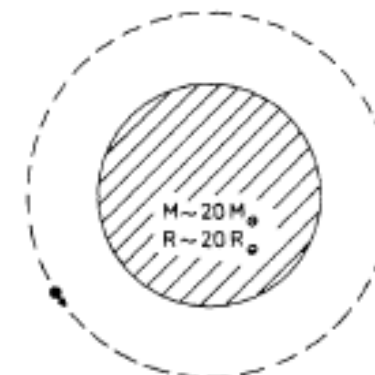


**LMXB**



**BeHMXB**

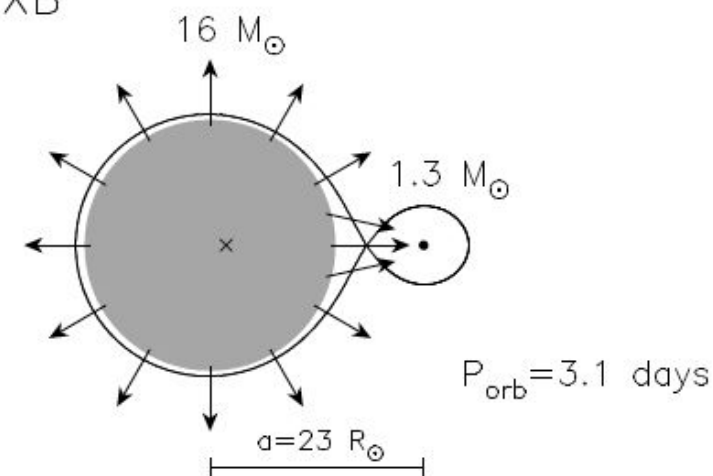
## STANDARD MASSIVE X-RAY BINARY



- Companion evolved to fill critical potential lobe
- $Z^d \lesssim P_{orb} \lesssim 10^d$
- Circular Orbit
- Eclipses likely
- "Steady" X-ray emission
- Mass transfer ( $10^{-10} - 10^{-8} M_{\odot} \text{yr}^{-1}$ ) by Roche lobe overflow, stellar wind or both

**sgHMXB**

## HMXB

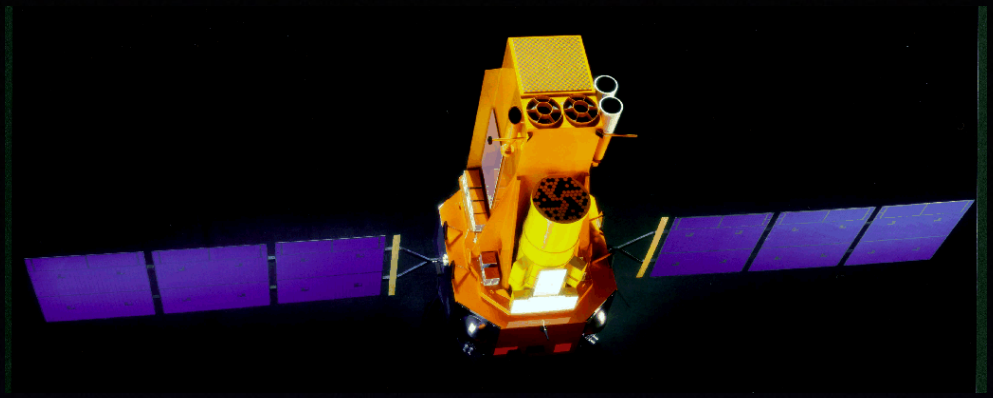


**RLO**

**HMXB**

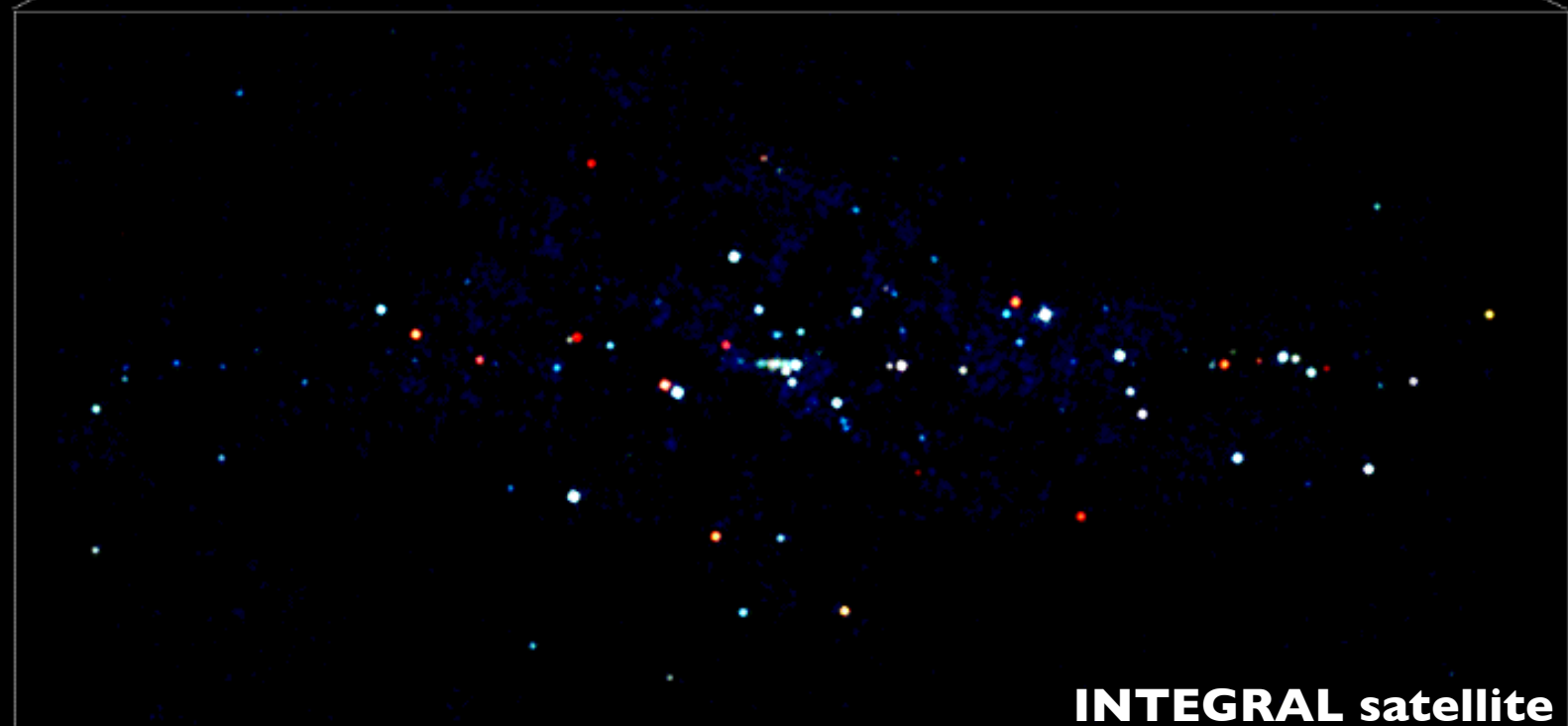
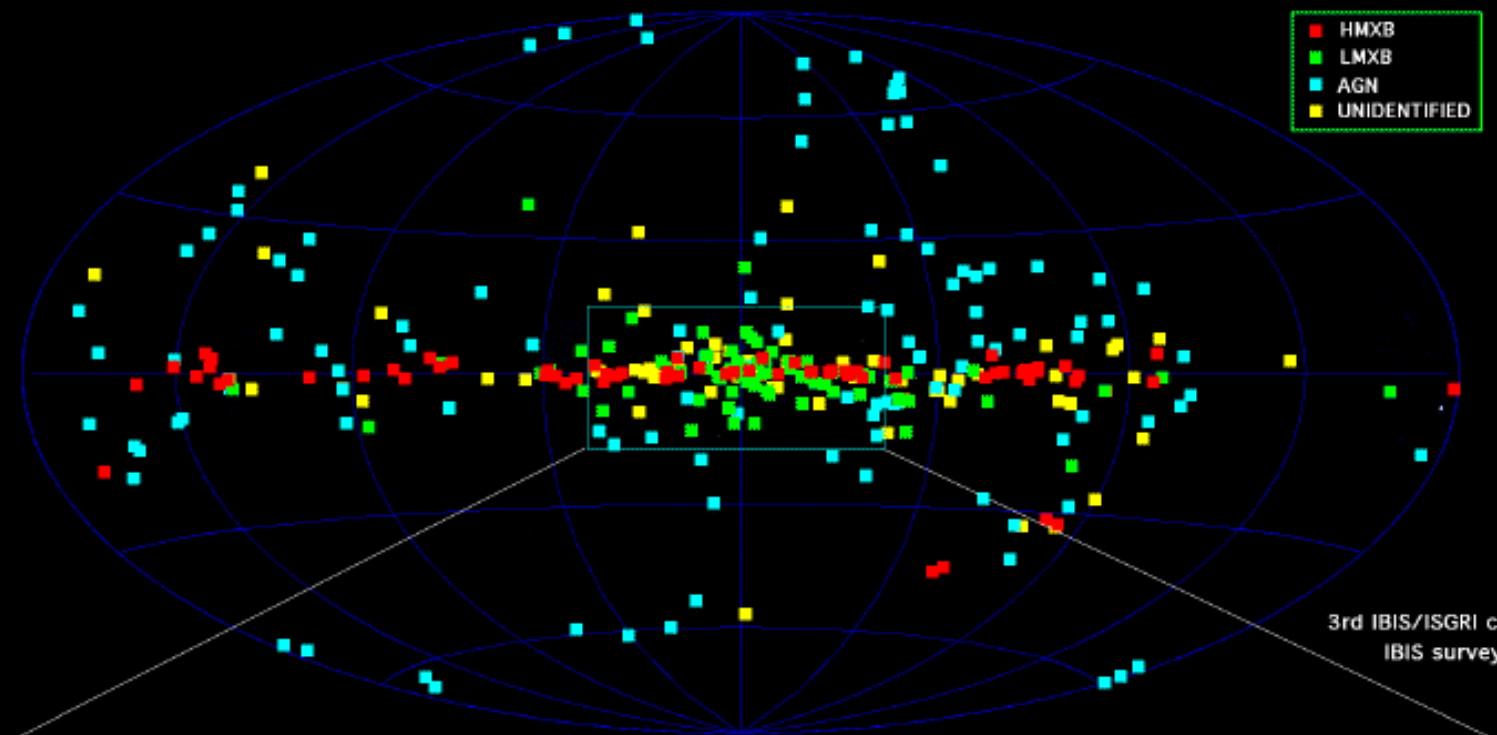
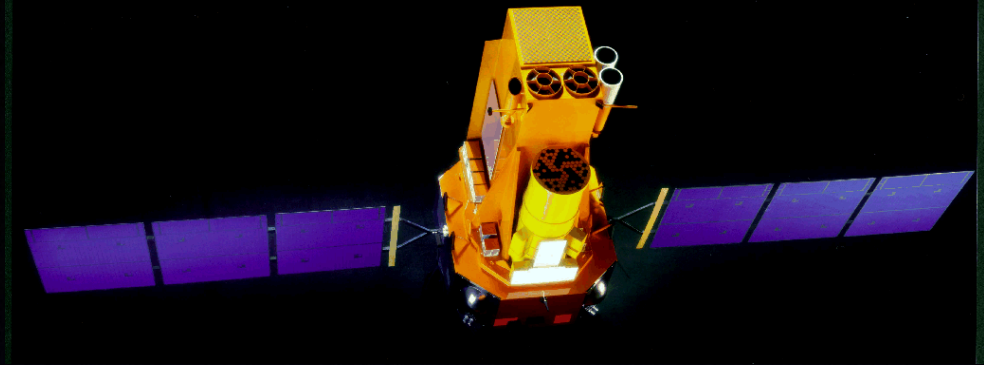


# Accreting binaries





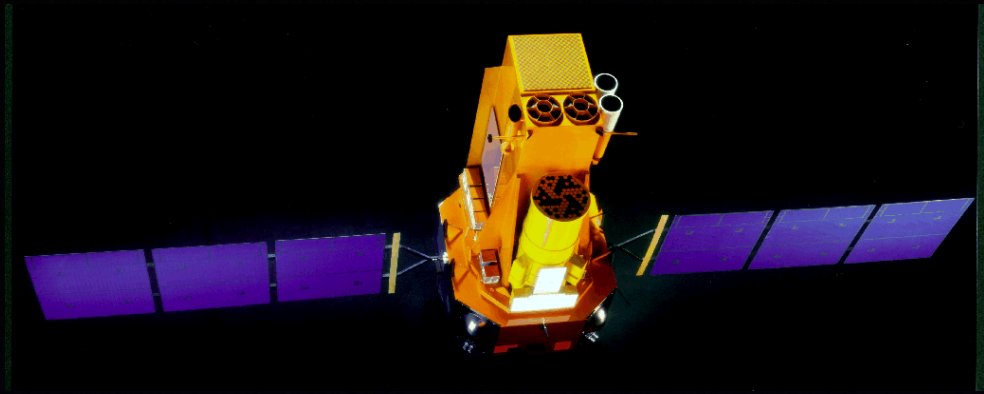
# Accreting binaries



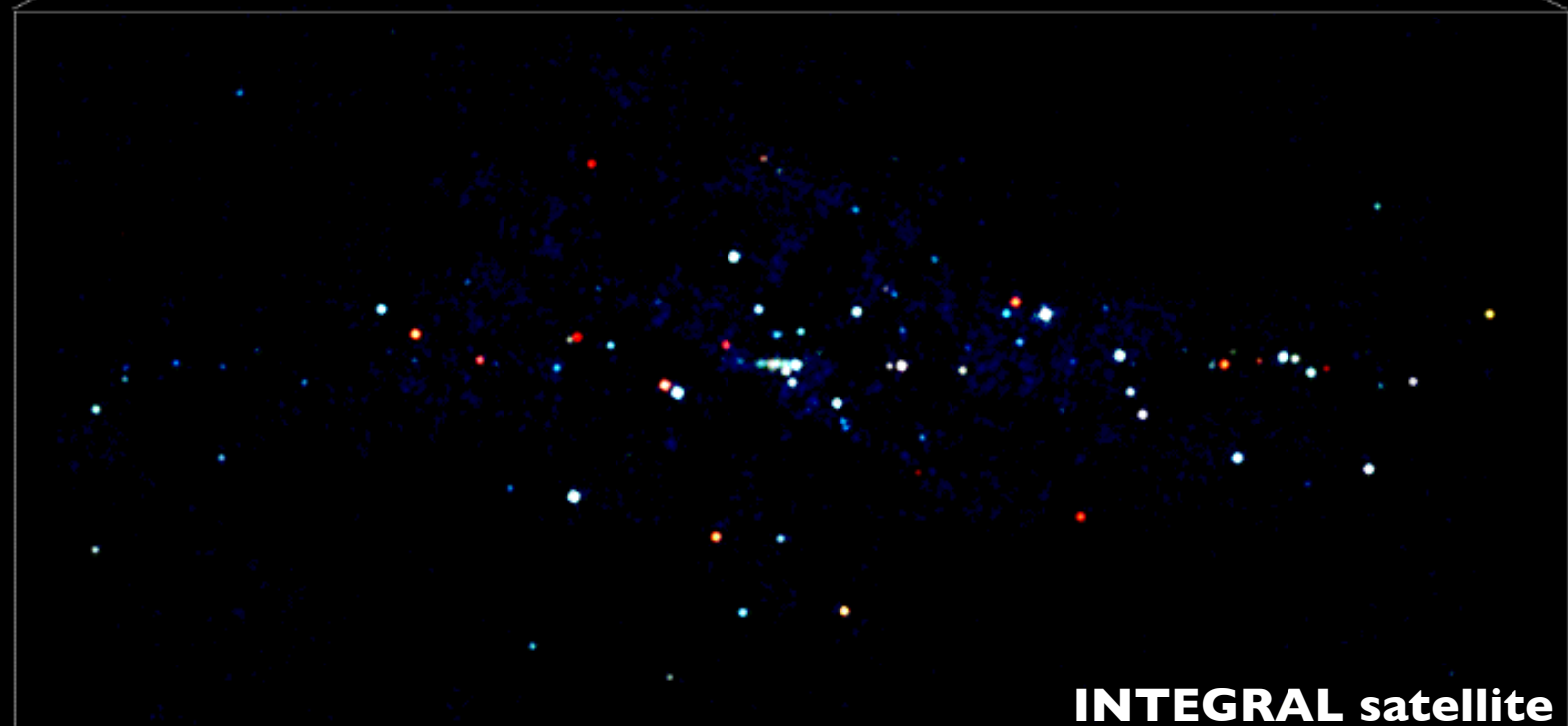
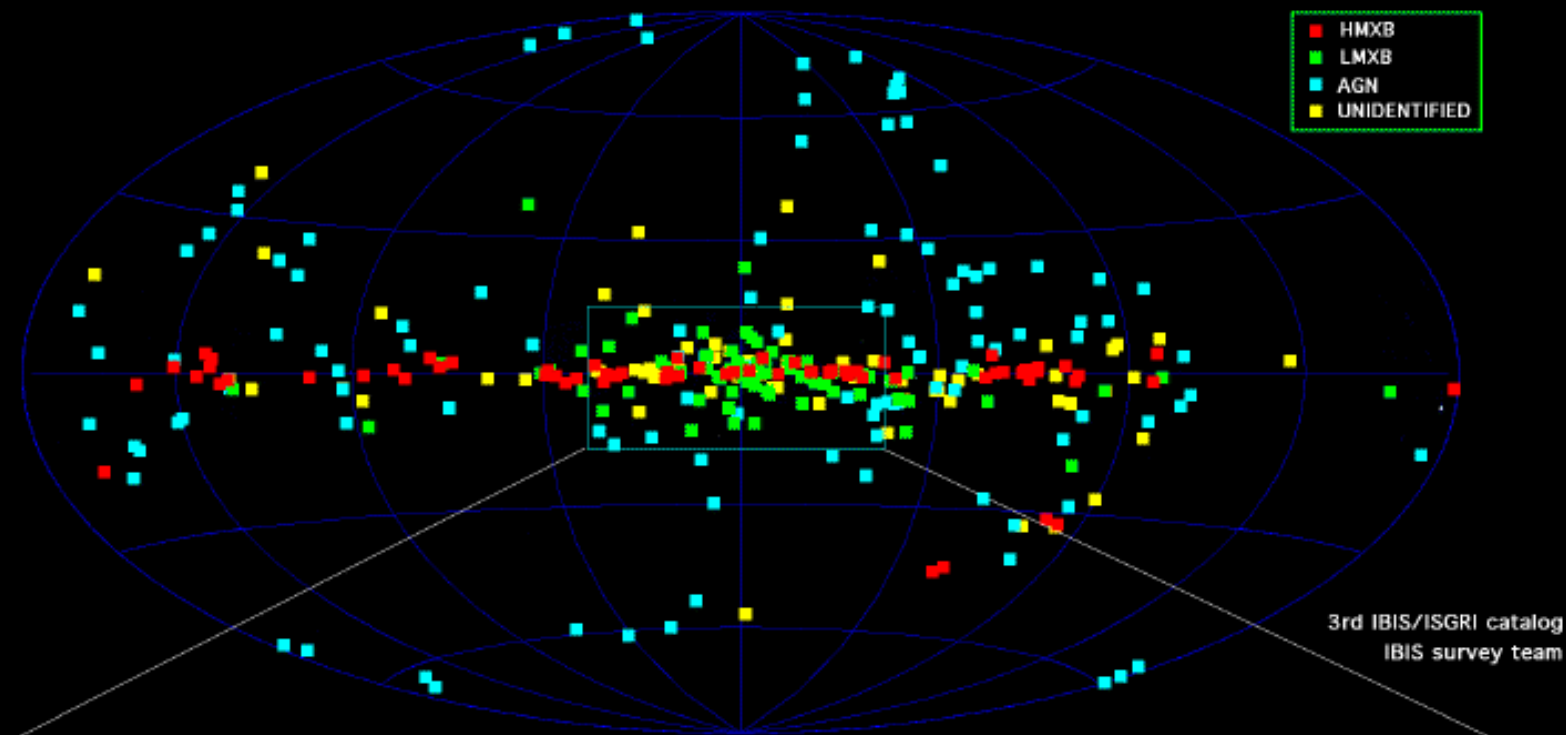
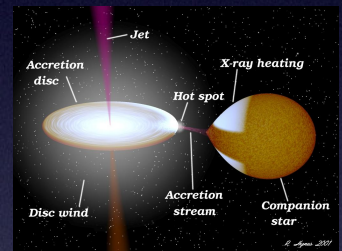
**INTEGRAL satellite**  
**Bird et al. 2018**



# Accreting binaries



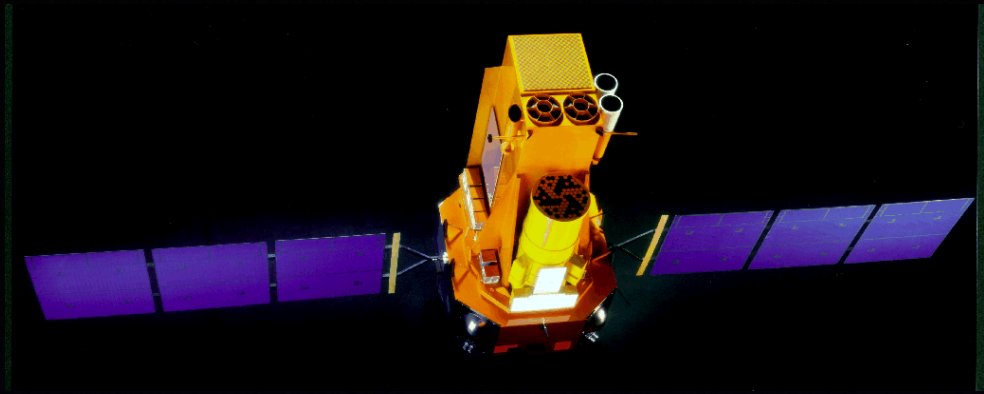
- LMXB (old stars) within Galactic bulge, migrating off the plane ( $|b| > 3-5^\circ$ )



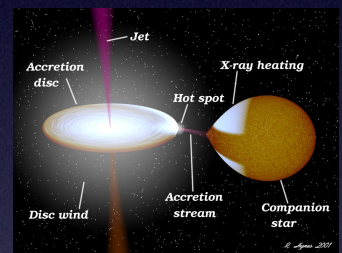
**INTEGRAL satellite**  
**Bird et al. 2018**



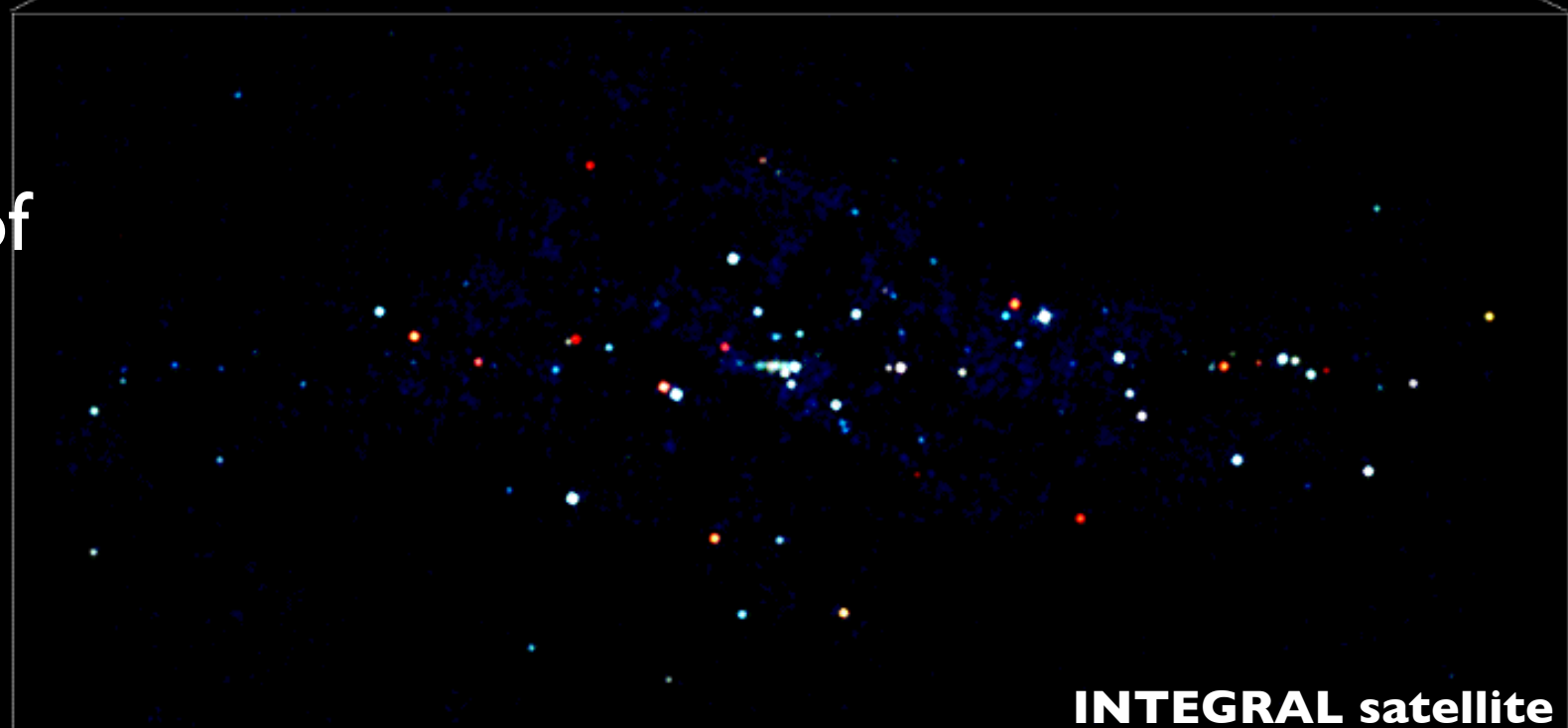
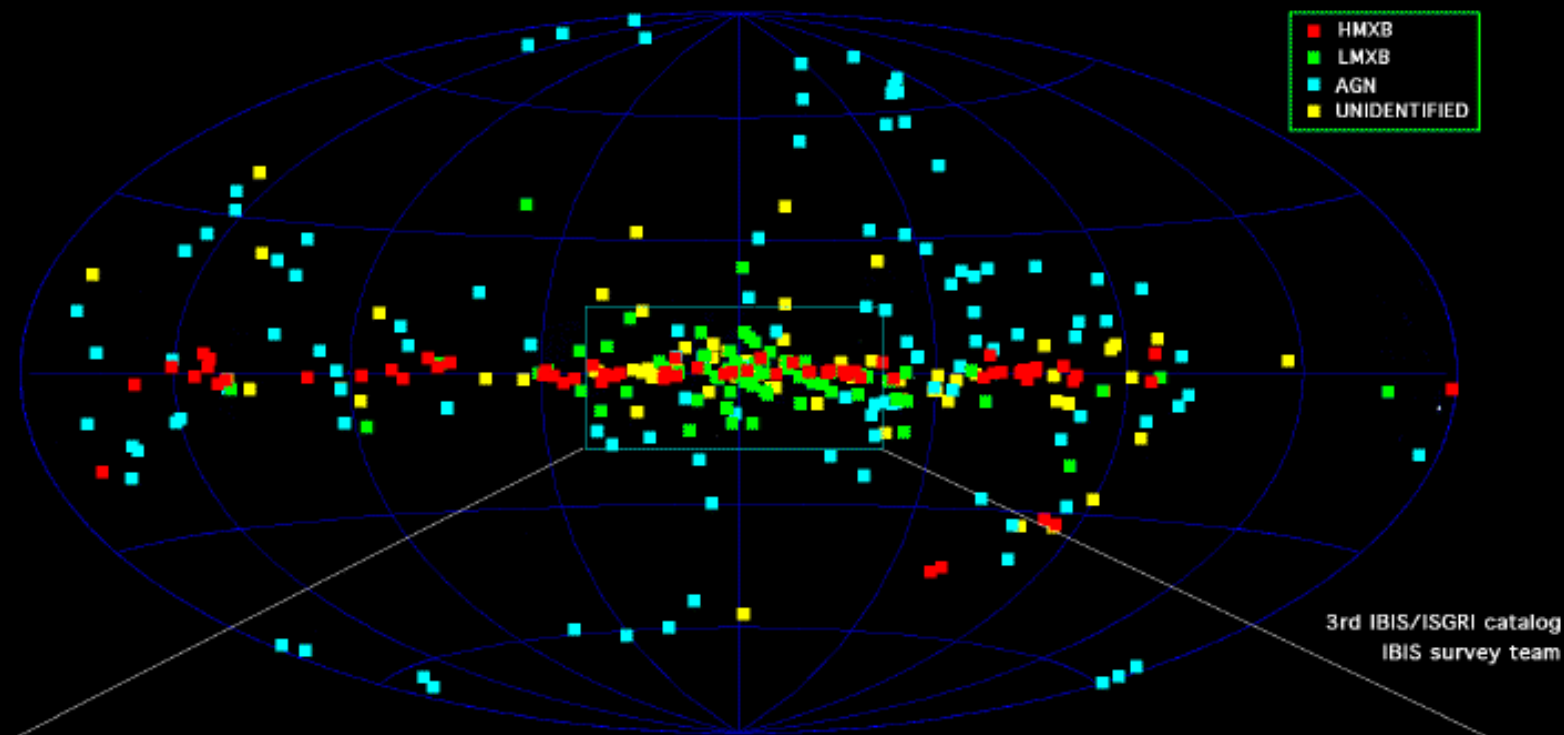
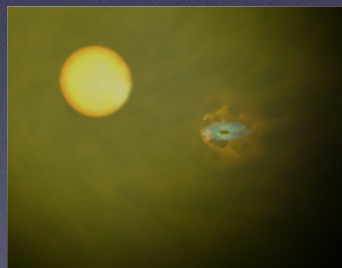
# Accreting binaries



- LMXB (old stars) within Galactic bulge, migrating off the plane ( $|b| > 3-5^\circ$ )



- HMXB (young stars): within Galactic plane, tangential directions of spiral arms



**INTEGRAL satellite**  
**Bird et al. 2018**

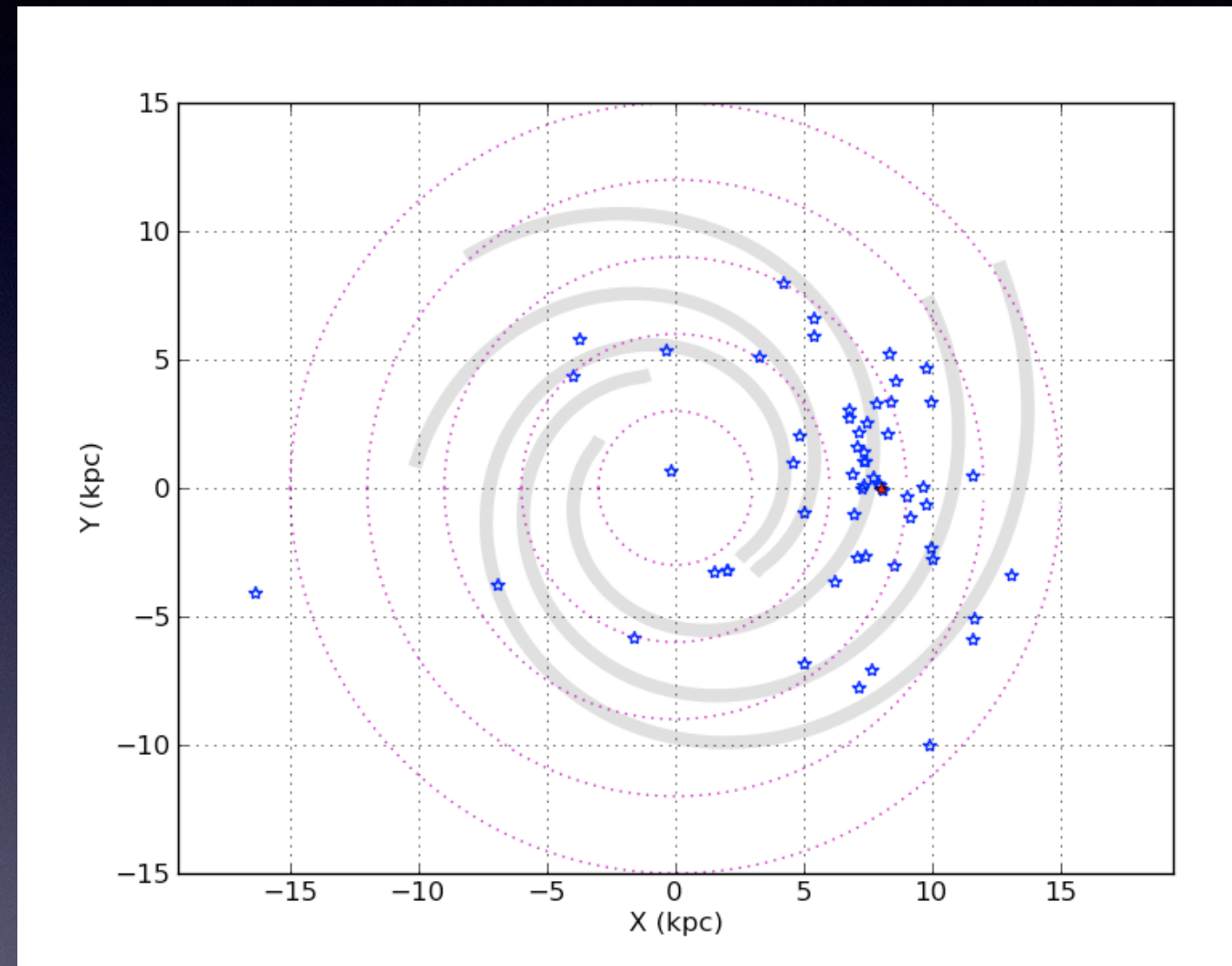


# Galactic distribution of HMXB



# Galactic distribution of HMXB

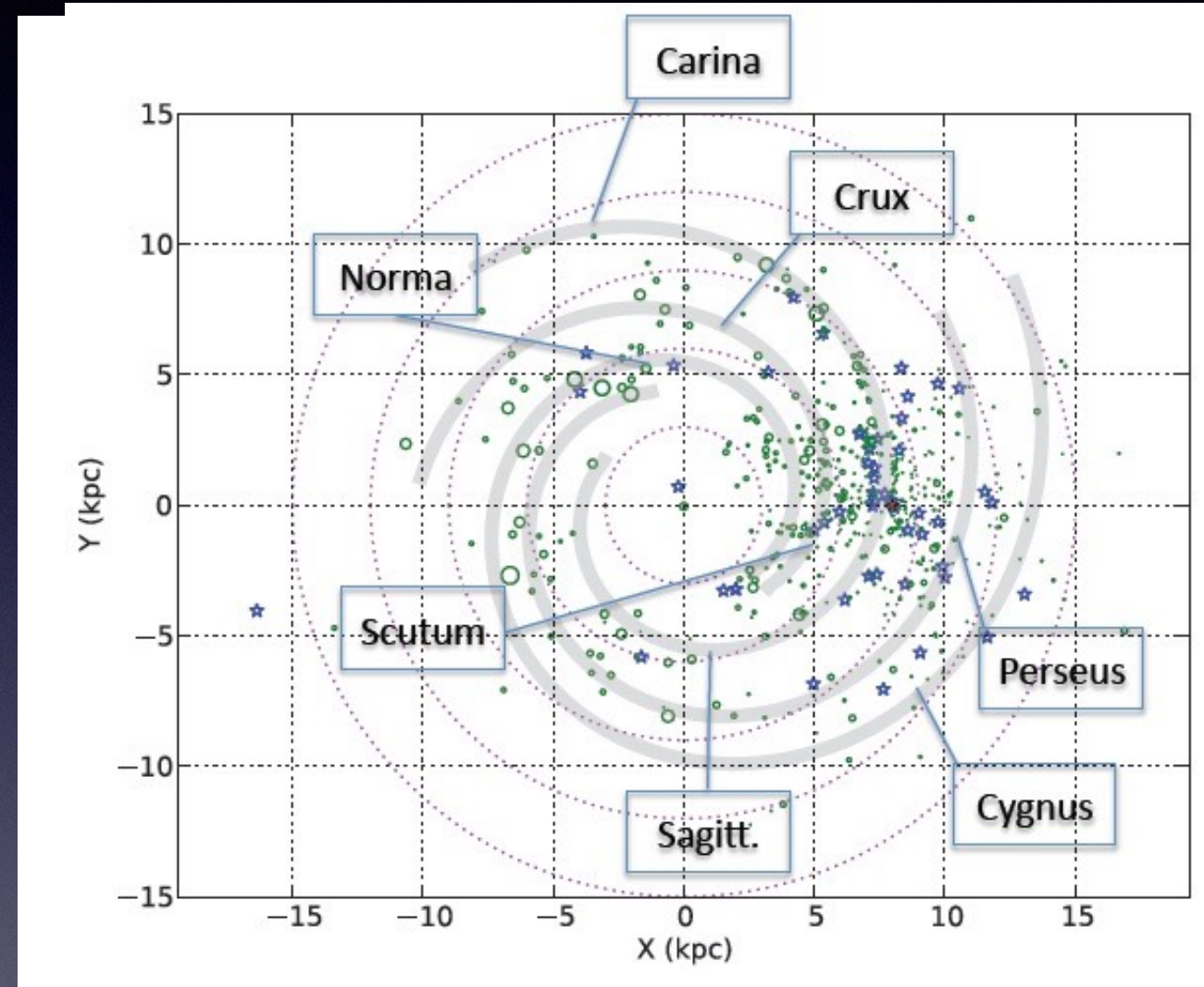
- 46 HMXB distributed on a 4-spiral arm Galactic model





# Galactic distribution of HMXB

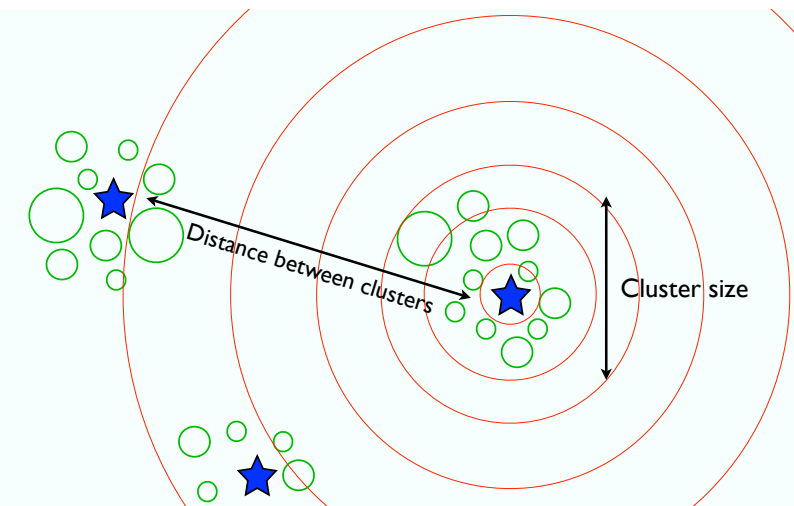
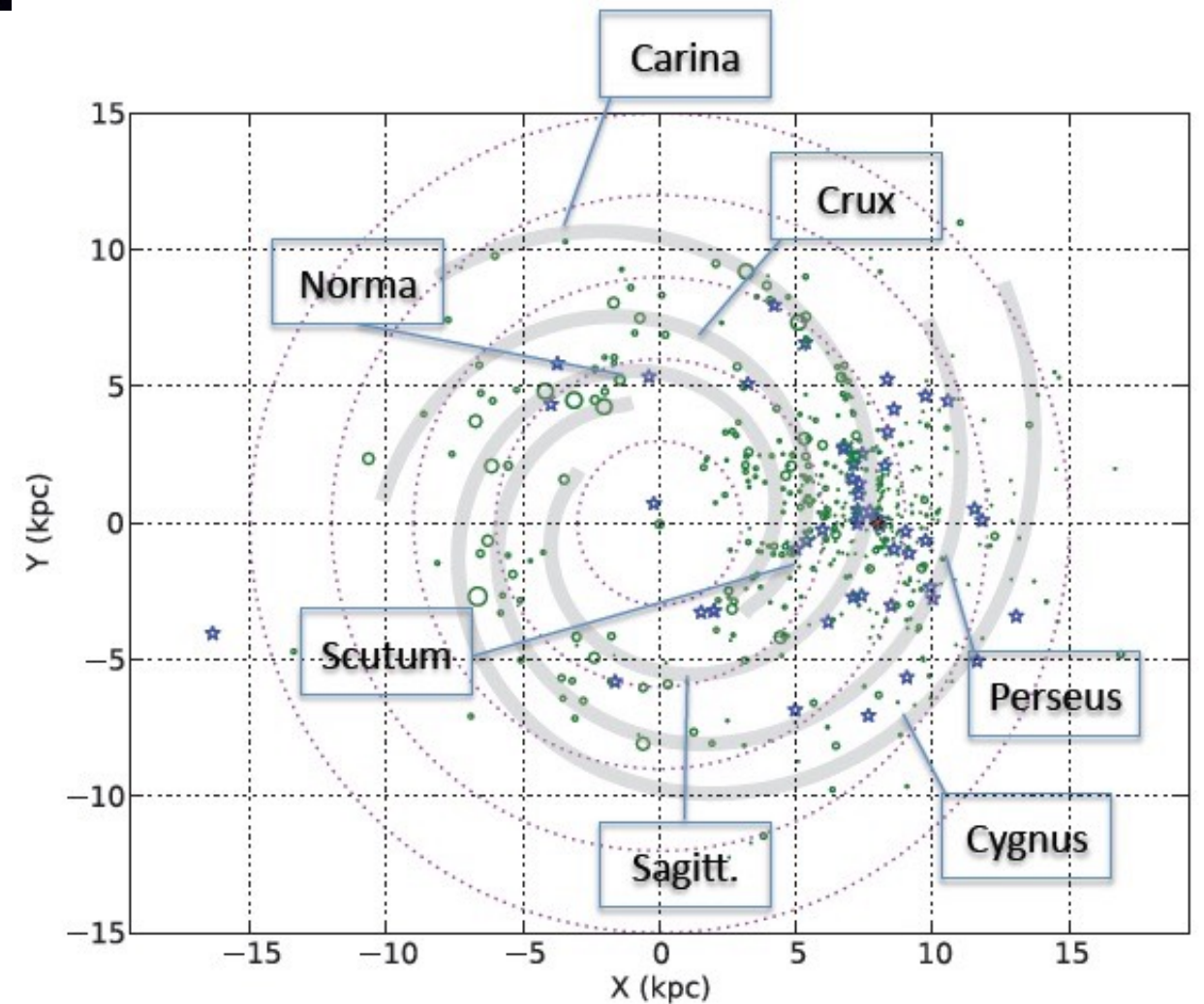
- 46 HMXB distributed on a 4-spiral arm Galactic model
- Star Forming Complexes (SFC)





# Galactic distribution of HMXB

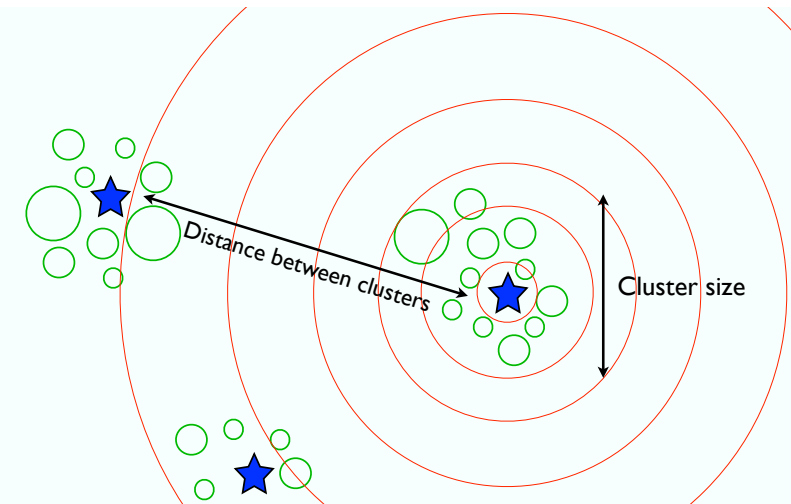
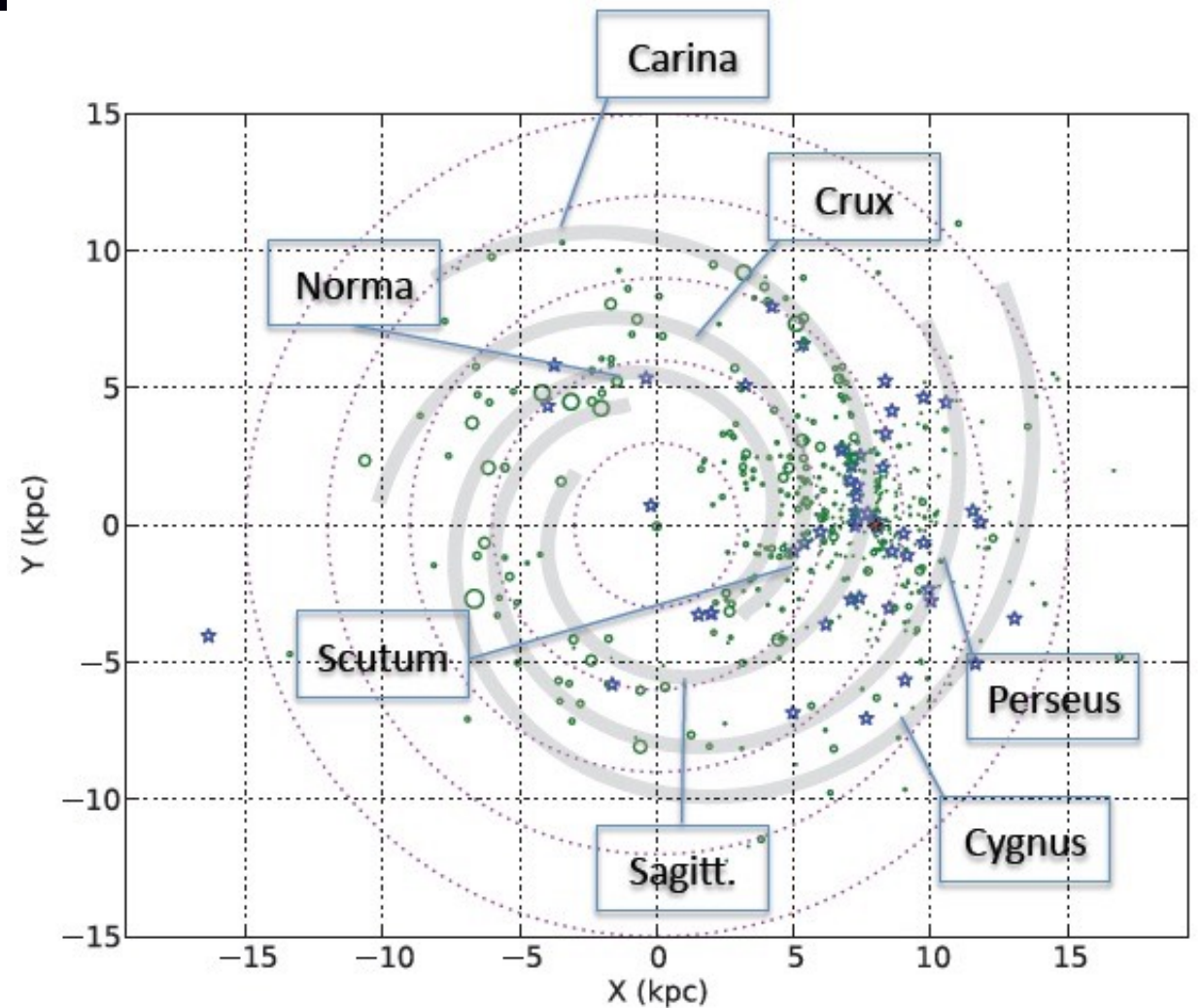
- 46 HMXB distributed on a 4-spiral arm Galactic model
- Star Forming Complexes (SFC)
- Search for correlation between HMXB & SFC





# Galactic distribution of HMXB

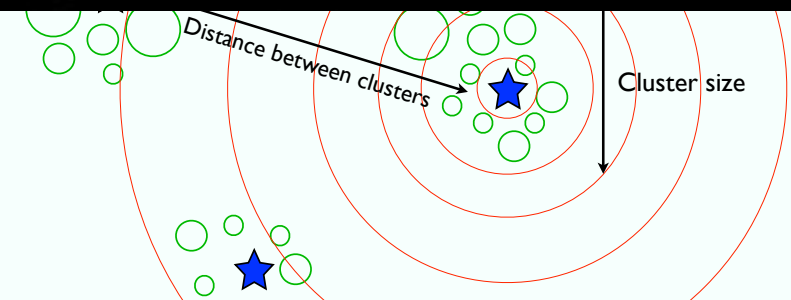
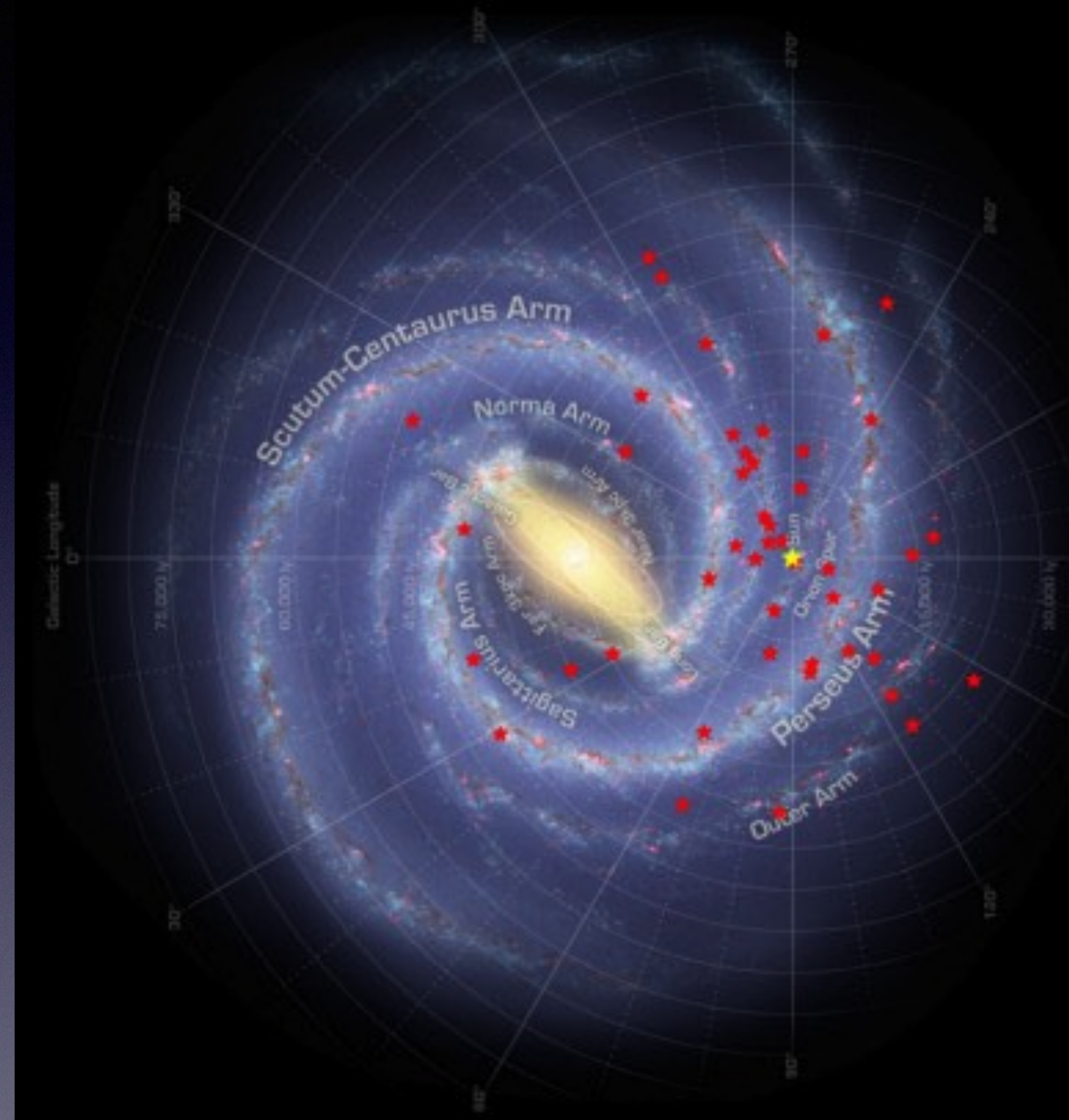
- 46 HMXB distributed on a 4-spiral arm Galactic model
- Star Forming Complexes (SFC)
- Search for correlation between HMXB & SFC
- $\Rightarrow$  HMXB clustered with SFC ( $\langle \text{size} \rangle = 0.3$  kpc,  $\langle \text{distance} \rangle = 1.7$  kpc), close to their birthplace





# Galactic distribution of HMXB

- 46 HMXB distributed on a 4-spiral arm Galactic model
- Star Forming Complexes (SFC)
- Search for correlation between HMXB & SFC
- => HMXB clustered with SFC ( $\langle \text{size} \rangle = 0.3 \text{ kpc}$ ,  $\langle \text{distance} \rangle = 1.7 \text{ kpc}$ ), close to their birthplace



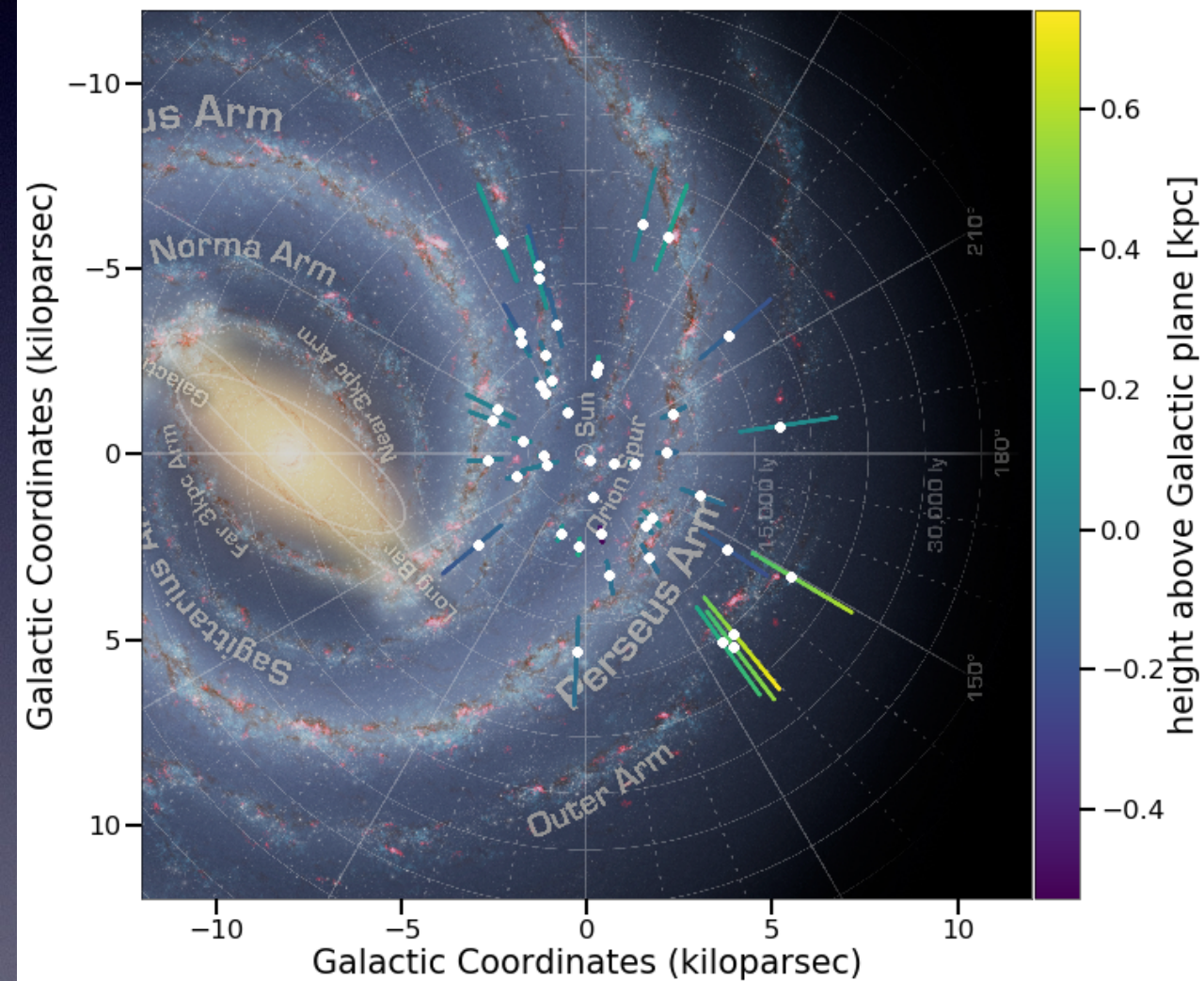


# Galactic distribution & natal kick of HMXB



# Galactic distribution & natal kick of HMXB

Gaia view of HMXBs in the Milky Way

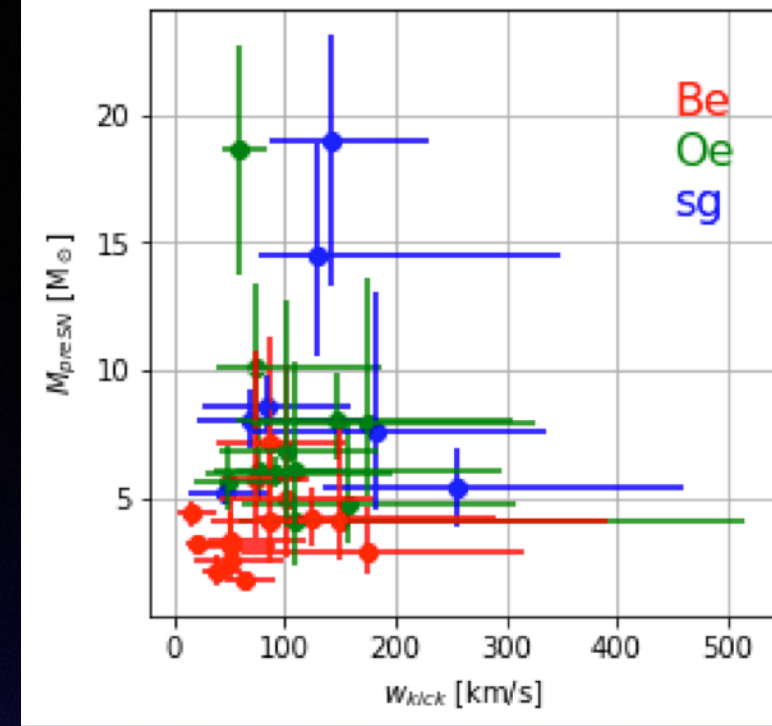


Galactic distribution of 39 NS-HMXB (Gaia EDR3)

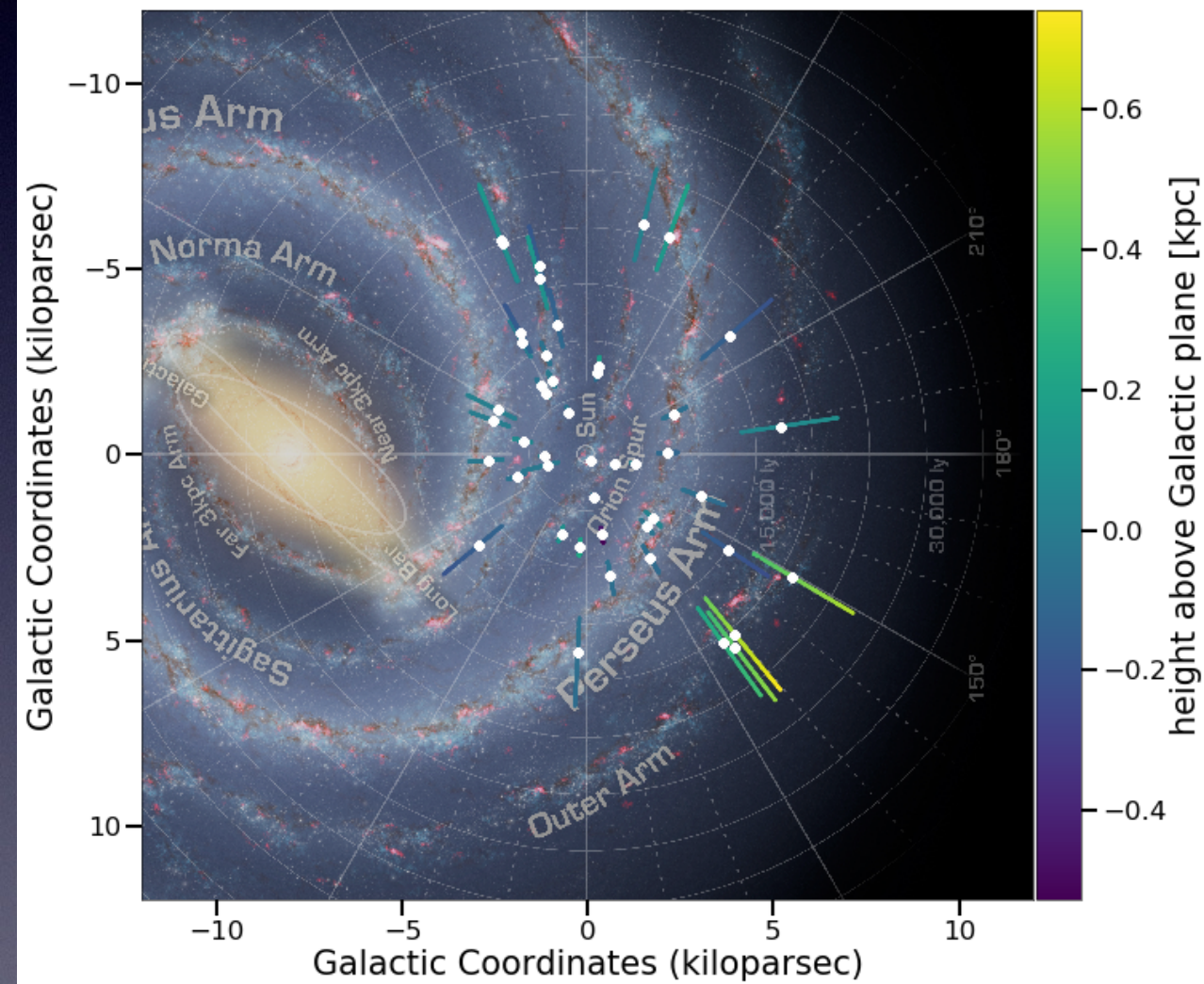
Fortin, Garcia, Chaty, Chassande Mottin, Simaz Bunzel, A&A subm.



# Galactic distribution & natal kick of HMXB



Gaia view of HMXBs in the Milky Way

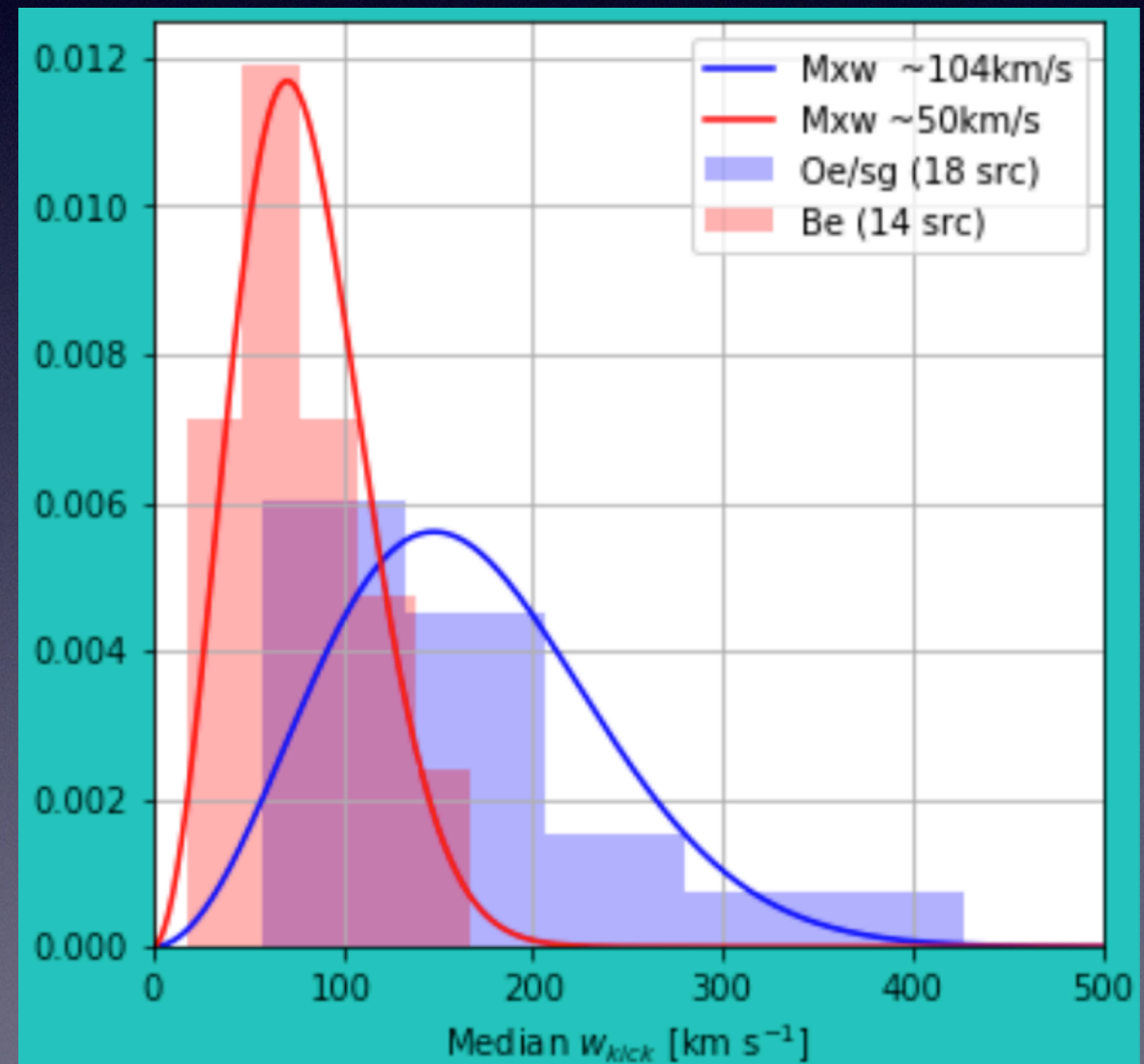
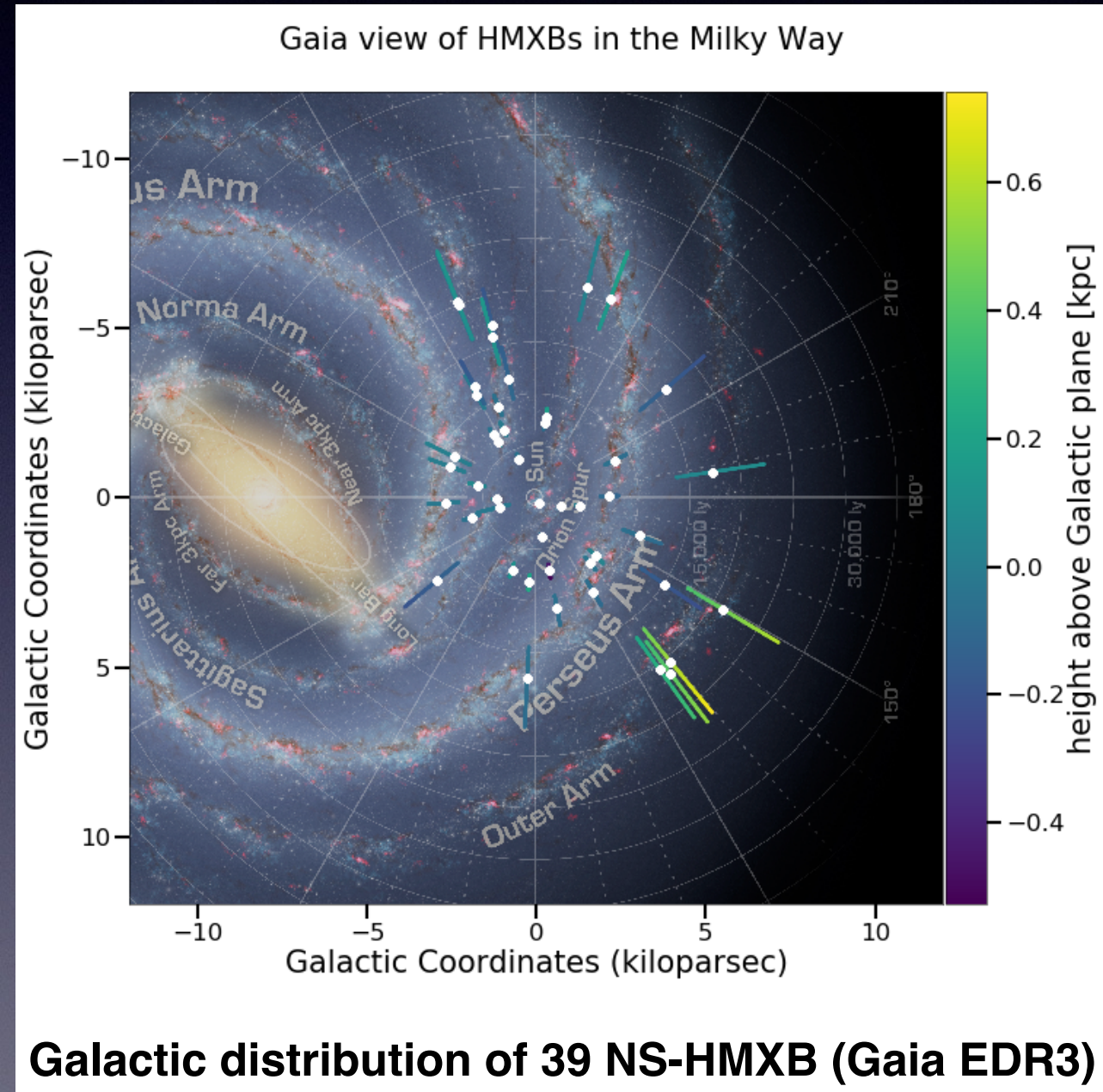
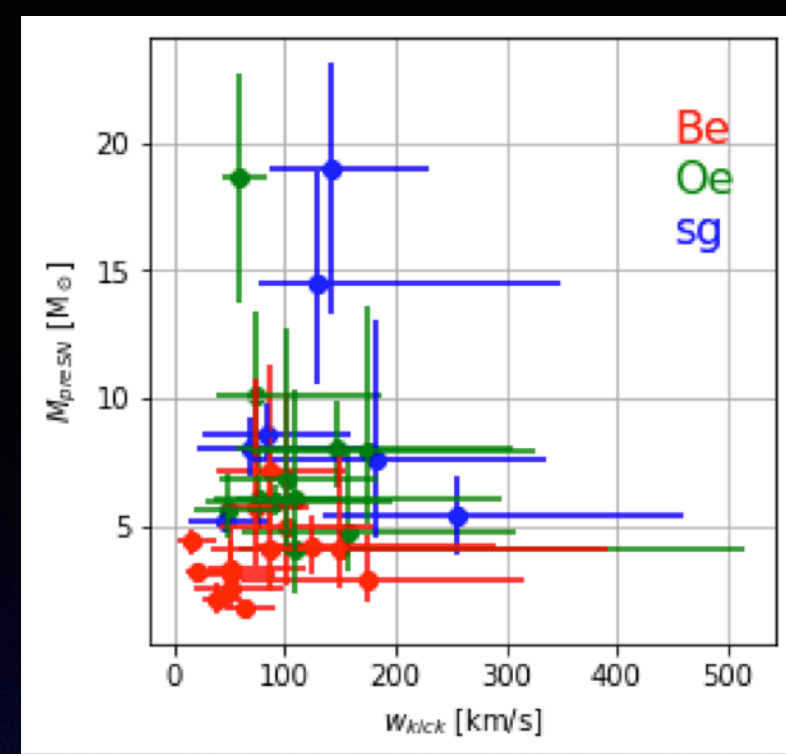


Galactic distribution of 39 NS-HMXB (Gaia EDR3)

Fortin, Garcia, Chaty, Chassande Mottin, Simaz Bunzel, A&A subm.



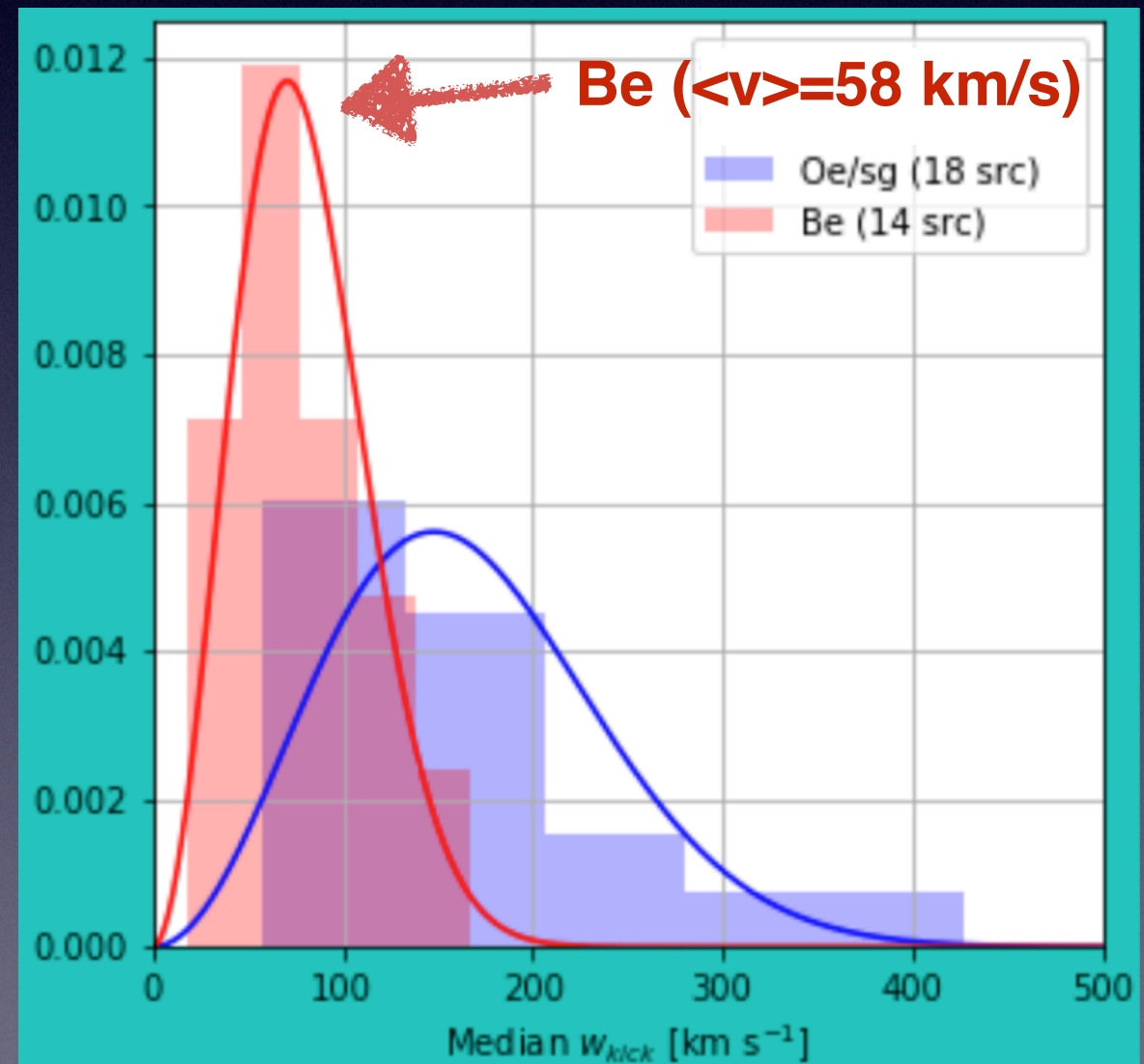
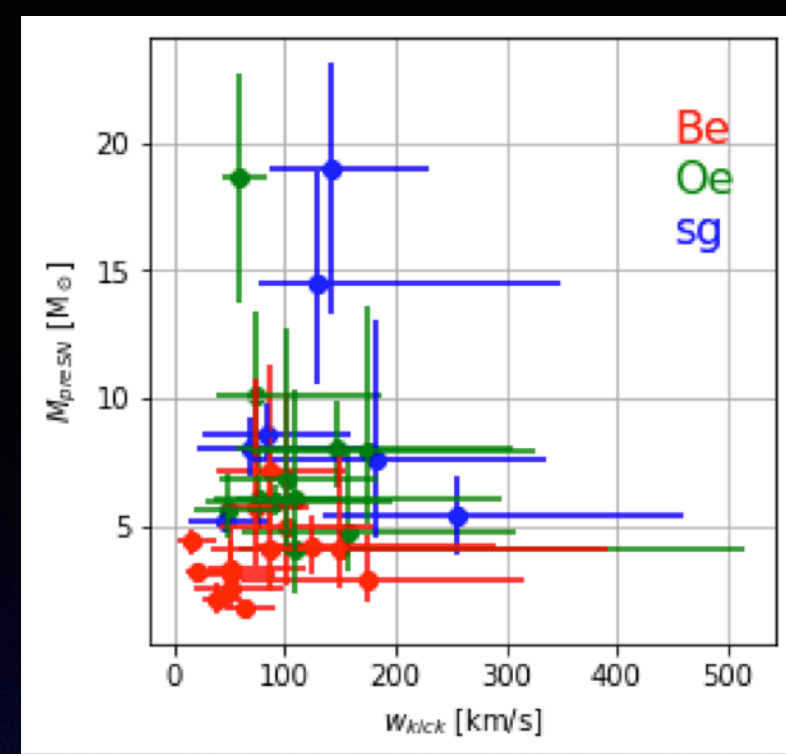
# Galactic distribution & natal kick of HMXB



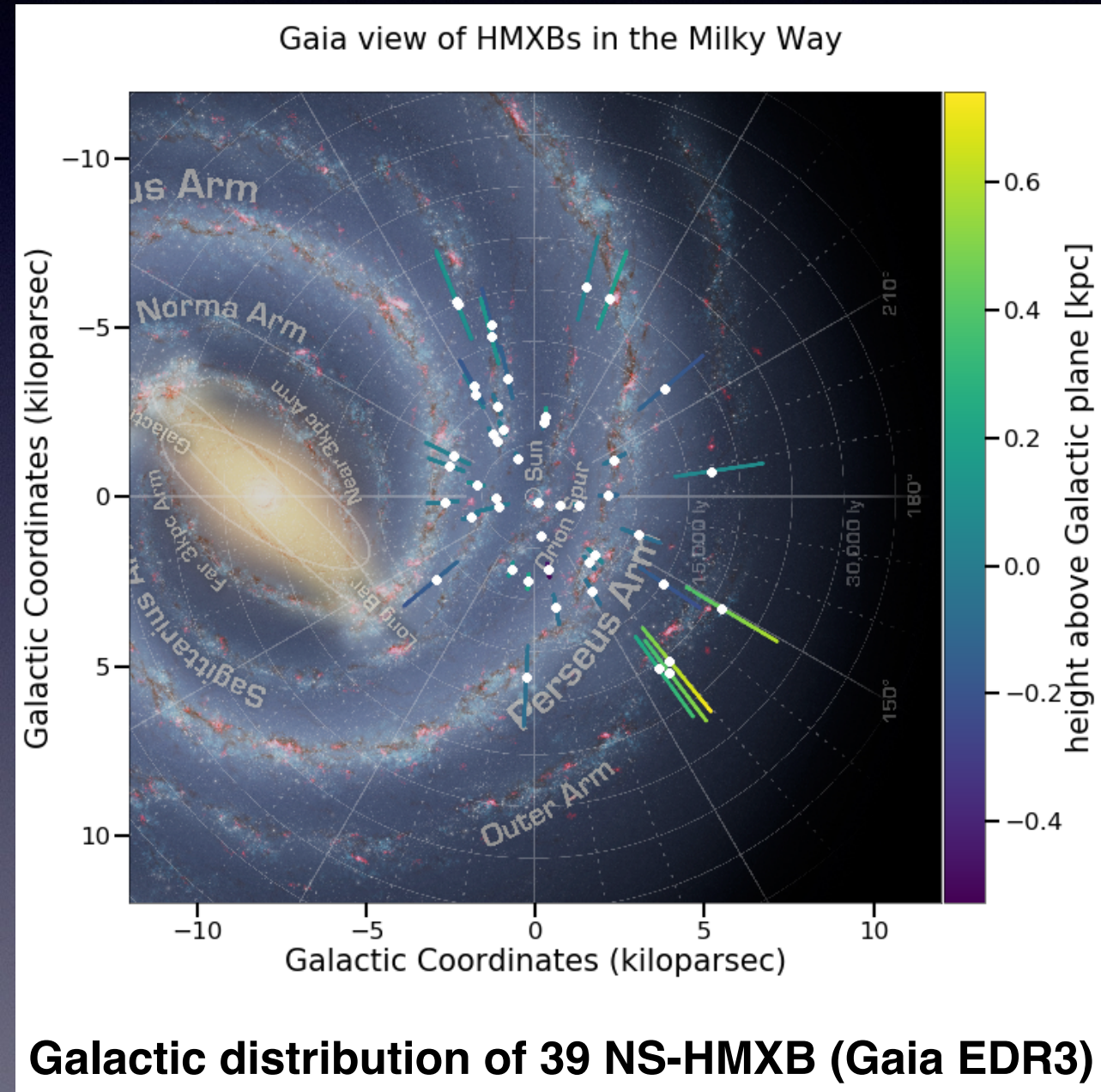
Fortin, Garcia, Chaty, Chassande Mottin, Simaz Bunzel, A&A subm.



# Galactic distribution & natal kick of HMXB



Gaia view of HMXBs in the Milky Way

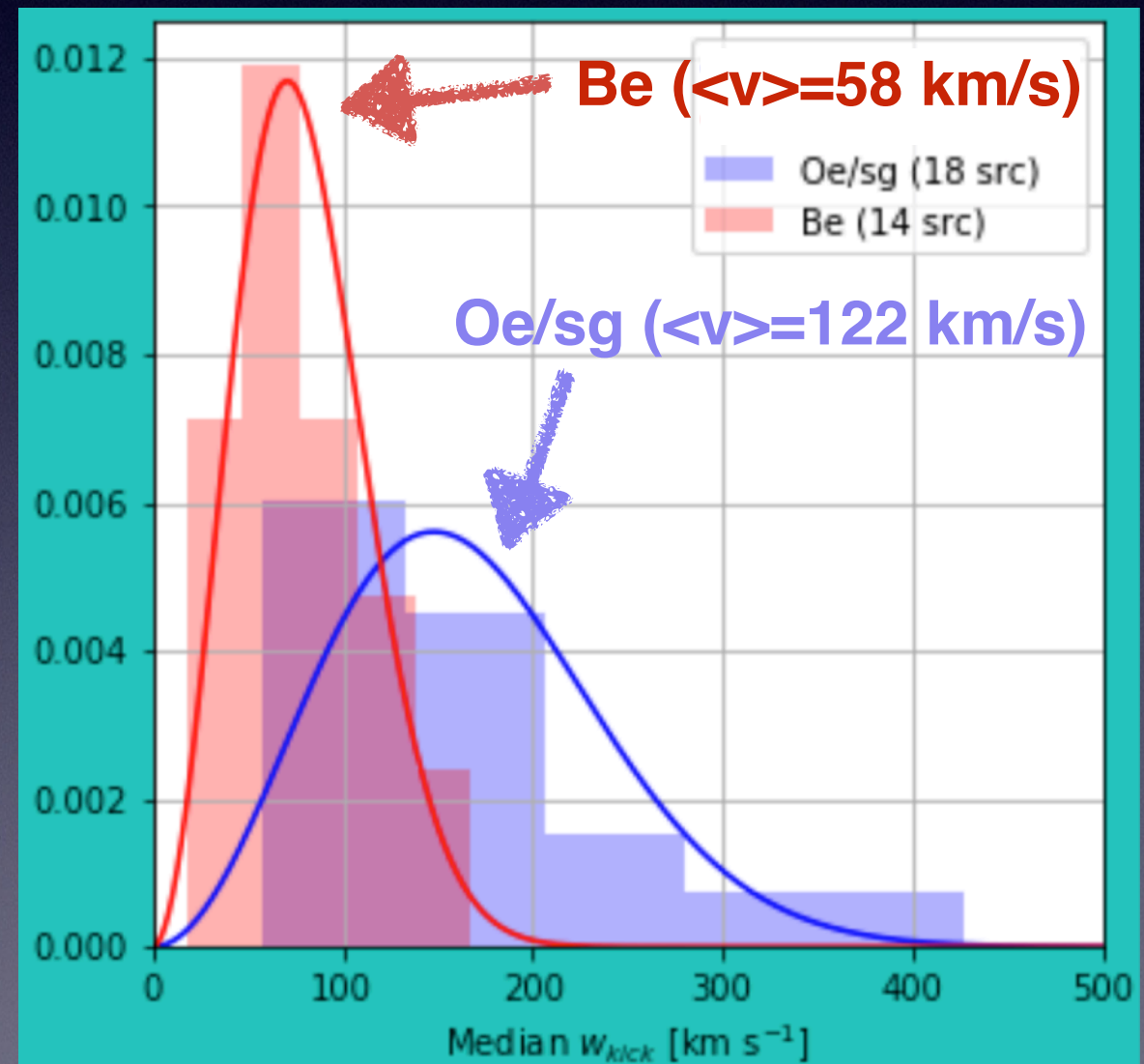
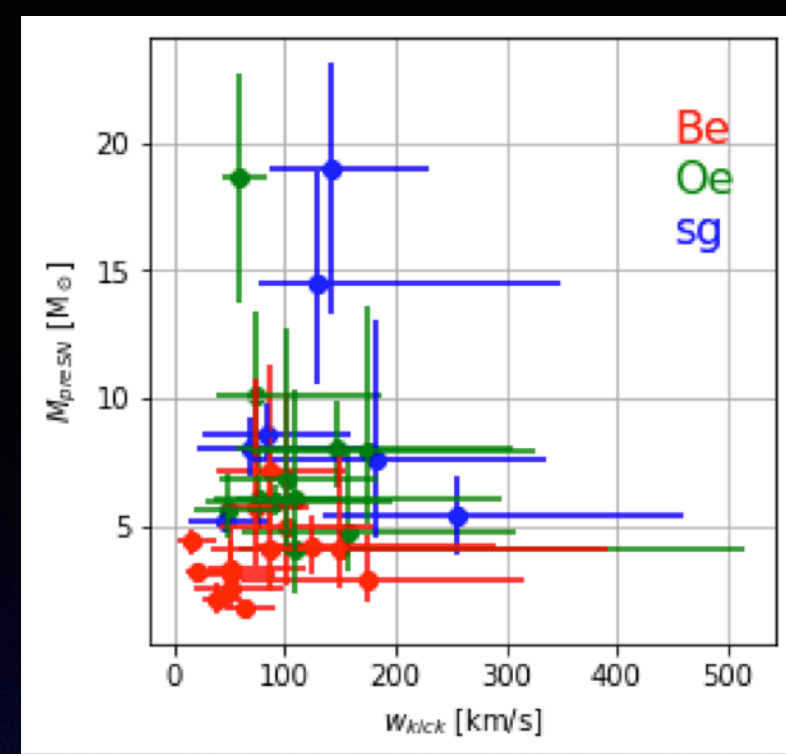


Galactic distribution of 39 NS-HMXB (Gaia EDR3)

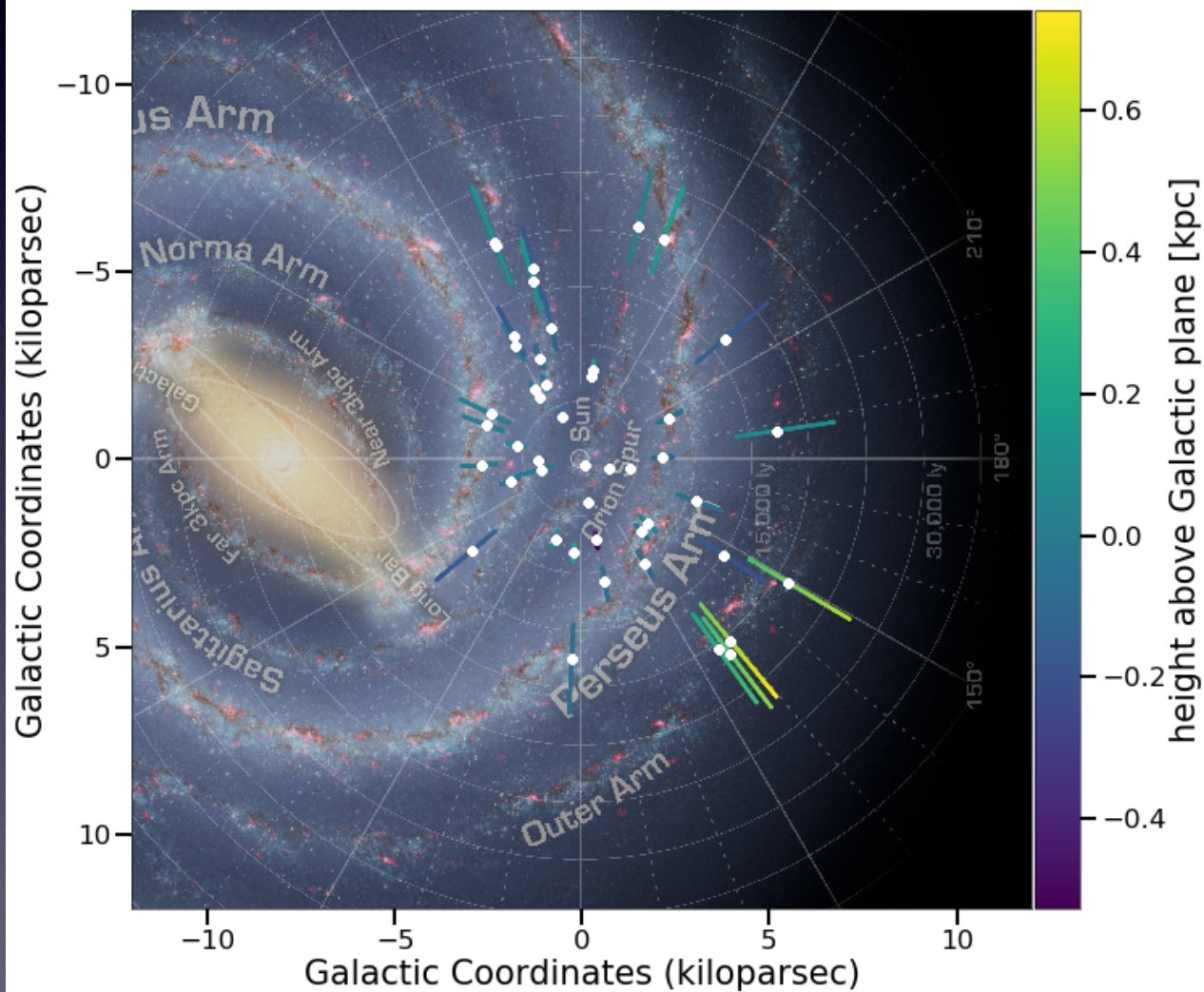
Fortin, Garcia, Chaty, Chassande Mottin, Simaz Bunzel, A&A subm.



# Galactic distribution & natal kick of HMXB



Gaia view of HMXBs in the Milky Way



Galactic distribution of 39 NS-HMXB (Gaia EDR3)

Fortin, Garcia, Chaty, Chassande Mottin, Simaz Bunzel, A&A subm.



# Accreting binaries

Name	BH mass [ $M_{\odot}$ ]	BH spin
M33 X-7	$15.65^{+1.45}_{-1.45}$	$0.84^{+0.05}_{-0.05}$
Cygnus X-1	$21.20^{+2.20}_{-2.20}$	$> 0.983$
LMC X-1	$10.90^{+1.40}_{-1.40}$	$0.92^{+0.05a}_{-0.07}$
Swift J1357.2-0933	$> 8.9$	–
XTE J1650-500	$< 7.3$	$0.79^{+0.01}_{-0.01}$
XTE J1118+480	$7.55^{+0.65}_{-0.65}$	–
XTE J1859+226 (V406 Vul)	$> 5.42$	–
SAX J1819.3-2525 (V4641 Sgr)	$6.40^{+0.60}_{-0.60}$	–
XTE J1550-564	$11.70^{+3.89}_{-3.89}$	$0.34^{+0.37b}_{-0.45}$
GRO J1655-40 (N. Sco 94)	$6.00^{+0.40}_{-0.40}$	$0.70^{+0.10c}_{-0.10}$
GRS 1009-45 (N. Vel 93)	$> 4.4$	–
GRS 1915+105	$12.00^{+2.00}_{-2.00}$	$0.88^{+0.06d}_{-0.13}$
GRO J0422+32	$8.50^{+6.50}_{-6.50}$	–
GRS 1124-684 (N. Mus 91)	$5.65^{+1.85}_{-1.85}$	$0.63^{+0.16}_{-0.19}$
GS 2023+338 (V404 Cyg)	$9.00^{+0.20}_{-0.60}$	$> 0.92$
GS 2000+251 (QZ Vul)	$7.15^{+1.65}_{-1.65}$	–
GS 1354-64 (BW Cir)	$> 6.9$	$> 0.98$
H 1705-250 (N. Oph 77)	$6.40^{+1.50}_{-1.50}$	–
3A0620-003	$6.60^{+0.30}_{-0.30}$	$0.12^{+0.19}_{-0.19}$
1H J1659-487 (GX 339-4)	$> 6.0$	$> 0.95$
4U 1543-475 (IL Lup)	$9.40^{+1.00}_{-1.00}$	$0.67^{+0.15e}_{-0.08}$
GRS 1716-249	$6.45^{+1.55}_{-1.55}$	$> 0.92$
LMC X-3	$6.98^{+0.56}_{-0.56}$	$0.25^{+0.20}_{-0.29}$
XTE J1652-453	–	$0.45^{+0.02}_{-0.02}$
XTE J1752-223	–	$0.92^{+0.06}_{-0.06}$
Swift J1910.2-0546	–	$> 0.32$
MAXI J1836-194	–	$0.88^{+0.03}_{-0.03}$
XTE J1908+094	–	$0.75^{+0.09}_{-0.09}$
Swift J1753.5-0127	–	$0.76^{+0.11}_{-0.15}$
4U 1630-472	–	$> 0.97$
SAX J1711.6-3808	–	$0.60^{+0.20}_{-0.40}$
EXO 1846-031	–	$> 0.99$



# Accreting binaries

All stellar mass BH  
of our galaxy have  
 $5 \leq M_{\text{BH}} \leq 21 M_{\odot}$

Name	BH mass [ $M_{\odot}$ ]	BH spin
M33 X-7	$15.65^{+1.45}_{-1.45}$	$0.84^{+0.05}_{-0.05}$
Cygnus X-1	$21.20^{+2.20}_{-2.20}$	$> 0.983$
LMC X-1	$10.90^{+1.40}_{-1.40}$	$0.92^{+0.05\text{a}}_{-0.07}$
Swift J1357.2-0933	$> 8.9$	—
XTE J1650-500	$< 7.3$	$0.79^{+0.01}_{-0.01}$
XTE J1118+480	$7.55^{+0.65}_{-0.65}$	—
XTE J1859+226 (V406 Vul)	$> 5.42$	—
SAX J1819.3-2525 (V4641 Sgr)	$6.40^{+0.60}_{-0.60}$	—
XTE J1550-564	$11.70^{+3.89}_{-3.89}$	$0.34^{+0.37\text{b}}_{-0.45}$
GRO J1655-40 (N. Sco 94)	$6.00^{+0.40}_{-0.40}$	$0.70^{+0.10\text{c}}_{-0.10}$
GRS 1009-45 (N. Vel 93)	$> 4.4$	—
GRS 1915+105	$12.00^{+2.00}_{-2.00}$	$0.88^{+0.06\text{d}}_{-0.13}$
GRO J0422+32	$8.50^{+6.50}_{-6.50}$	—
GRS 1124-684 (N. Mus 91)	$5.65^{+1.85}_{-1.85}$	$0.63^{+0.16}_{-0.19}$
GS 2023+338 (V404 Cyg)	$9.00^{+0.20}_{-0.60}$	$> 0.92$
GS 2000+251 (QZ Vul)	$7.15^{+1.65}_{-1.65}$	—
GS 1354-64 (BW Cir)	$> 6.9$	$> 0.98$
H 1705-250 (N. Oph 77)	$6.40^{+1.50}_{-1.50}$	—
3A0620-003	$6.60^{+0.30}_{-0.30}$	$0.12^{+0.19}_{-0.19}$
1H J1659-487 (GX 339-4)	$> 6.0$	$> 0.95$
4U 1543-475 (IL Lup)	$9.40^{+1.00}_{-1.00}$	$0.67^{+0.15\text{e}}_{-0.08}$
GRS 1716-249	$6.45^{+1.55}_{-1.55}$	$> 0.92$
LMC X-3	$6.98^{+0.56}_{-0.56}$	$0.25^{+0.20}_{-0.29}$
XTE J1652-453	—	$0.45^{+0.02}_{-0.02}$
XTE J1752-223	—	$0.92^{+0.06}_{-0.06}$
Swift J1910.2-0546	—	$> 0.32$
MAXI J1836-194	—	$0.88^{+0.03}_{-0.03}$
XTE J1908+094	—	$0.75^{+0.09}_{-0.09}$
Swift J1753.5-0127	—	$0.76^{+0.11}_{-0.15}$
4U 1630-472	—	$> 0.97$
SAX J1711.6-3808	—	$0.60^{+0.20}_{-0.40}$
EXO 1846-031	—	$> 0.99$





# Binary evolution



# Binary evolution

- Binaries form and evolve... until eventually they merge...



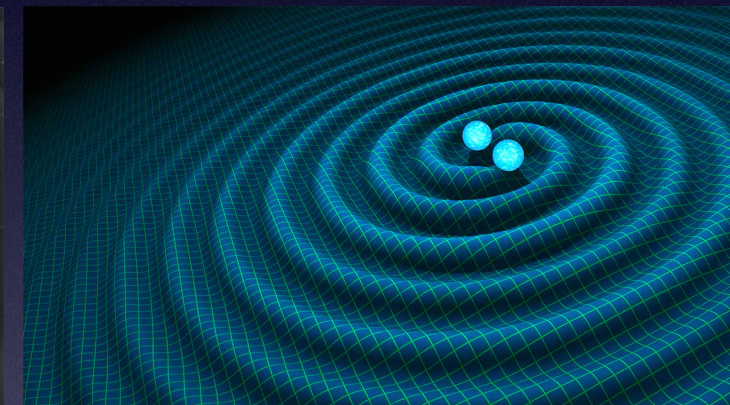


# Binary evolution

- Binaries form and evolve... until eventually they merge...
- ... leading to the emission of gravitational waves (GW), detected by LIGO-Virgo-KAGRA collaboration



• BBH



• BNS

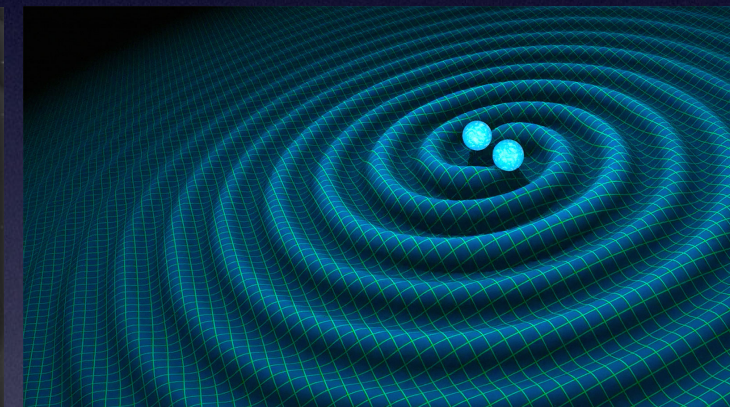


# Binary evolution

- Binaries form and evolve... until eventually they merge...
- ... leading to the emission of gravitational waves (GW), detected by LIGO-Virgo-KAGRA collaboration
- The tip of the iceberg?
- « Today's binaries might be tomorrow's GW! »



• BBH



• BNS



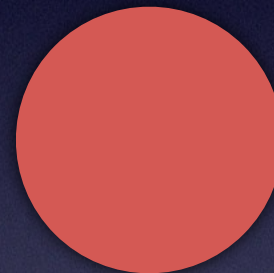




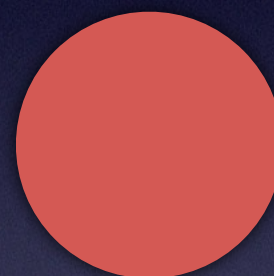




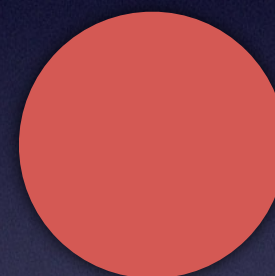
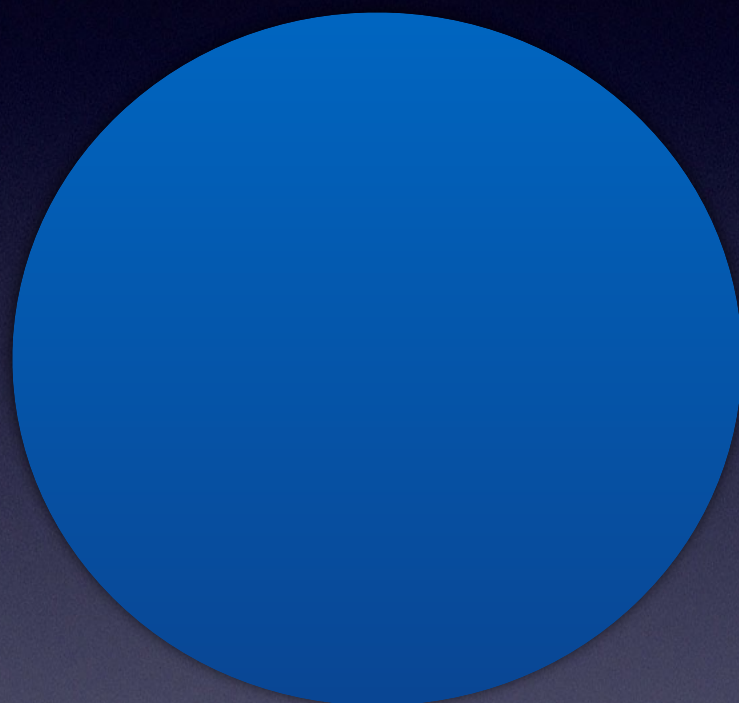




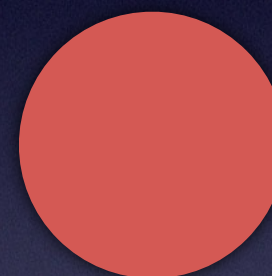
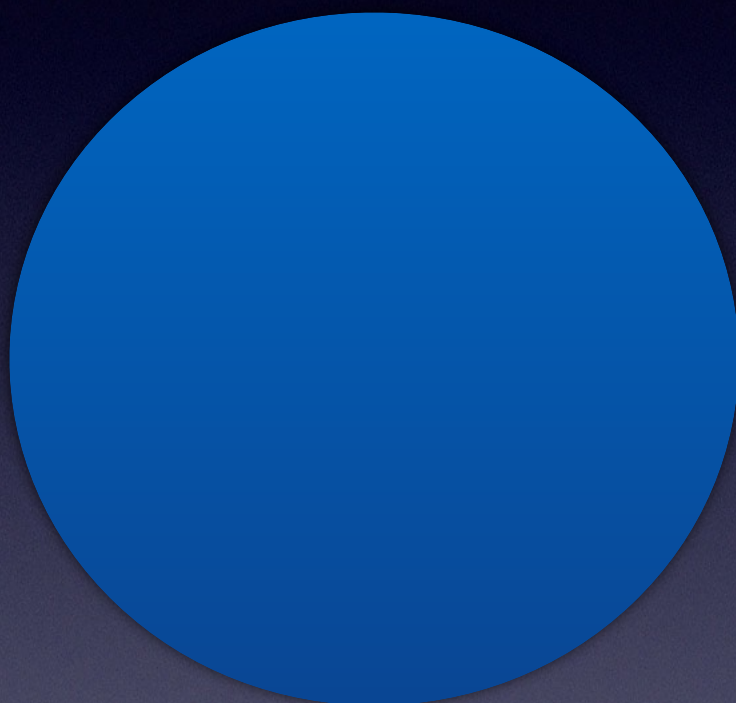
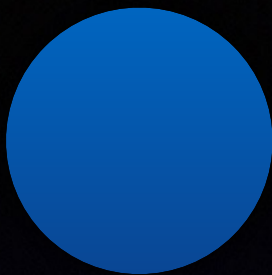




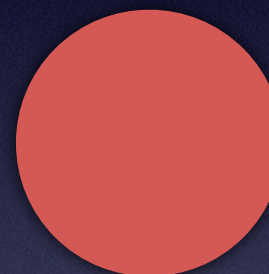
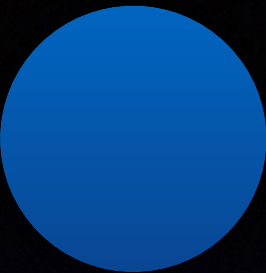




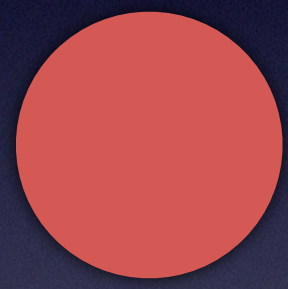
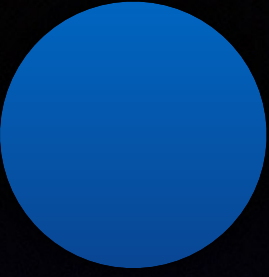
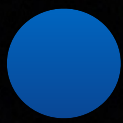




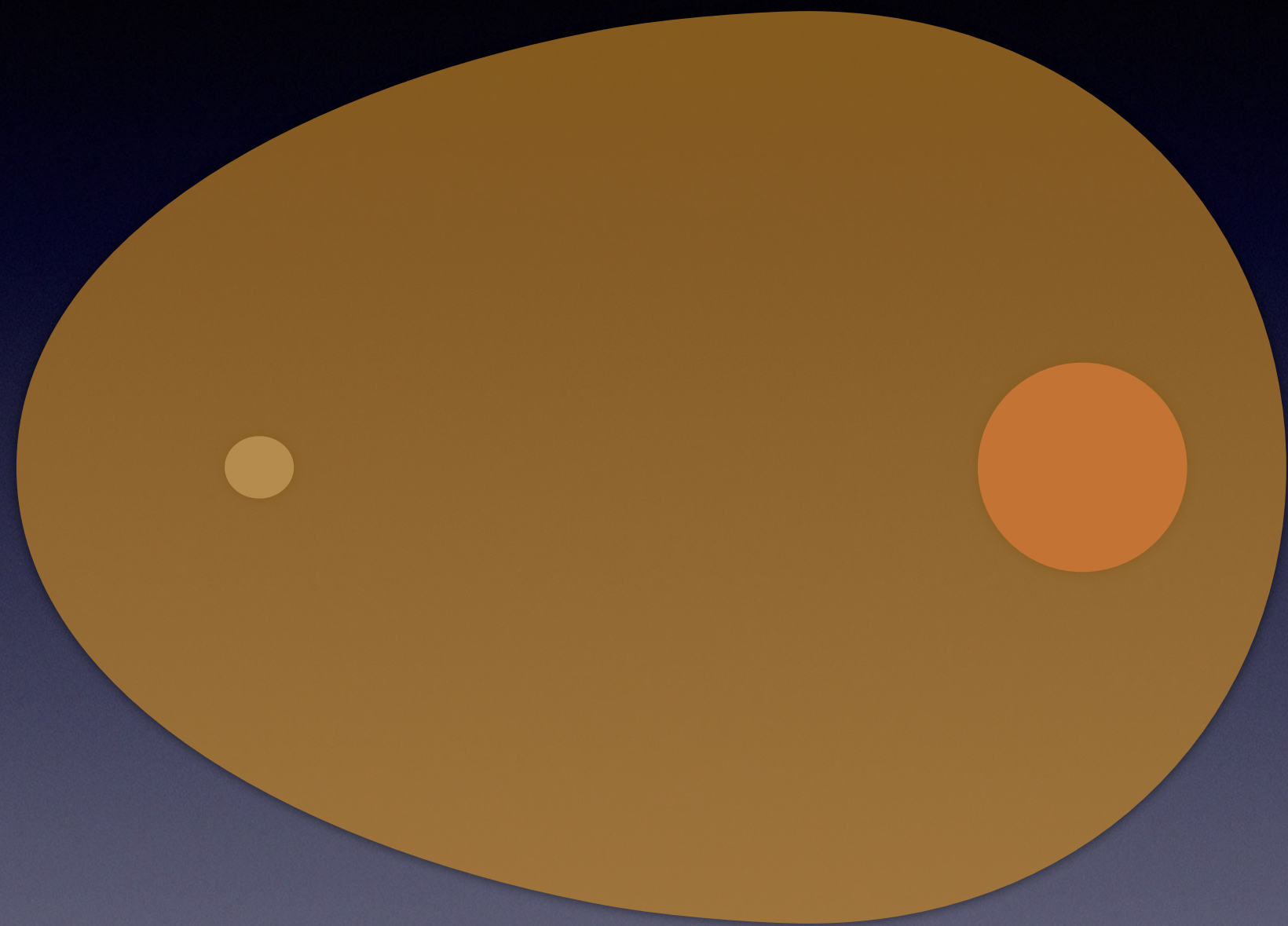
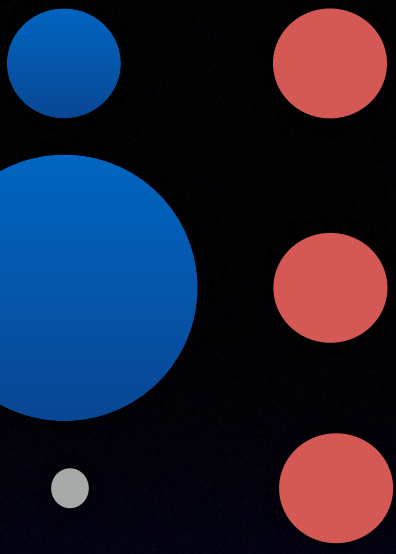




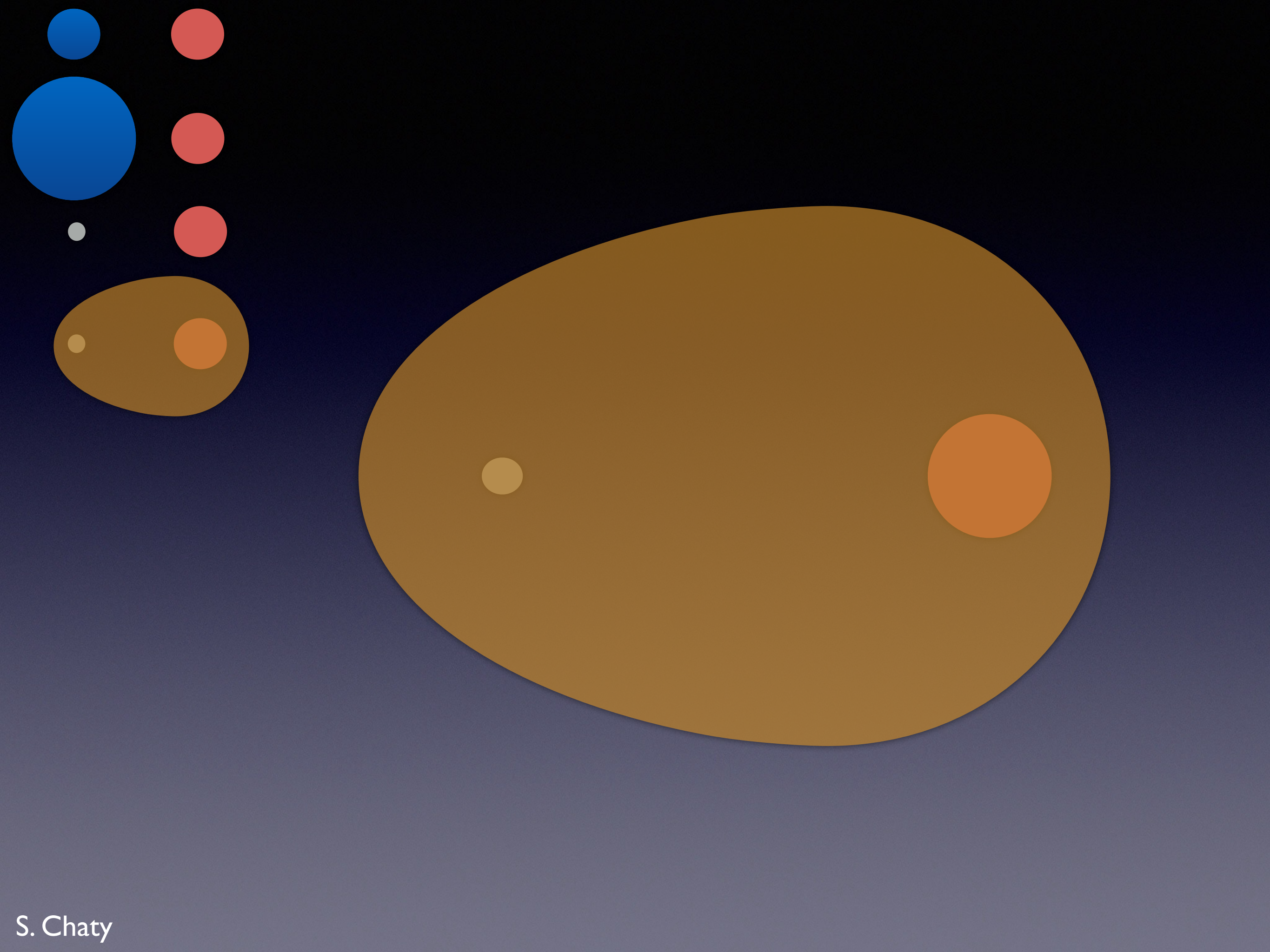




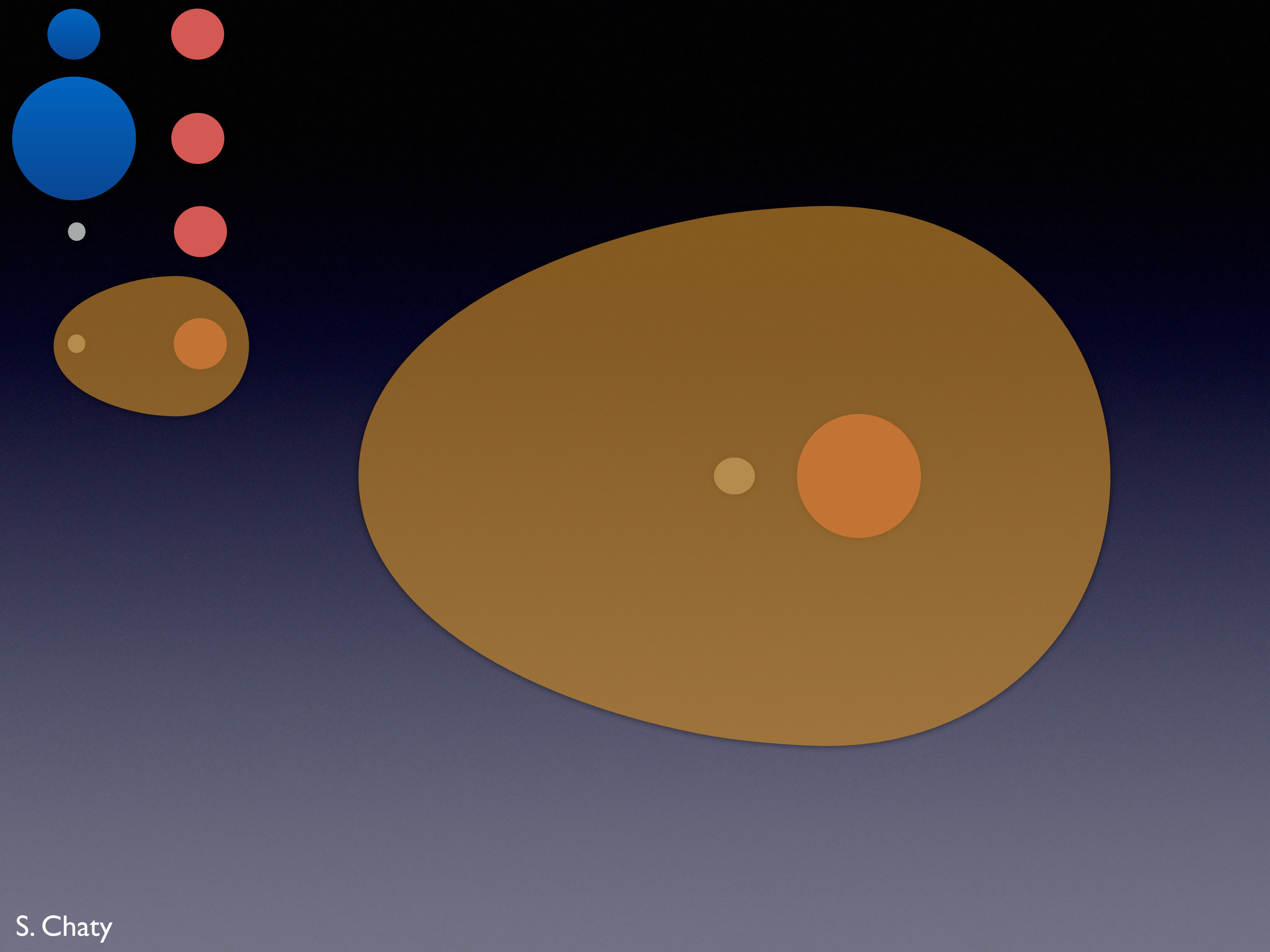




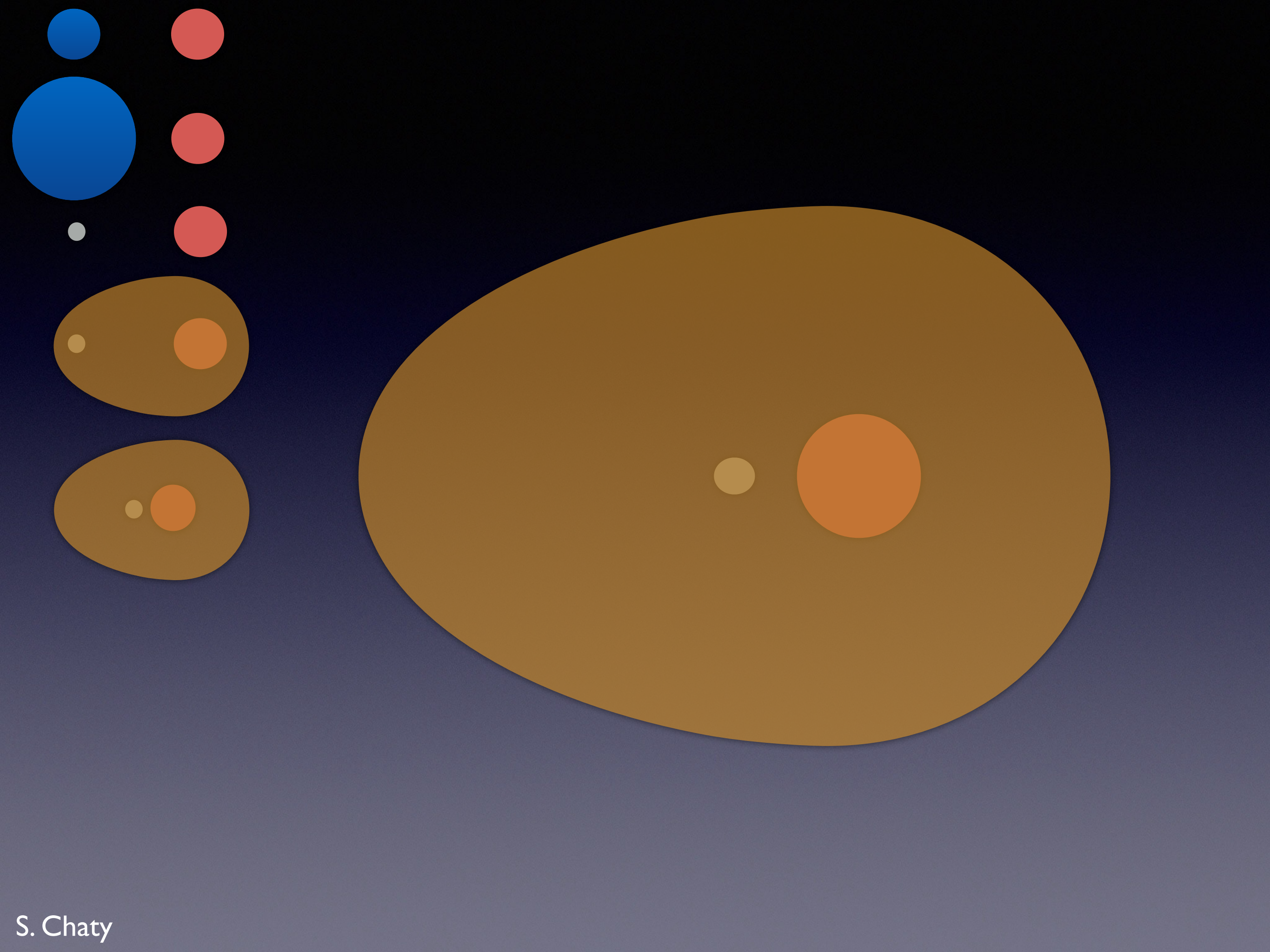




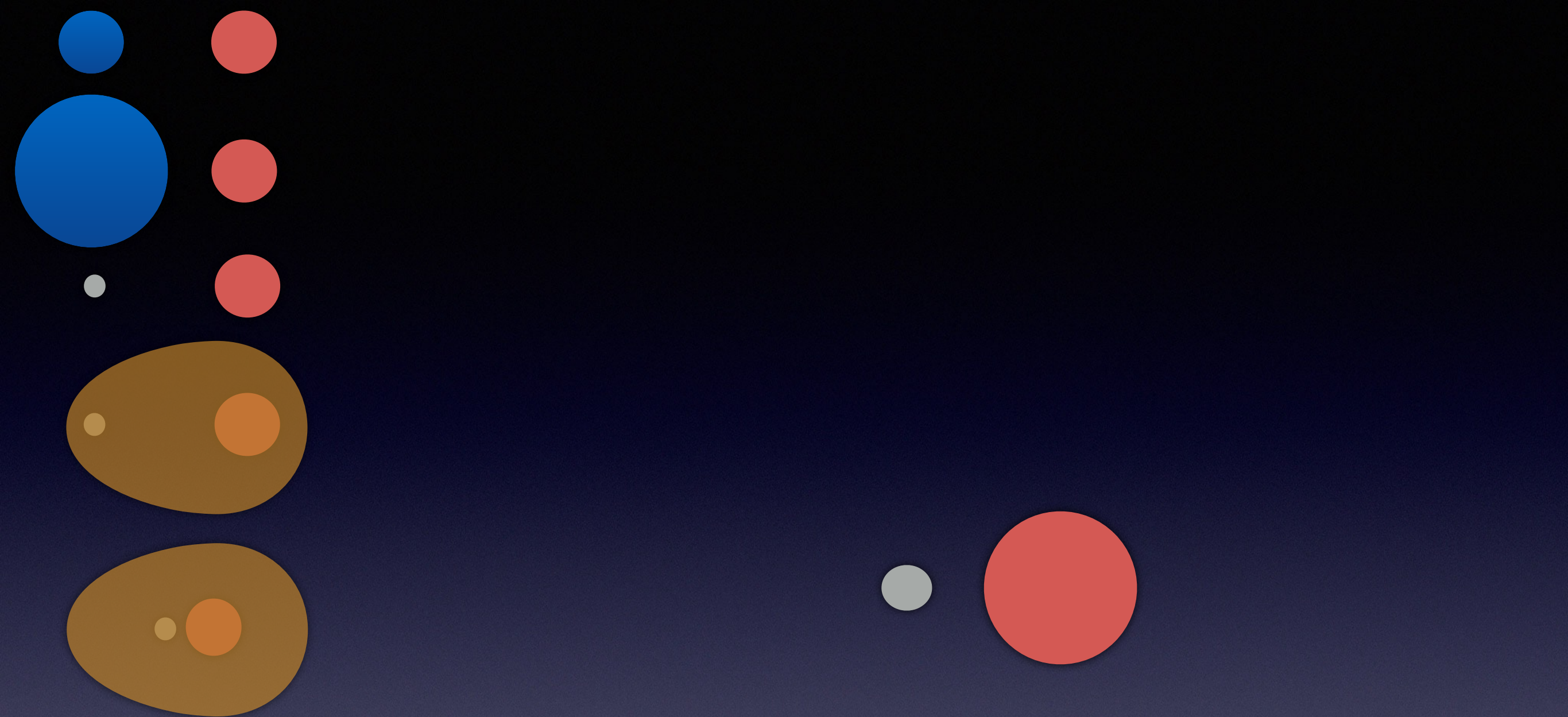




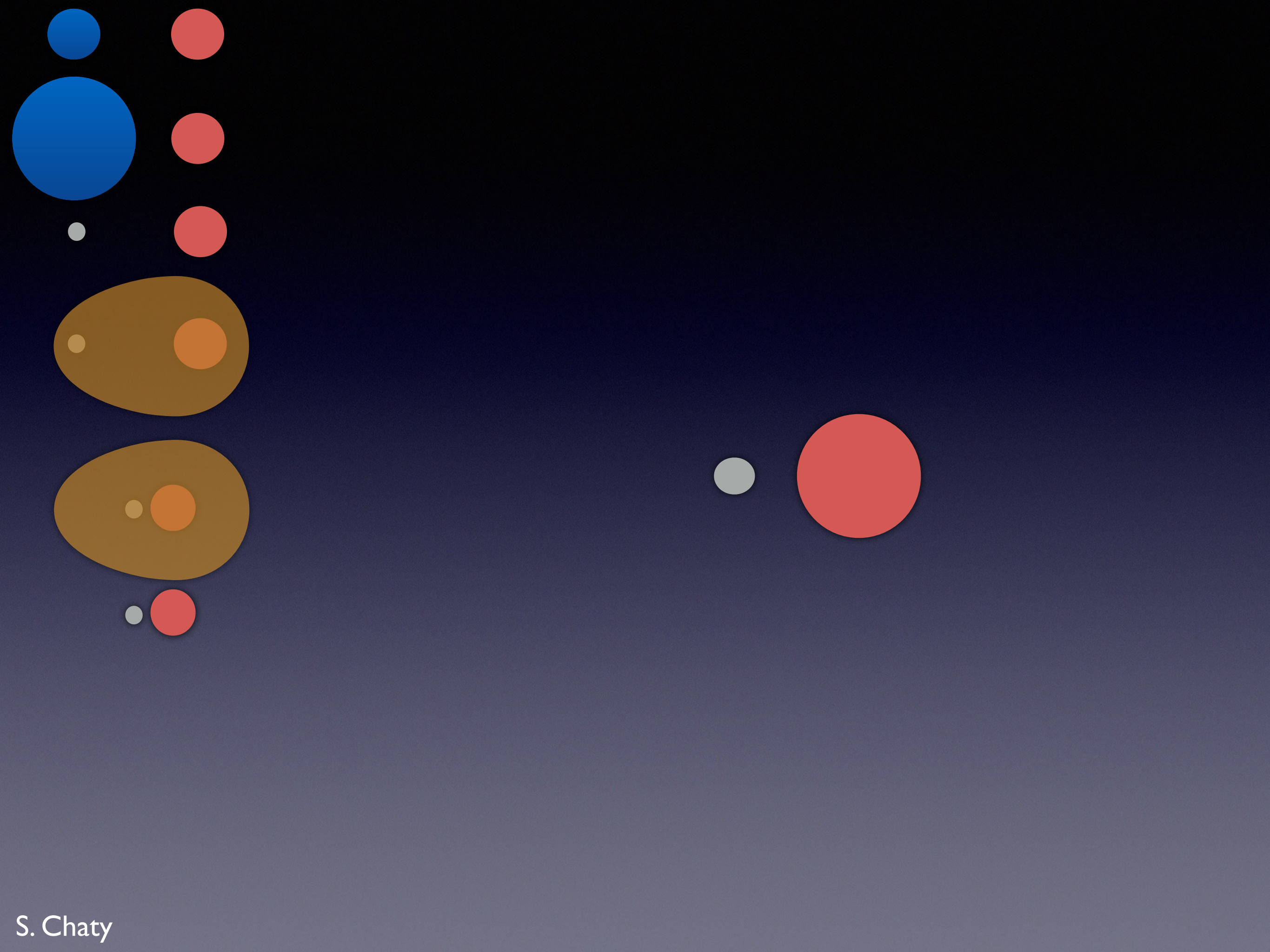




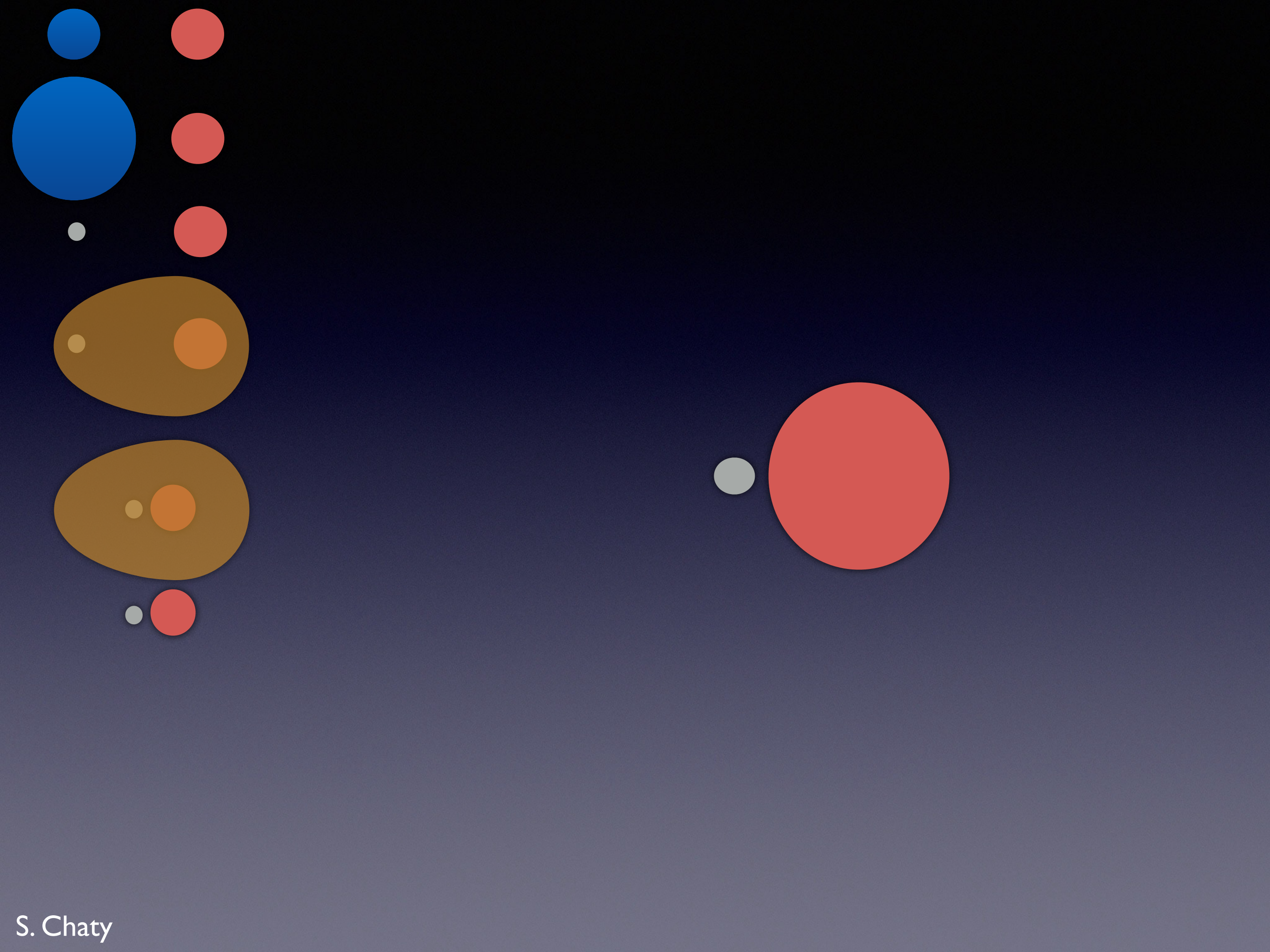




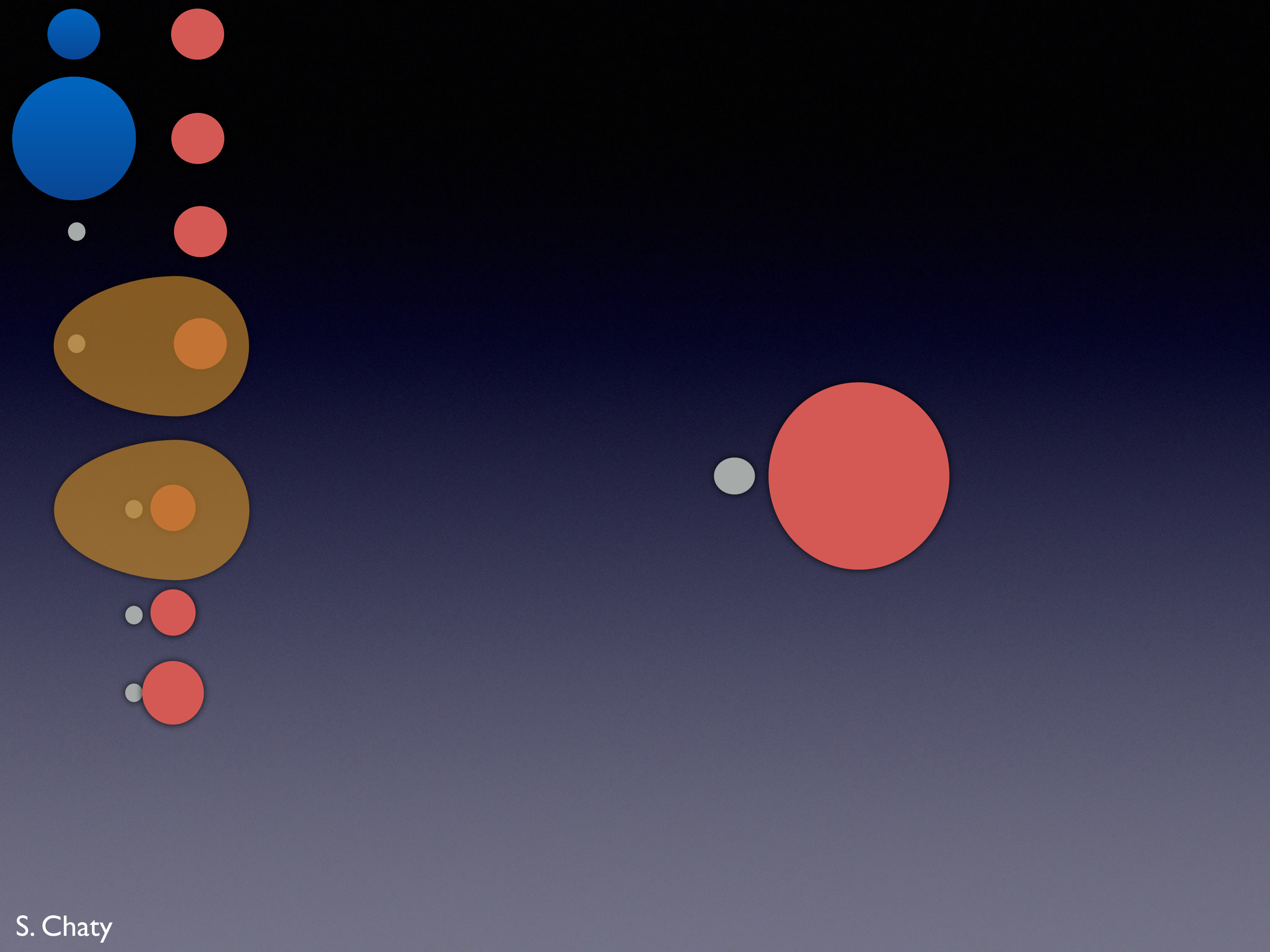




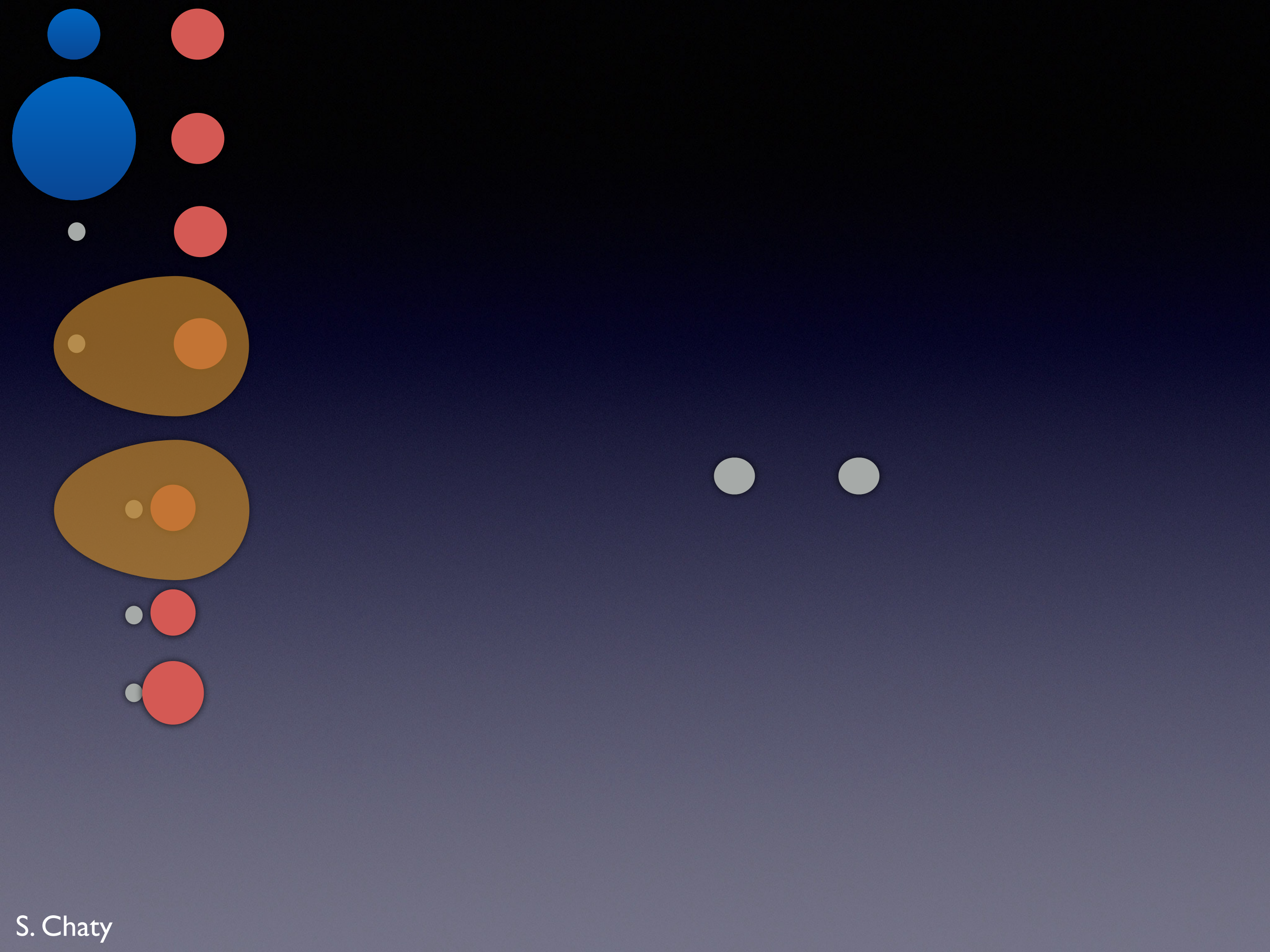




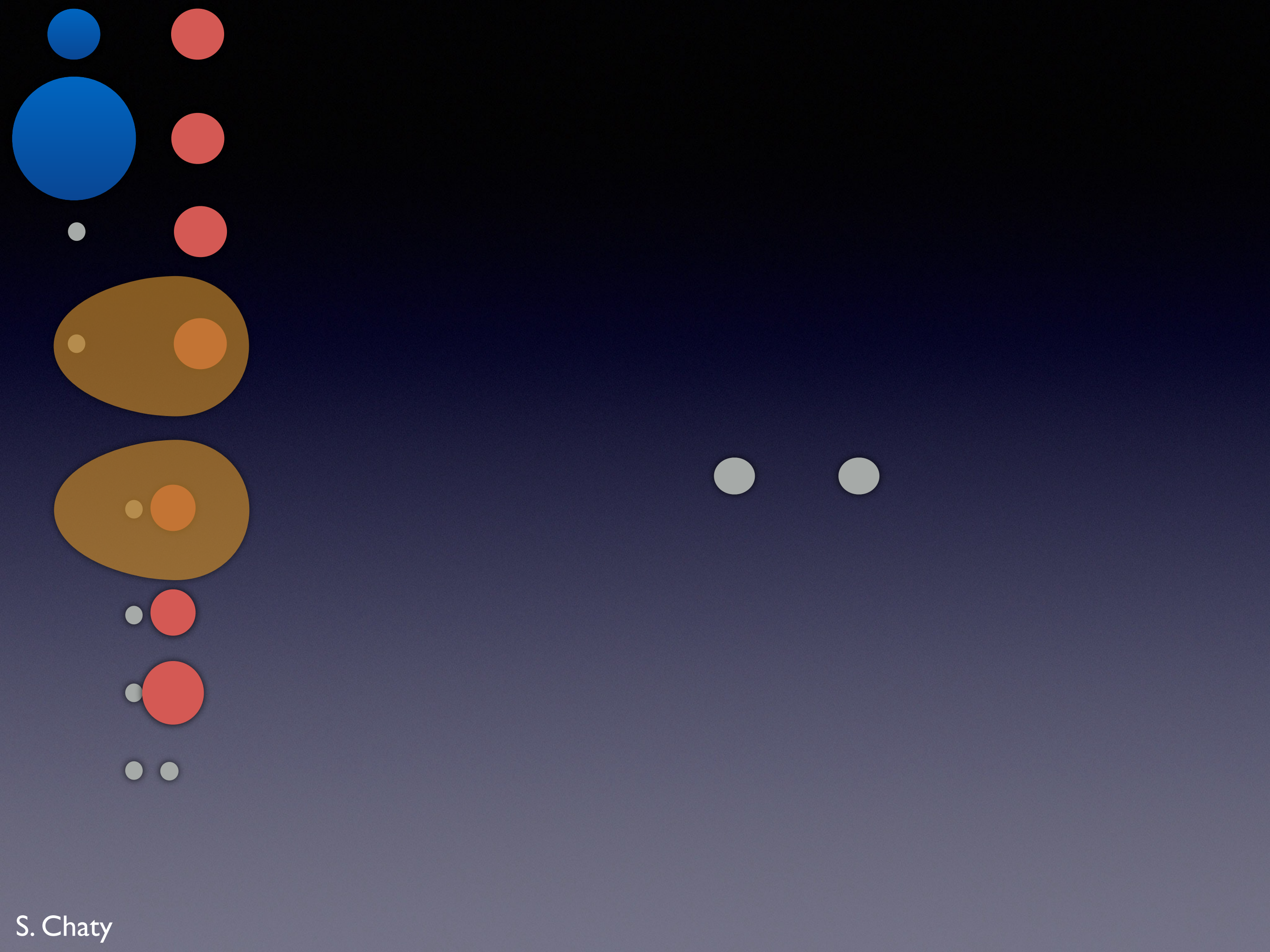




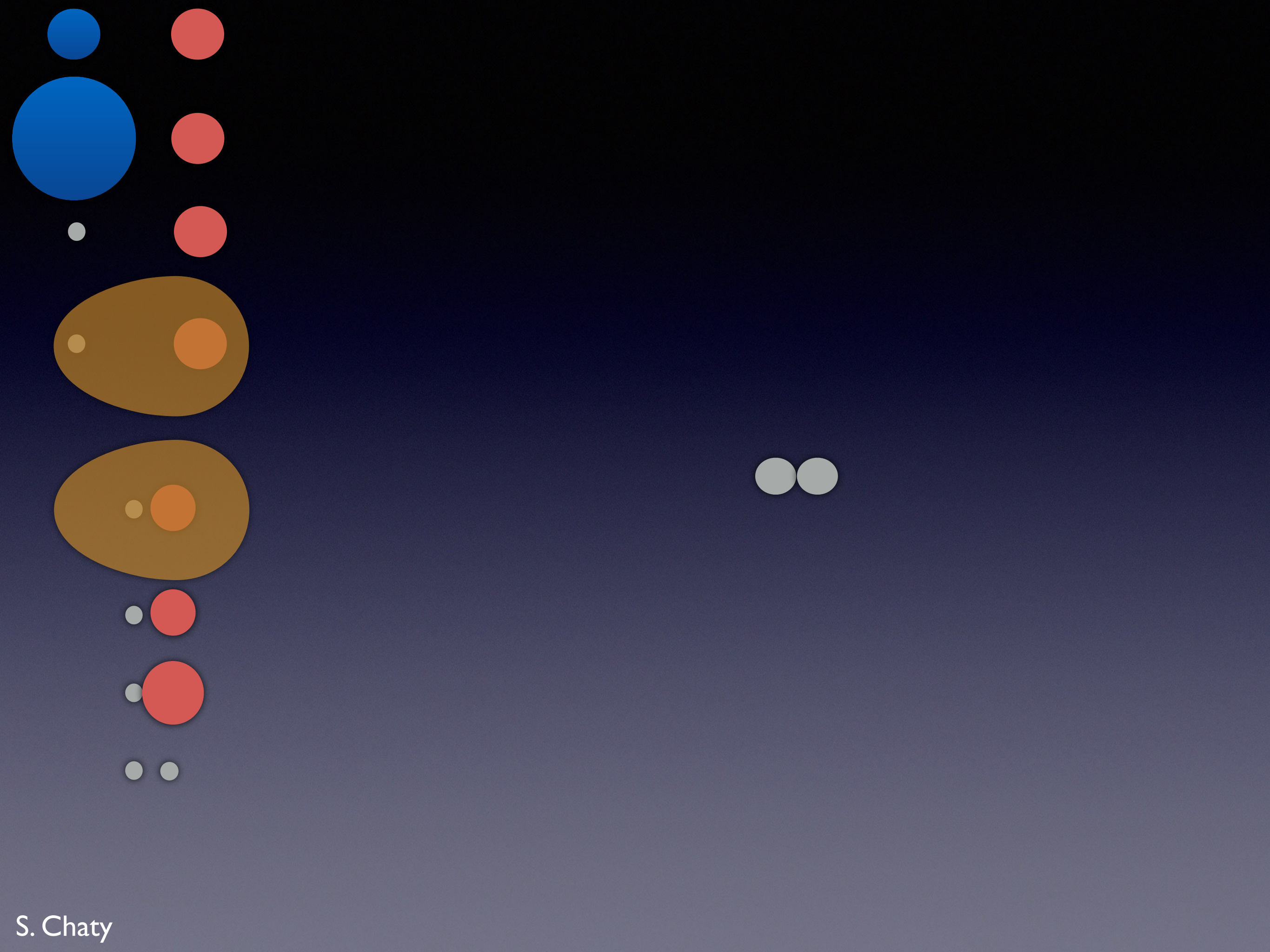




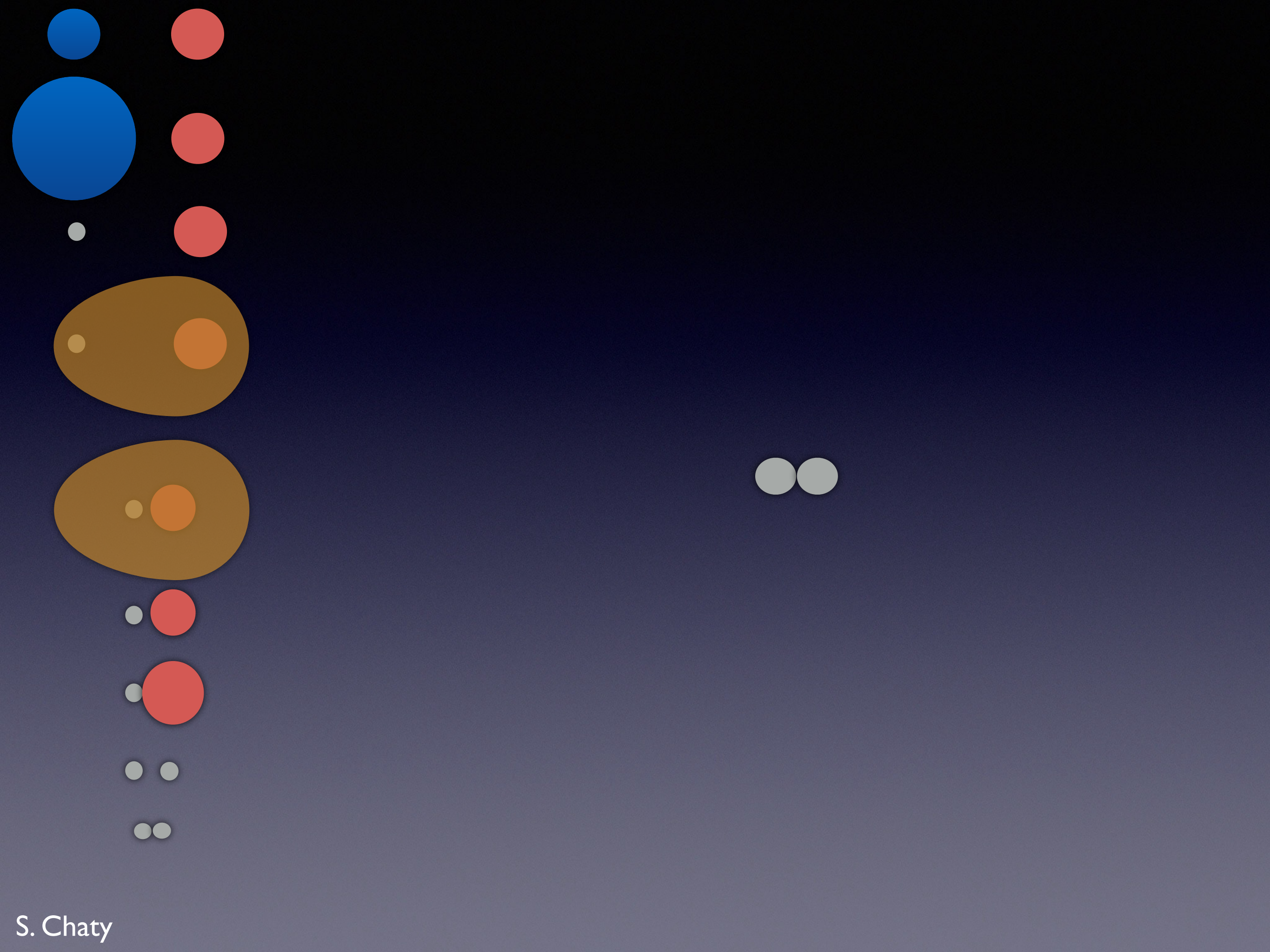




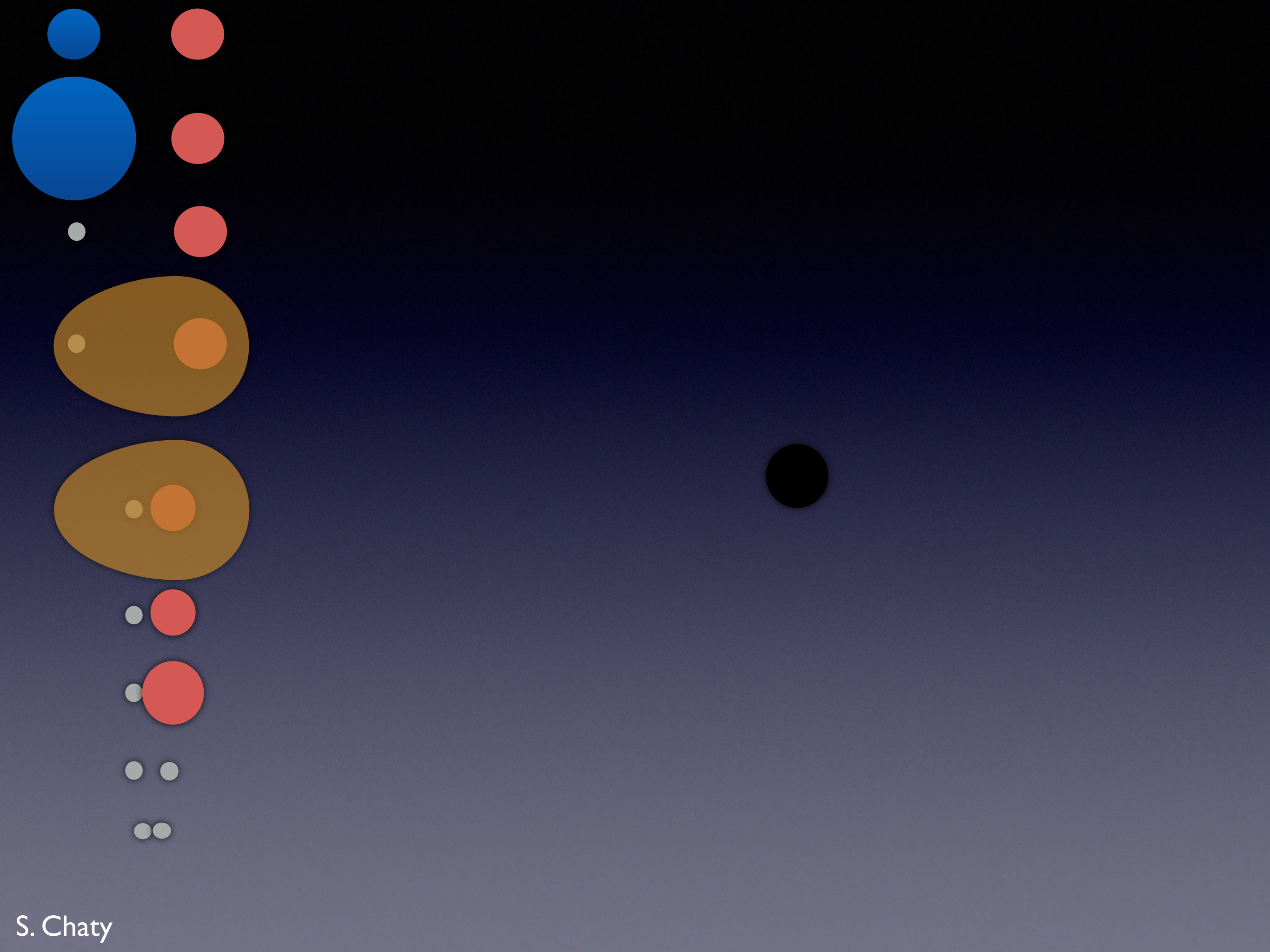




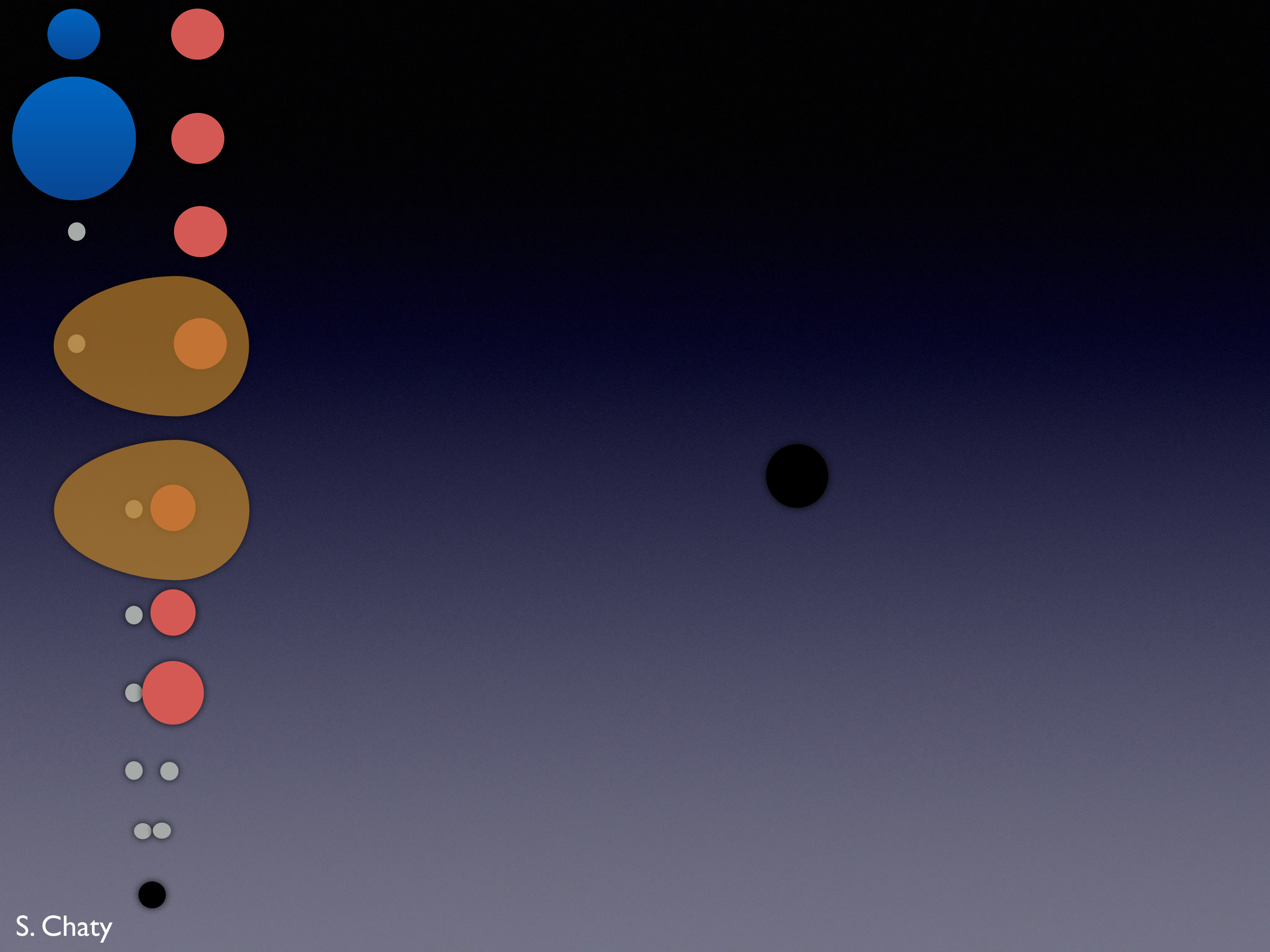














**Question 1:**  
To be or not to be  
a merger progenitor?



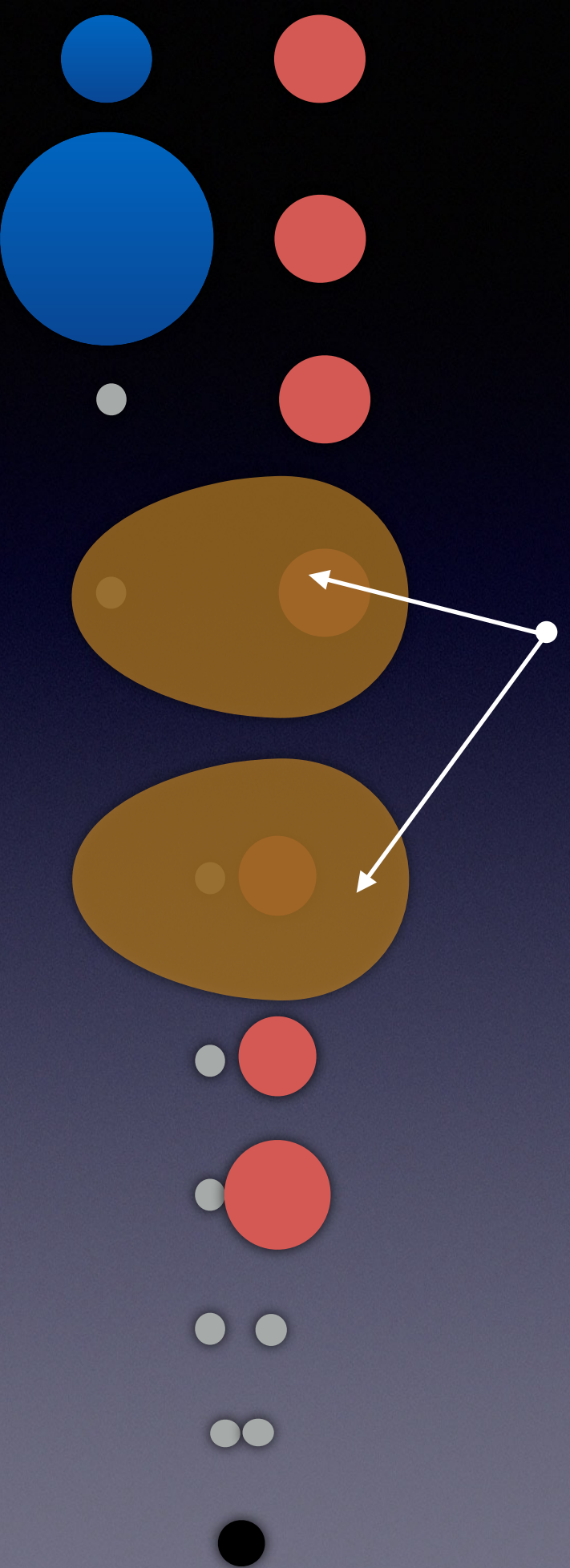


# Question 1:

To be or not to be  
a merger progenitor?



Common envelope: has to be ejected,  
or the couple merge during this phase



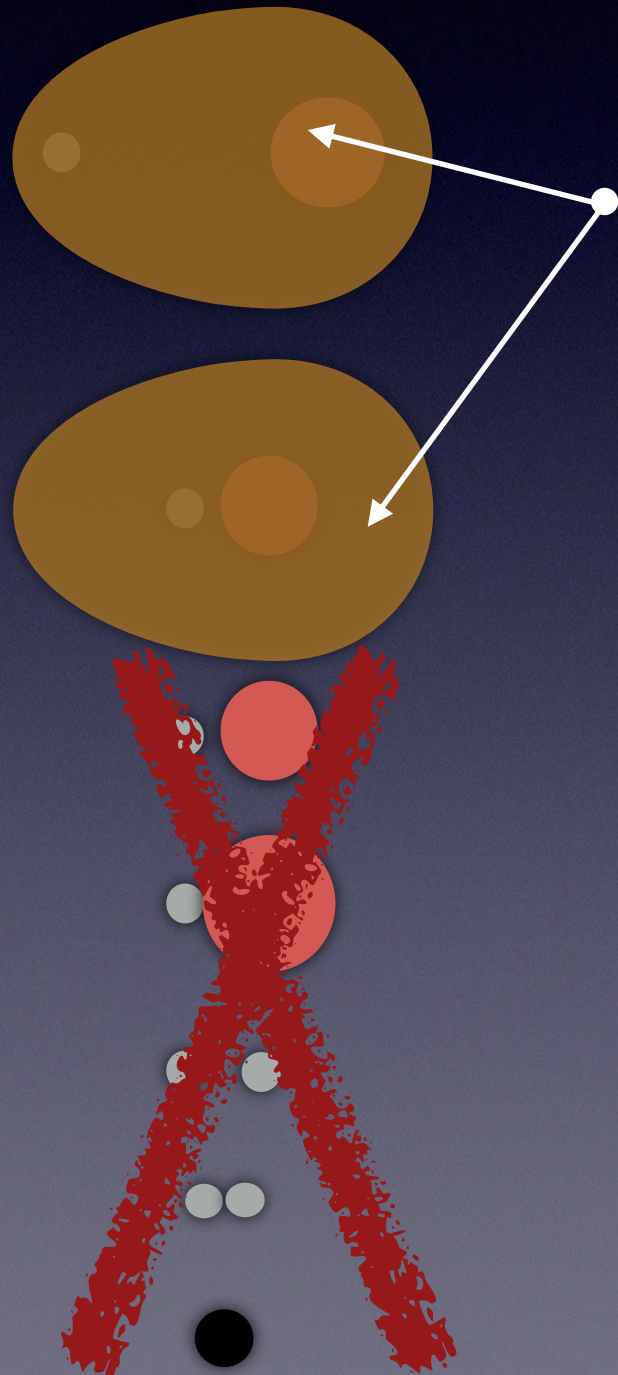


# Question 1:

To be or not to be  
a merger progenitor?



Common envelope: has to be ejected,  
or the couple merge during this phase







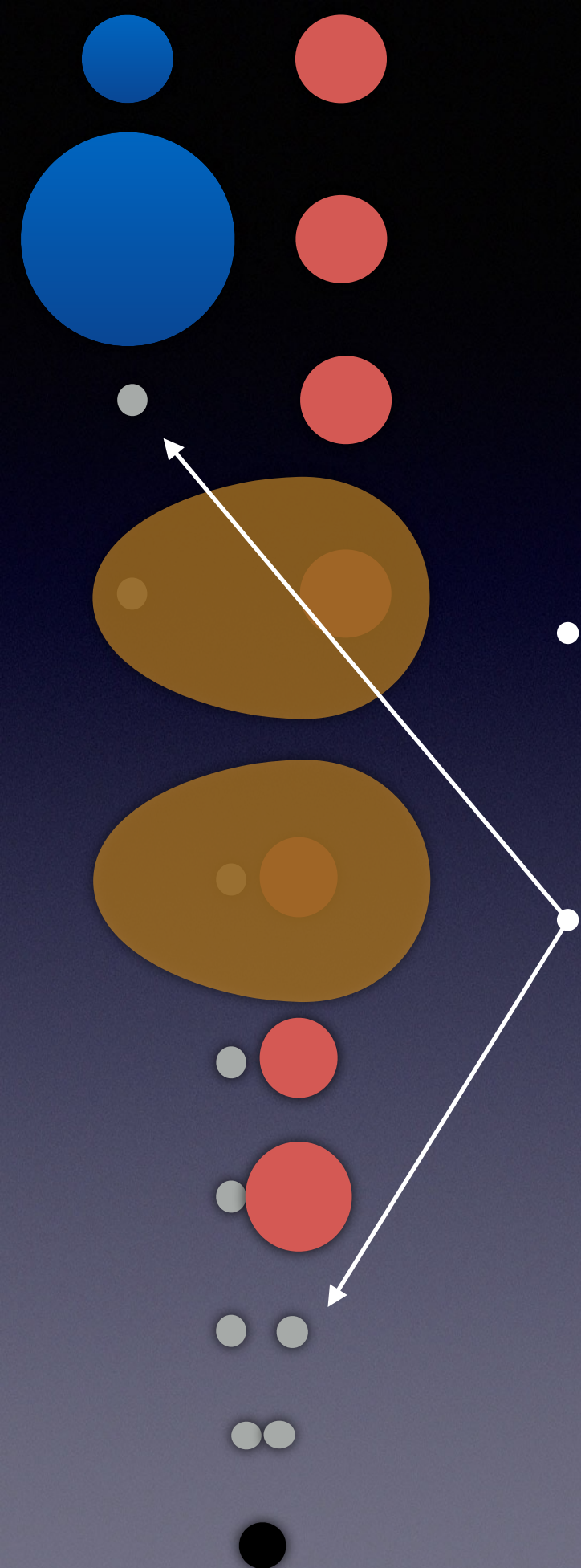


# Question 1:

To be or not to be  
a merger progenitor?



- Common envelope: has to be ejected, or the couple merge during this phase
- Natal kick: has to be low (vs  $M$ ,  $q$ ,  $a$ ), or the couple is unbound



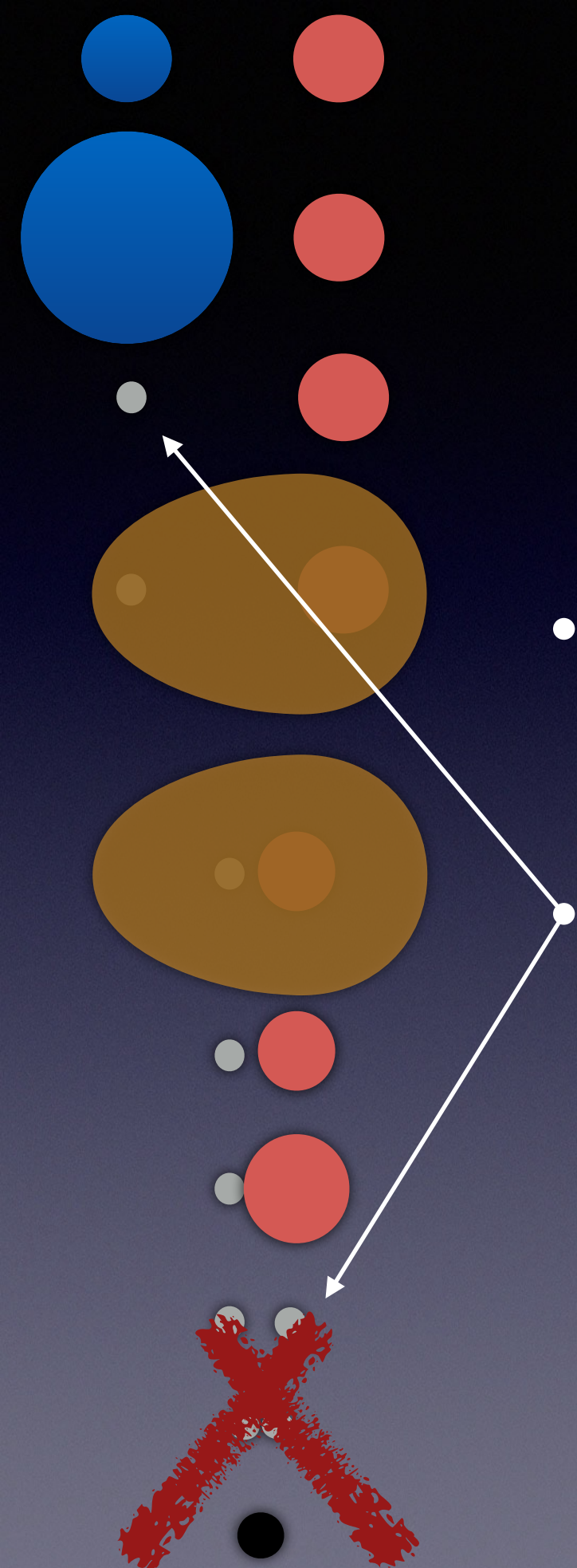


# Question 1:

To be or not to be  
a merger progenitor?



- Common envelope: has to be ejected, or the couple merge during this phase
- Natal kick: has to be low (vs  $M$ ,  $q$ ,  $a$ ), or the couple is unbound



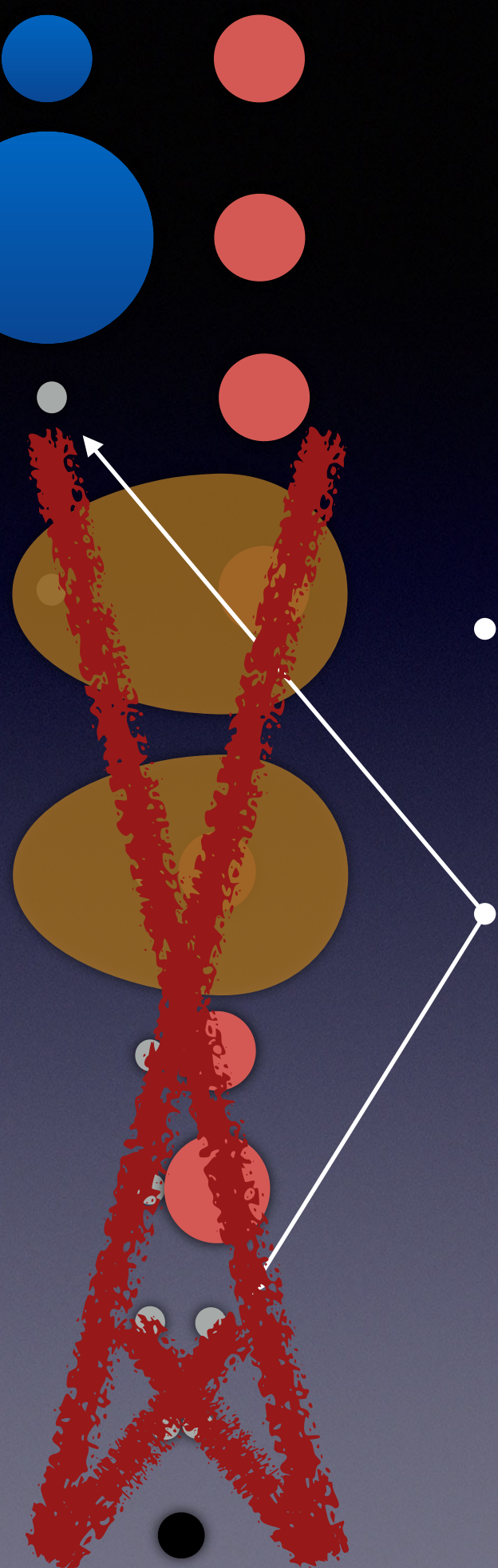


# Question 1:

To be or not to be  
a merger progenitor?



- Common envelope: has to be ejected, or the couple merge during this phase
- Natal kick: has to be low (vs  $M$ ,  $q$ ,  $a$ ), or the couple is unbound





# Question 1:

To be or not to be  
a merger progenitor?



- Common envelope: has to be ejected, or the couple merge during this phase
- Natal kick: has to be low (vs  $M$ ,  $q$ ,  $a$ ), or the couple is unbound



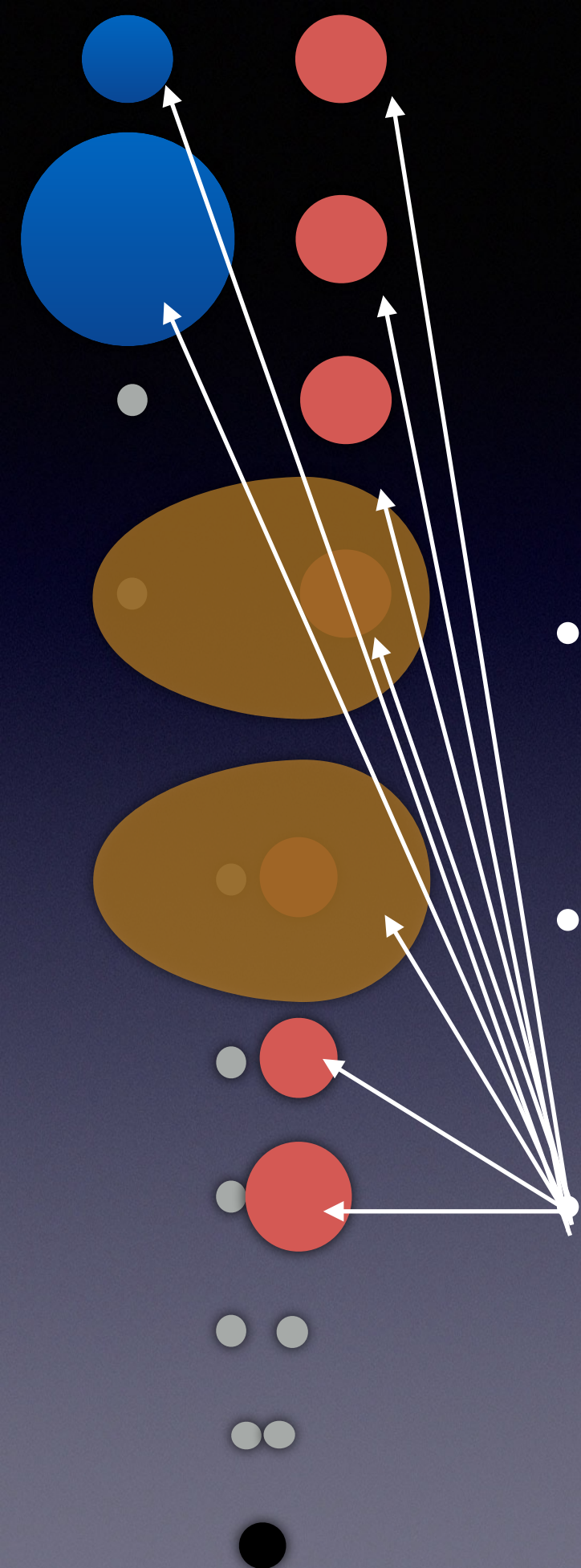
# Question 1:

To be or not to be  
a merger progenitor?



- Common envelope: has to be ejected, or the couple merge during this phase
- Natal kick: has to be low (vs  $M$ ,  $q$ ,  $a$ ), or the couple is unbound

Metallicity: has to be low to form massive final black hole





# Question 1:

To be or not to be  
a merger progenitor?



- Common envelope: has to be ejected, or the couple merge during this phase
- Natal kick: has to be low (vs  $M$ ,  $q$ ,  $a$ ), or the couple is unbound
- Metallicity: has to be low to form massive final black hole



# Question 1:

To be or not to be  
a merger progenitor?



- Common envelope: has to be ejected, or the couple merge during this phase
- Natal kick: has to be low (vs  $M$ ,  $q$ ,  $a$ ), or the couple is unbound
- Metallicity: has to be low to form massive final black hole

A good candidate to merger progenitor!



# Question 2:

To form or not to form  
a stellar couple?





## Question 2:

To form or not to form  
a stellar couple?



- Isolated binary evolution (« in the field »)



## Question 2:

To form or not to form  
a stellar couple?

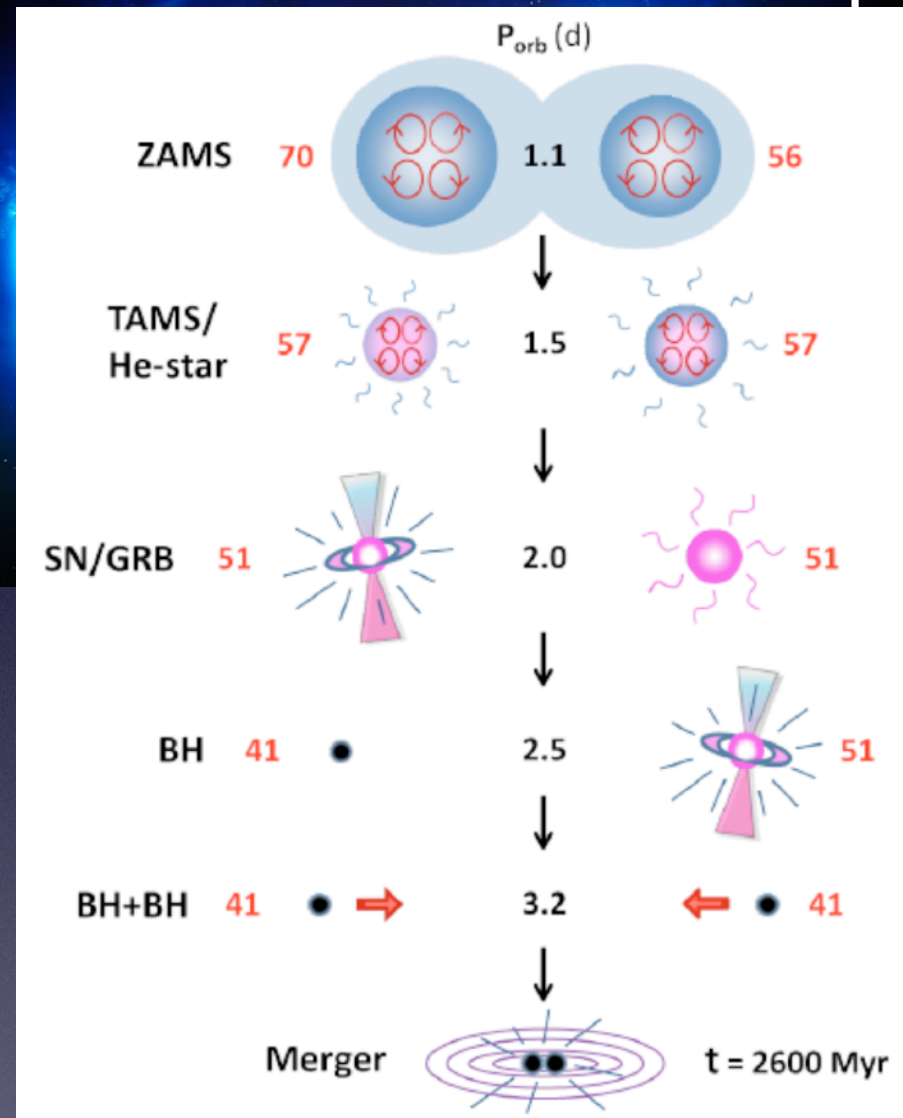


- Isolated binary evolution (« in the field »)
- Chemical Homogeneous Evolution (CHE)



# Question 2:

To form or not to form  
a stellar couple?



- Evolution (« in the field »)
- Chemical Homogeneous Evolution (CHE)



## Question 2:

To form or not to form  
a stellar couple?

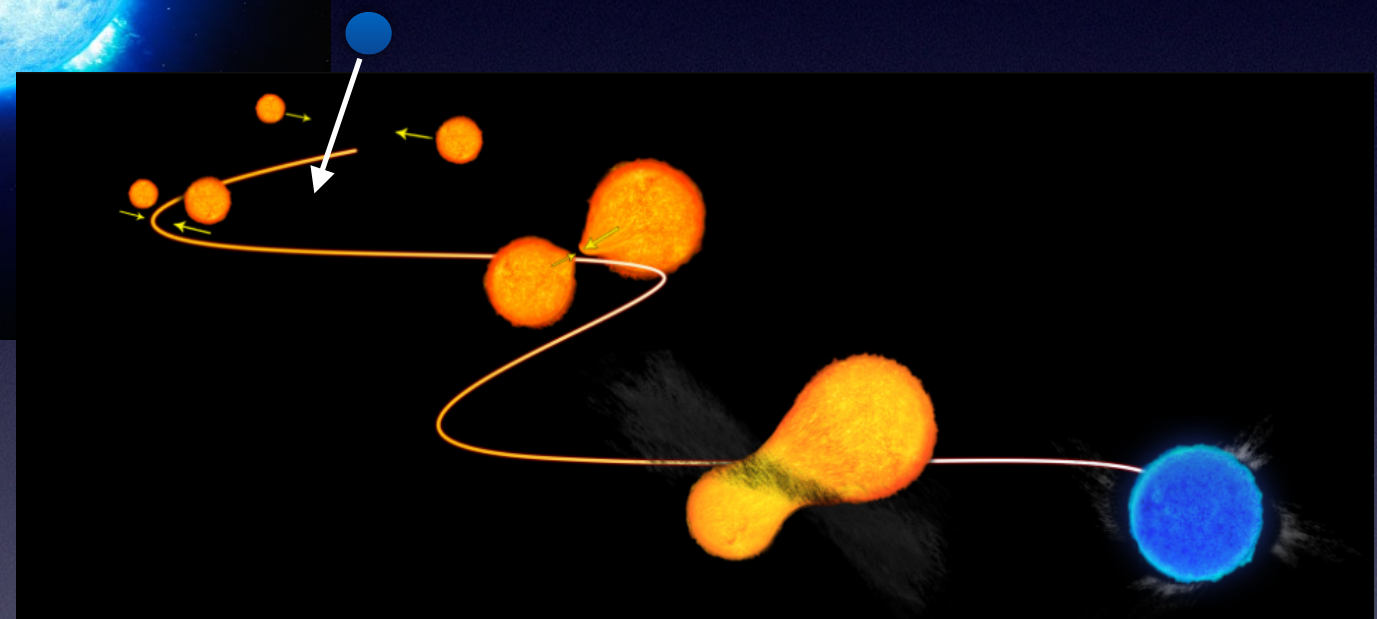


- Isolated binary evolution (« in the field »)
- Chemical Homogeneous Evolution (CHE)



## Question 2:

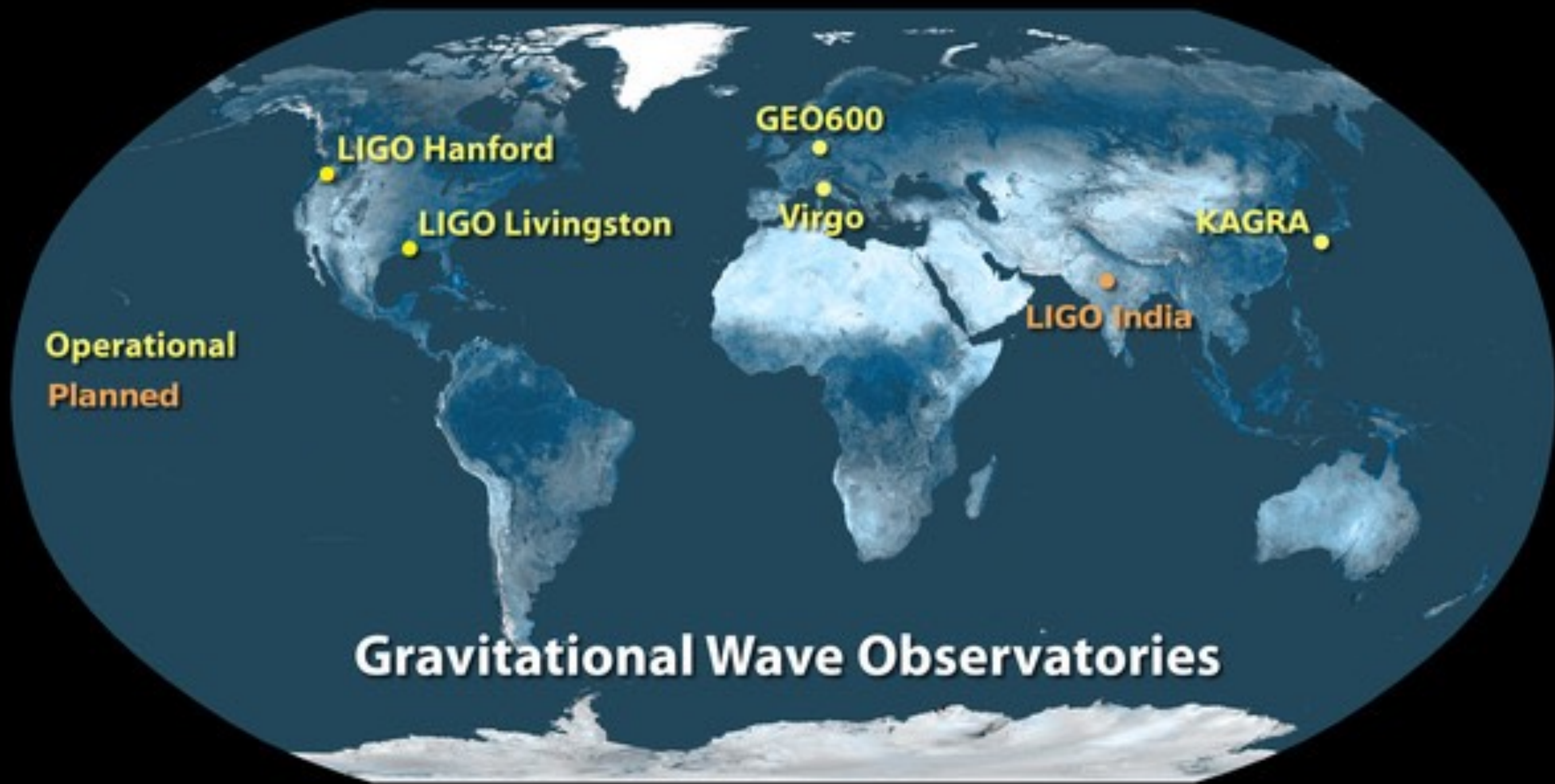
To form or not to form  
a stellar couple?



- Isolated binary evolution (« in the field »)
- Chemical Homogeneous Evolution (CHE)
- Dynamical capture in dense cluster



# Gravitational waves

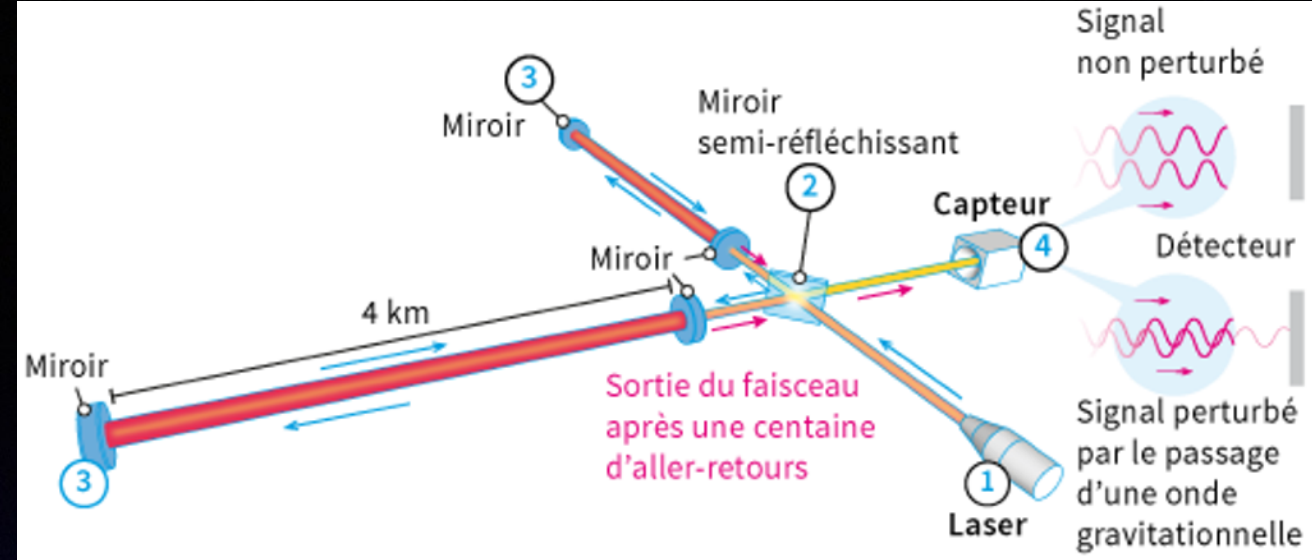




# Gravitational waves

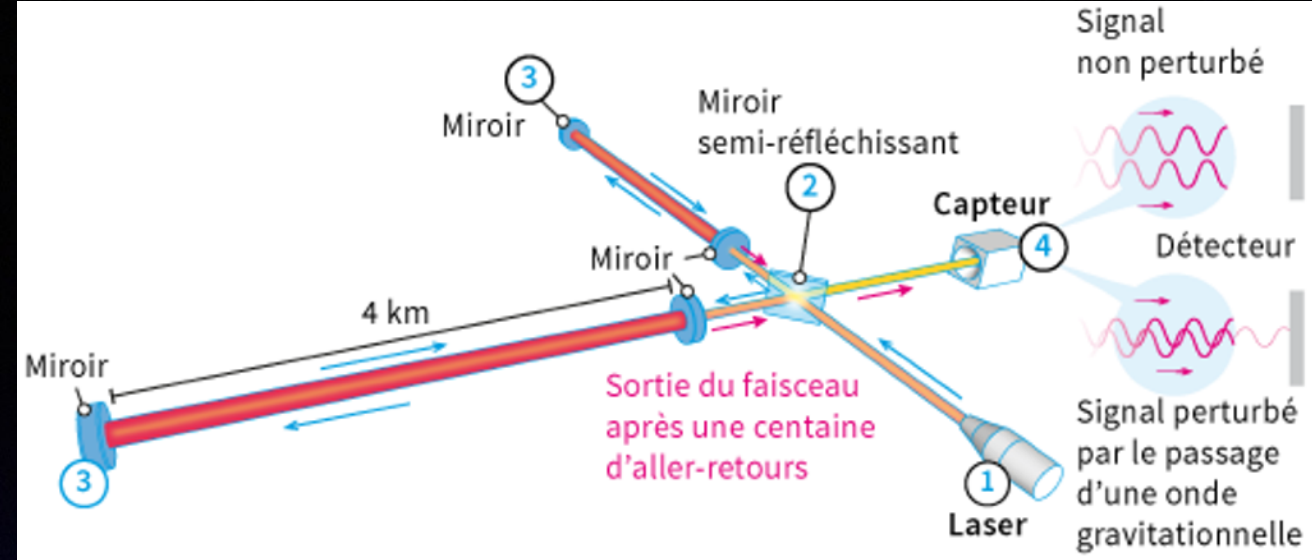


# Gravitational waves





# Gravitational waves

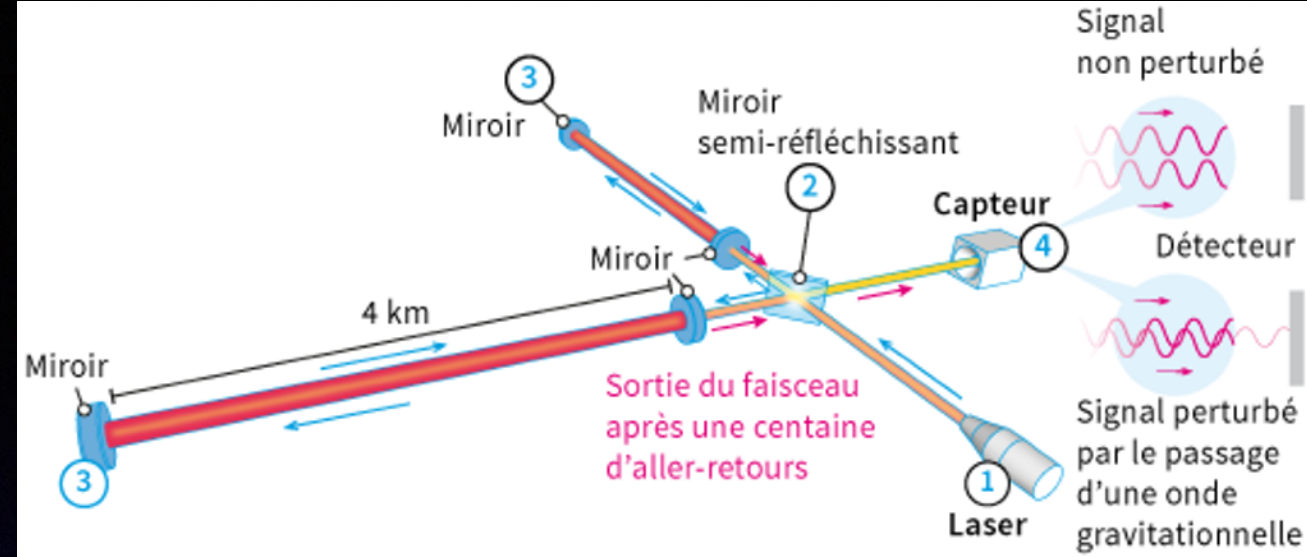


LIGO (US): 4 km (Louisiana/Washington)





# Gravitational waves



LIGO (US): 4 km (Louisiana/Washington)

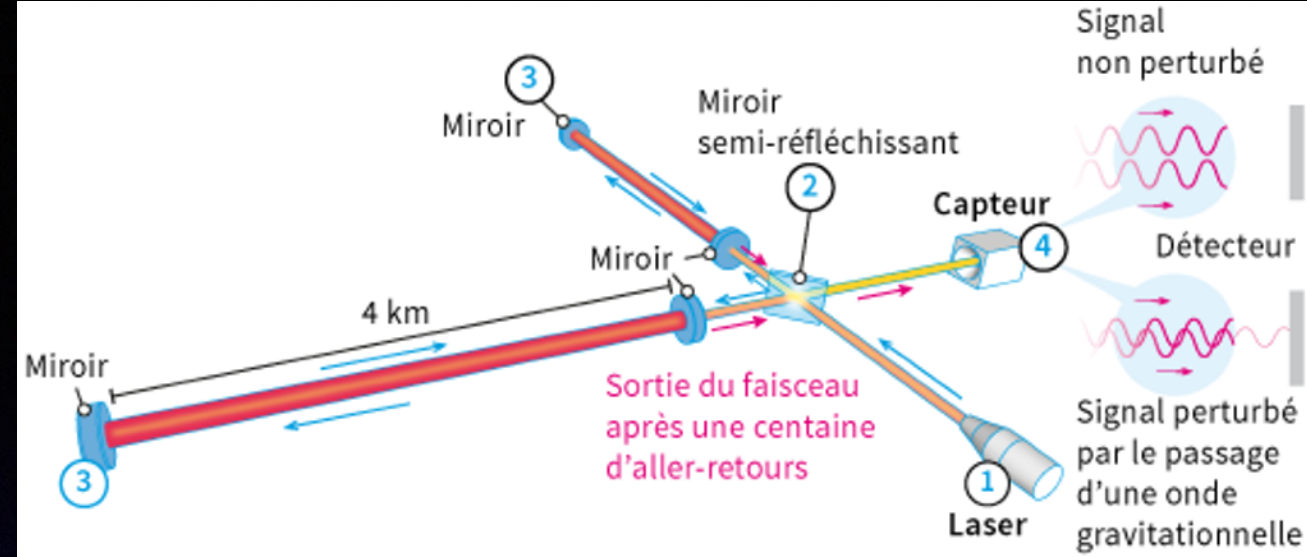


Virgo (EU): 3 km (Pisa, Italy)





# Gravitational waves



LIGO (US): 4 km (Louisiana/Washington)

Virgo (EU): 3 km (Pisa, Italy)

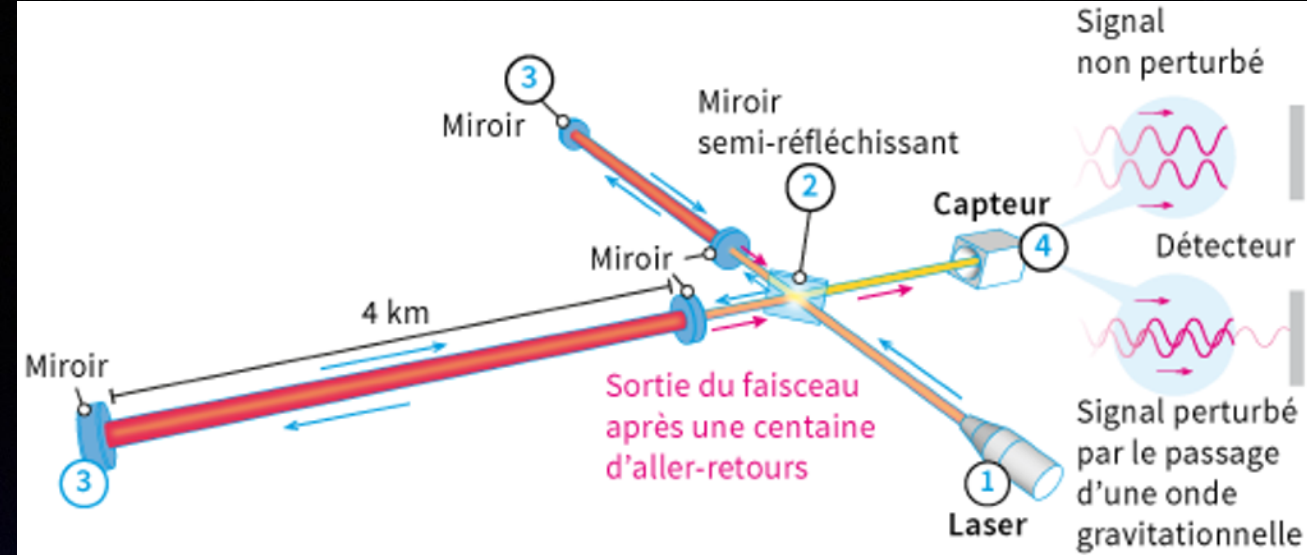


The LIGO equipment and observatories were jointly designed and operated by Caltech and MIT scientists.





# Gravitational waves



LIGO (US): 4 km (Louisiana/Washington)

Virgo (EU): 3 km (Pisa, Italy)



The LIGO equipment and observatories were jointly designed and operated by Caltech and MIT scientists.



PERSPECTIVES

An interior view is shown of one of the arms of the Virgo interferometer.



# Gravitational waves



LIGO (US): 4 km (Louisiana/Washington)

Virgo (EU): 3 km (Pisa, Italy)



The LIGO equipment and observatories were jointly designed and operated by Caltech and MIT scientists.



PERSPECTIVES

An interior view is shown of one of the arms of the Virgo interferometer.



# Gravitational waves

## Massive black holes and gravitational waves

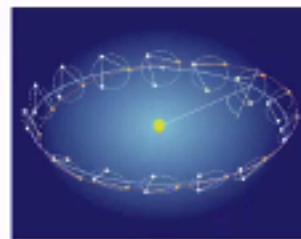
$$f \sim \frac{c}{2\pi R_s} \sim 10^4 \text{ Hz} \frac{M_\odot}{M}$$

$$r_s = \frac{2GM}{c^2}$$

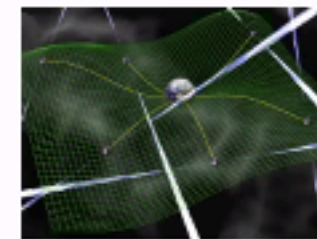
10  $M_{\text{sun}}$  binary  
 $f < 10^3$  Hz  
LIGO/Virgo  
inspiral/merger



$10^6$  Msun binary  
 $f < 10^{-2}$  Hz  
LISA  
inspiral/merger



$10^9$  Msun binary  
 $f < 10^{-6}$  Hz  
PTA  
inspiral+bk





# Gravitational waves

## Massive black holes and gravitational waves

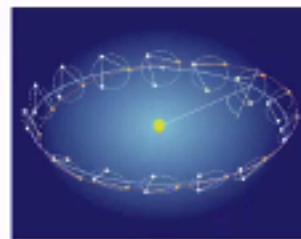
$$f \sim \frac{c}{2\pi R_s} \sim 10^4 \text{ Hz} \frac{M_\odot}{M}$$

$$r_s = \frac{2GM}{c^2}$$

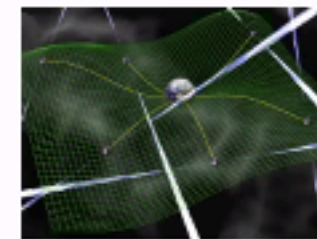
10  $M_{\text{sun}}$  binary  
 $f < 10^3$  Hz  
LIGO/Virgo  
inspiral/merger



$10^6$  Msun binary  
 $f < 10^{-2}$  Hz  
LISA  
inspiral/merger

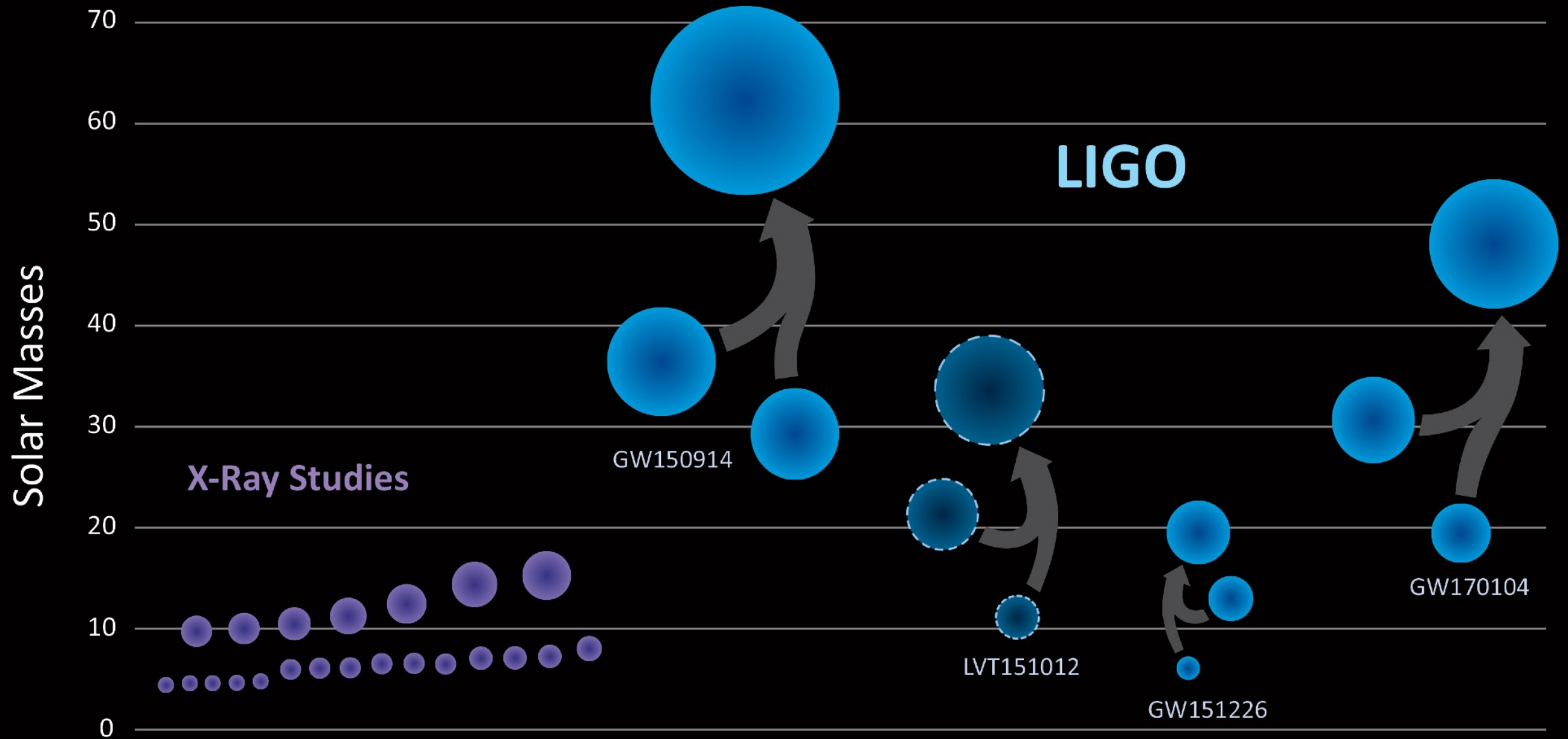


$10^9$  Msun binary  
 $f < 10^{-6}$  Hz  
PTA  
inspiral+bk



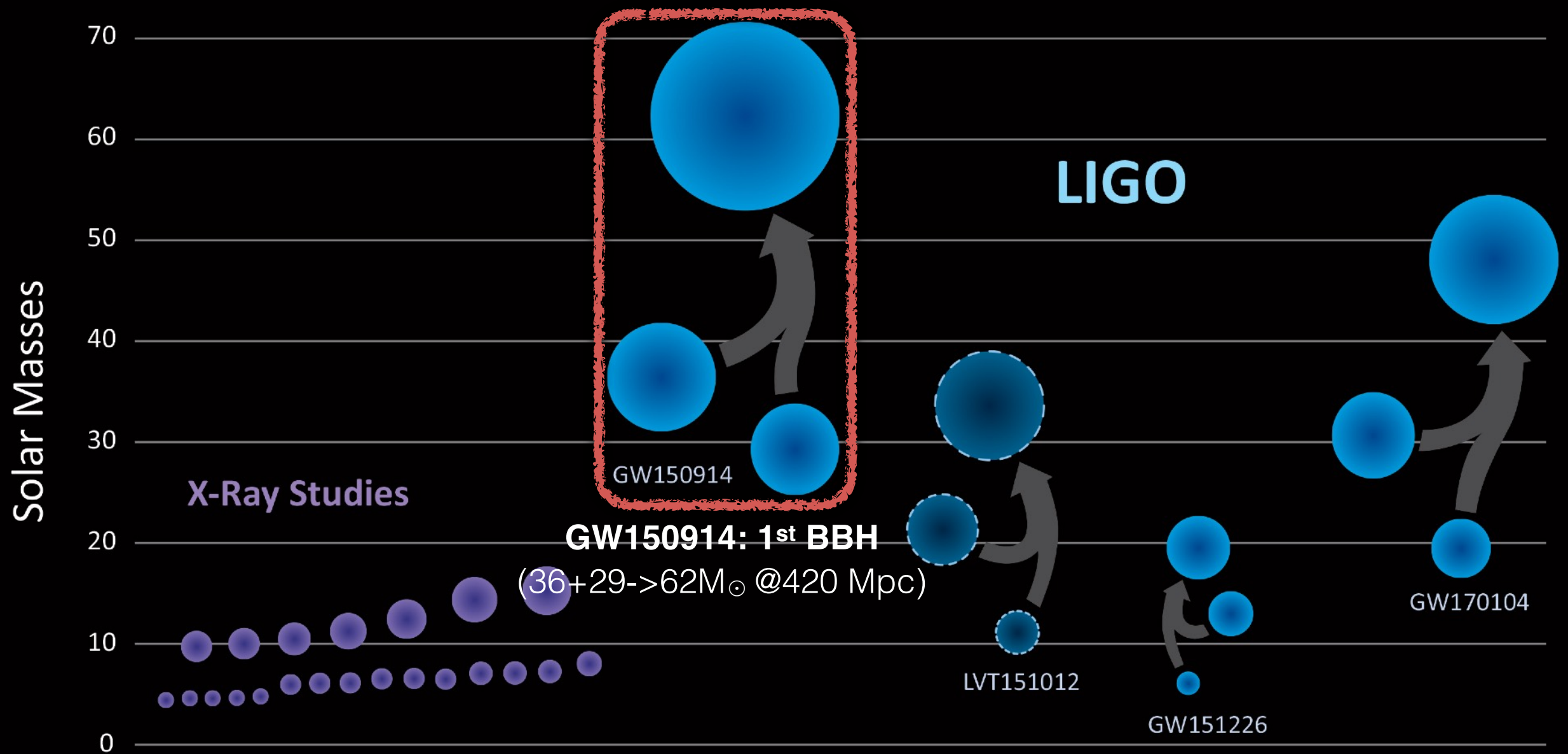


OI detections  
(09-12/2015):  
3 BBH



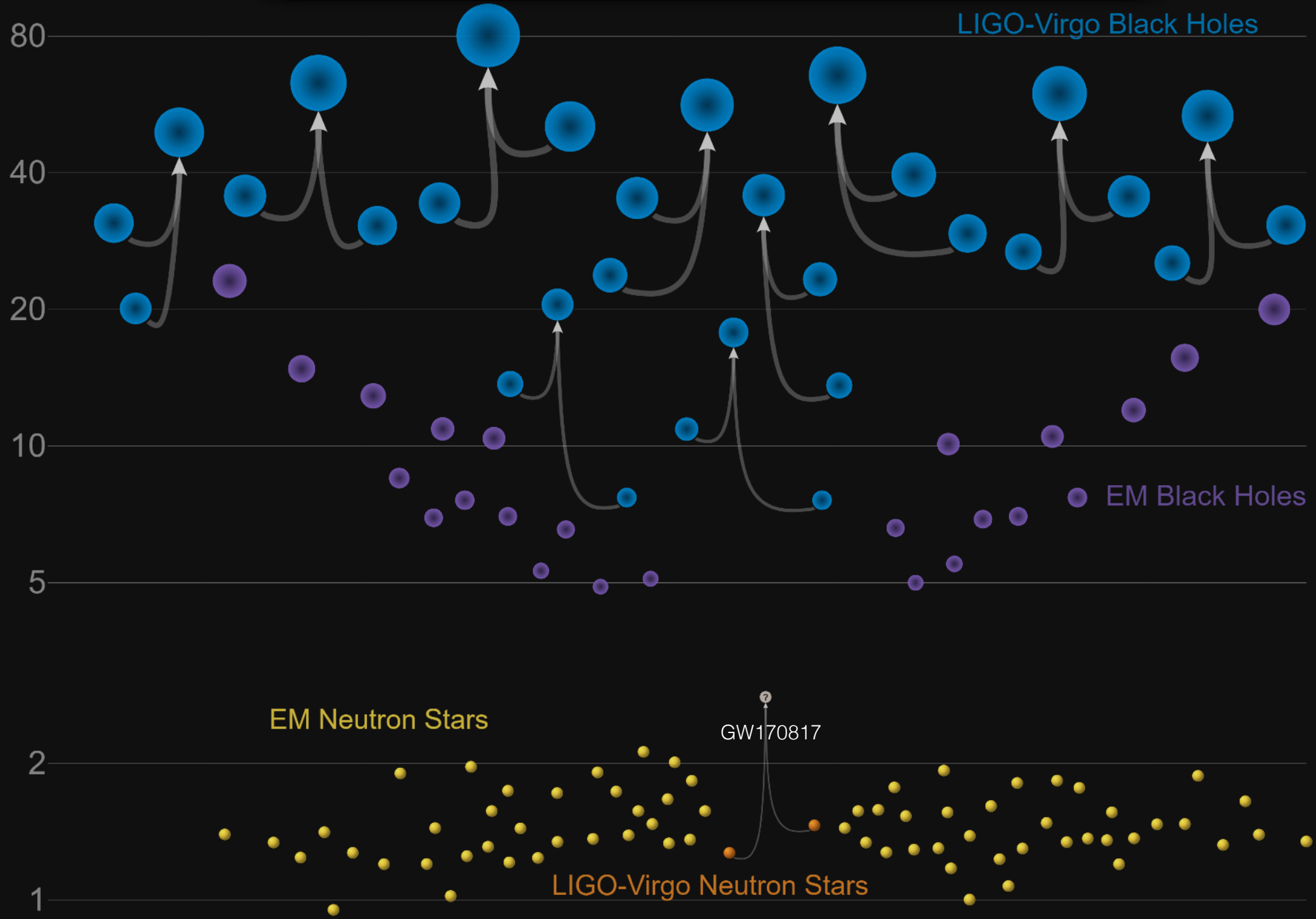


OI detections  
(09-12/2015):  
3 BBH



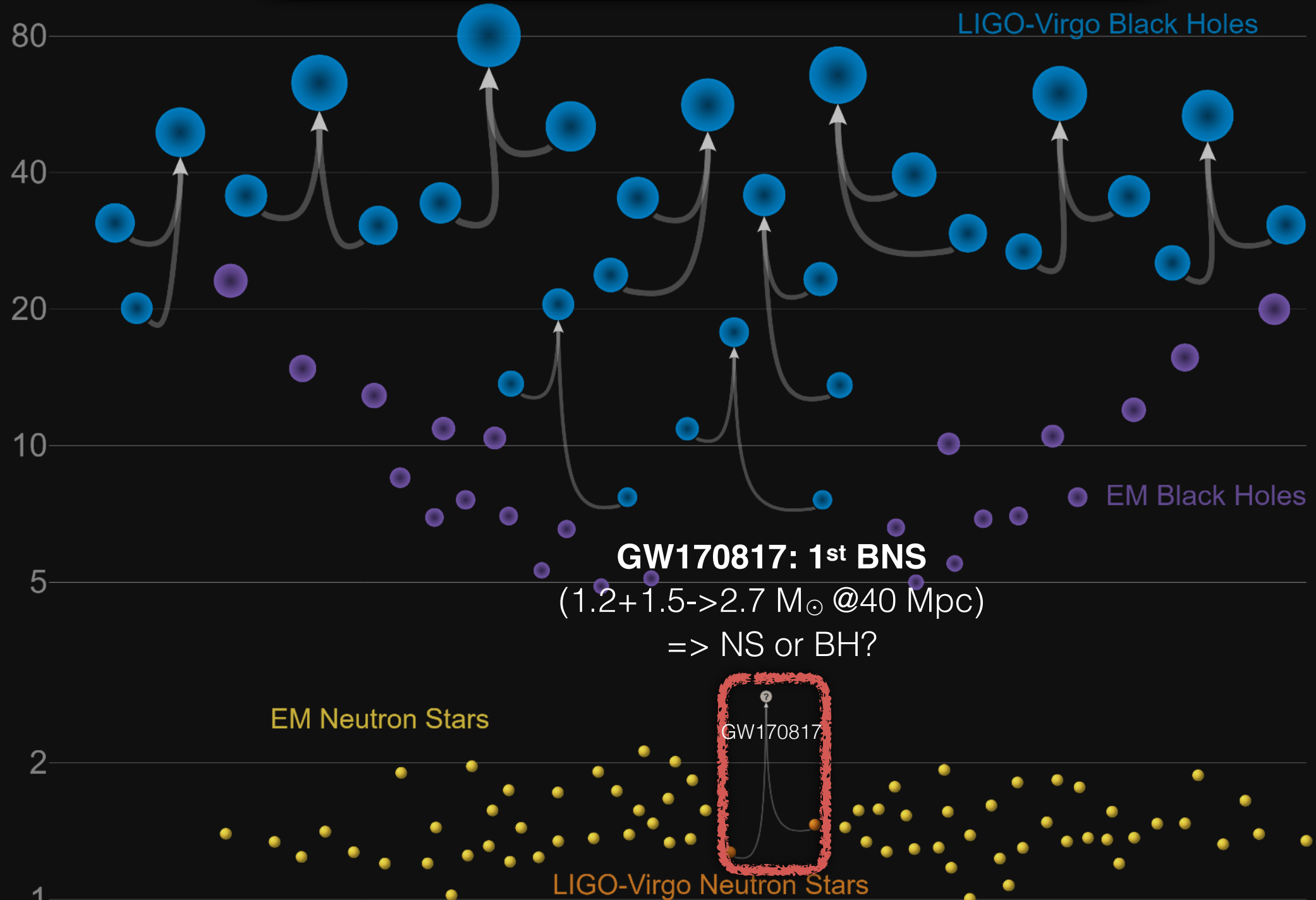


# O1+O2 detections (GWTC-1, 09/2015-08/2017): 10 BBH + 1 BNS





# O1+O2 detections (GWTC-1, 09/2015-08/2017): 10 BBH + 1 BNS





# O3a detections

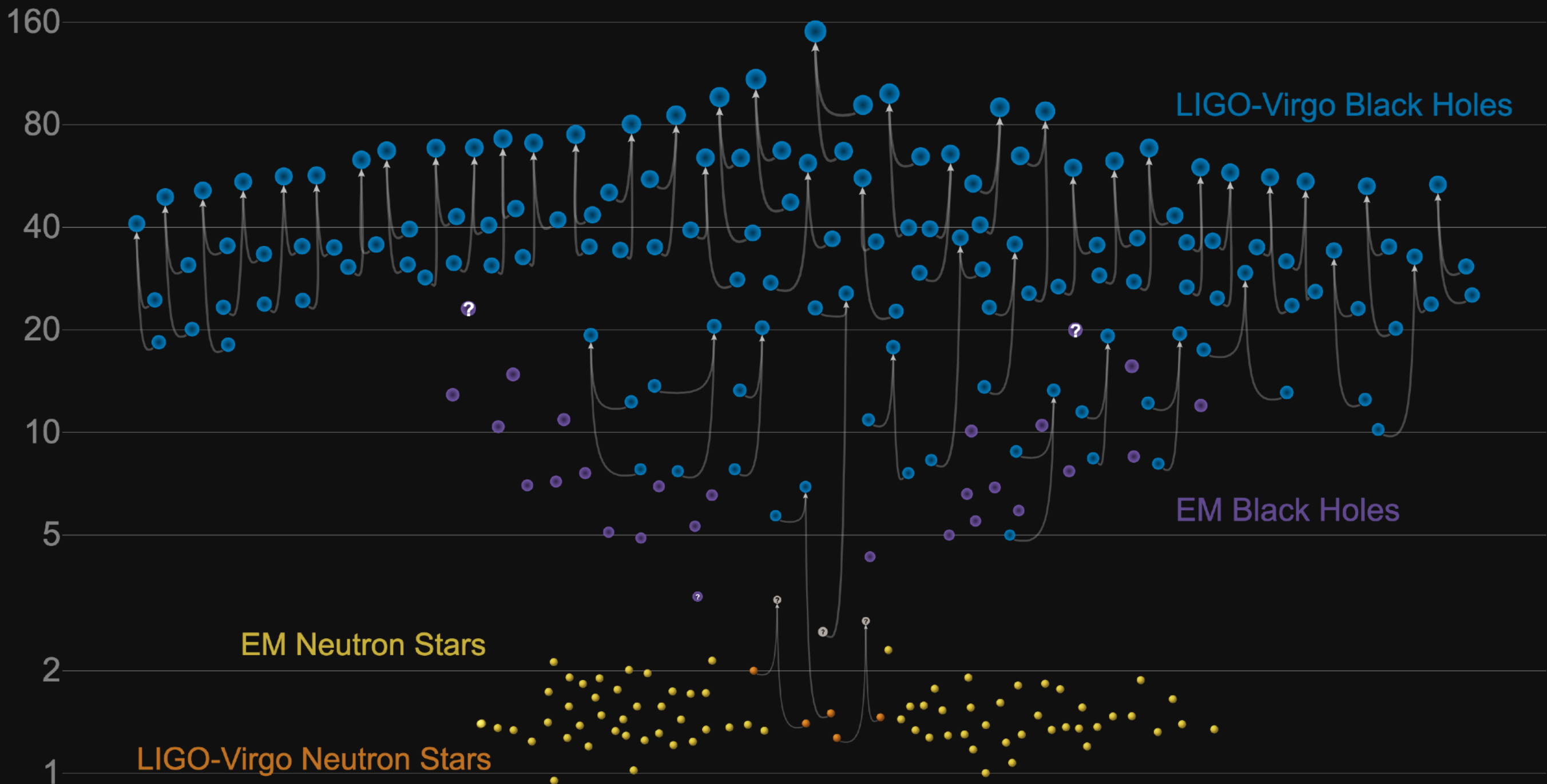
(GWTC-2, 04/2019-09/2019)

39 BBH/BNS/NSBH

# O3b detections

(GWTC-3, 11/2019-03/2020)

35 BBH/BNS/NSBH



GWTC-2 plot v1.0

LIGO-Virgo | Frank Elavsky, Aaron Geller | Northwestern



# O3a detections

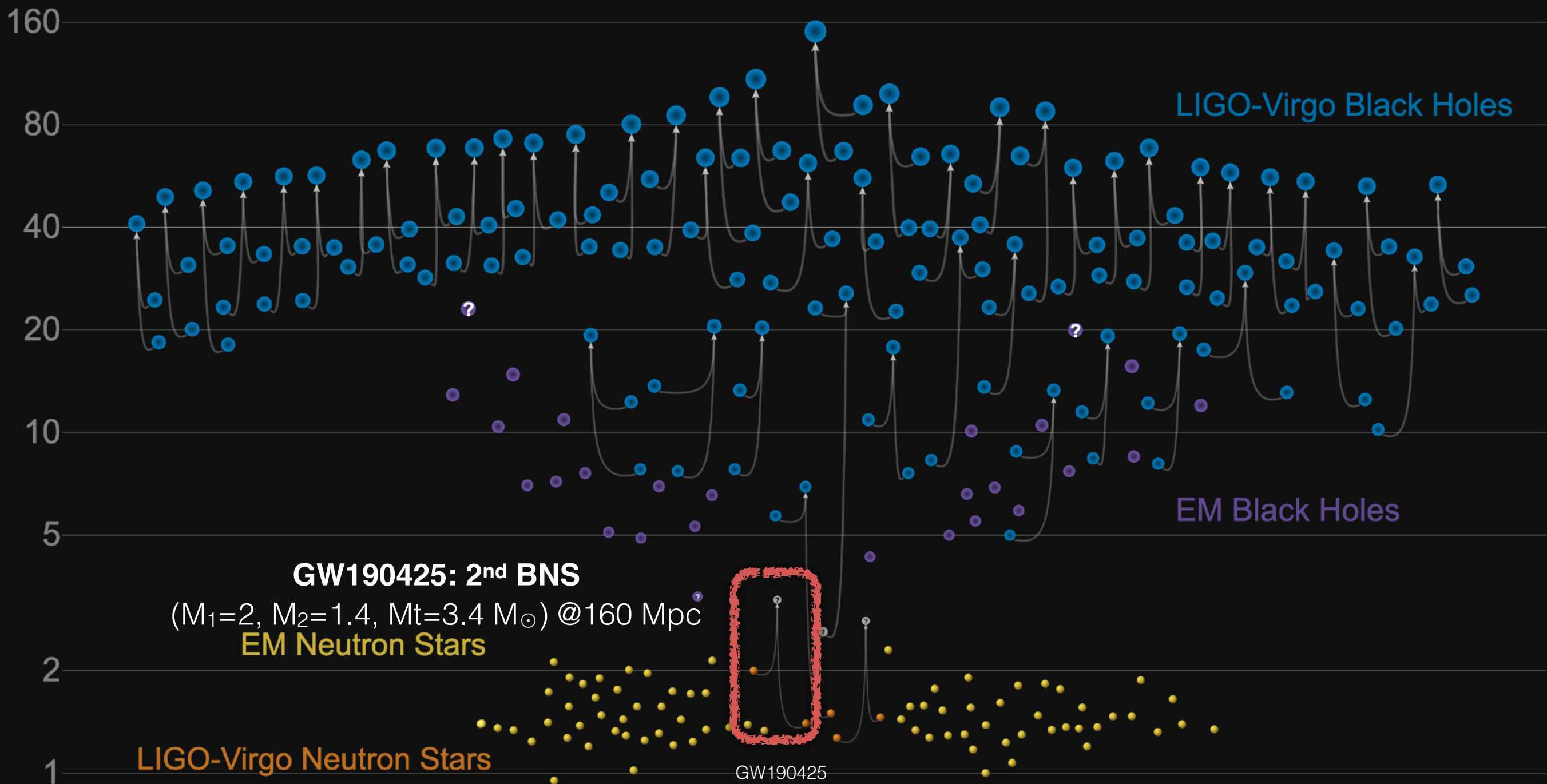
(GWTC-2, 04/2019-09/2019)

39 BBH/BNS/NSBH

# O3b detections

(GWTC-3, 11/2019-03/2020)

35 BBH/BNS/NSBH



GWTC-2 plot v1.0

LIGO-Virgo | Frank Elavsky, Aaron Geller | Northwestern



# O3a detections

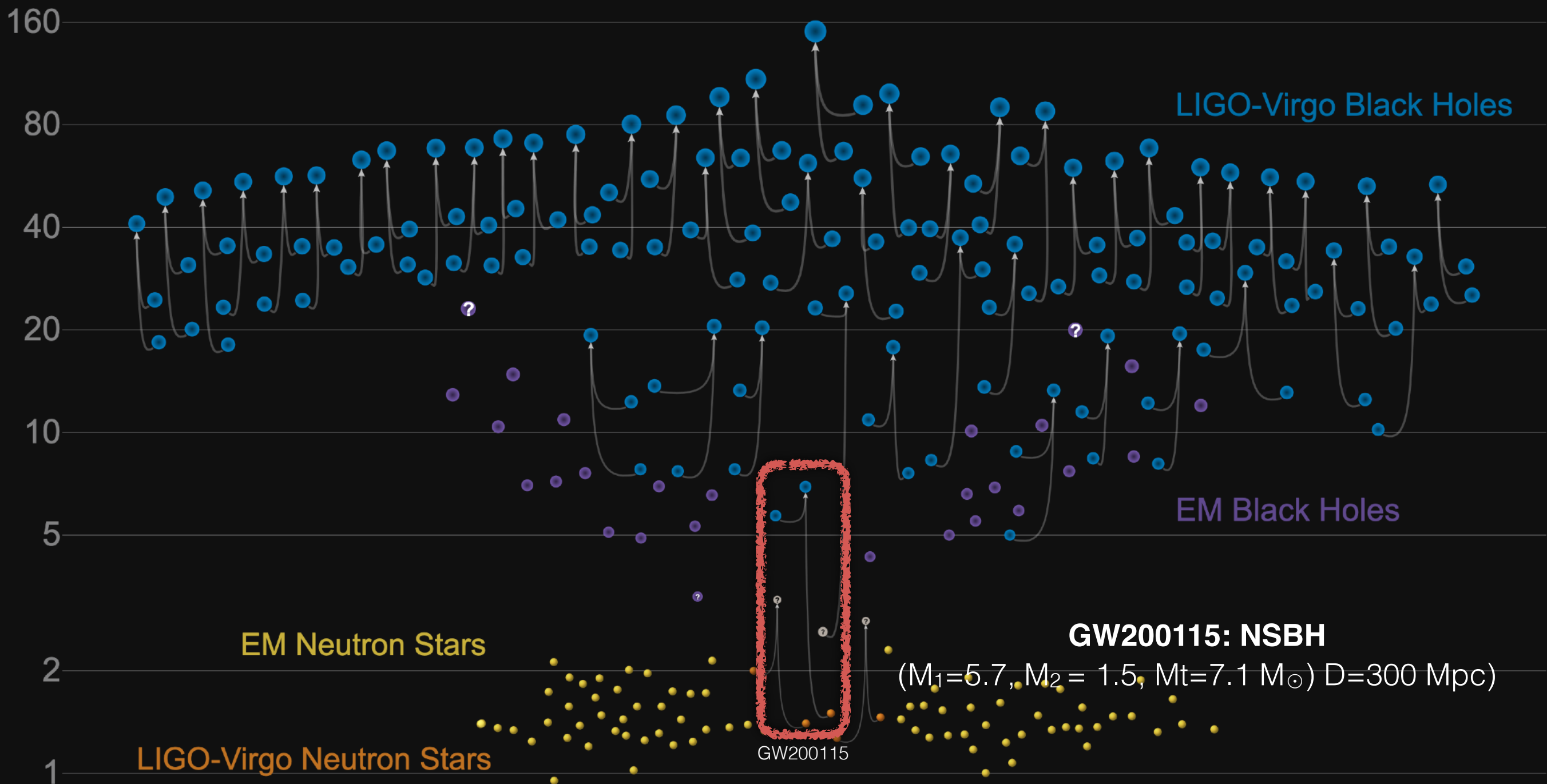
(GWTC-2, 04/2019-09/2019)

39 BBH/BNS/NSBH

# O3b detections

(GWTC-3, 11/2019-03/2020)

35 BBH/BNS/NSBH



GWTC-2 plot v1.0

LIGO-Virgo | Frank Elavsky, Aaron Geller | Northwestern



# O3a detections

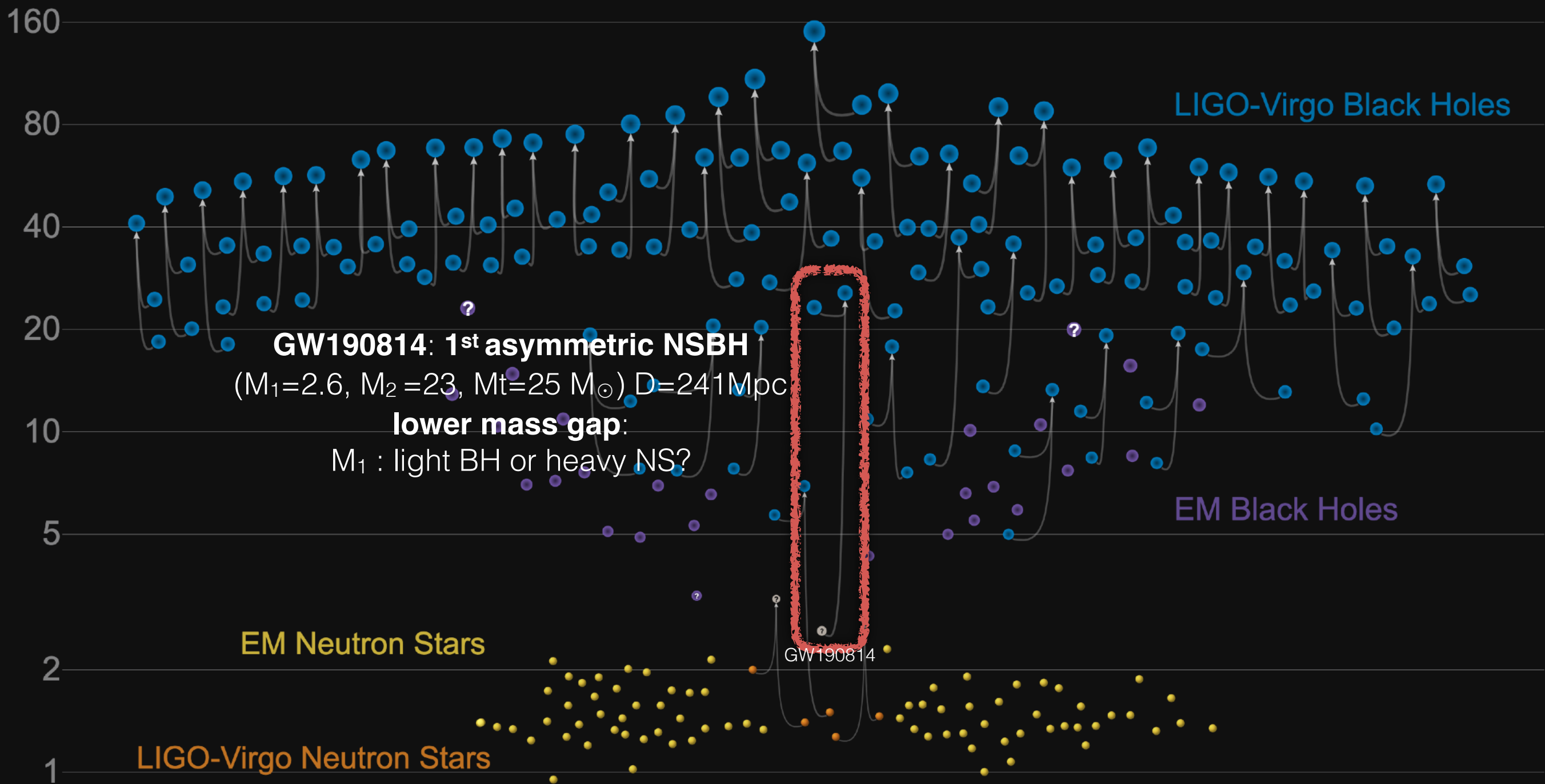
(GWTC-2, 04/2019-09/2019)

39 BBH/BNS/NSBH

# O3b detections

(GWTC-3, 11/2019-03/2020)

35 BBH/BNS/NSBH



GWTC-2 plot v1.0

LIGO-Virgo | Frank Elavsky, Aaron Geller | Northwestern



# O3a detections

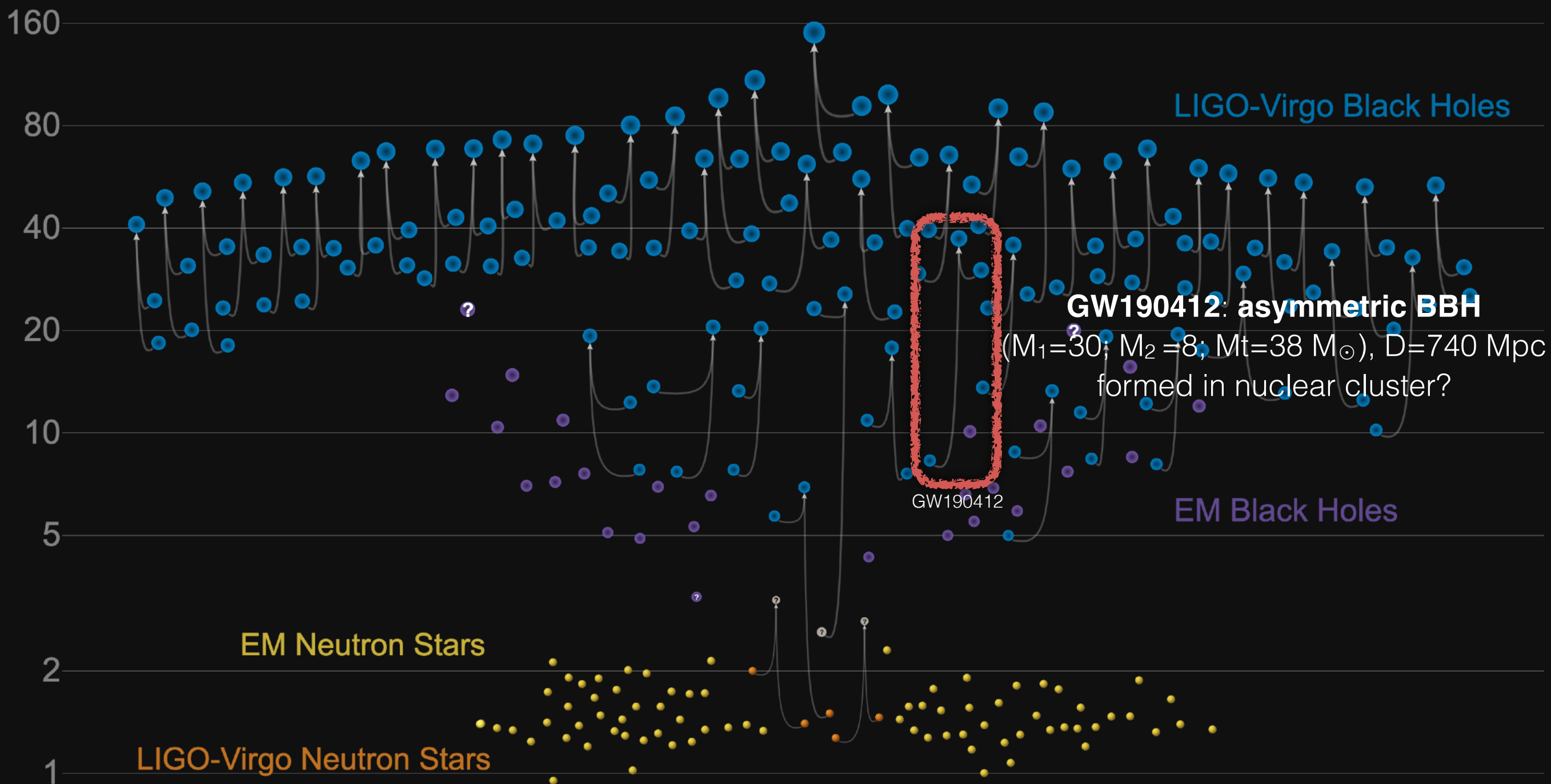
(GWTC-2, 04/2019-09/2019)

39 BBH/BNS/NSBH

# O3b detections

(GWTC-3, 11/2019-03/2020)

35 BBH/BNS/NSBH



GWTC-2 plot v1.0

LIGO-Virgo | Frank Elavsky, Aaron Geller | Northwestern



# O3a detections

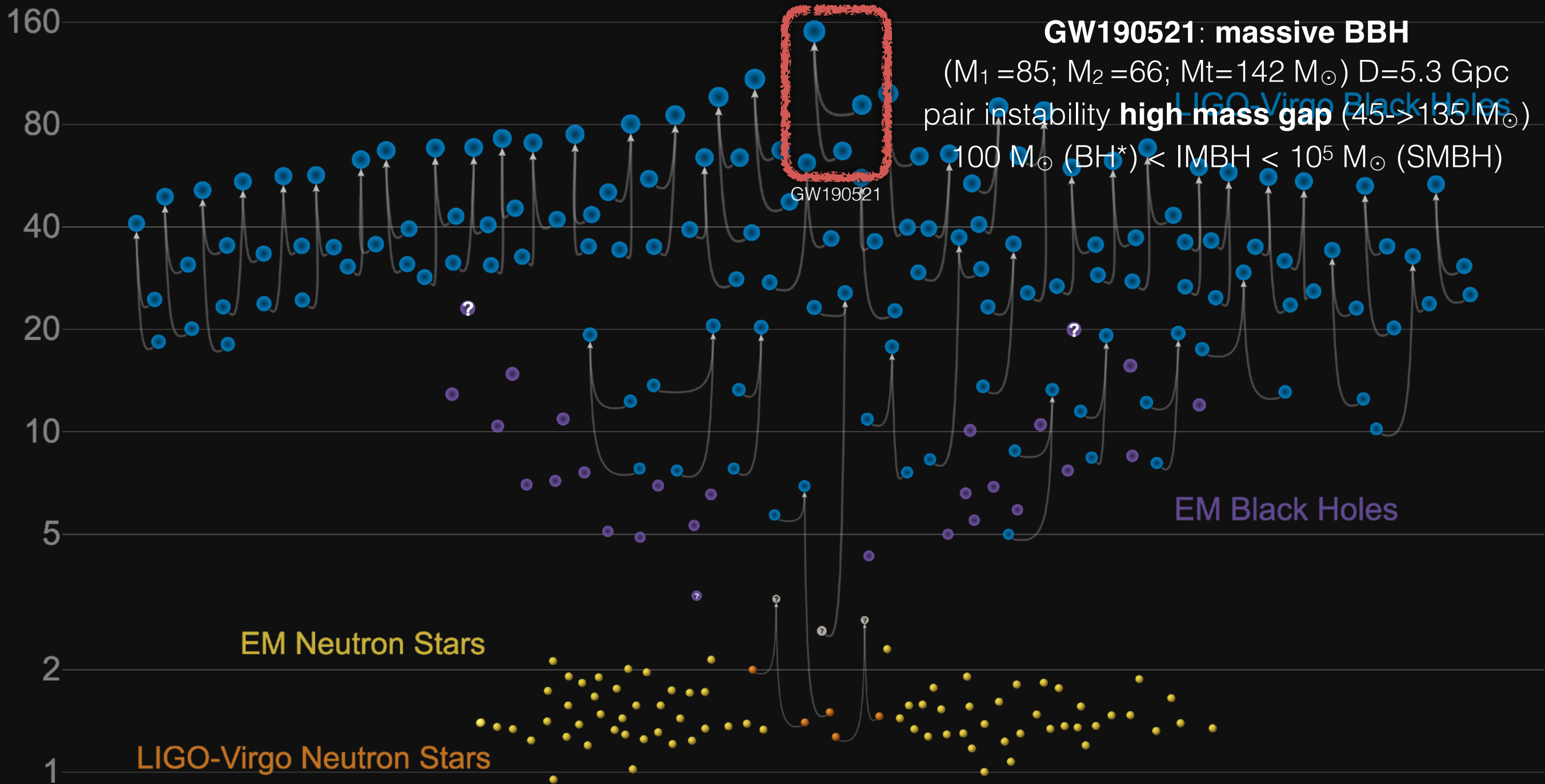
(GWTC-2, 04/2019-09/2019)

39 BBH/BNS/NSBH

# O3b detections

(GWTC-3, 11/2019-03/2020)

35 BBH/BNS/NSBH



GWTC-2 plot v1.0

LIGO-Virgo | Frank Elavsky, Aaron Geller | Northwestern



# O3a detections

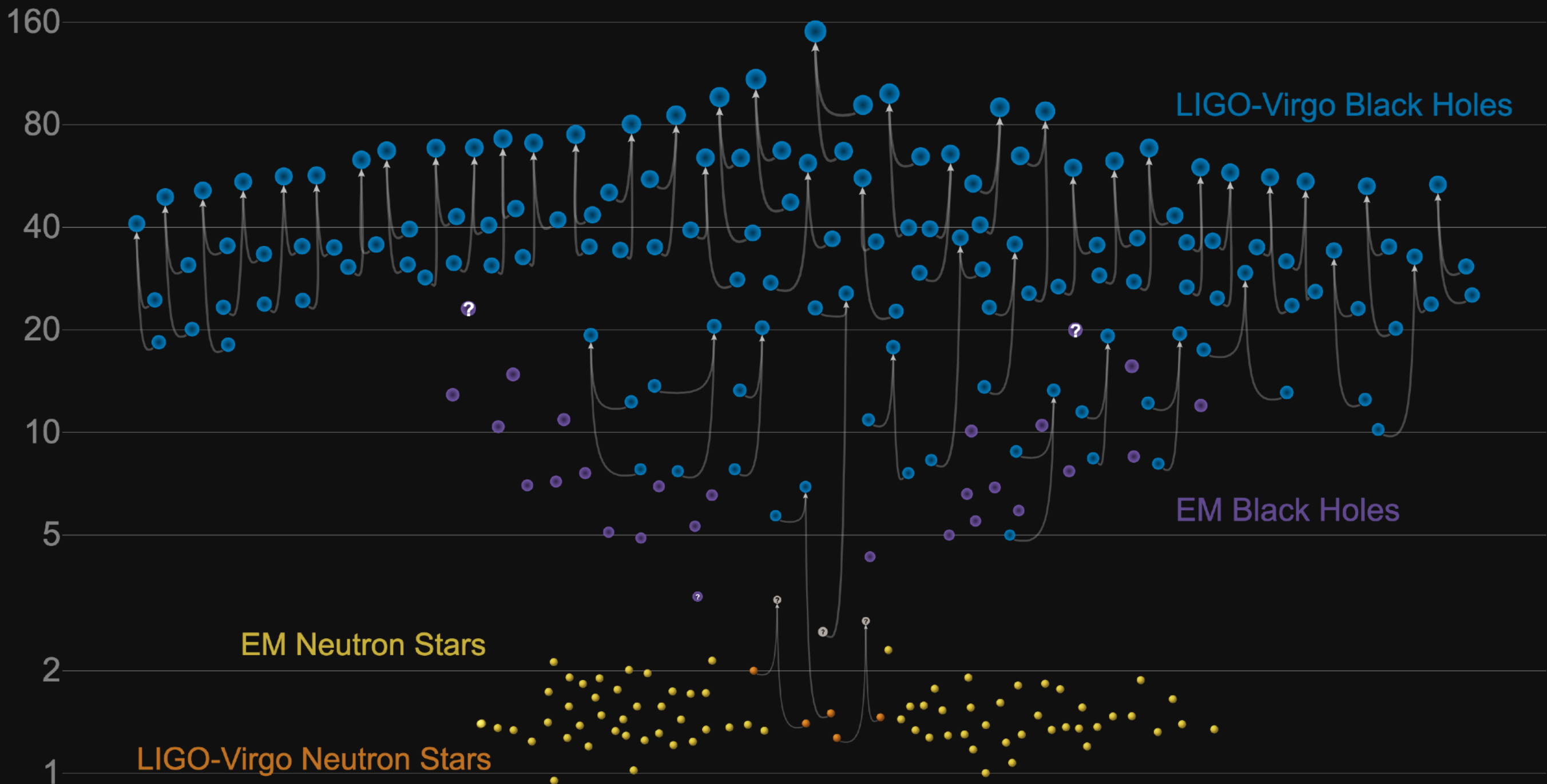
(GWTC-2, 04/2019-09/2019)

39 BBH/BNS/NSBH

# O3b detections

(GWTC-3, 11/2019-03/2020)

35 BBH/BNS/NSBH

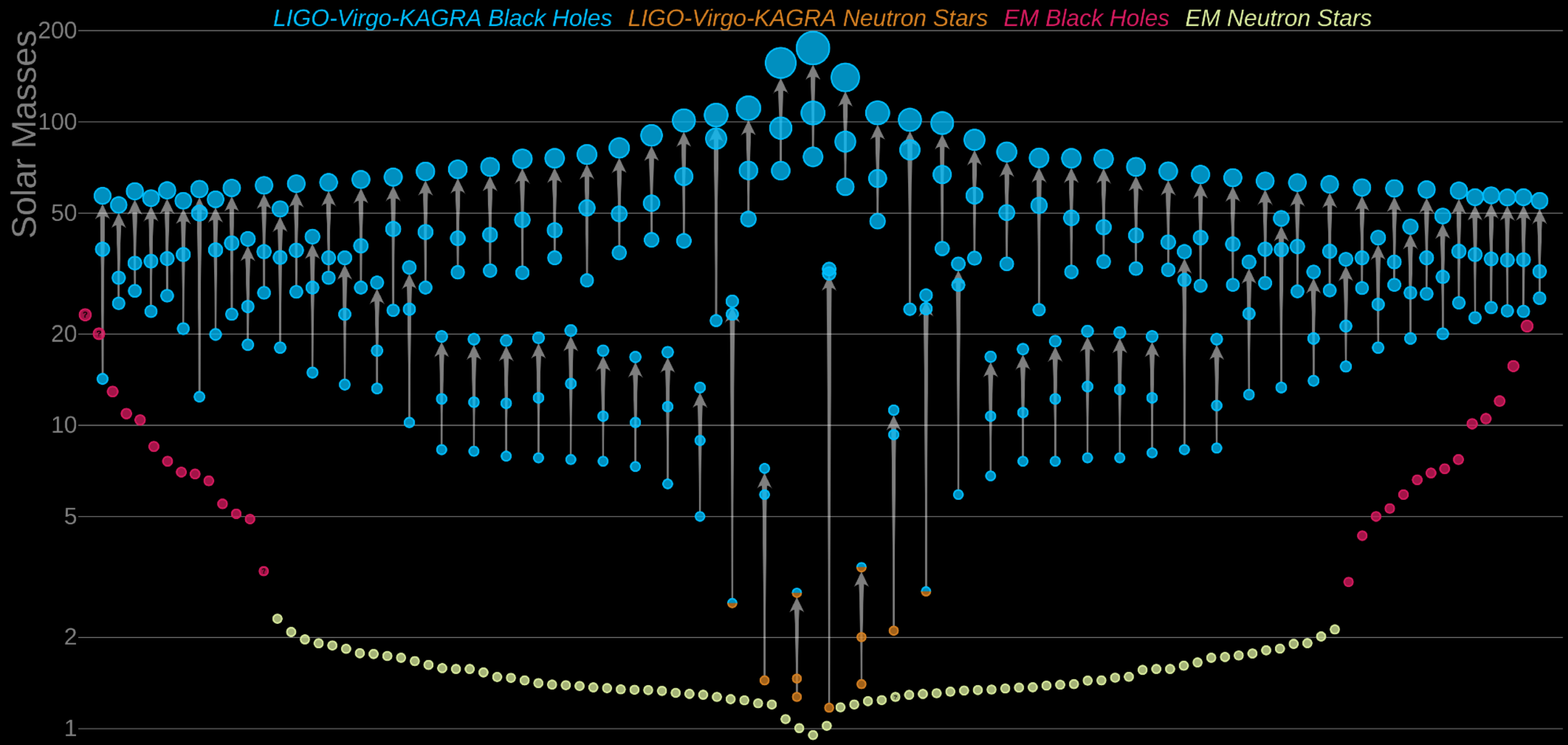


GWTC-2 plot v1.0

LIGO-Virgo | Frank Elavsky, Aaron Geller | Northwestern



# ○ | — ○3 detections (GWTC-1+2+3, 09/2015-03/2020): 90 BBH/BNS/NSBH

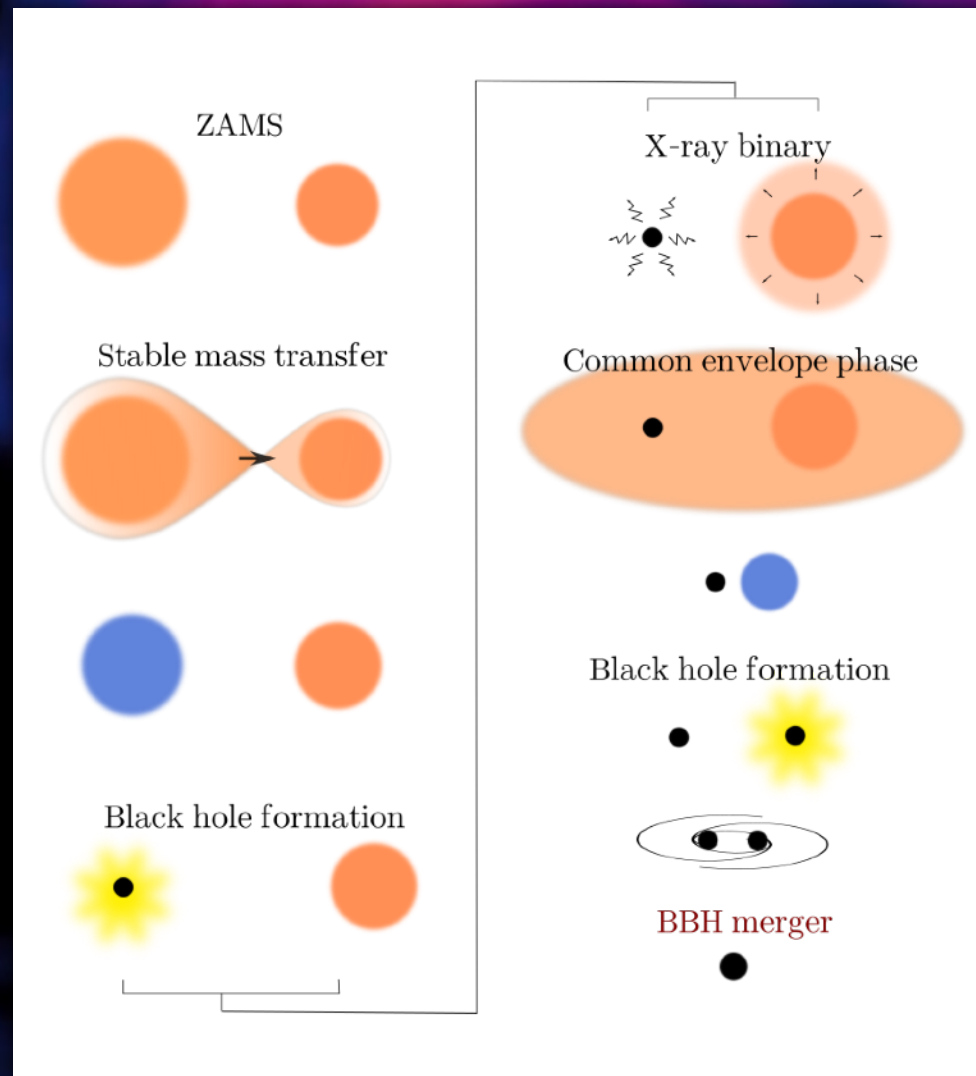


LIGO-Virgo-KAGRA | Aaron Geller | Northwestern



# Progenitors of low-mass binary BH mergers in the isolated binary evolution scenario

F. García, A. Simaz Bunzel, S. Chaty, E. Porter, E. Chassande-Mottin, A&A



A&A 649, A114 (2021)  
<https://doi.org/10.1051/0004-6361/202038357>  
 © ESO 2021

**Astronomy  
& Astrophysics**

## Progenitors of low-mass binary black-hole mergers in the isolated binary evolution scenario

Federico García<sup>1,2</sup>, Adolfo Simaz Bunzel<sup>3,\*</sup>, Sylvain Chaty<sup>1,4</sup>, Edward Porter<sup>4</sup>, and Eric Chassande-Mottin<sup>4</sup>

<sup>1</sup> AIM, CEA, CNRS, Université Paris-Saclay, Université de Paris, 91191 Gif-sur-Yvette, France  
 e-mail: fgarcia@cea.fr, asbunzel@unlp.edu.ar  
<sup>2</sup> Kapteyn Astronomical Institute, University of Groningen, PO Box 800, 9700, AV Groningen, The Netherlands  
<sup>3</sup> Instituto Argentino de Radioastronomía, Universidad Nacional de La Plata, 1900 La Plata, Argentina  
<sup>4</sup> Université de Paris, CNRS, Astroparticule et Cosmologie, 75013 Paris, France

Received 6 May 2020 / Accepted 2 March 2021

**ABSTRACT**

**Context.** The formation history, progenitor properties, and expected rates of the binary black holes discovered by the LIGO-Virgo collaboration via the gravitational-wave emission during their coalescence are a topic of active research.

**Aims.** We aim to study the progenitor properties and expected rates of the two lowest-mass binary black hole mergers, GW151226 and GW170608, detected within the first two Advanced LIGO-Virgo observing runs, in the context of the classical isolated binary-evolution scenario.

**Methods.** We used the publicly available 1D-hydrodynamic stellar-evolution code MESA, which we adapted to include the black-hole formation and the unstable mass transfer developed during the so-called common-envelope phase. Using more than 60 000 binary simulations, we explored a wide parameter space for initial stellar masses, separations, metallicities, and mass-transfer efficiencies. We obtained the expected distributions for the chirp mass, mass ratio, and merger time delay by accounting for the initial stellar binary distributions. We predicted the expected merger rates and compared them with those of the detected gravitational-wave events. We studied the dependence of our predictions with respect to the (as yet) unconstrained parameters inherent to binary stellar evolution.

**Results.** Our simulations for both events show that while the progenitors we obtained are compatible over the entire range of explored metallicities, they show a strong dependence on the initial masses of the stars, according to stellar winds. All the progenitors we found follow a similar evolutionary path, starting from binaries with initial separations in the 30–200  $R_{\odot}$  range experiencing a stable mass transfer interaction before the formation of the first black hole, followed by a second unstable mass-transfer episode leading to a common-envelope ejection that occurs either when the secondary star crosses the Hertzsprung gap or when it is burning He in its core. The common-envelope phase plays a fundamental role in the considered low-mass range: only progenitors experiencing such an unstable mass-transfer phase are able to merge in less than a Hubble time.

**Conclusions.** We find integrated merger-rate densities in the range  $0.2\text{--}5.0\text{ yr}^{-1}\text{ Gpc}^{-3}$  in the Local Universe for the highest mass-transfer efficiencies explored here. The highest rate densities lead to detection rates of  $1.2\text{--}3.3\text{ yr}^{-1}$ , which are compatible with the observed rates. The common-envelope efficiency  $\alpha_{\text{CE}}$  has a strong impact on the progenitor populations. A high-efficiency scenario with  $\alpha_{\text{CE}} = 2.0$  is favoured when comparing the expected rates with the observations.

**Key words.** gravitational waves – binaries: general – stars: evolution – stars: black holes

### 1. Introduction

In 2015, the Advanced LIGO (LIGO Scientific Collaboration 2015) and Advanced Virgo (Acernese et al. 2015) Collaboration (LVC) began a series of observation runs. During both the O1 (12 September 2015–19 January 2016) and O2 (30 November 2016–25 August 2017) observation runs, a total of 11 gravitational wave (GW) events were observed. Ten of these events involved the detection of signals from the merger of a binary black hole (BBH, Abbott et al. 2019a) and one corresponded to the merger of two neutron stars (Abbott et al. 2017a, GW170817).

While the detected BBHs are mainly dominated by high-mass components ( $M \gtrsim 35 M_{\odot}$ ), two detections in particular, GW151226 (Abbott et al. 2016a) and GW170608 (Abbott et al. 2017b), are shown to be low-mass systems having BH masses consistent with those found in X-ray binaries (i.e.,  $M \lesssim 20 M_{\odot}$ ). Despite the fact that all these events could belong to the same population (Abbott et al. 2019b), the existence and abundance of these objects have triggered questions regarding their formation history. Several scenarios have been proposed in the literature, including the isolated binary evolution (our main focus here, Bethe & Brown 1998; Mandel & de Mink 2016; Tauris et al. 2017) and the dynamical formation channels (Portegies Zwart & McMillan 2000; Bae et al. 2014; Rodriguez et al. 2016).

In the dynamical formation scenario, BBHs are produced by three-body encounters in stellar clusters. In the chemically homogeneous evolutionary channel, compact BBHs are formed from rapidly rotating stars in near contact binaries that experience efficient internal mixing. It is estimated that dynamical encounters in globular clusters contributed to less than a few percent of all observed events (Bae et al. 2014; Rodriguez et al. 2016), while BBH rates in open and young star clusters can be an order of magnitude higher (Di Carlo et al. 2019; Kumamoto et al. 2020). On the other hand, the chemically homogeneous scenario is not able to produce a BBH in the

\* Fellow of CONICET.

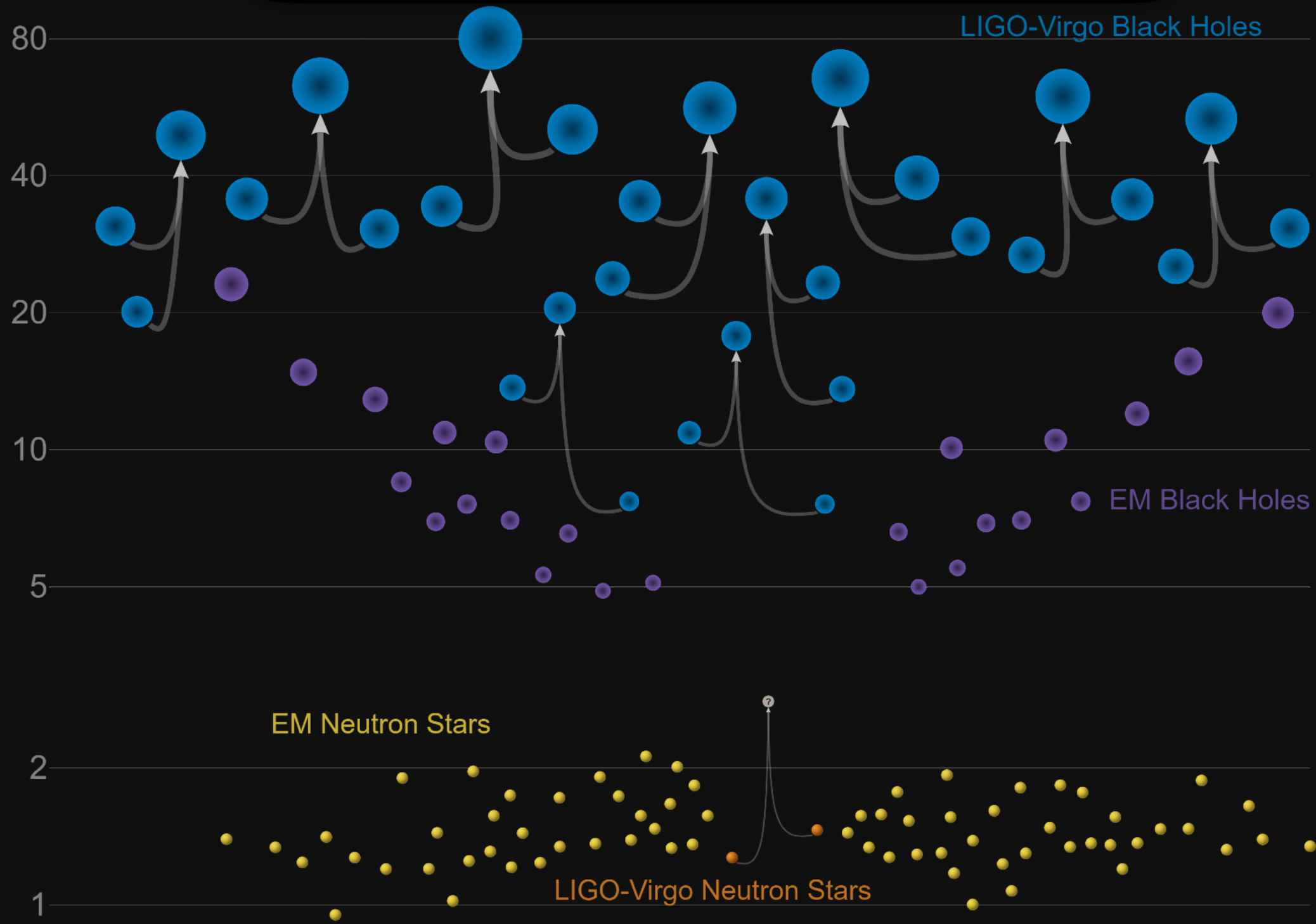
Article published by EDP Sciences A114, page 1 of 21

This work was supported by the LabEx UnivEarthS, Interface project I10  
 “From evolution of binaries to merging of compact objects” (ANR-10-LABX-0023 & ANR-18-IDEX-0001).  
 We acknowledge use of Arago Cluster from Astroparticule et Cosmologie (APC) for our calculations

S. Chaty

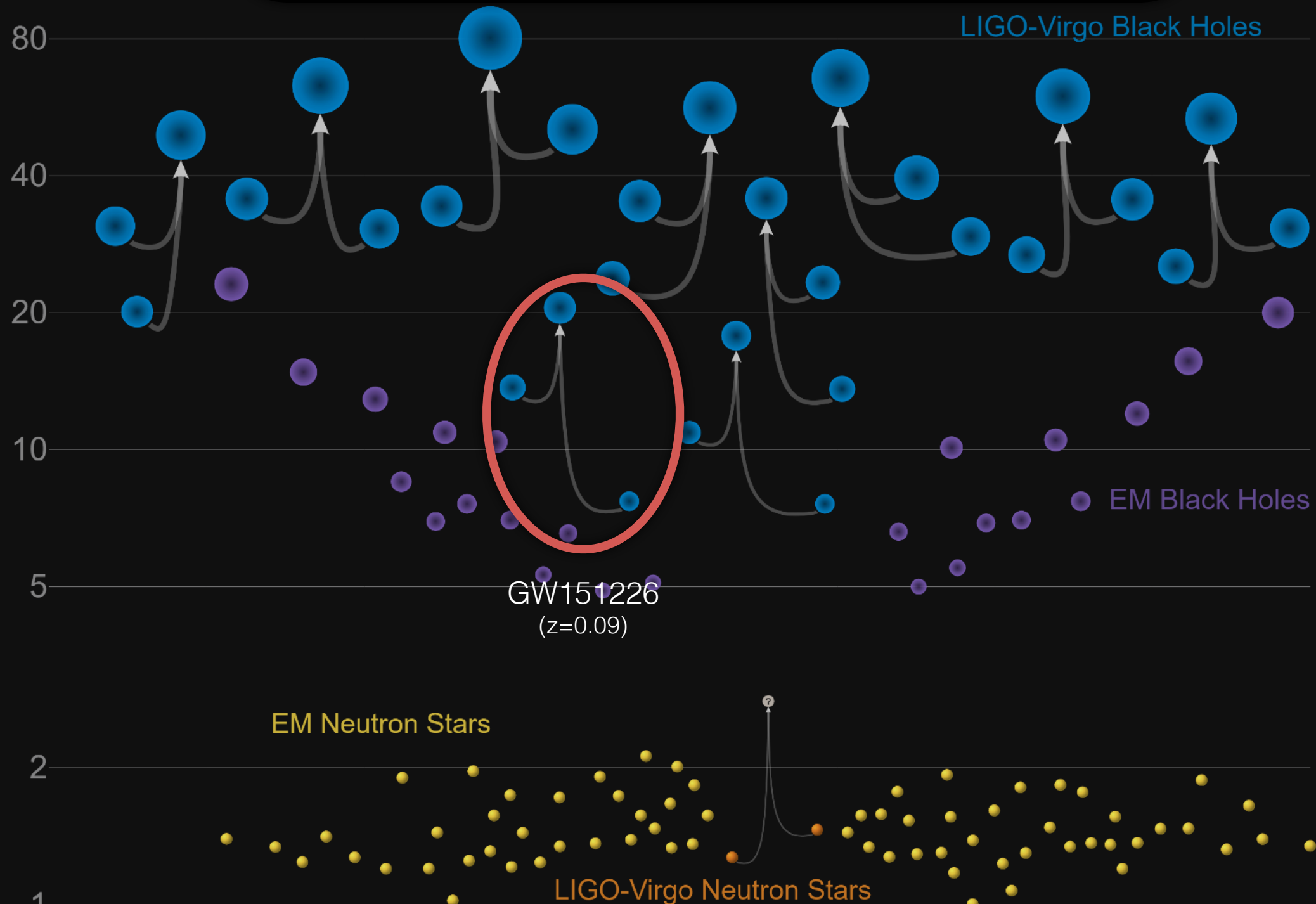


# GW151226 & GW170608: the lowest mass binary BH mergers in O1/O2 runs



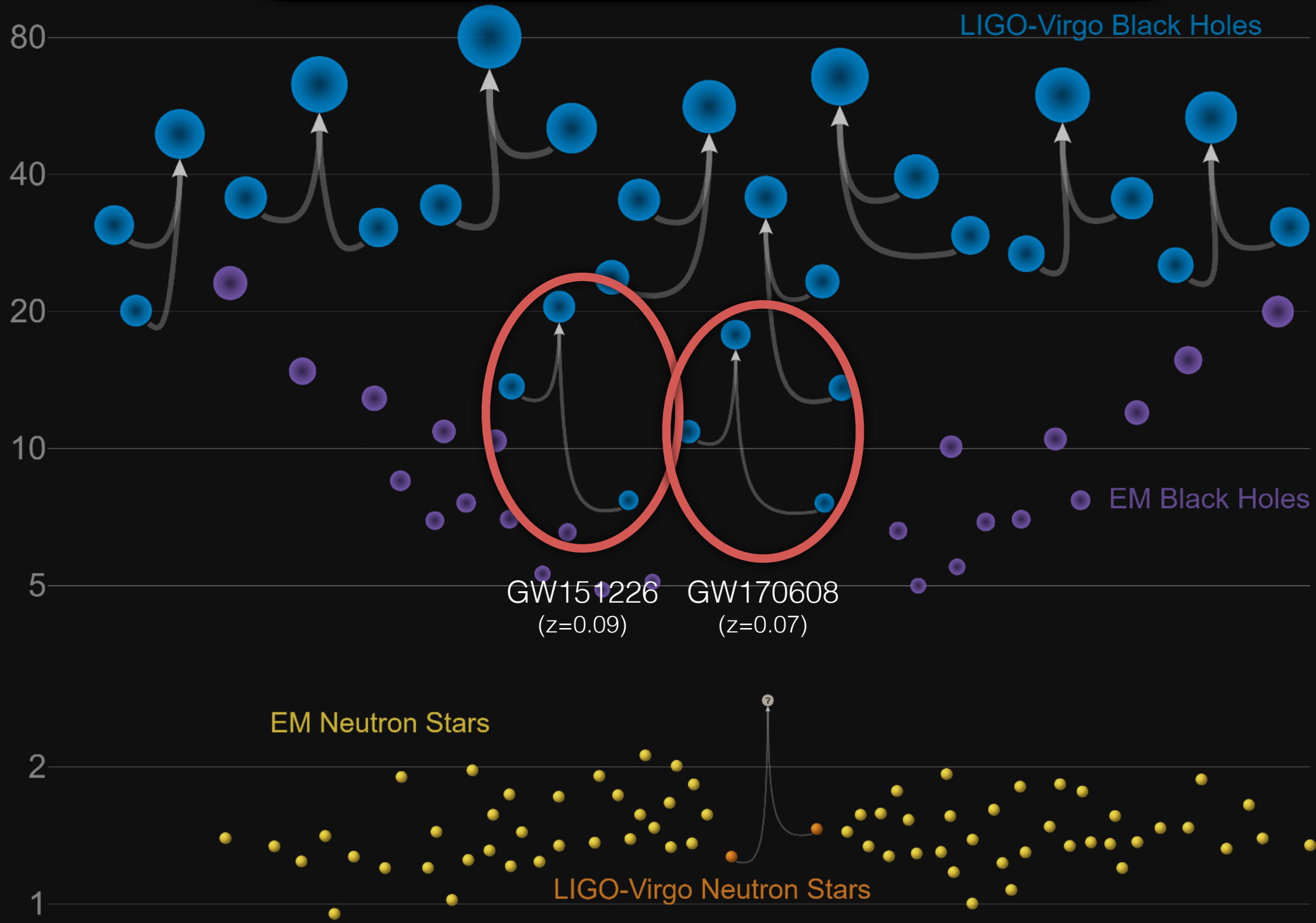


# GW151226 & GW170608: the lowest mass binary BH mergers in O1/O2 runs



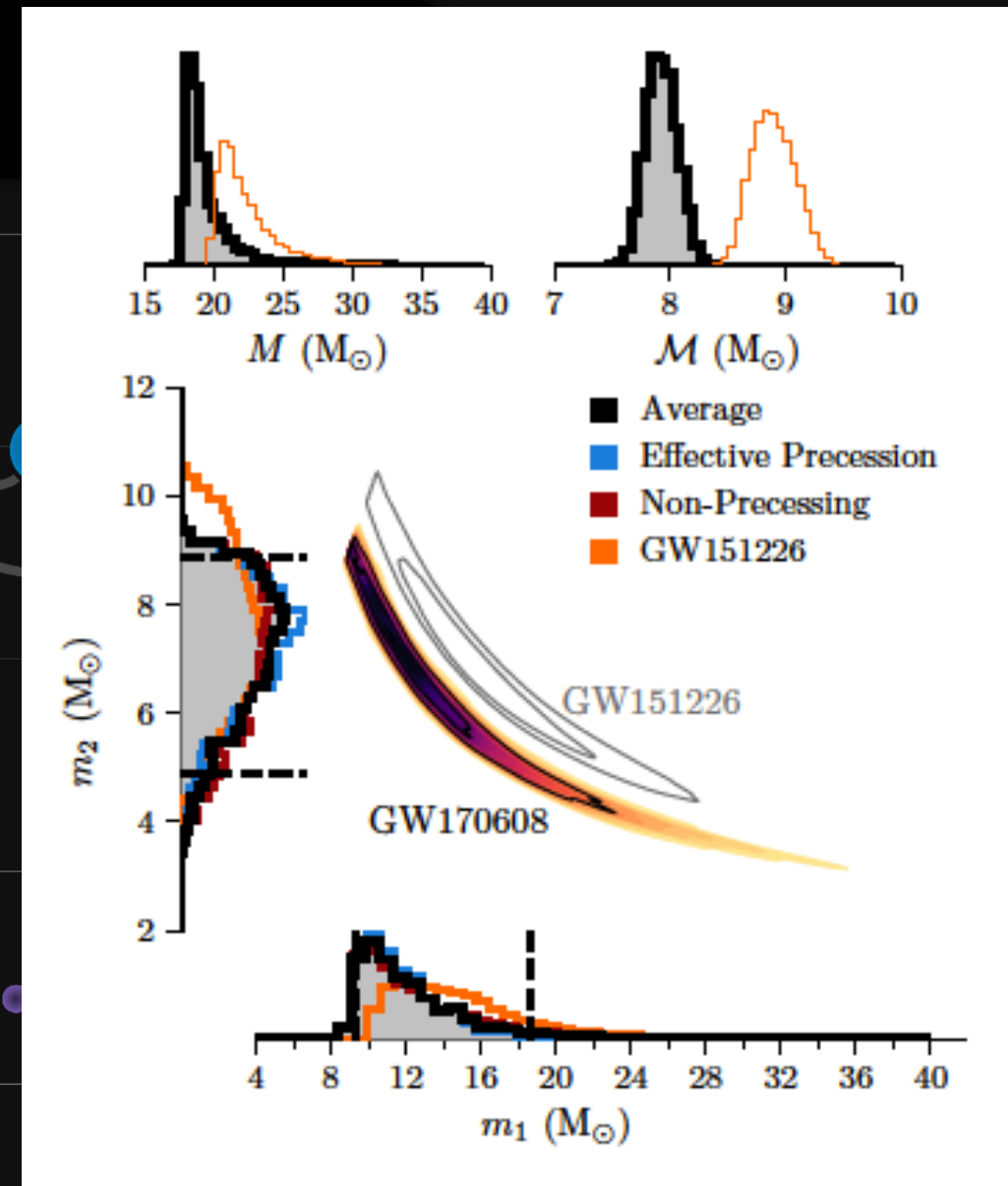
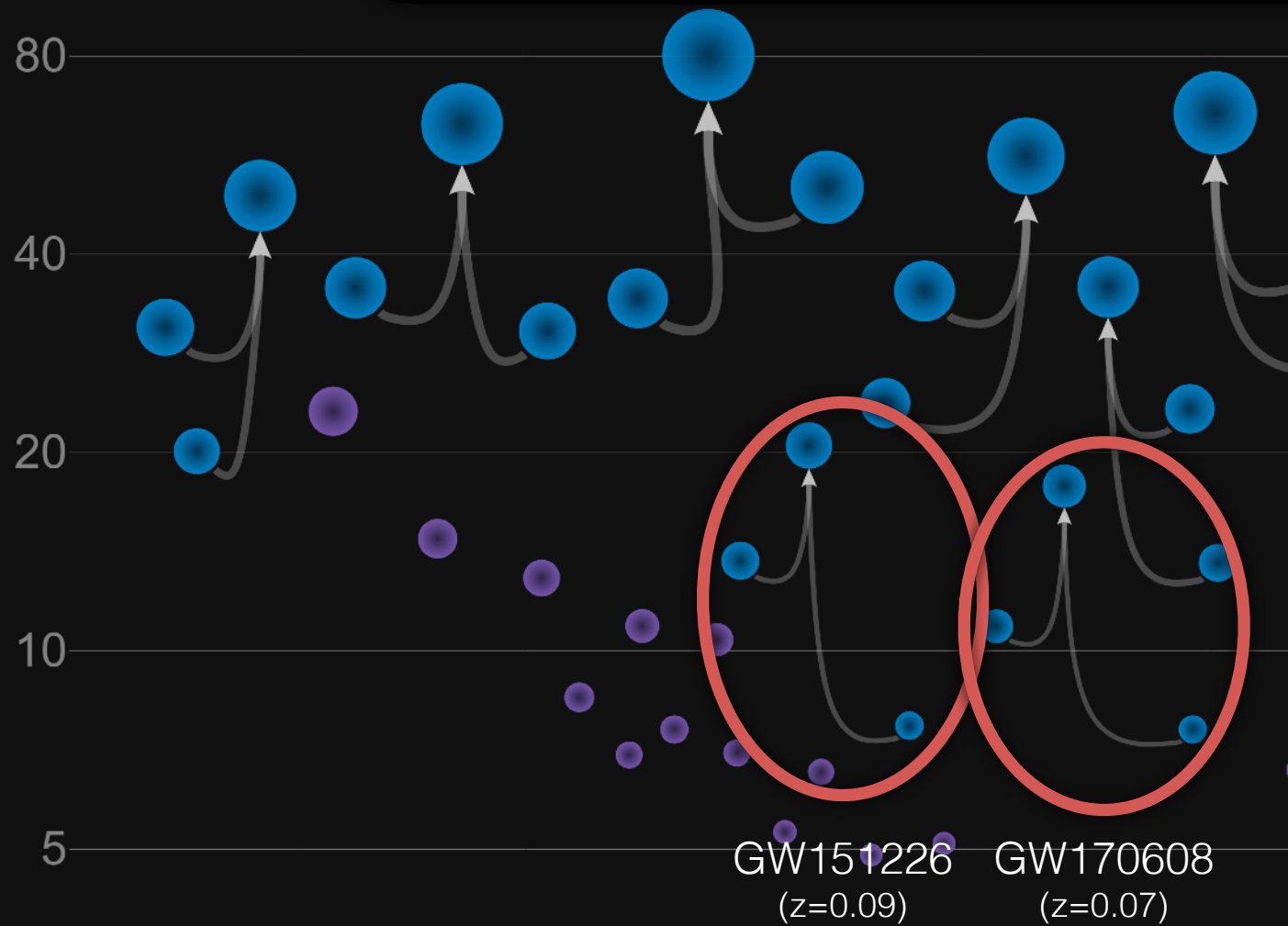


# GW151226 & GW170608: the lowest mass binary BH mergers in O1/O2 runs





# GW151226 & GW170608: the lowest mass binary BH mergers in O1/O2 runs



EM Neutron Stars

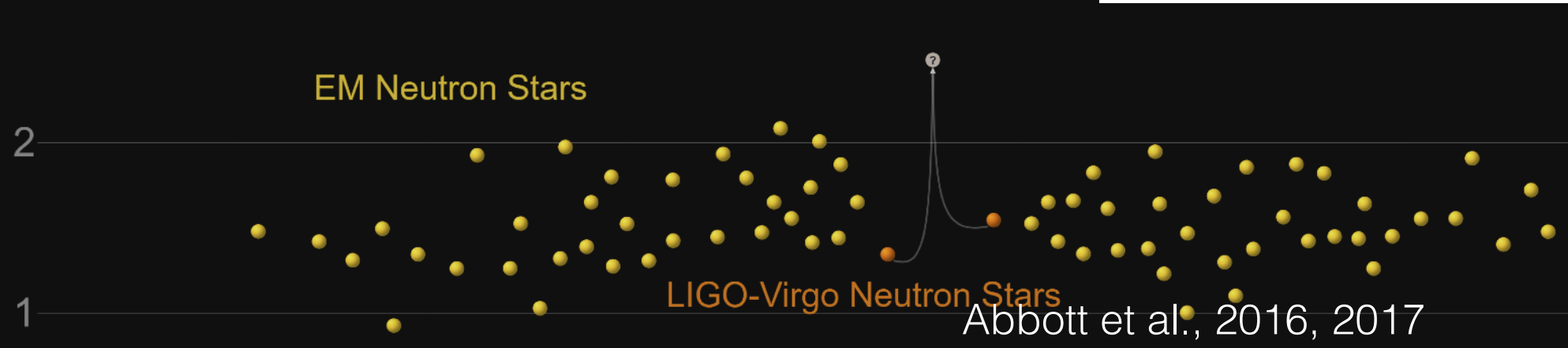
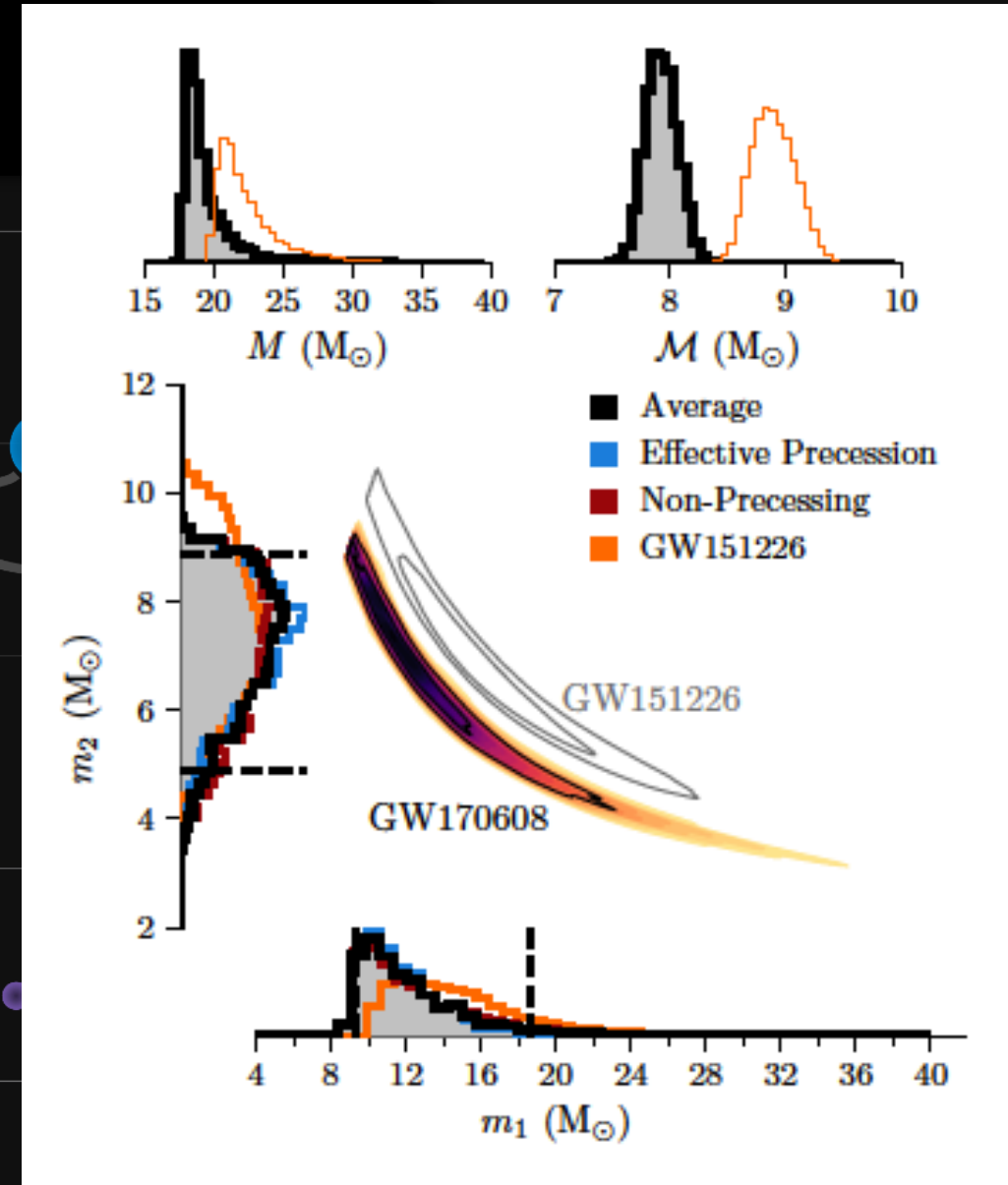
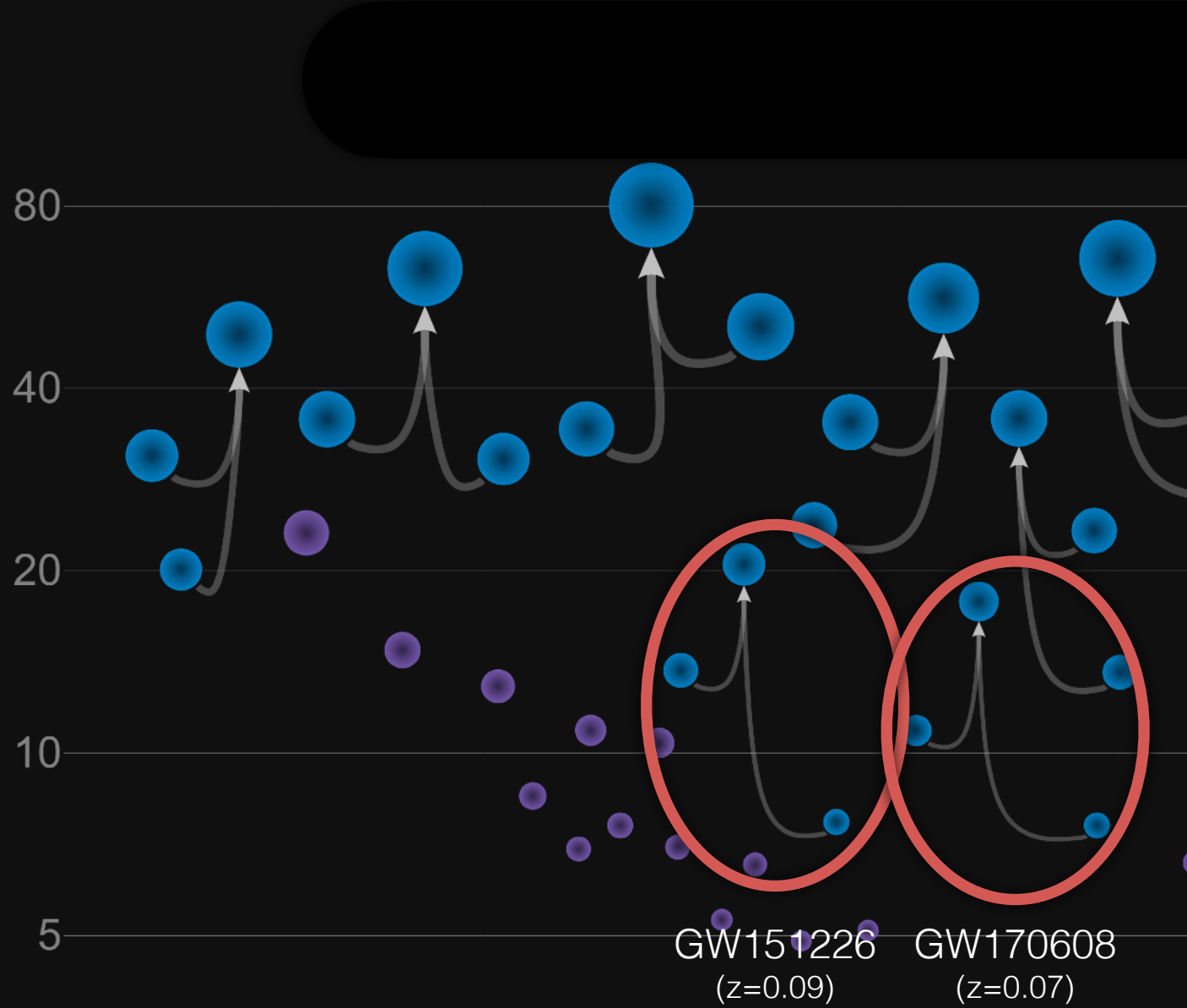


LIGO-Virgo Neutron Stars

Abbott et al., 2016, 2017



# GW151226 & GW170608: the lowest mass binary BH mergers in O1/O2 runs



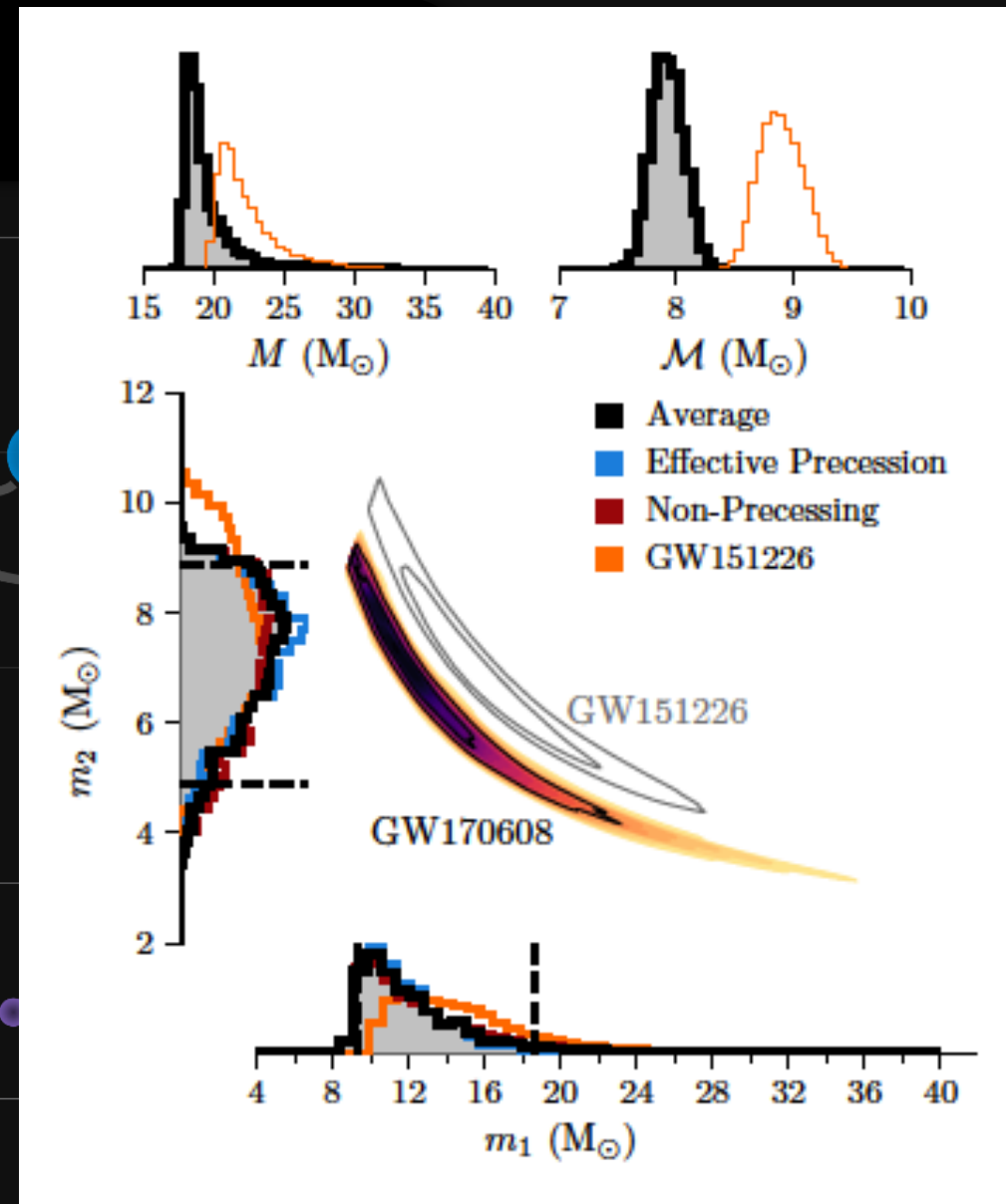
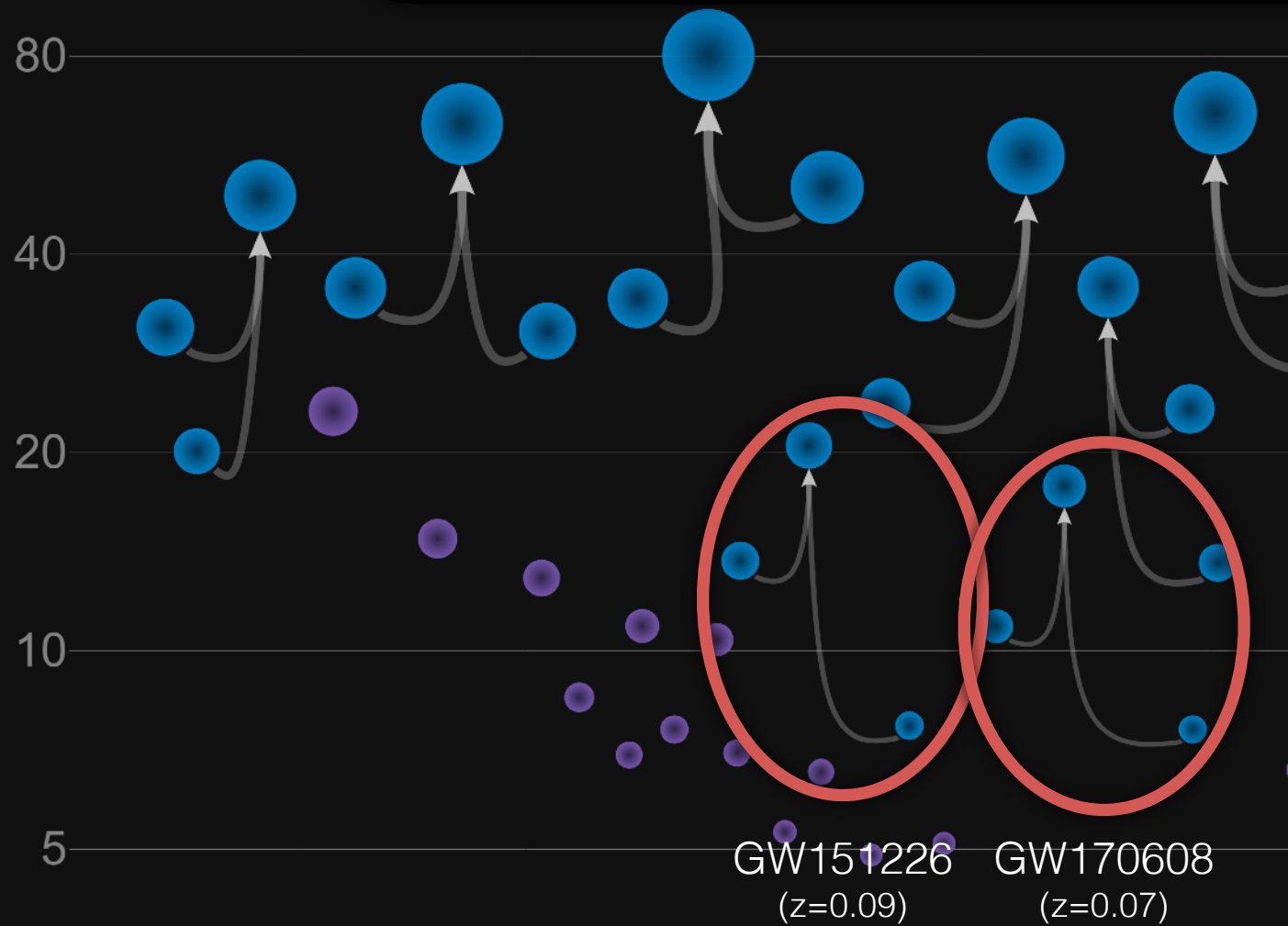
GW151226 ( $z=0.09$ )  
 $\mathcal{M}_{\text{chirp}} = 8.83^{+0.74}_{-0.66}$   
 $q_{\text{BBH}} = 0.56^{+0.44}_{-0.49}$   
 (100% CI de-redshifted)

GW170608 ( $z=0.07$ )  
 $\mathcal{M}_{\text{chirp}} = 7.91^{+0.43}_{-0.37}$   
 $q_{\text{BBH}} = 0.69^{+0.31}_{-0.56}$   
 (100% CI de-redshifted)

Abbott et al., 2016, 2017



# GW151226 & GW170608: the lowest mass binary BH mergers in O1/O2 runs



GW151226 ( $z=0.09$ )  
 $\mathcal{M}_{\text{chirp}} = 8.83^{+0.74}_{-0.66}$   
 $q_{\text{BBH}} = 0.56^{+0.44}_{-0.49}$   
 (100% CI de-redshifted)

GW170608 ( $z=0.07$ )  
 $\mathcal{M}_{\text{chirp}} = 7.91^{+0.43}_{-0.37}$   
 $q_{\text{BBH}} = 0.69^{+0.31}_{-0.56}$   
 (100% CI de-redshifted)

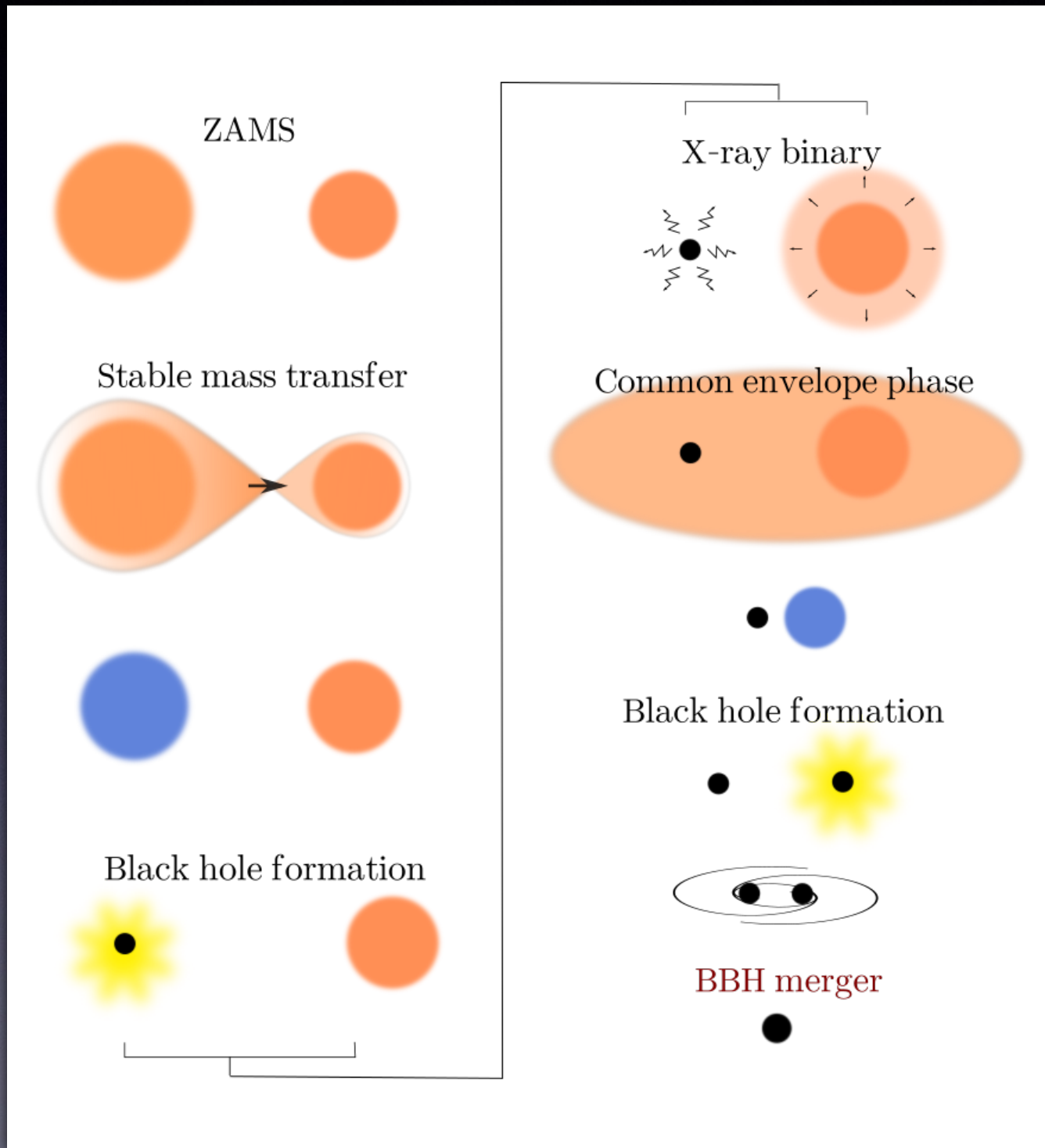
- Aims:** formation history, progenitor properties and expected rates of binary BH mergers detected during LIGO/Virgo O1/O2 runs, **low mass BH compatible with Galactic X-ray binaries** ( $M < 20 M_{\odot}$ )

LIGO-Virgo Neutron Stars

Abbott et al., 2016, 2017



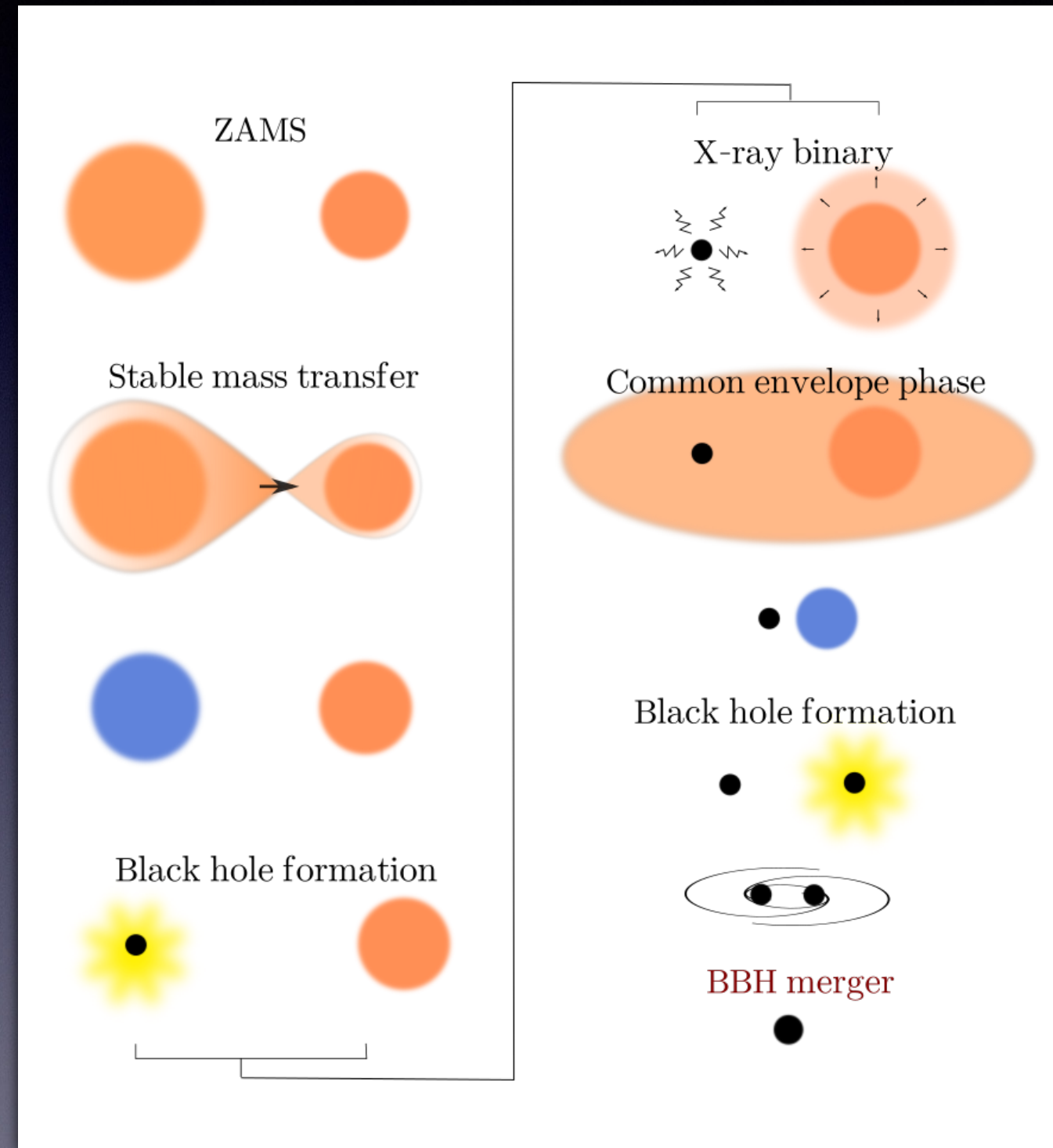
# Isolated binary evolution





# Isolated binary evolution

- « In the field »

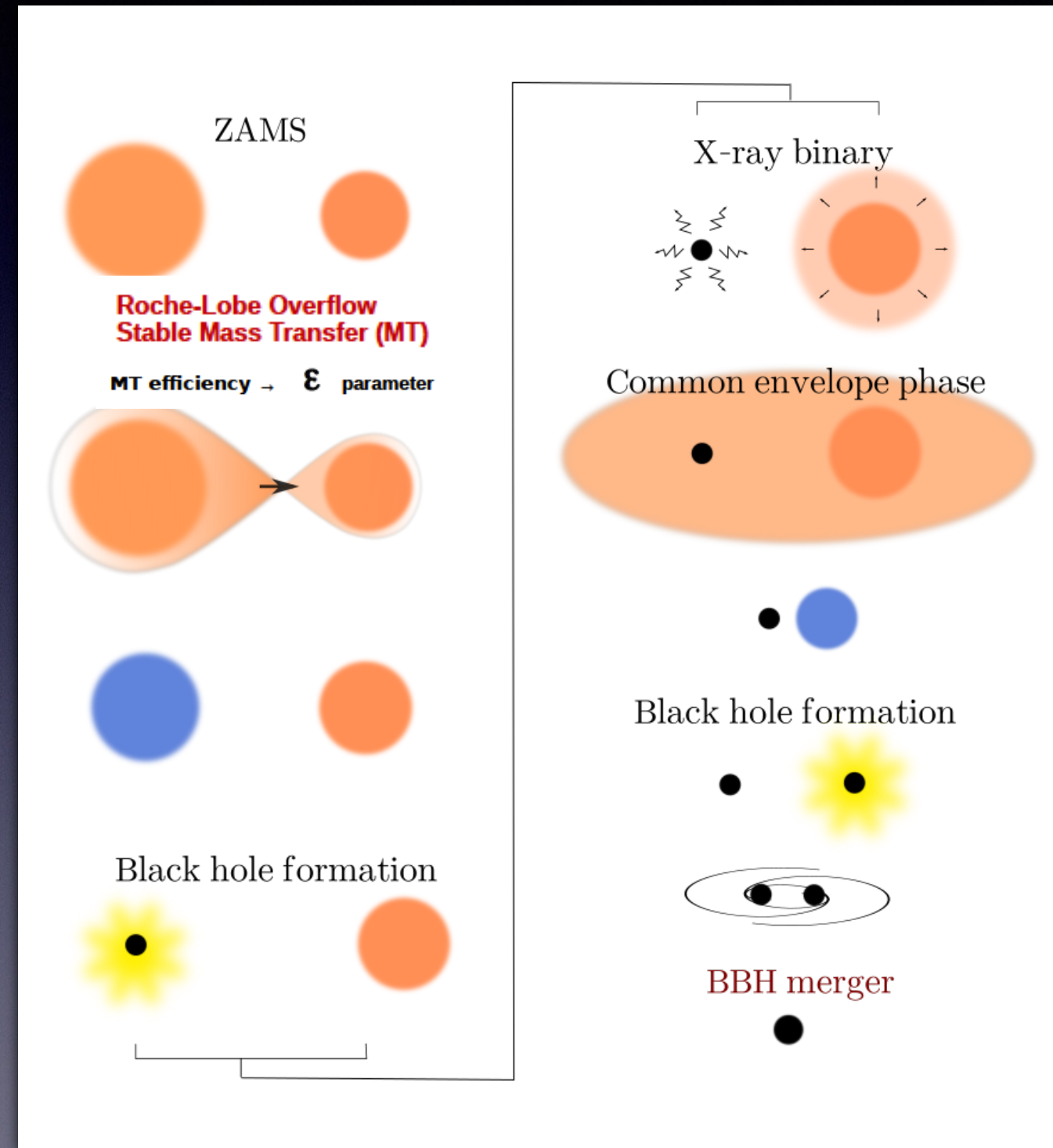


Scenario that we explored with 1D-hydrodynamical simulations



# Isolated binary evolution

- « In the field »

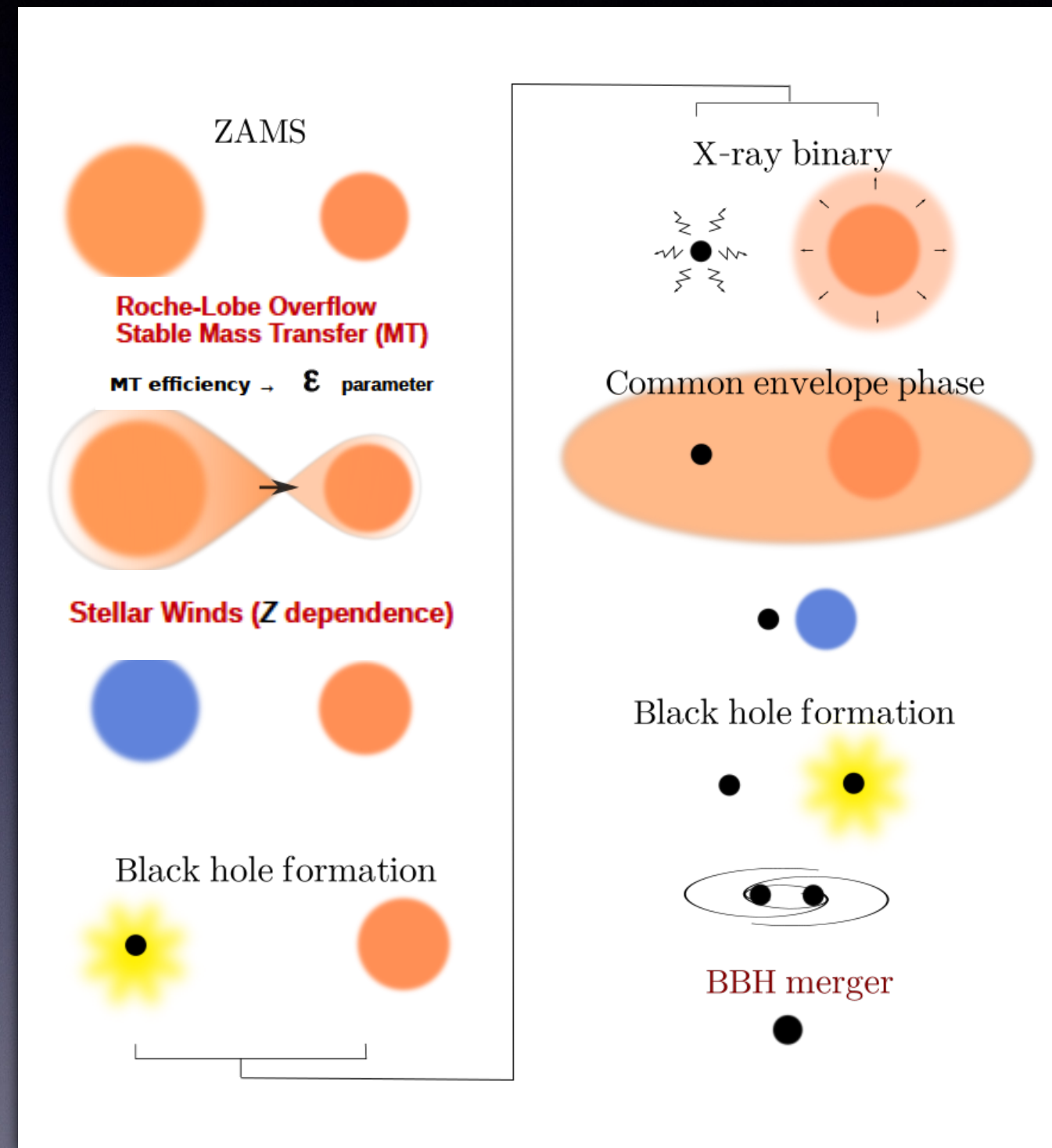


Scenario that we explored with 1D-hydrodynamical simulations



# Isolated binary evolution

- « In the field »

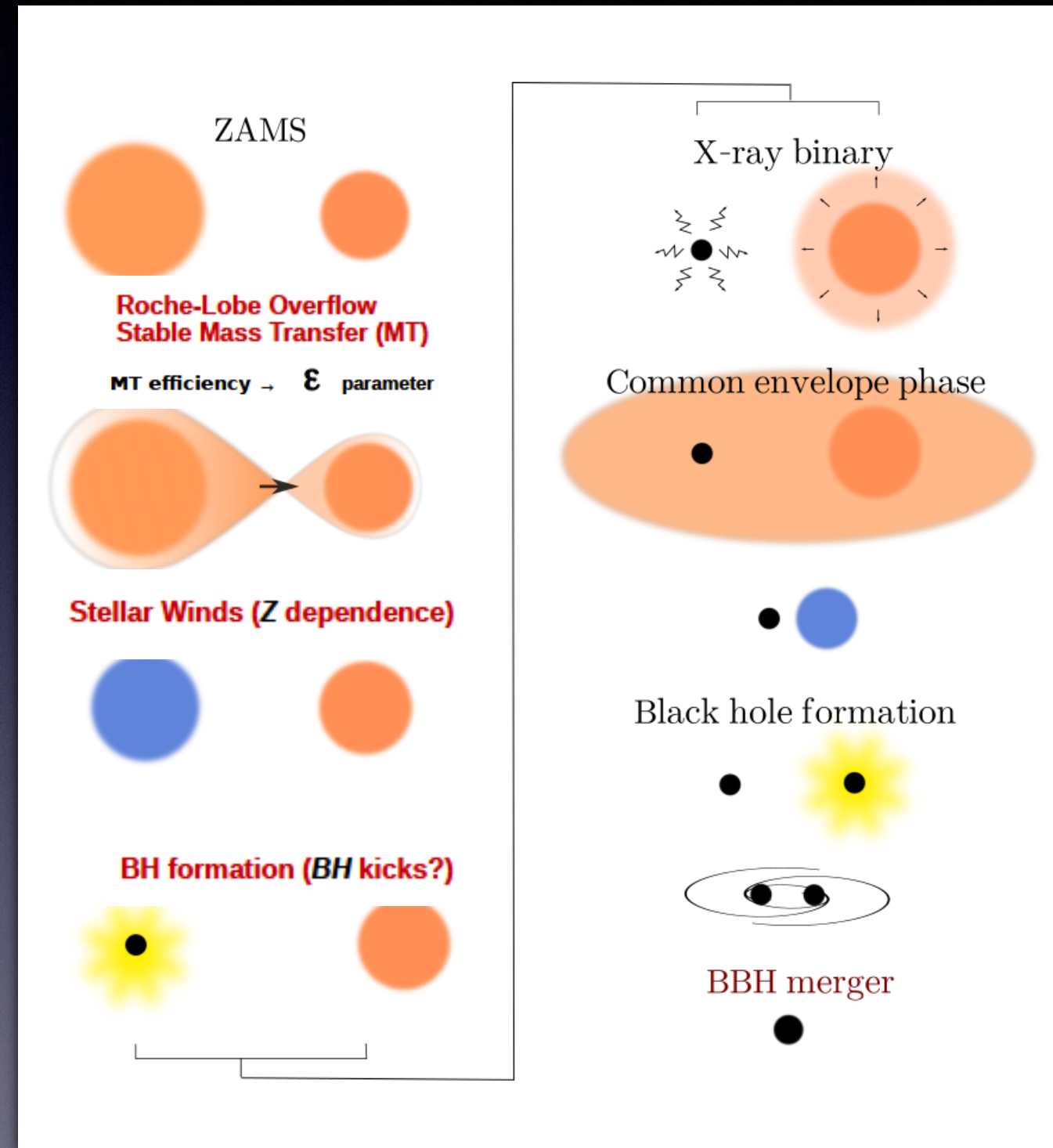


Scenario that we explored with 1D-hydrodynamical simulations



# Isolated binary evolution

- « In the field »

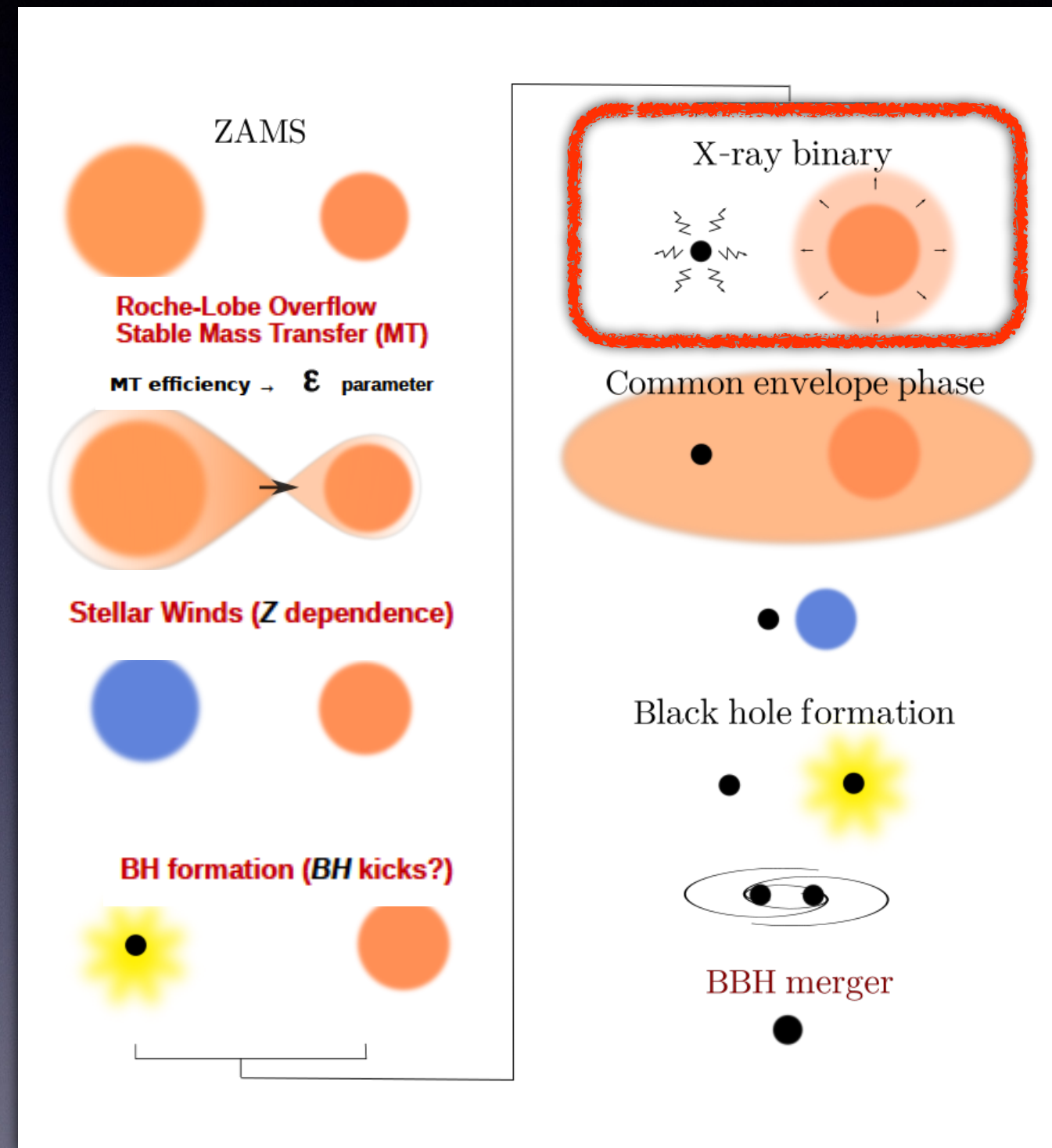


Scenario that we explored with 1D-hydrodynamical simulations



# Isolated binary evolution

- « In the field »

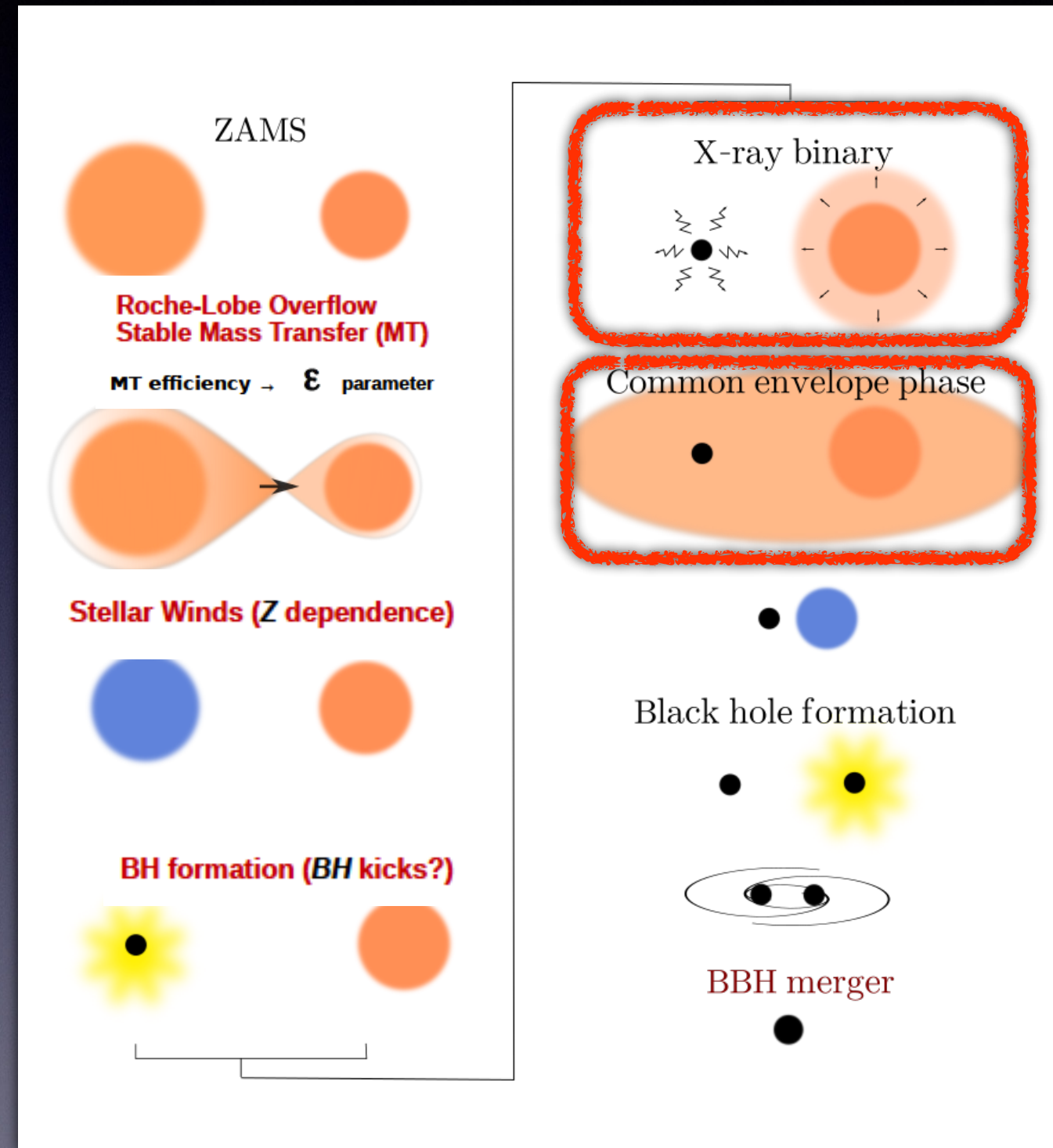


Scenario that we explored with 1D-hydrodynamical simulations



# Isolated binary evolution

- « In the field »
- Common Enveloppe Phase occurs **after HMXB**



Scenario that we explored with 1D-hydrodynamical simulations



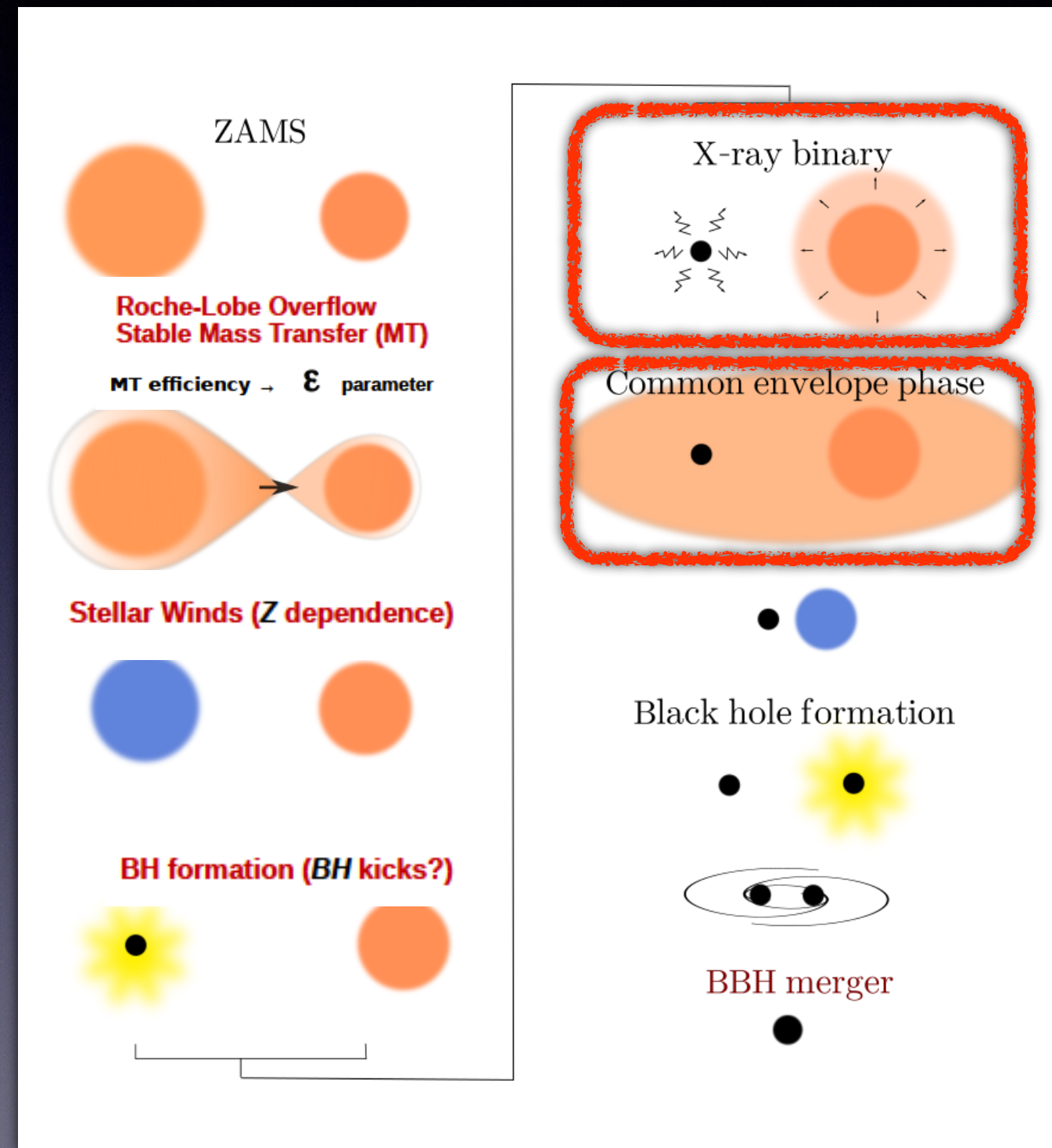
# Isolated binary evolution

**Common-envelope phase**  
**Unstable Mass Transfer**  
**(envelope unbinding)**

$$\Delta E_{\text{bind}} = \alpha_{\text{CE}} \Delta E_{\text{orb}},$$

$\alpha_{\text{CE}}$  efficiency parameter

- « In the field »
- Common Enveloppe Phase occurs **after HMXB**



Scenario that we explored with 1D-hydrodynamical simulations



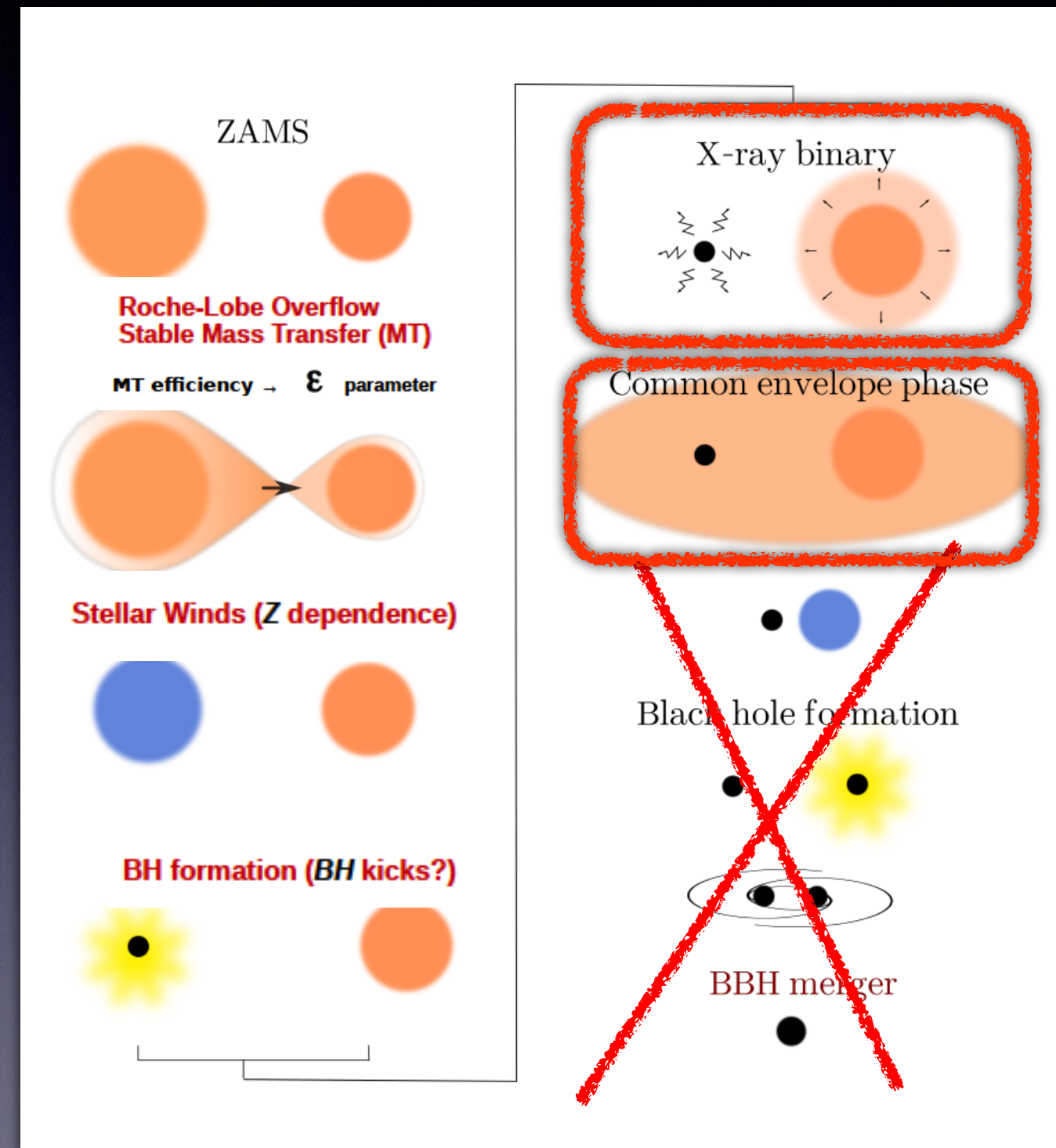
# Isolated binary evolution

Common-envelope phase  
Unstable Mass Transfer  
(envelope unbinding)

$$\Delta E_{\text{bind}} = \alpha_{\text{CE}} \Delta E_{\text{orb}},$$

$\alpha_{\text{CE}}$  efficiency parameter

- « In the field »
- Common Enveloppe Phase occurs **after HMXB**
- Short  $P_{\text{orb}}$  (<1yr) HMXB do not survive CE => Thorne-Zytkow objects!  
(Tauris+2017 ApJ)



Scenario that we explored with 1D-hydrodynamical simulations



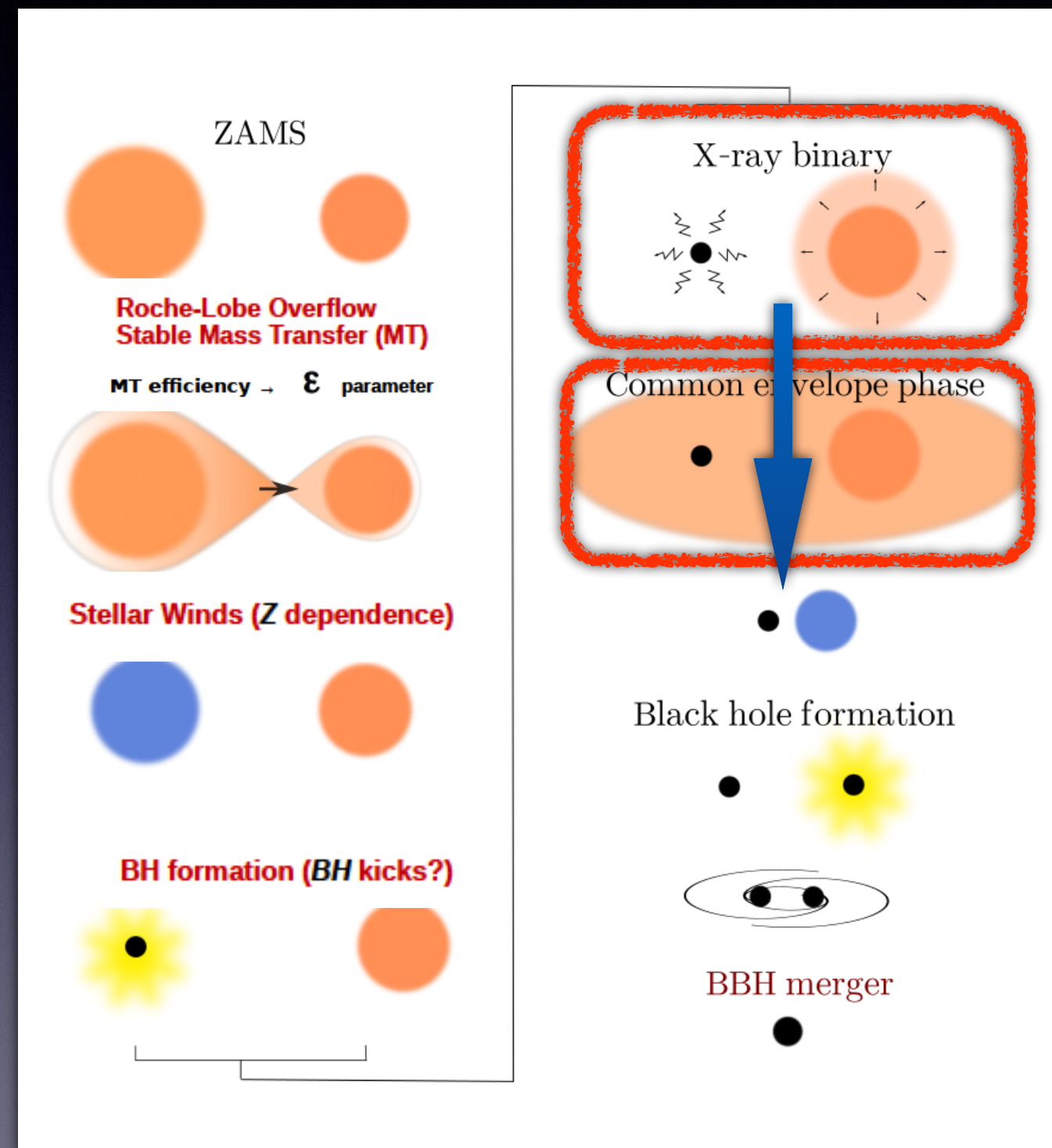
# Isolated binary evolution

**Common-envelope phase  
Unstable Mass Transfer  
(envelope unbinding)**

$$\Delta E_{\text{bind}} = \alpha_{\text{CE}} \Delta E_{\text{orb}},$$

$\alpha_{\text{CE}}$  efficiency parameter

- « In the field »
- Common Enveloppe Phase occurs **after HMXB**
- Short  $P_{\text{orb}} (< 1 \text{ yr})$  HMXB do not survive CE => Thorne-Zytkow objects!  
(Tauris+2017 ApJ)
- Long  $P_{\text{orb}} (> 1 \text{ yr})$  HMXB will go through, survive CE, until eventually BNS or BBH will merge in BH



Scenario that we explored with 1D-hydrodynamical simulations



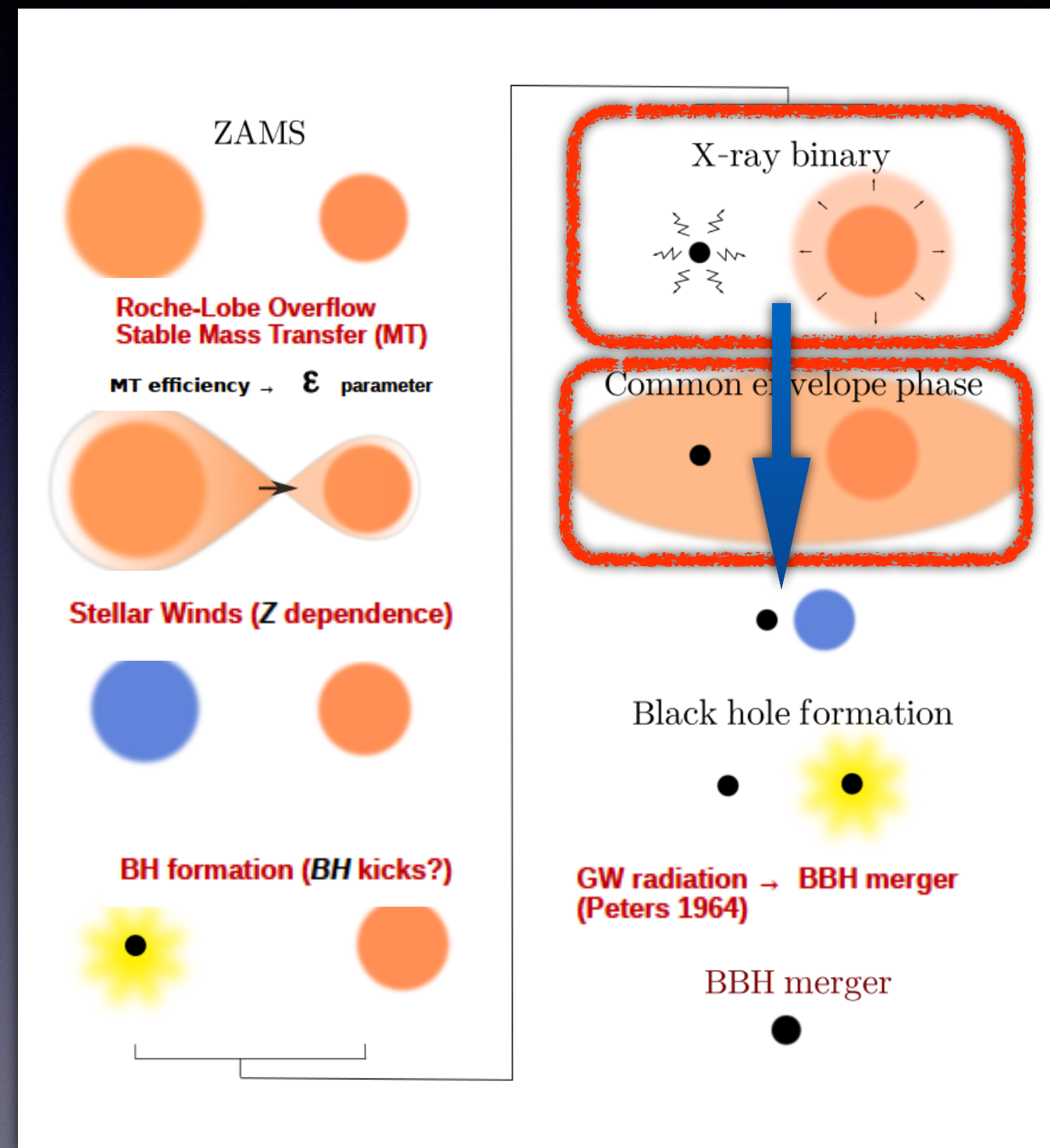
# Isolated binary evolution

**Common-envelope phase**  
**Unstable Mass Transfer**  
**(envelope unbinding)**

$$\Delta E_{\text{bind}} = \alpha_{\text{CE}} \Delta E_{\text{orb}},$$

$\alpha_{\text{CE}}$  efficiency parameter

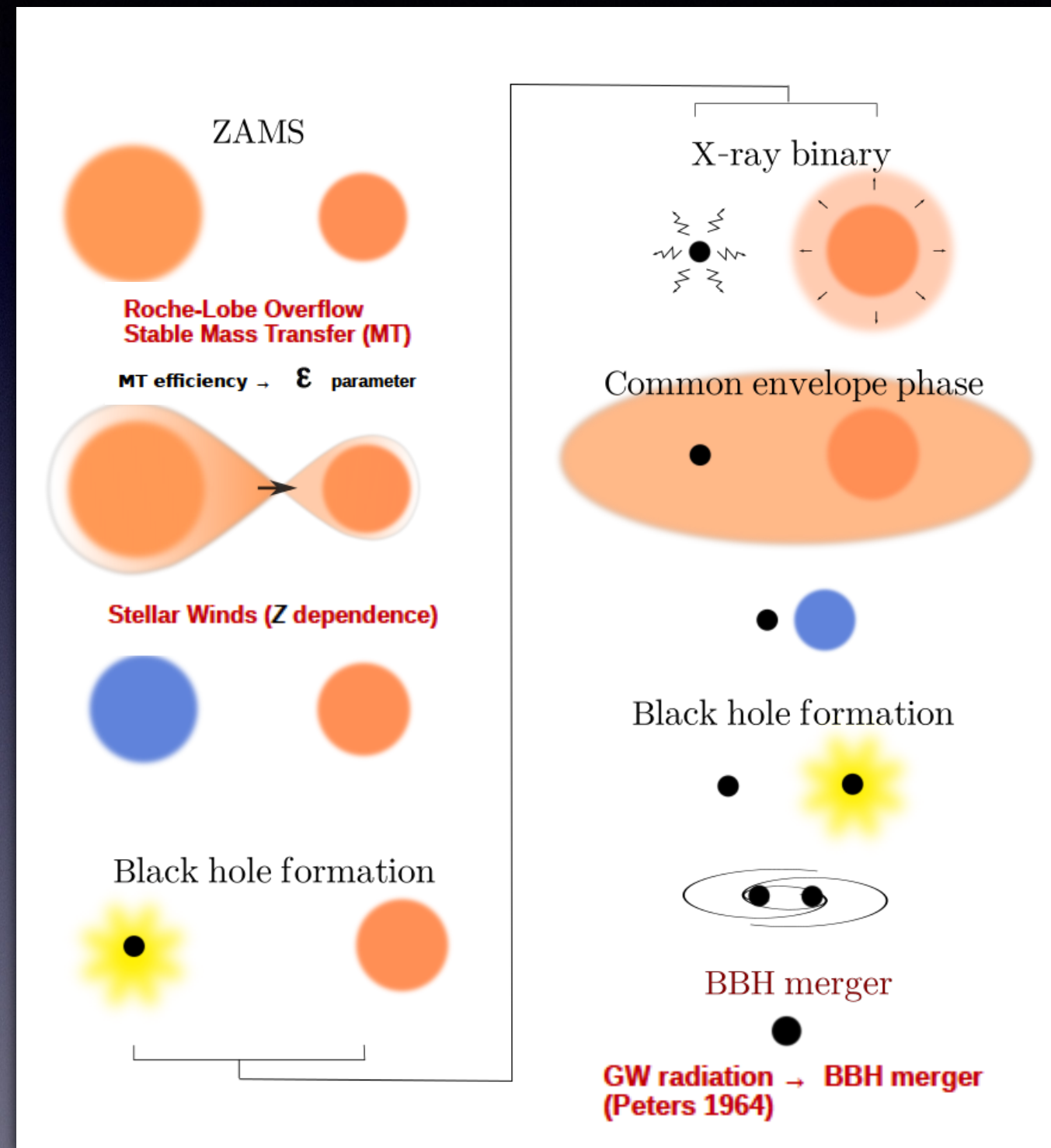
- « In the field »
- Common Enveloppe Phase occurs **after HMXB**
- Short  $P_{\text{orb}} (< 1 \text{ yr})$  HMXB do not survive CE => Thorne-Zytkow objects!  
 (Tauris+2017 ApJ)
- Long  $P_{\text{orb}} (> 1 \text{ yr})$  HMXB will go through, survive CE, until eventually BNS or BBH will merge in BH



Scenario that we explored with 1D-hydrodynamical simulations



# Isolated binary evolution

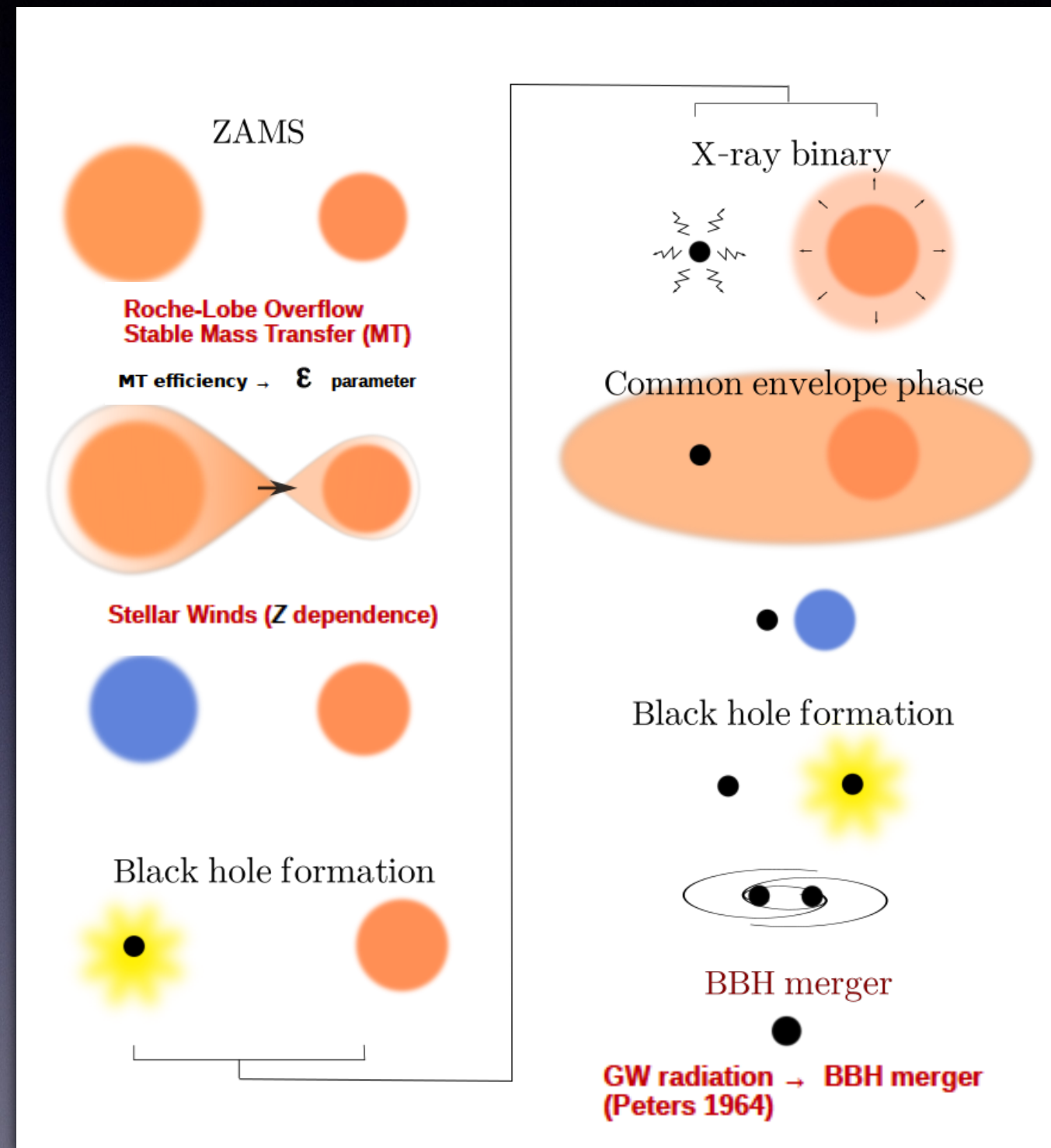


Non-rotating stars, circular orbits and no asymmetric kicks



# Isolated binary evolution

- **Method:** simulations with **MESA**<sup>1</sup> (1D-hydrodynamic stellar code) inc. binary evolution package [**MESAbinary**]



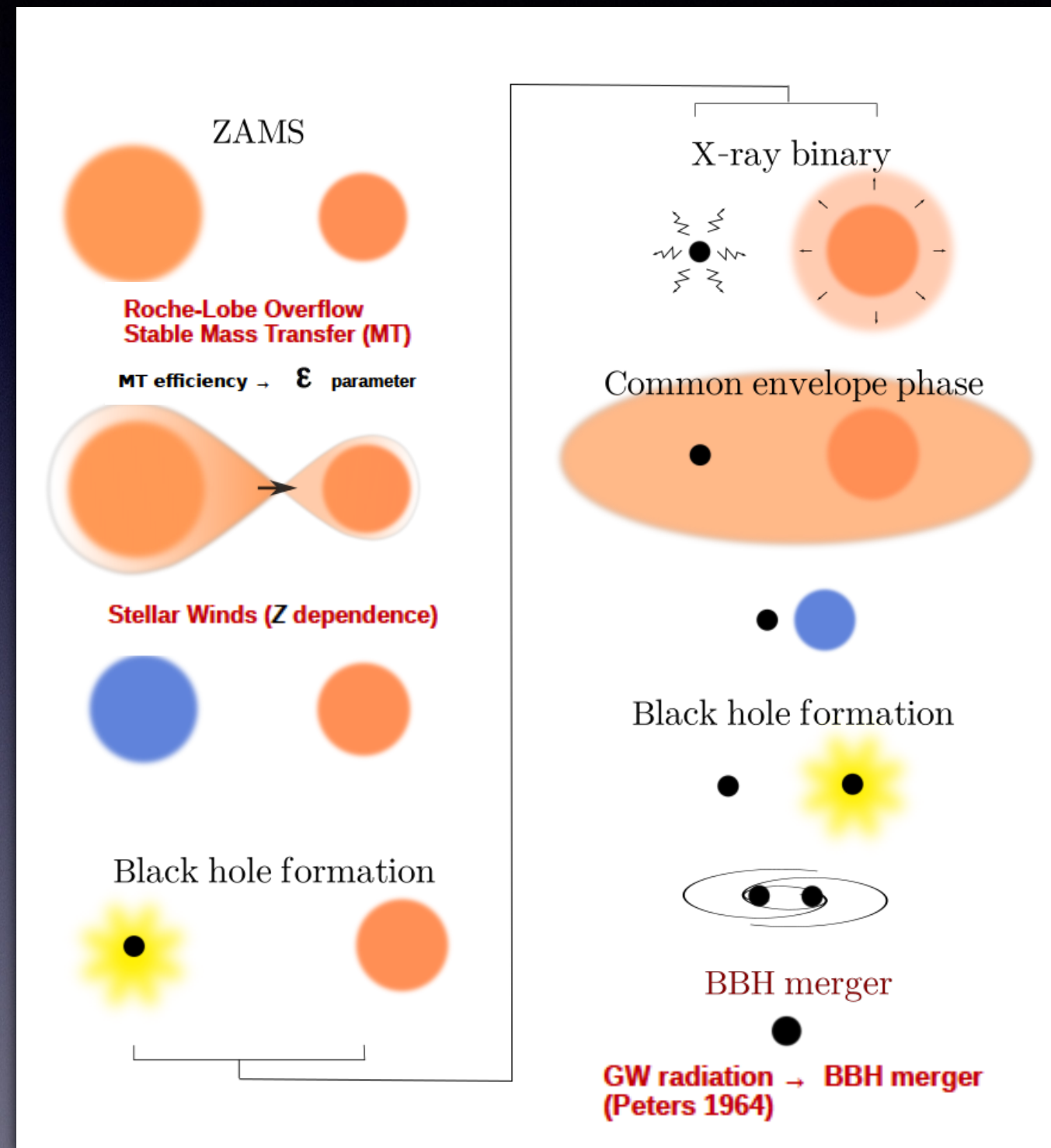
Non-rotating stars, circular orbits and no asymmetric kicks

• <sup>1</sup><http://mesa.sourceforge.net>  
S. Chaty



# Isolated binary evolution

- **Method:** simulations with **MESA**<sup>1</sup> (1D-hydrodynamic stellar code) inc. binary evolution package [**MESAbinary**]
- To model full binary evolution in a single run from its formation to BBH merger, we incorporated 2 packages in MESA:



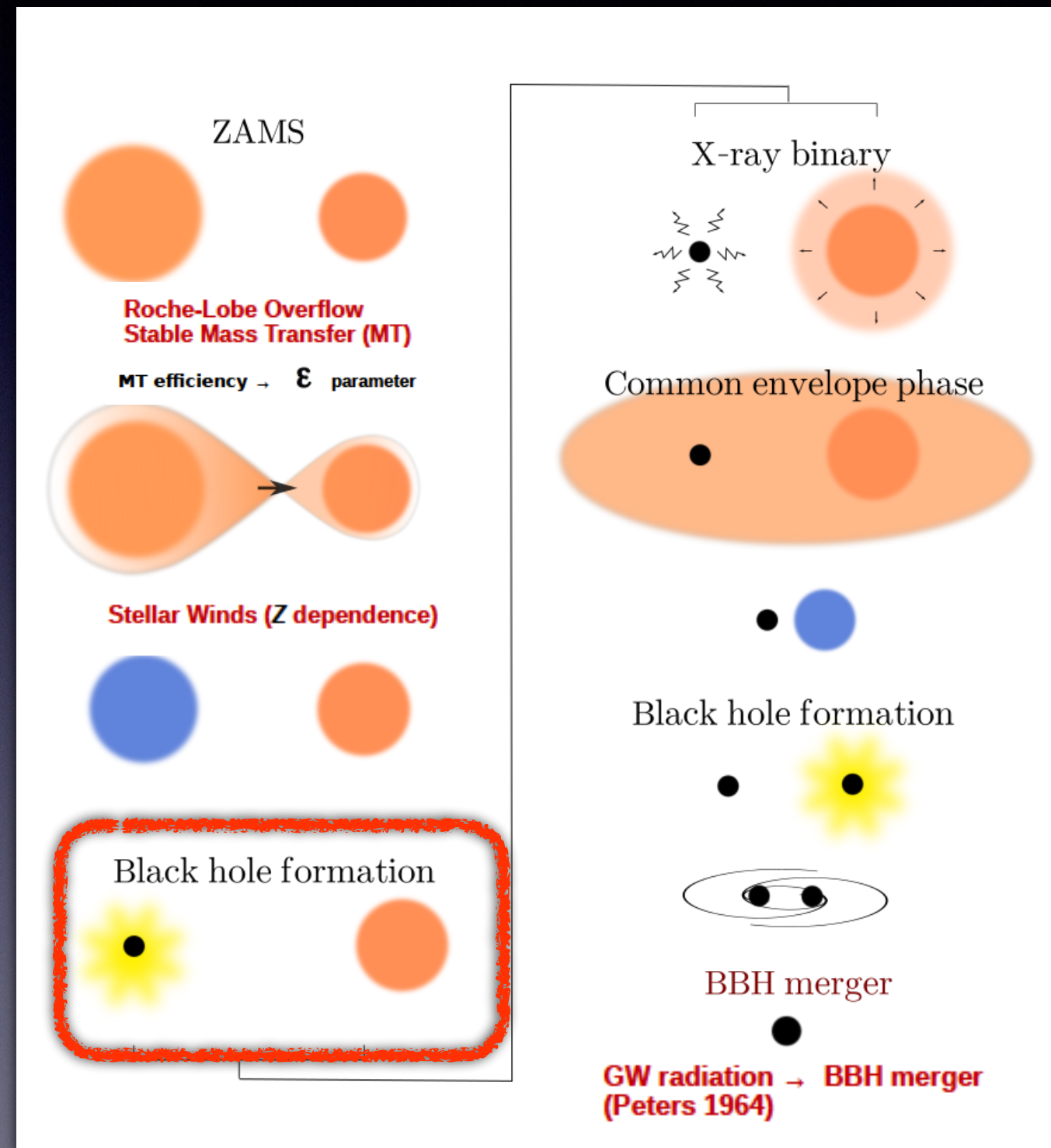
Non-rotating stars, circular orbits and no asymmetric kicks

• <sup>1</sup><http://mesa.sourceforge.net>  
S. Chaty



# Isolated binary evolution

- **Method:** simulations with **MESA**<sup>1</sup> (1D-hydrodynamic stellar code) inc. binary evolution package [**MESAbinary**]
- To model full binary evolution in a single run from its formation to BBH merger, we incorporated 2 packages in MESA:
  - **BH formation:** *delayed CO* core-collapse prescription (Fryer+2012)



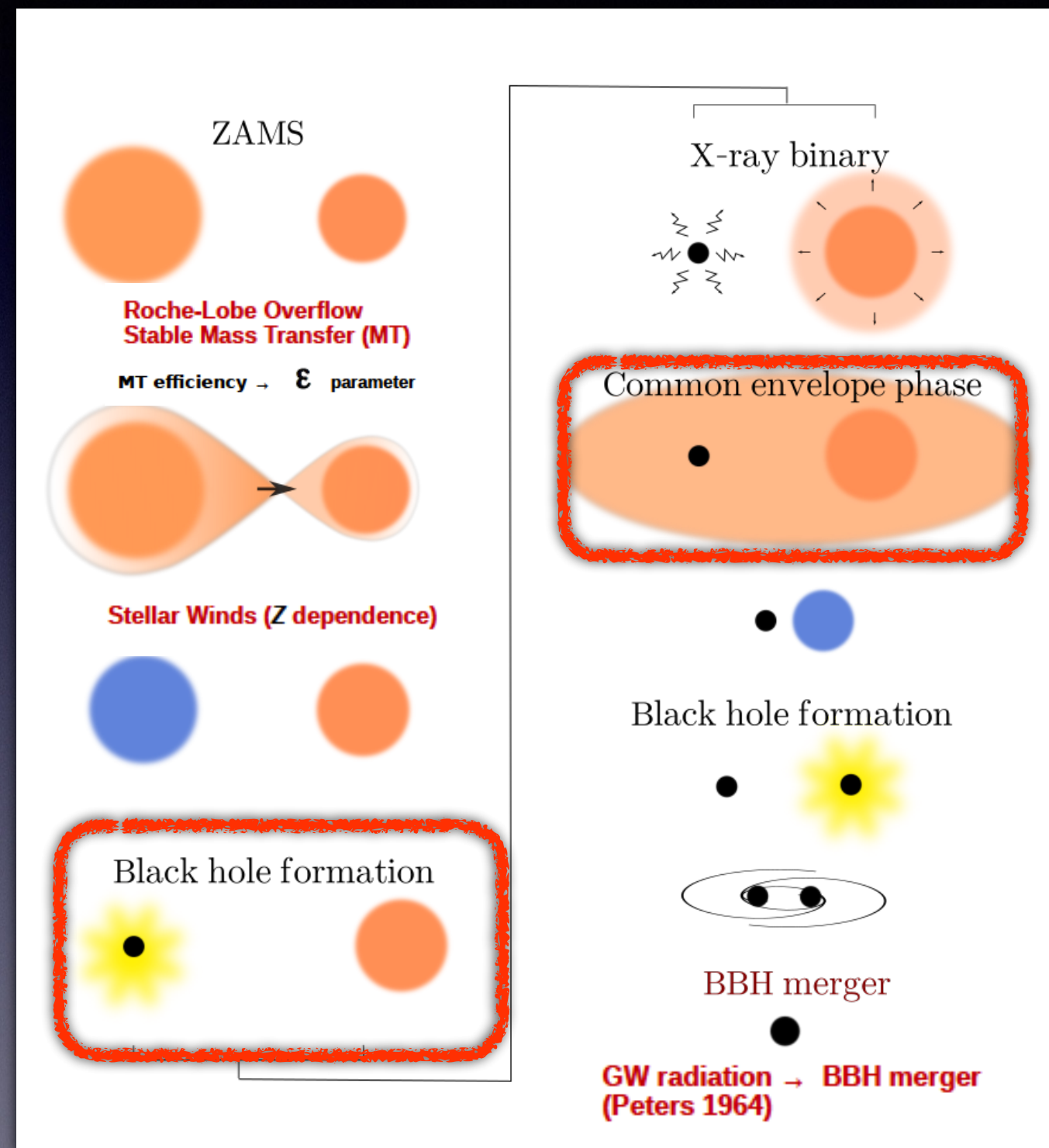
Non-rotating stars, circular orbits and no asymmetric kicks

• <sup>1</sup><http://mesa.sourceforge.net>  
S. Chaty



# Isolated binary evolution

- **Method:** simulations with **MESA**<sup>1</sup> (1D-hydrodynamic stellar code) inc. binary evolution package [**MESAbinary**]
- To model full binary evolution in a single run from its formation to BBH merger, we incorporated 2 packages in MESA:
  - **BH formation:** *delayed CO* core-collapse prescription (Fryer+2012)
  - **Common envelope** (CE) phase: unstable mass transfer ( $\alpha_{CE}$ )

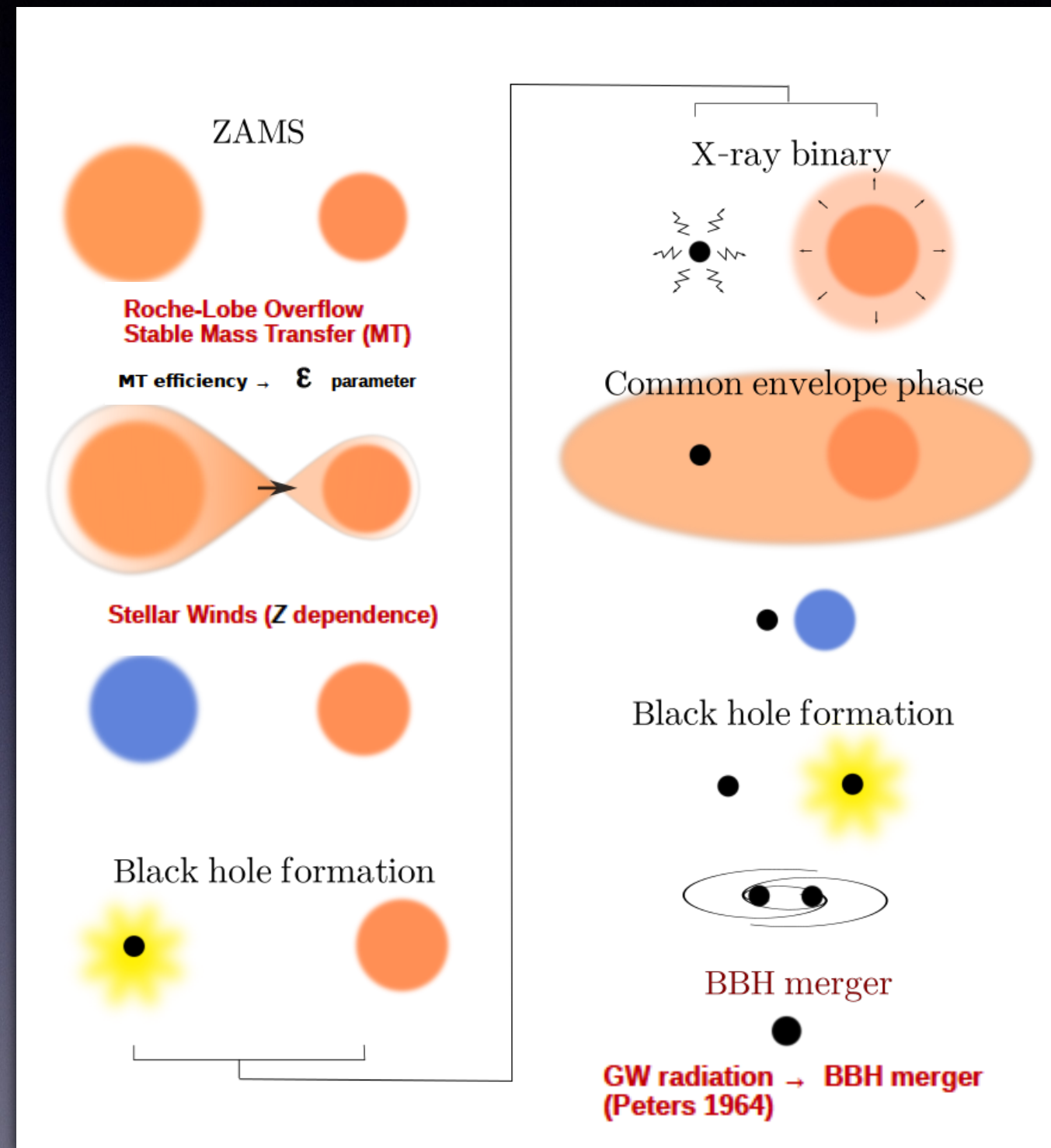


Non-rotating stars, circular orbits and no asymmetric kicks

• <sup>1</sup><http://mesa.sourceforge.net>  
S. Chaty



# Isolated binary evolution



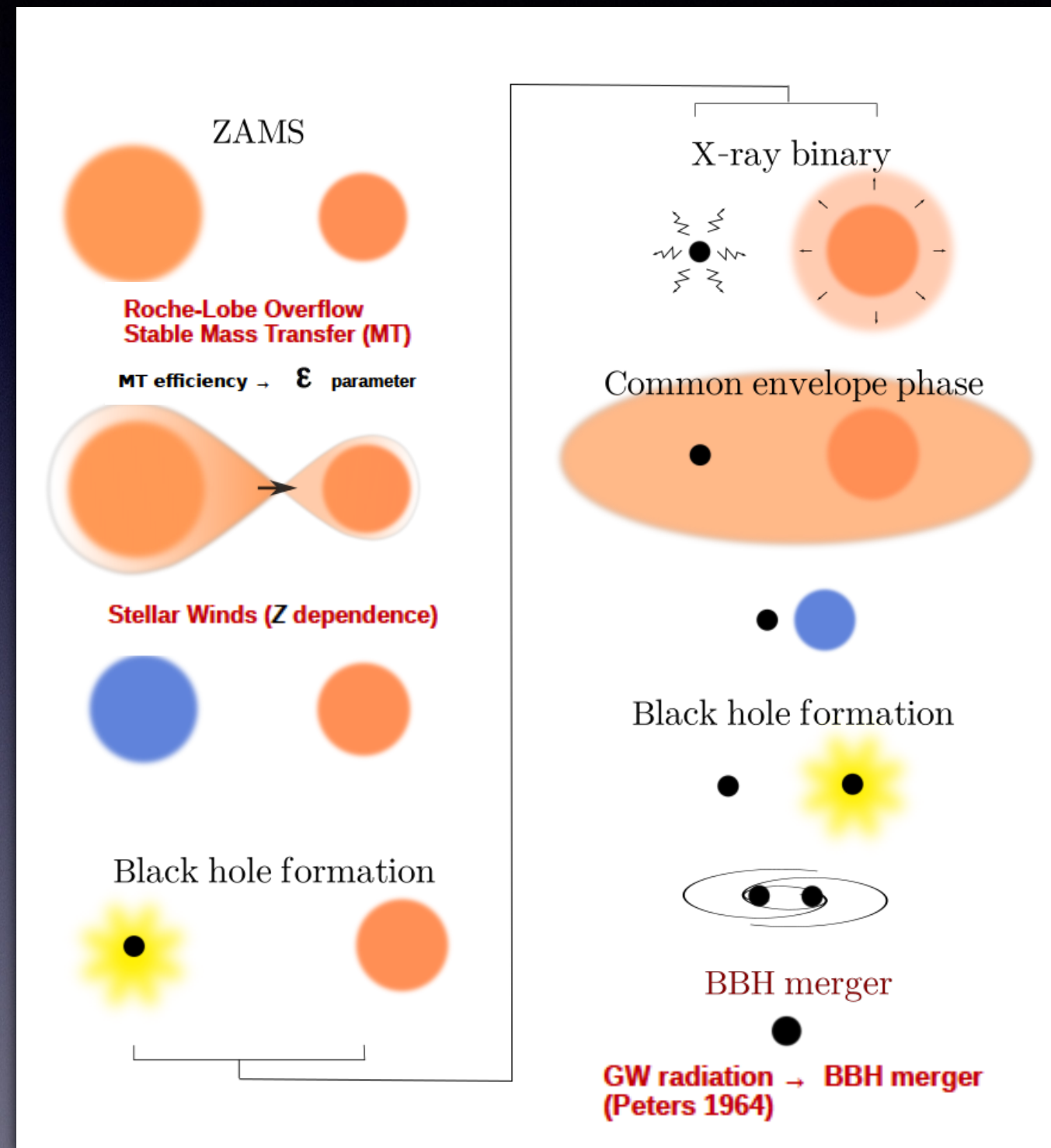
$[Z_{\odot} = 12 \times 10^{-3}]$

Non-rotating stars, circular orbits and no asymmetric kicks



# Isolated binary evolution

- Explore a wide parameter space (+66 000 simulations):



$[Z_{\odot} = 12 \times 10^{-3}]$

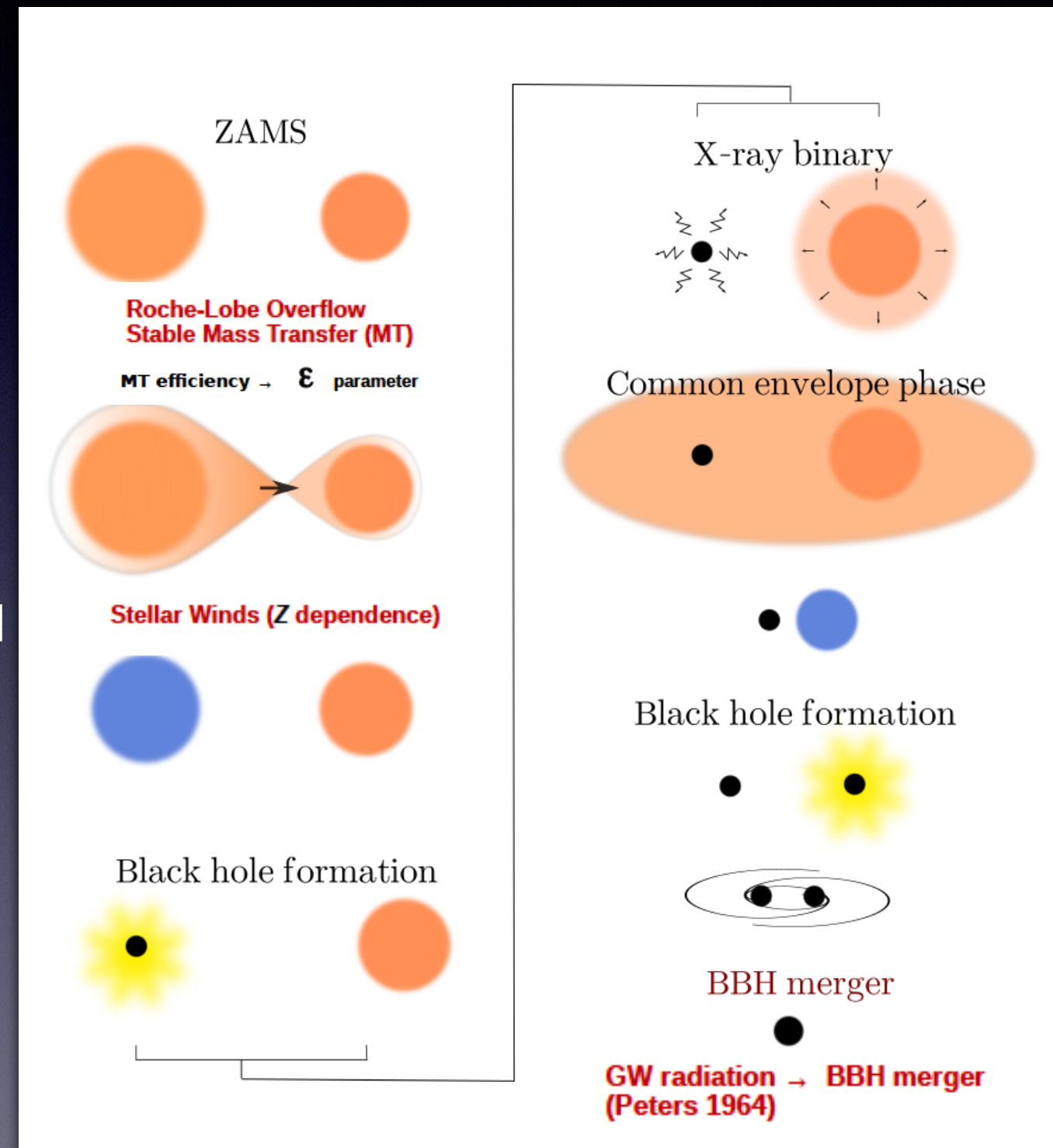
Non-rotating stars, circular orbits and no asymmetric kicks



# Isolated binary evolution

- **Explore a wide parameter space (+66 000 simulations):**

- initial stellar masses [ 20 - 34  $M_{\odot}$  ]
- orbital separations [ 30 - 200  $R_{\odot}$  ]
- 4 metallicities [  $Z = 0.1, 1, 4, 7, 15$  ]  $\times 10^{-3}$
- 4 stable MT efficiencies [  $\epsilon = 0.0, 0.2, 0.4, 0.6$  ]
- 2 unstable MT efficiencies [  $\alpha_{CE} = 1.0, 2.0$  ]



[ $Z_{\odot} = 12 \times 10^{-3}$ ]

Non-rotating stars, circular orbits and no asymmetric kicks

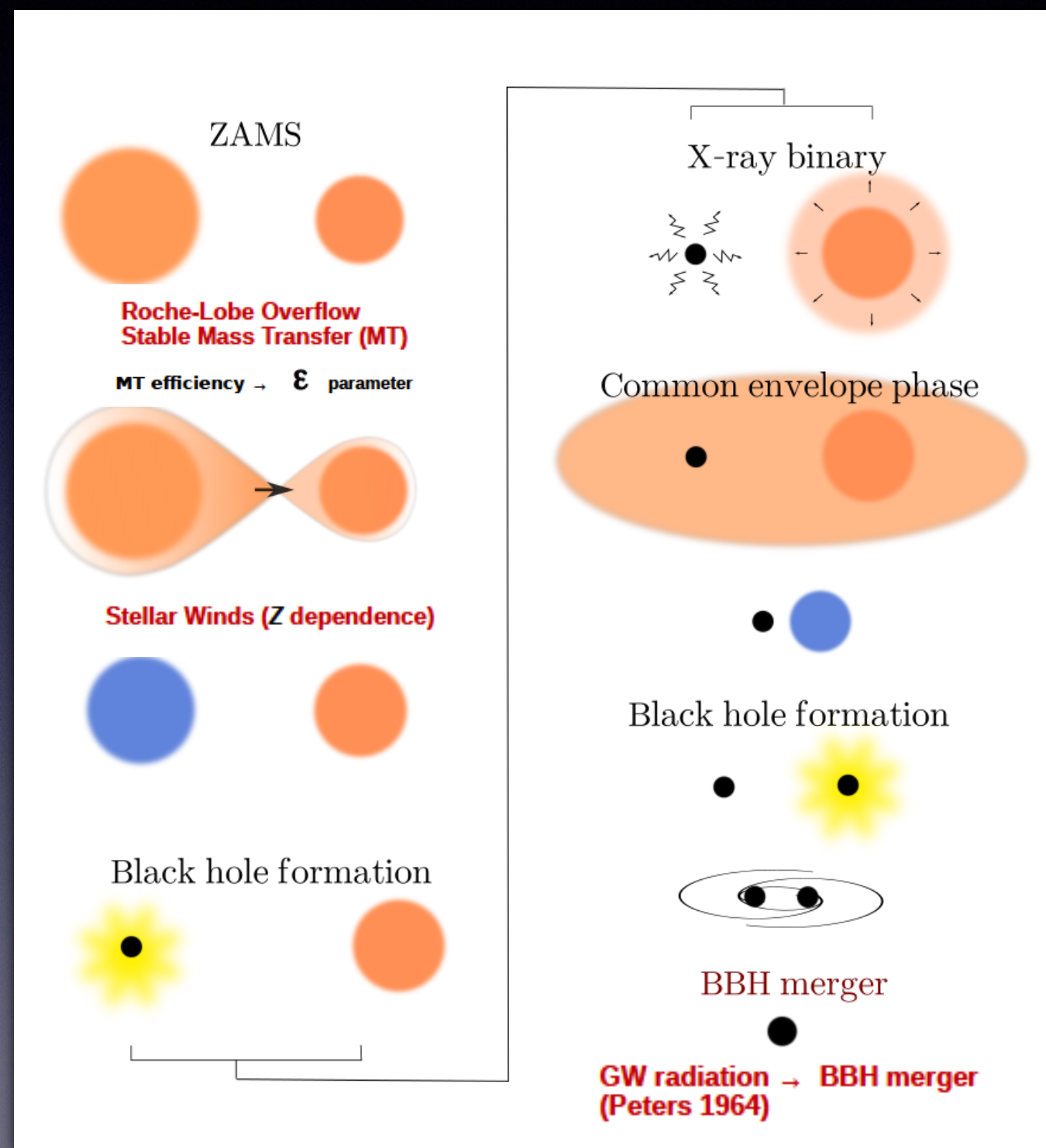


# Isolated binary evolution

- **Explore a wide parameter space (+66 000 simulations):**

- initial stellar masses [ 20 - 34  $M_{\odot}$  ]
- orbital separations [ 30 - 200  $R_{\odot}$  ]
- 4 metallicities [  $Z = 0.1, 1, 4, 7, 15$  ]  $\times 10^{-3}$
- 4 stable MT efficiencies [  $\epsilon = 0.0, 0.2, 0.4, 0.6$  ]
- 2 unstable MT efficiencies [  $\alpha_{CE} = 1.0, 2.0$  ]

- **Looking for:** binary progenitors leading to BBH with mass & merger-time delay compatible with detected GW events



Non-rotating stars, circular orbits and no asymmetric kicks

$$[Z_{\odot} = 12 \times 10^{-3}]$$



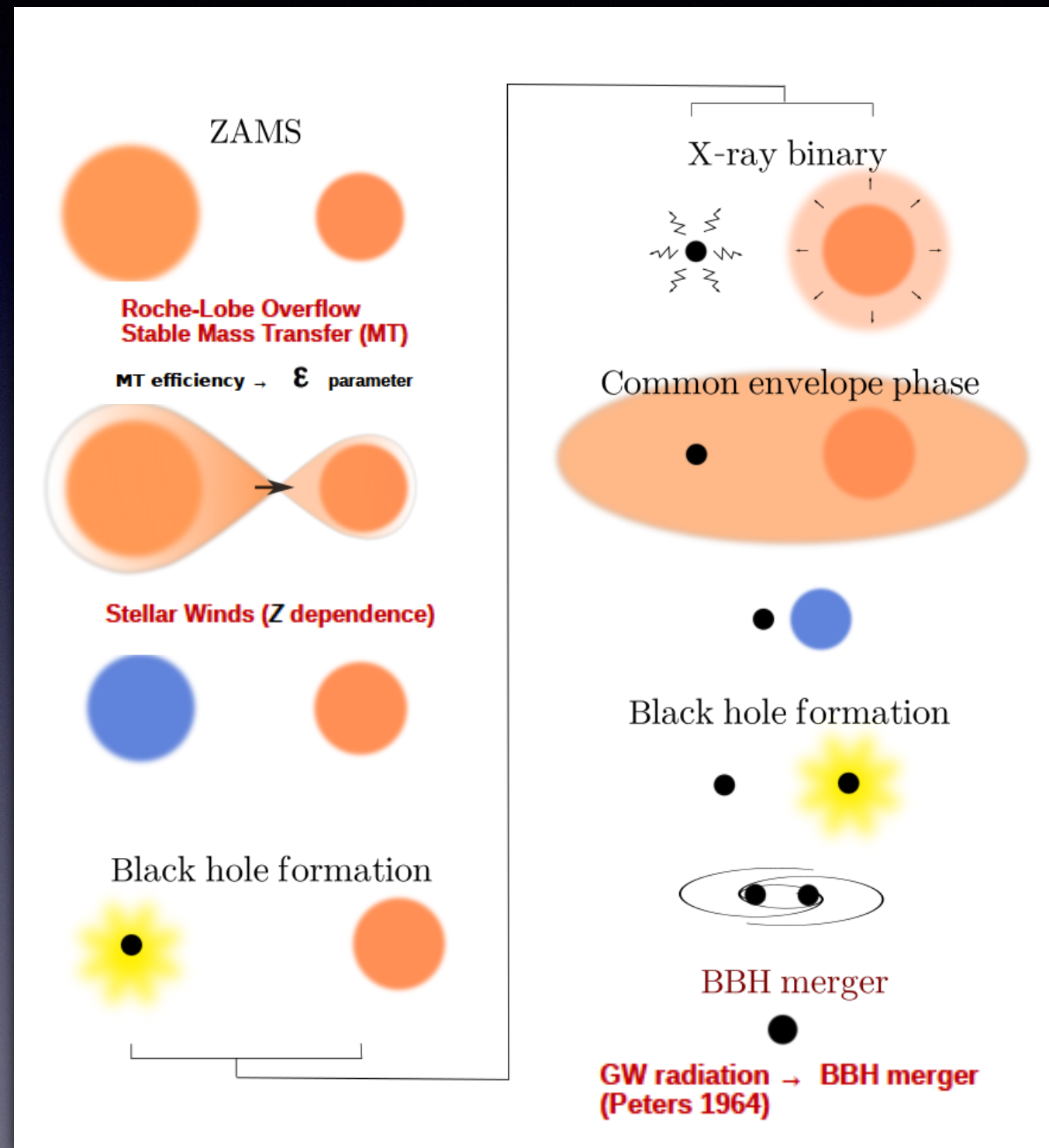
# Isolated binary evolution

- **Explore a wide parameter space (+66 000 simulations):**

- initial stellar masses [ 20 - 34  $M_{\odot}$  ]
- orbital separations [ 30 - 200  $R_{\odot}$  ]
- 4 metallicities [  $Z = 0.1, 1, 4, 7, 15$  ]  $\times 10^{-3}$
- 4 stable MT efficiencies [  $\epsilon = 0.0, 0.2, 0.4, 0.6$  ]
- 2 unstable MT efficiencies [  $\alpha_{CE} = 1.0, 2.0$  ]

- **Looking for:** binary progenitors leading to BBH with mass & merger-time delay compatible with detected GW events

- **Compare** local merger-rate densities with GW events detected by LIGO-Virgo

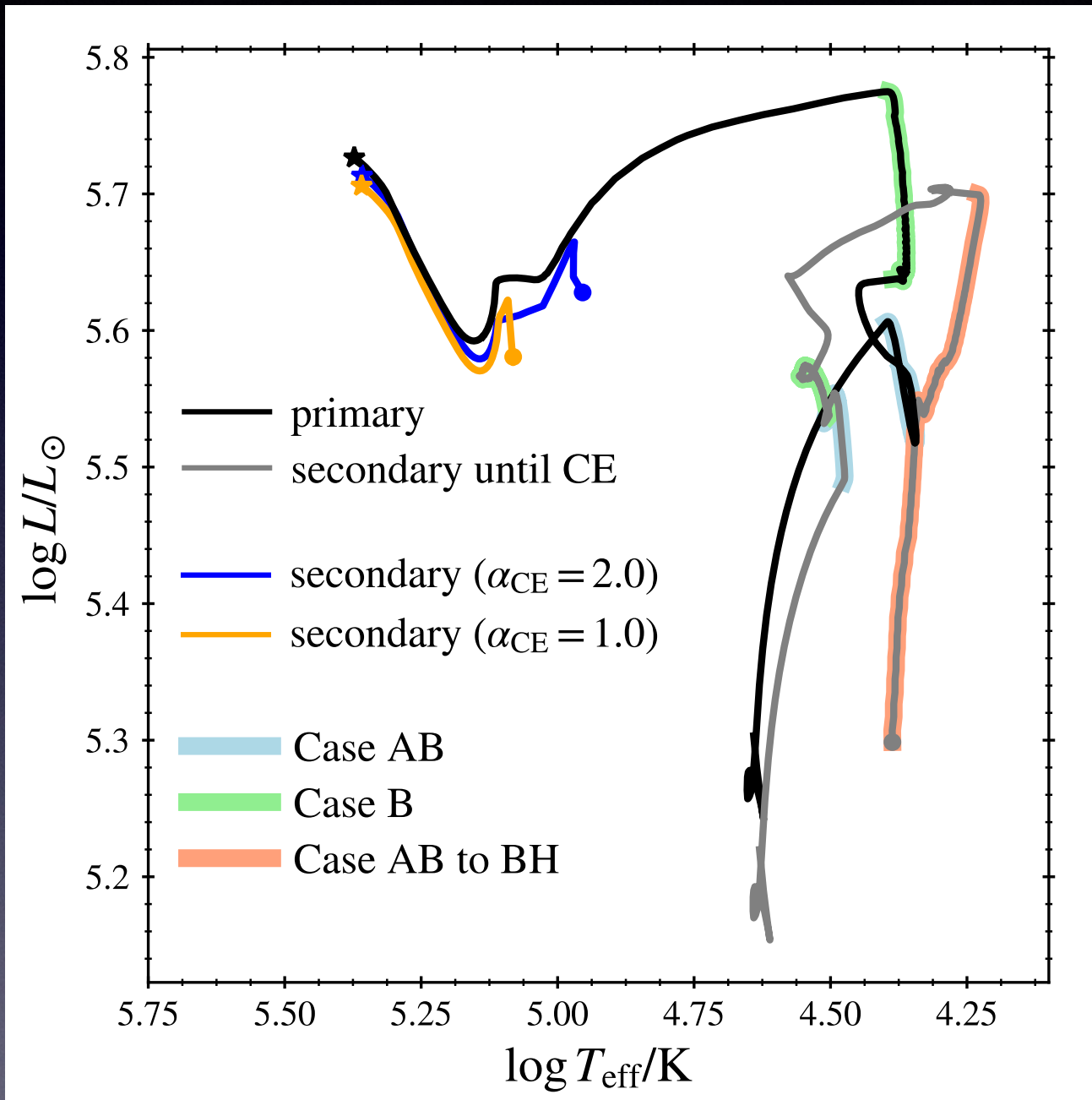


Non-rotating stars, circular orbits and no asymmetric kicks

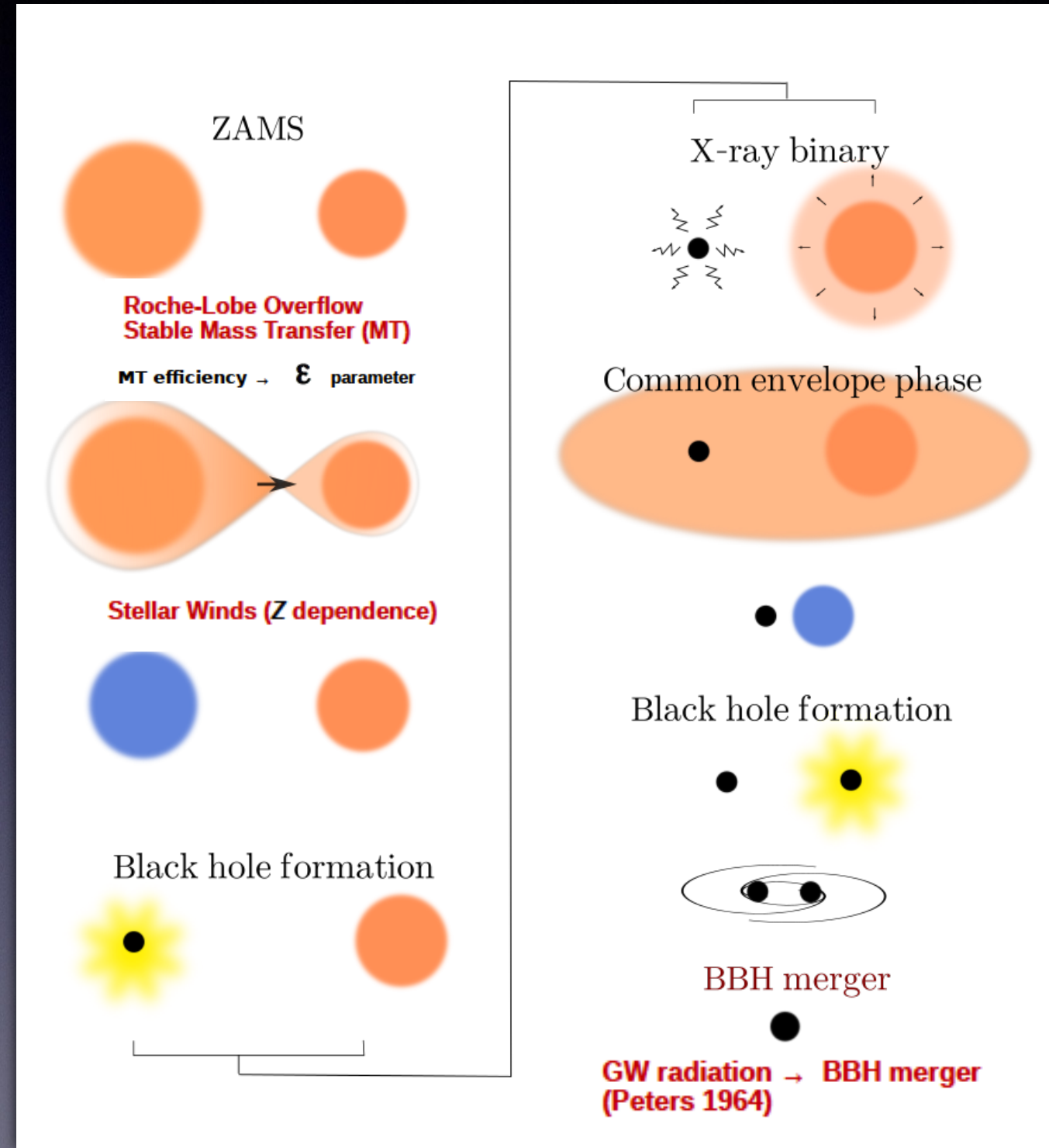
$$[Z_{\odot} = 12 \times 10^{-3}]$$



# Isolated binary evolution



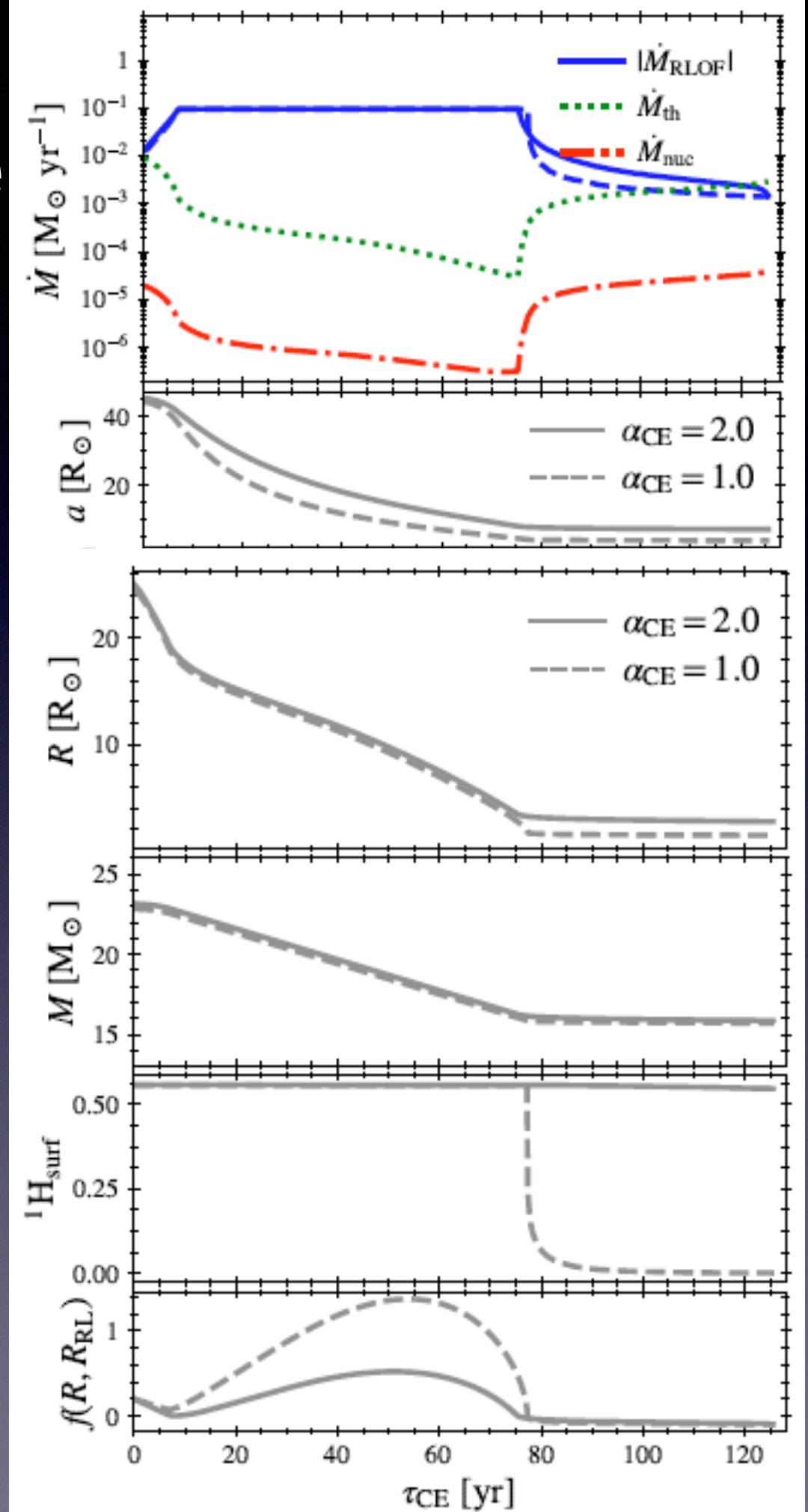
**Full binary evolution simulation leading to the formation of a BBH**



Non-rotating stars, circular orbits and no asymmetric kicks



# Common Envelope Phase



Common-envelope phase  
Unstable Mass Transfer  
(envelope unbinding)

$$\Delta E_{\text{bind}} = \alpha_{\text{CE}} \Delta E_{\text{orb}},$$

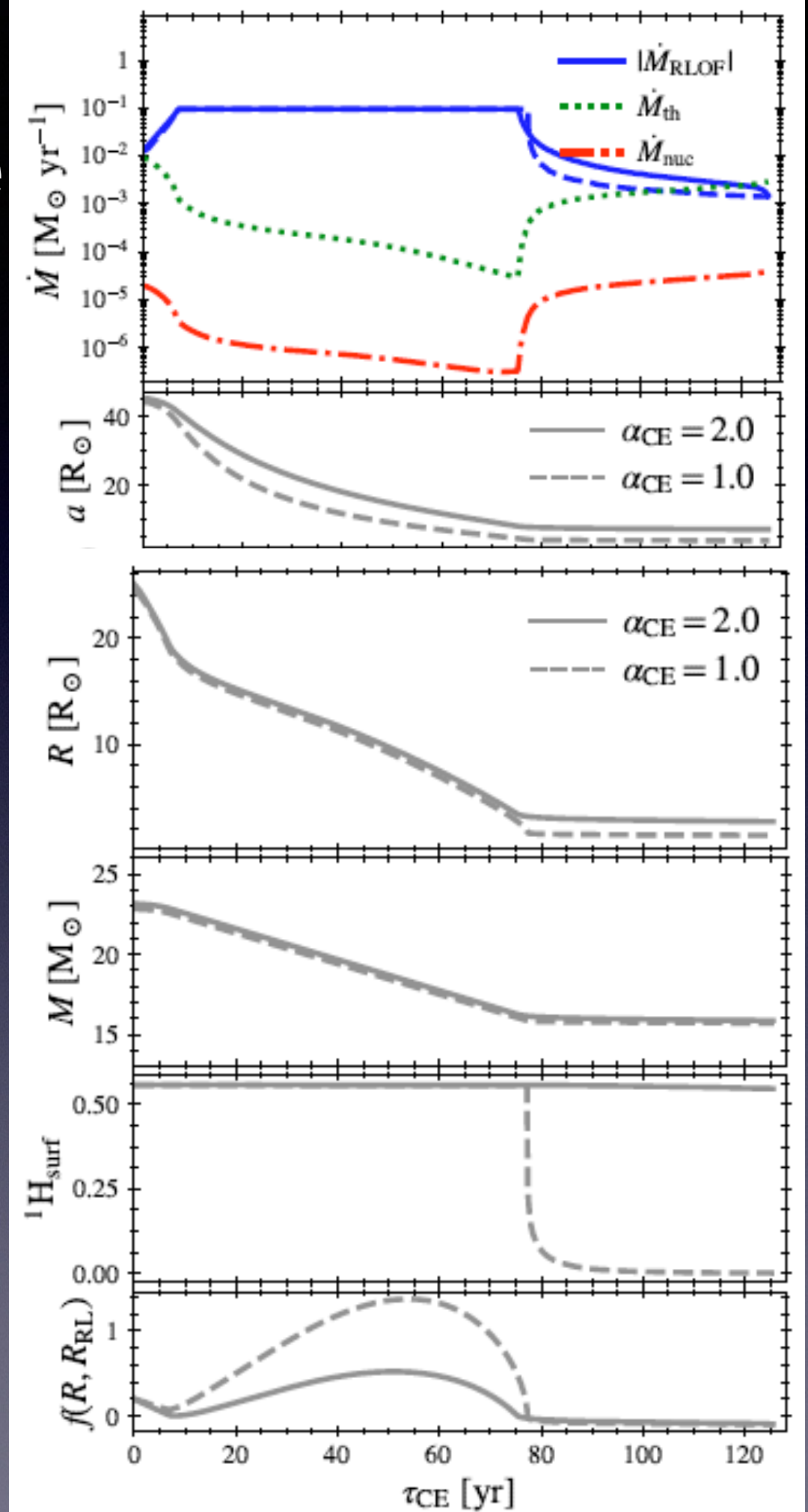
$\alpha_{\text{CE}}$  efficiency parameter

Unstable MT rates  
 $\sim 10^{-2} M_{\odot}/\text{yr}$



# Common Envelope Phase

- The most uncertain phase of binary evolution, with 2 possible outcomes:



Common-envelope phase  
Unstable Mass Transfer  
(envelope unbinding)

$$\Delta E_{\text{bind}} = \alpha_{\text{CE}} \Delta E_{\text{orb}},$$

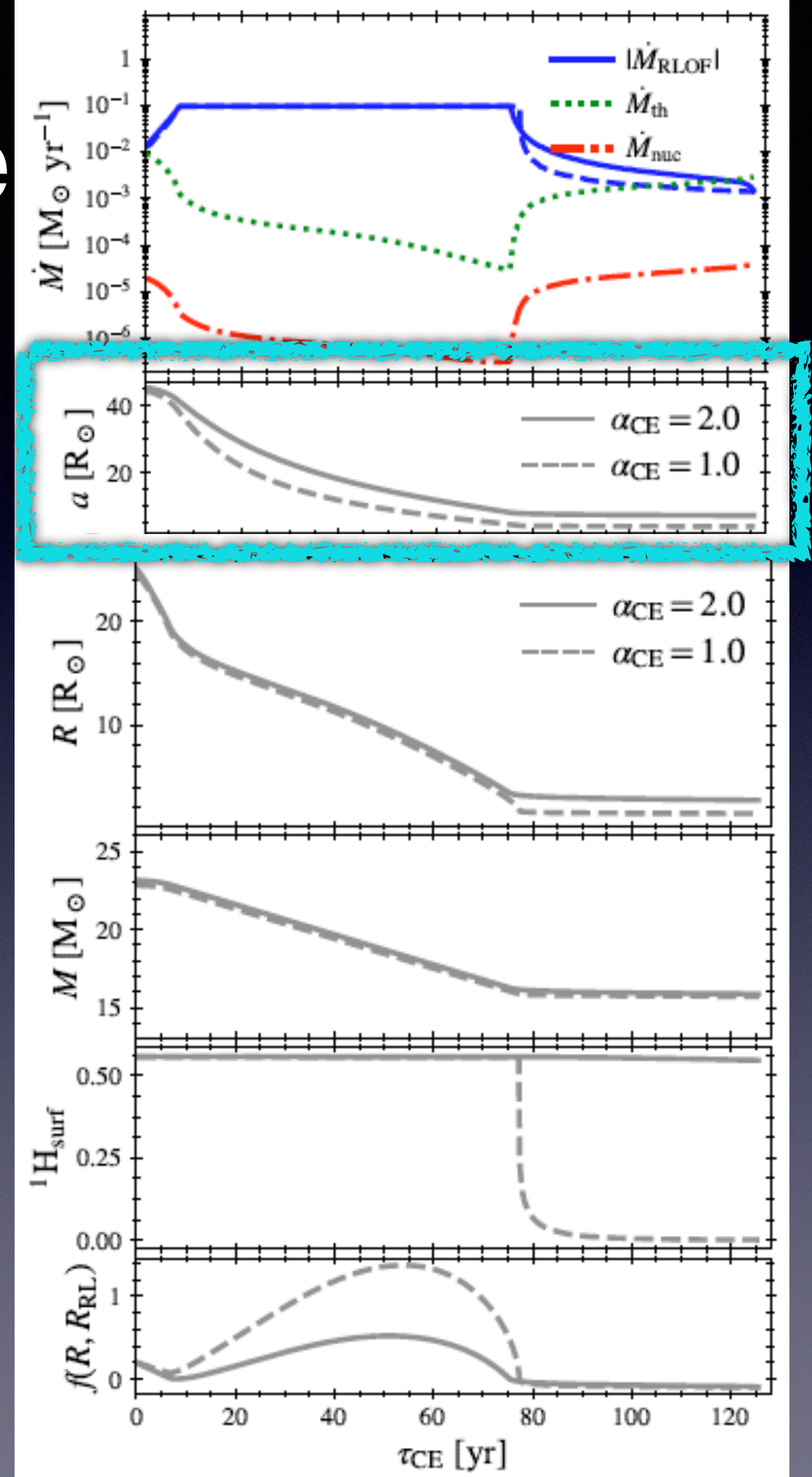
$\alpha_{\text{CE}}$  efficiency parameter

Unstable MT rates  
 $\sim 10^{-2} M_{\odot}/\text{yr}$



# Common Envelope Phase

- The most uncertain phase of binary evolution, with 2 possible outcomes:



Common-envelope phase  
Unstable Mass Transfer  
(envelope unbinding)

$$\Delta E_{\text{bind}} = \alpha_{\text{CE}} \Delta E_{\text{orb}},$$

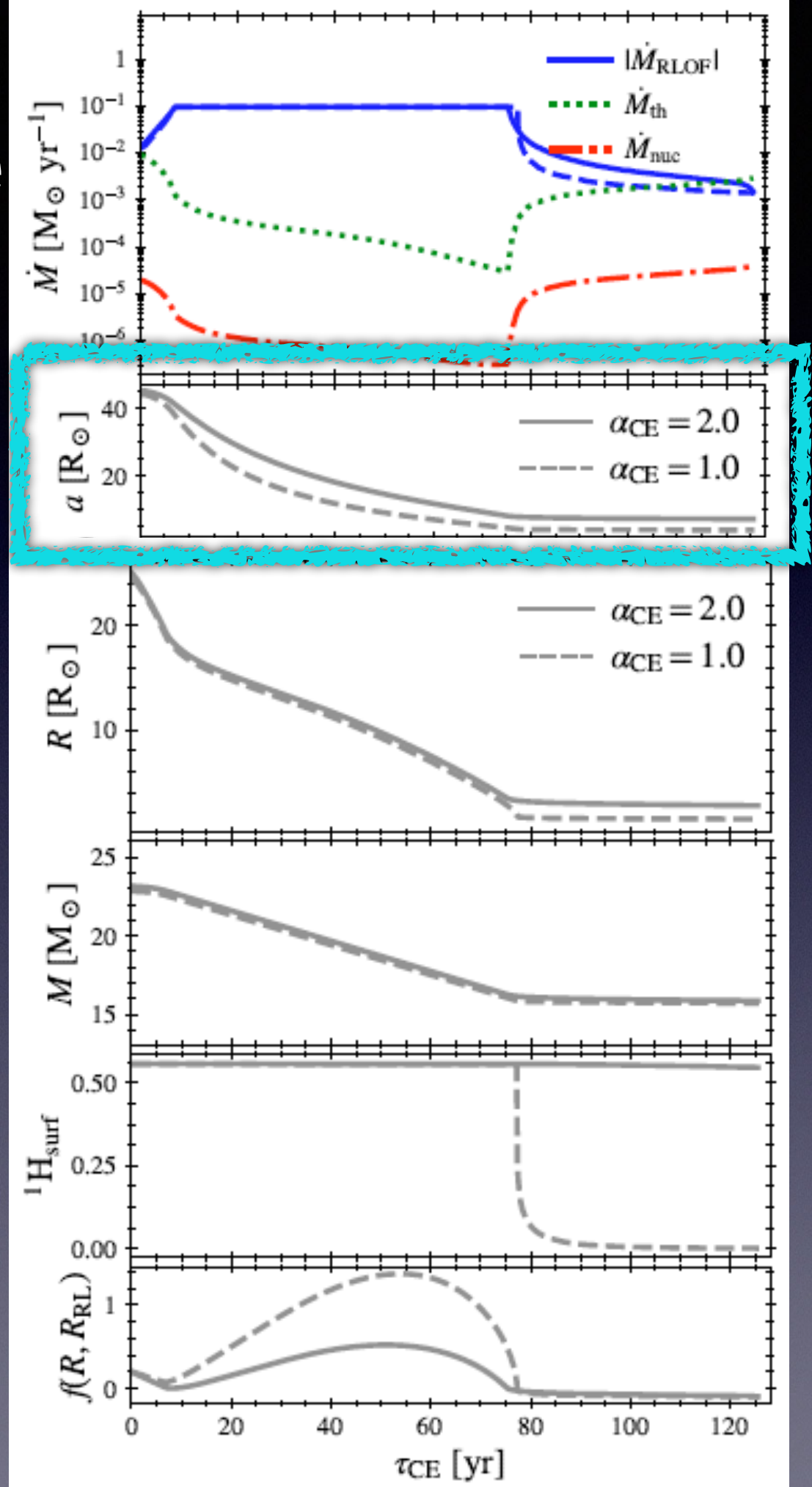
$\alpha_{\text{CE}}$  efficiency parameter

Unstable MT rates  
 $\sim 10^{-2} M_{\odot}/\text{yr}$



# Common Envelope Phase

- **The most uncertain phase of binary evolution,** with 2 possible outcomes:
  - 1. if envelope not ejected -> premature merger of compact object at the center of red giant



**Common-envelope phase  
Unstable Mass Transfer  
(envelope unbinding)**

$$\Delta E_{\text{bind}} = \alpha_{\text{CE}} \Delta E_{\text{orb}},$$

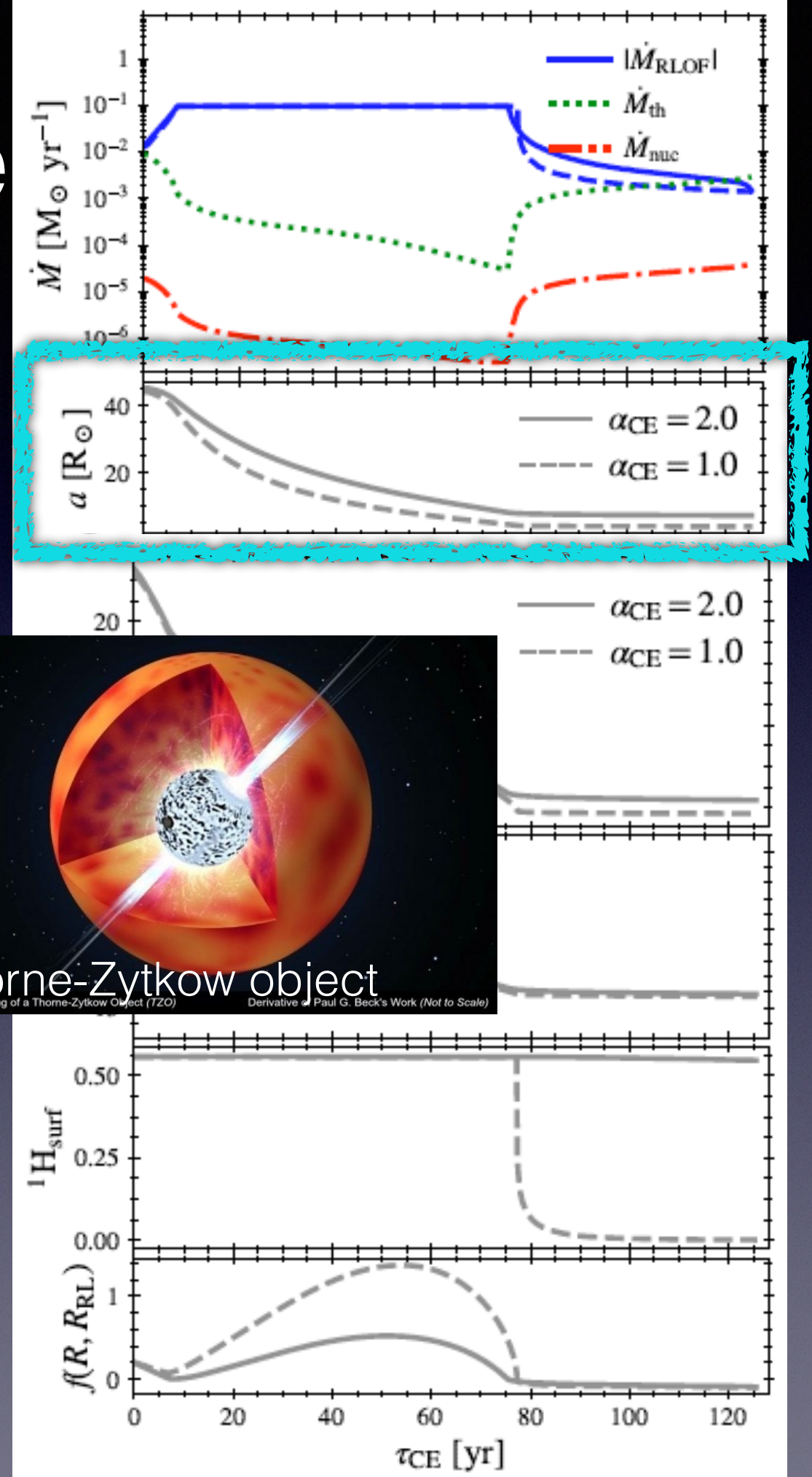
$\alpha_{\text{CE}}$  efficiency parameter

Unstable MT rates  
 $\sim 10^{-2} M_{\odot}/\text{yr}$



# Common Envelope Phase

- **The most uncertain phase of binary evolution,** with 2 possible outcomes:
  - 1. if envelope not ejected -> premature merger of compact object at the center of red giant



**Common-envelope phase  
Unstable Mass Transfer  
(envelope unbinding)**

$$\Delta E_{\text{bind}} = \alpha_{\text{CE}} \Delta E_{\text{orb}},$$

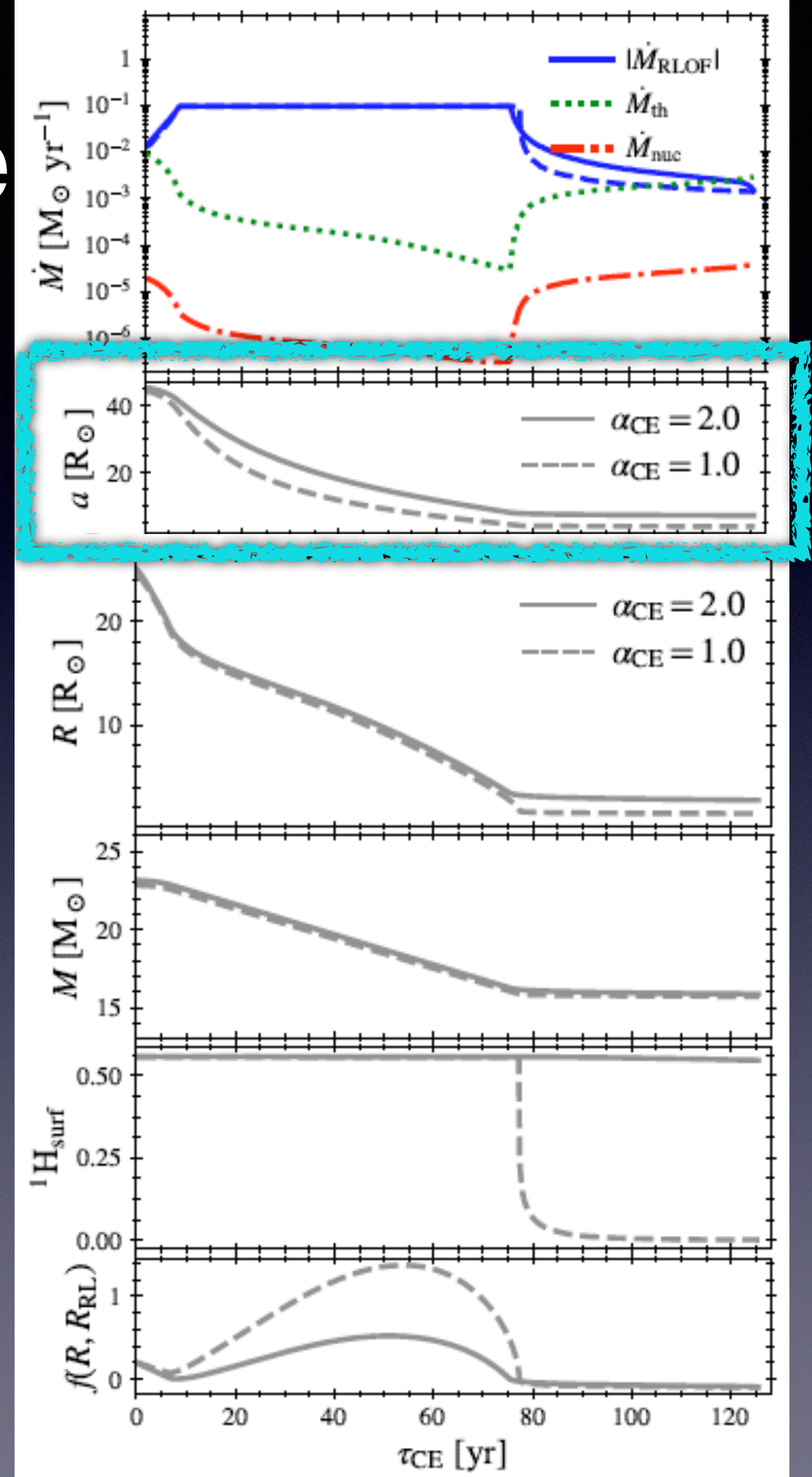
$\alpha_{\text{CE}}$  efficiency parameter

Unstable MT rates  
 $\sim 10^{-2} M_{\odot}/\text{yr}$



# Common Envelope Phase

- **The most uncertain phase of binary evolution,** with 2 possible outcomes:
  - 1. if envelope not ejected -> premature merger of compact object at the center of red giant



**Common-envelope phase  
Unstable Mass Transfer  
(envelope unbinding)**

$$\Delta E_{bind} = \alpha_{CE} \Delta E_{orb},$$

$\alpha_{CE}$  efficiency parameter

Unstable MT rates  
 $\sim 10^{-2} M_{\odot}/\text{yr}$



# Common Envelope Phase

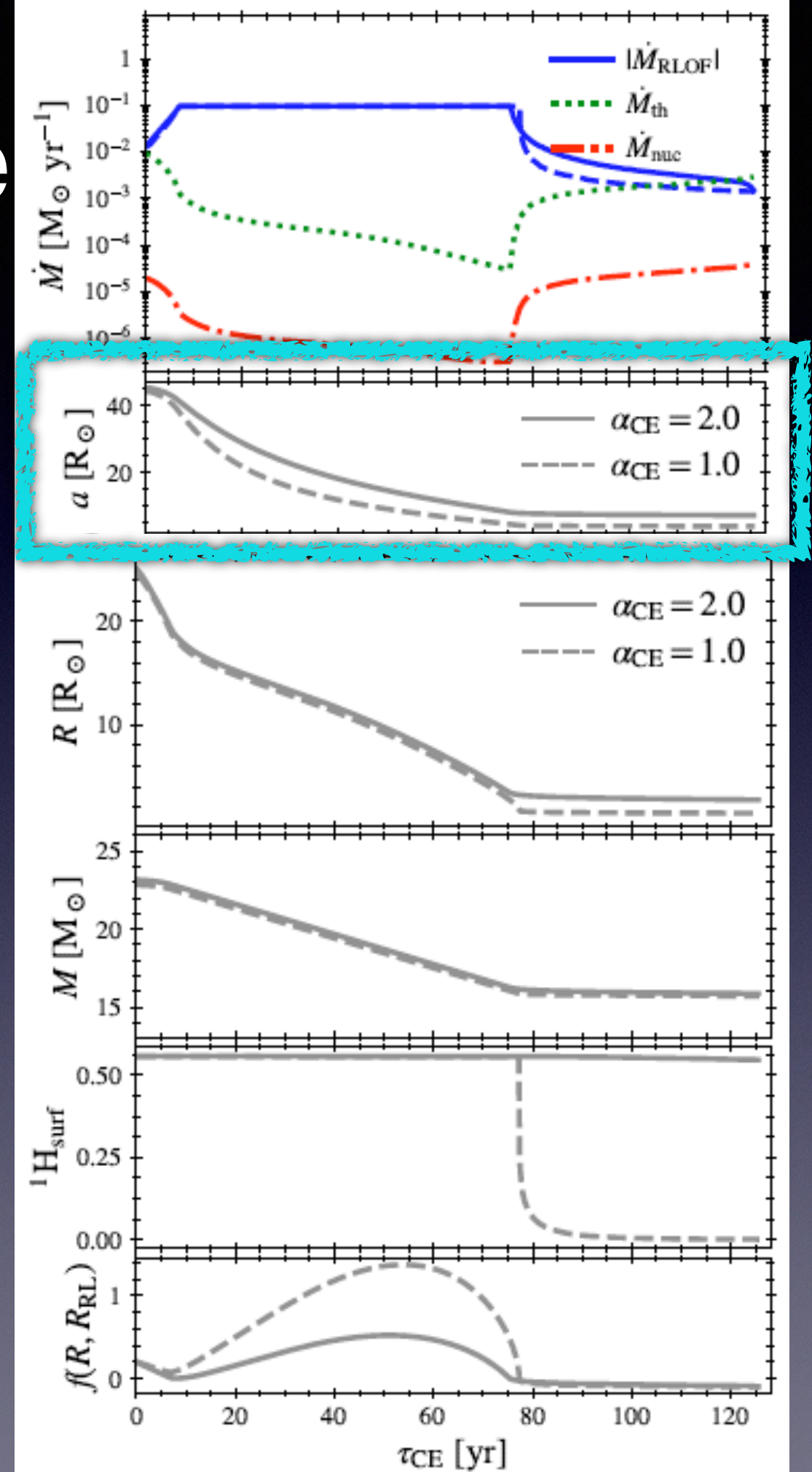
- **The most uncertain phase of binary evolution,** with 2 possible outcomes:
  - 1. if envelope not ejected -> premature merger of compact object at the center of red giant
  - 2. if envelope ejected ( $\alpha_{\text{CE}}=2.0$ ) -> ultra-compact BBH + red giant (orbital separation reduced by factor  $\sim 100$ )

Common-envelope phase  
Unstable Mass Transfer  
(envelope unbinding)

$$\Delta E_{\text{bind}} = \alpha_{\text{CE}} \Delta E_{\text{orb}},$$

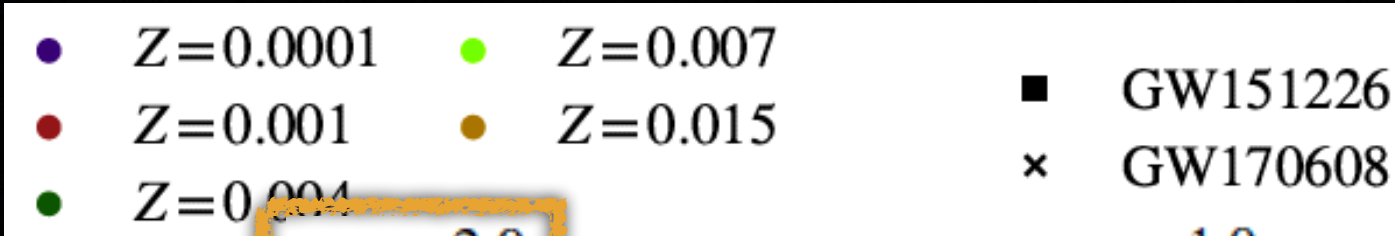
$\alpha_{\text{CE}}$  efficiency parameter

Unstable MT rates  
 $\sim 10^{-2} M_{\odot}/\text{yr}$



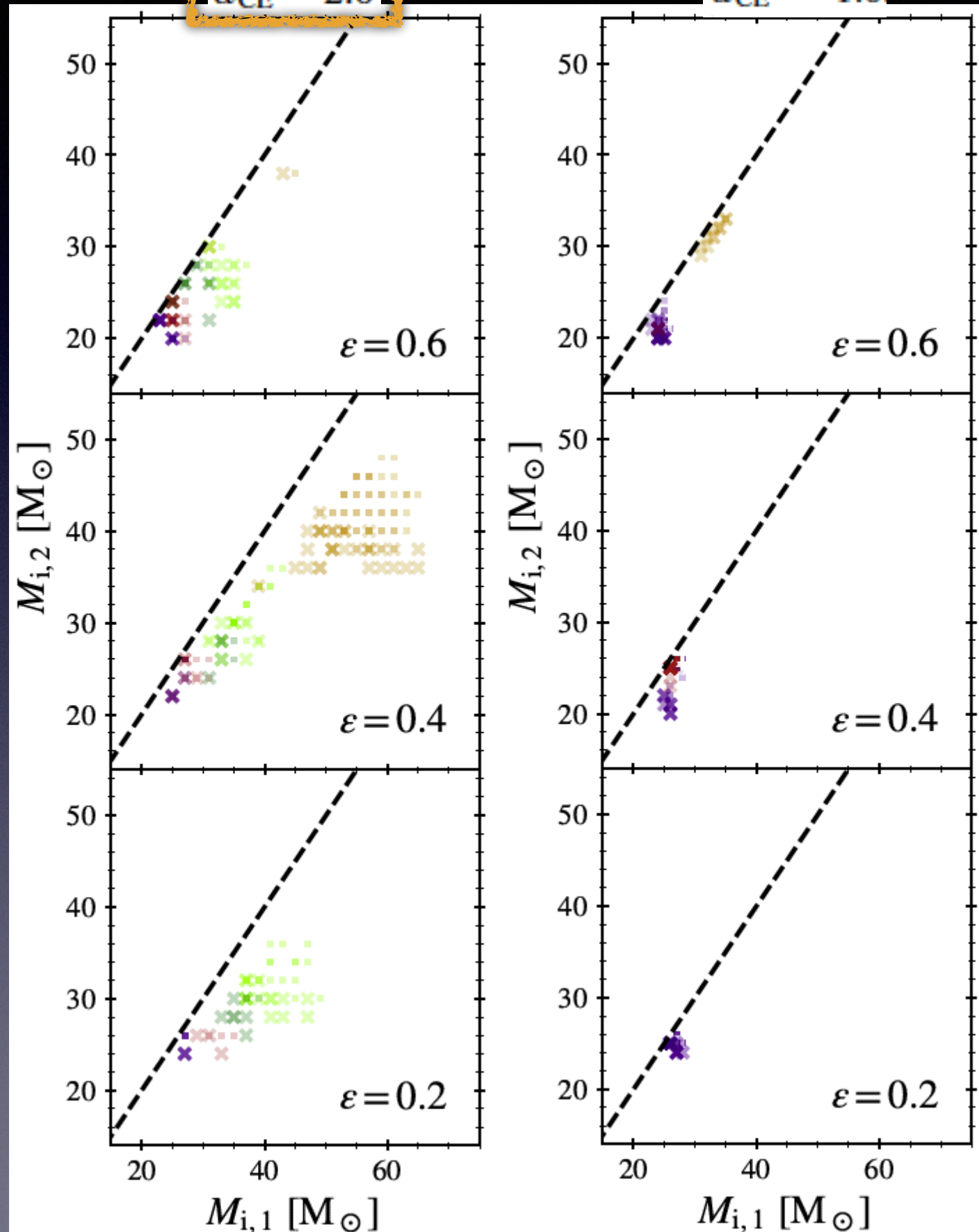


# Properties of binary progenitors ( $M_{i,2}$ vs $M_{i,1}$ )



$\alpha_{CE} = 2.0$

$\alpha_{CE} = 1.0$



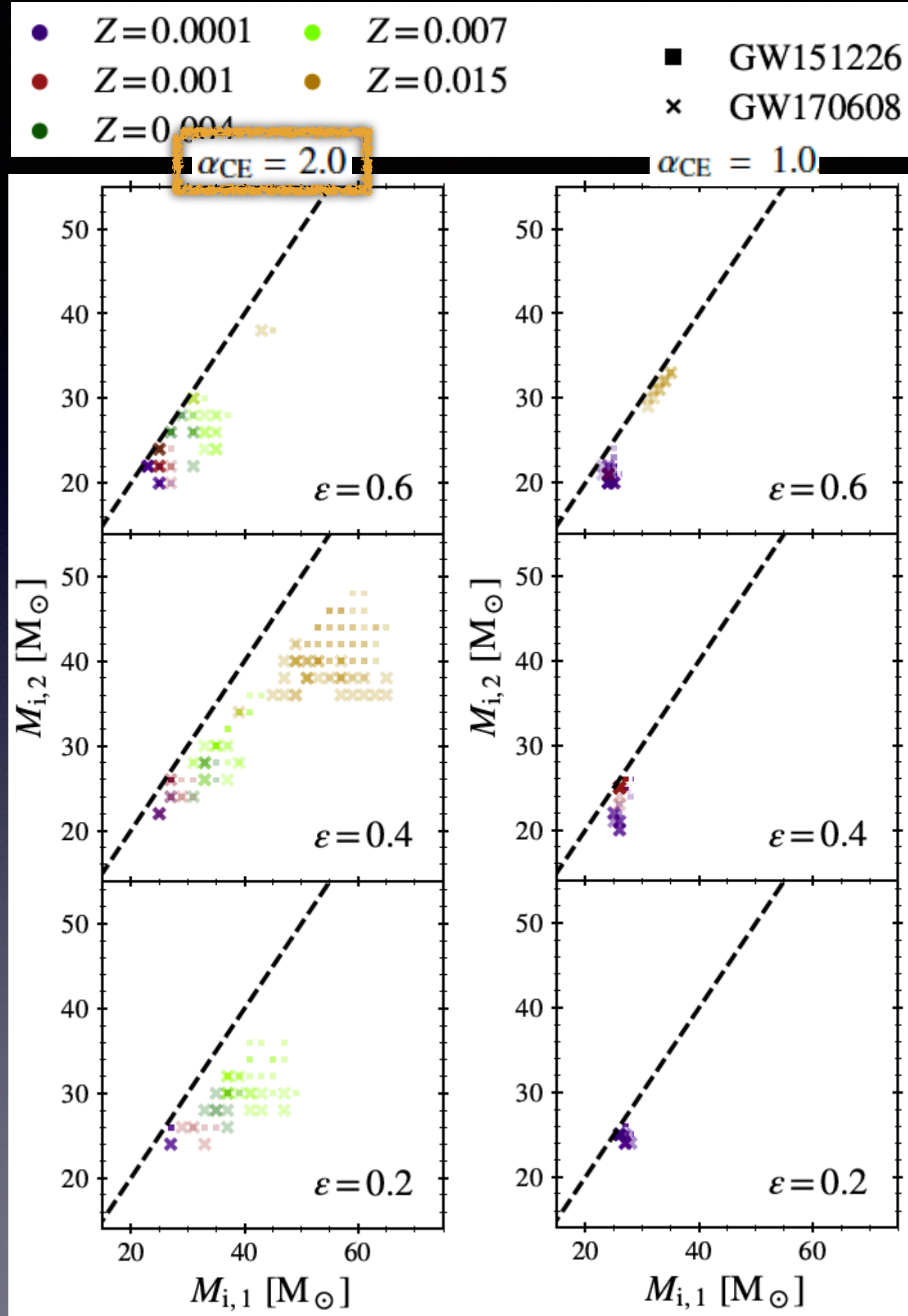
$$\mathcal{M} = \frac{(m_1 m_2)^{3/5}}{(m_1 + m_2)^{1/5}}$$



# Properties of binary progenitors ( $M_{i,2}$ vs $M_{i,1}$ )

- We obtain **>1000s binary progenitors** distributed for metallicities ( $Z$ ), MT ( $\epsilon$ ) & CE ( $\alpha_{CE}$ ) efficiencies

$$\mathcal{M} = \frac{(m_1 m_2)^{3/5}}{(m_1 + m_2)^{1/5}}$$





# Properties of binary progenitors ( $M_{i,2}$ vs $M_{i,1}$ )

- **We obtain >1000s binary progenitors** distributed for metallicities ( $Z$ ), MT ( $\epsilon$ ) & CE ( $\alpha_{CE}$ ) efficiencies
- **Stellar progenitors** of GW151226 **more massive** than GW170608 (in agreement with final BH mass)

$$\mathcal{M} = \frac{(m_1 m_2)^{3/5}}{(m_1 + m_2)^{1/5}}$$

GW151226 ( $z=0.09$ )

$$\mathcal{M}_{\text{chirp}} = 8.83^{+0.71}_{-0.66}$$

$$q_{\text{BBH}} = 0.56^{+0.44}_{-0.49}$$

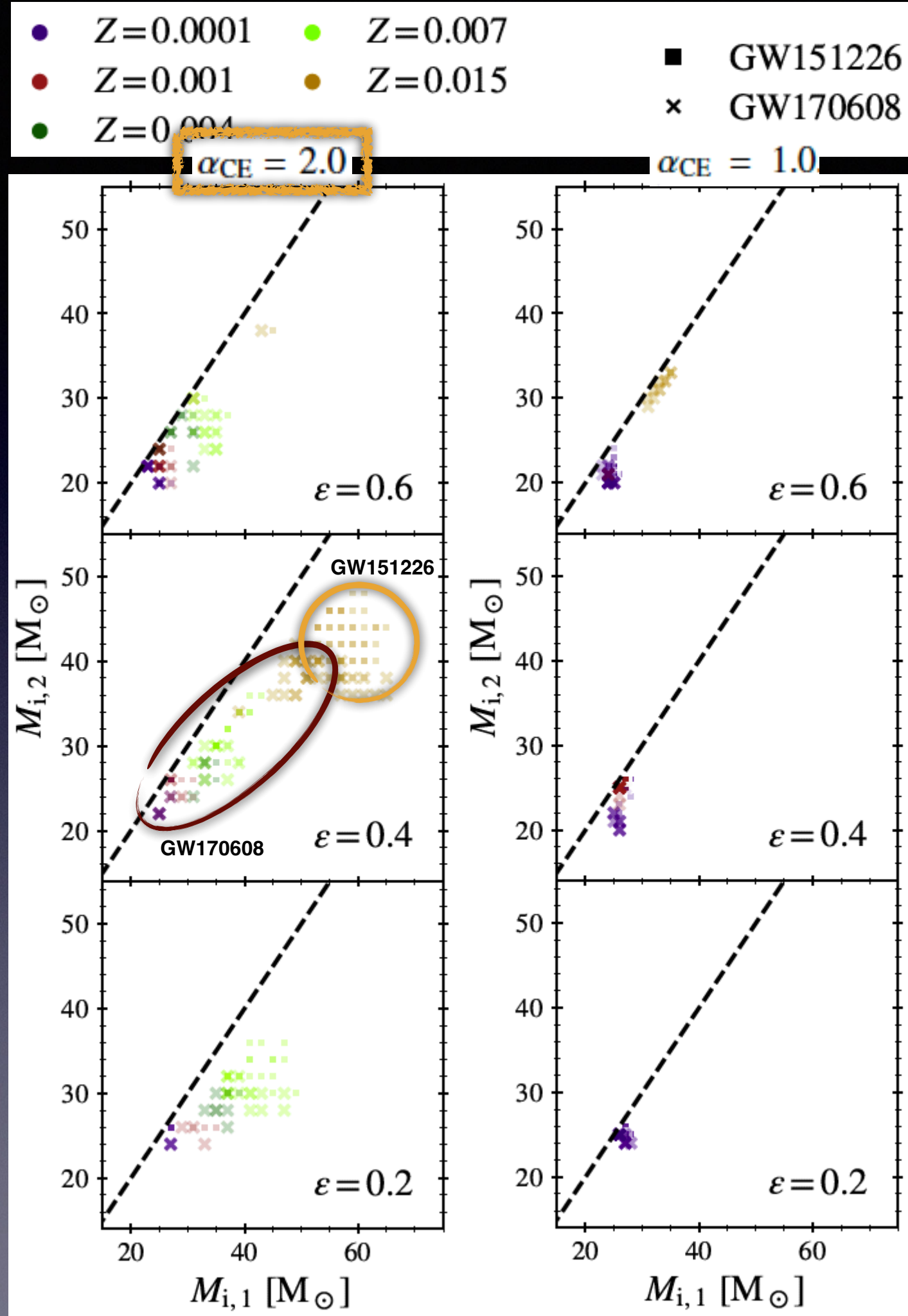
(100% CI de-redshifted)

GW170608 ( $z=0.07$ )

$$\mathcal{M}_{\text{chirp}} = 7.91^{+0.43}_{-0.37}$$

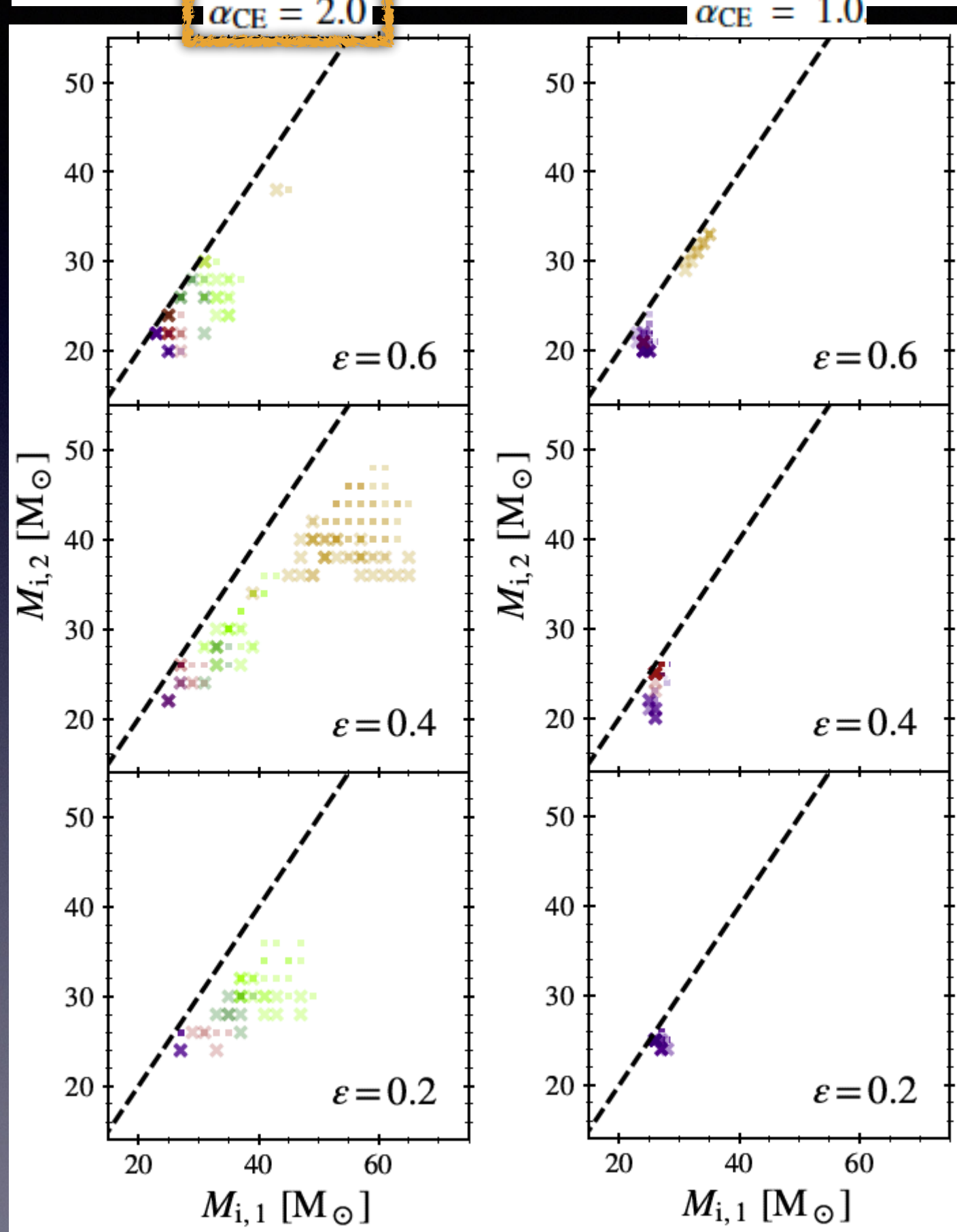
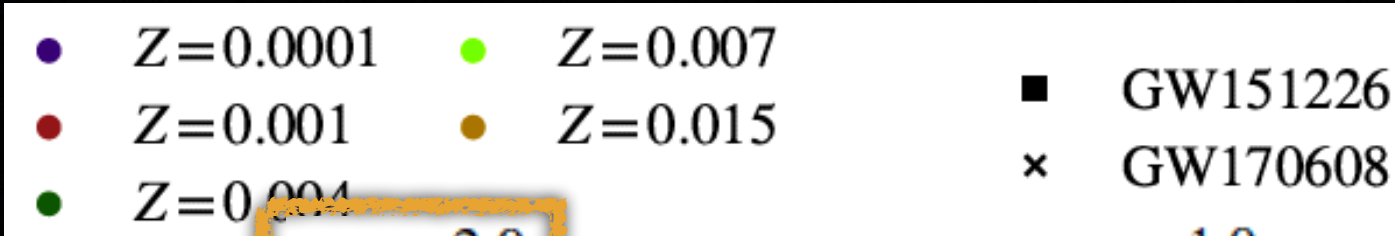
$$q_{\text{BBH}} = 0.69^{+0.31}_{-0.56}$$

(100% CI de-redshifted)





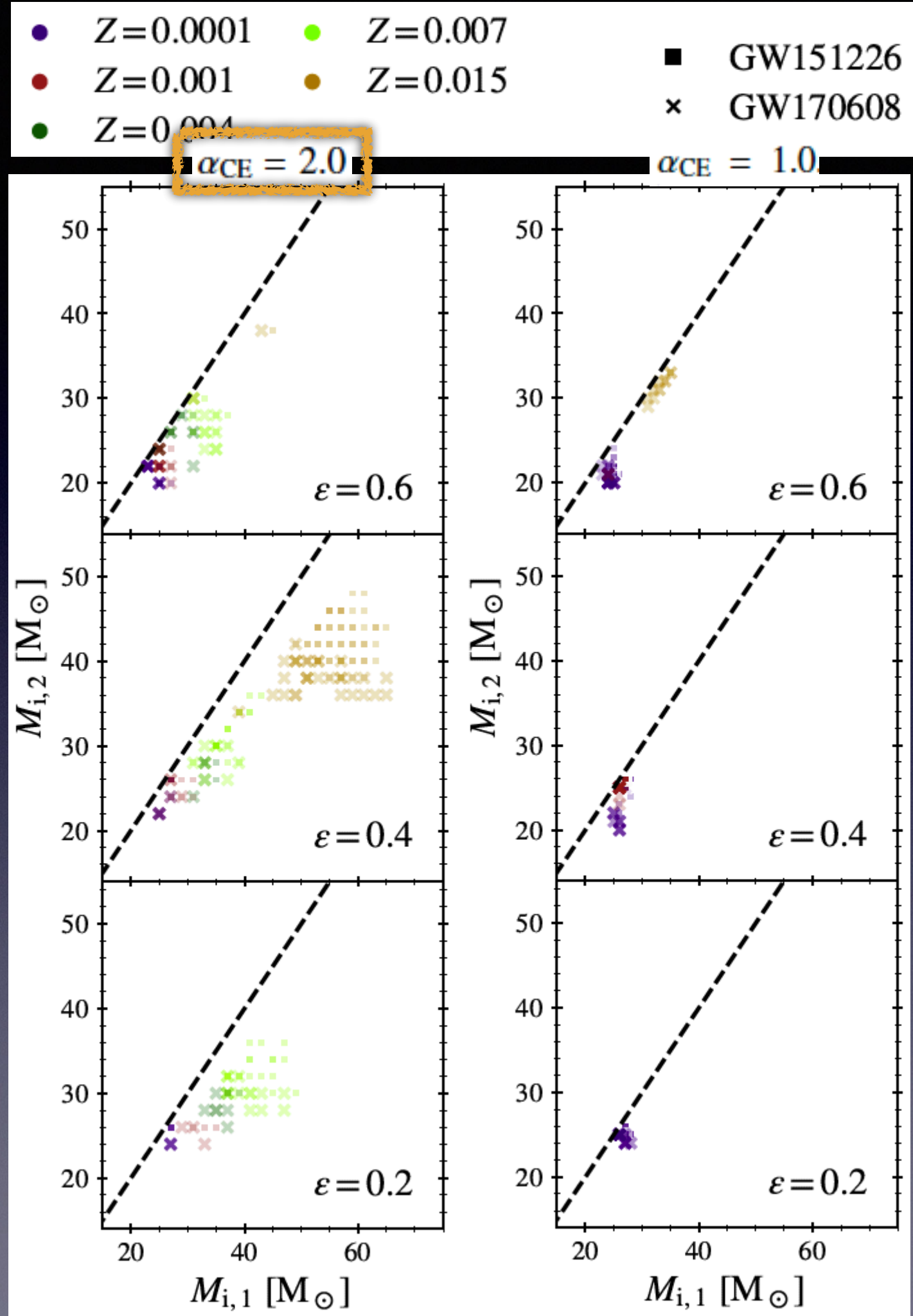
# Properties of binary progenitors ( $M_{i,2}$ vs $M_{i,1}$ )





# Properties of binary progenitors ( $M_{i,2}$ vs $M_{i,1}$ )

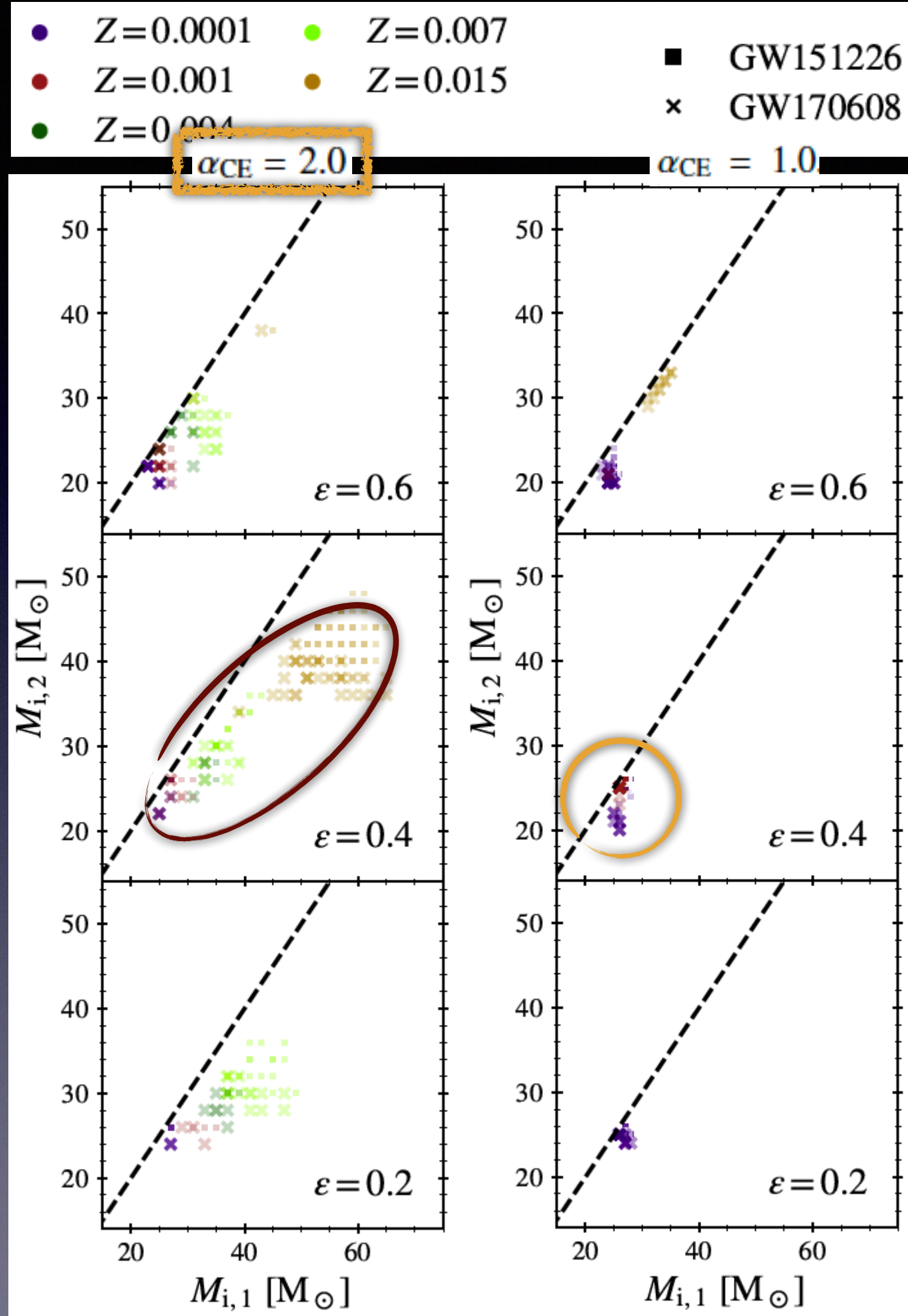
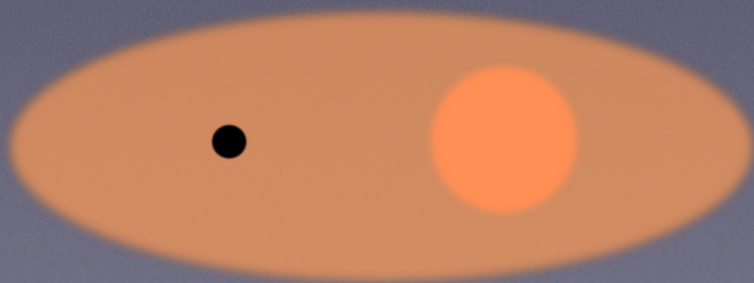
- **CE phase required for all progenitors**, to reduce orbital separation, and merge in  $t < t_{\text{Hubble}}$





# Properties of binary progenitors ( $M_{i,2}$ vs $M_{i,1}$ )

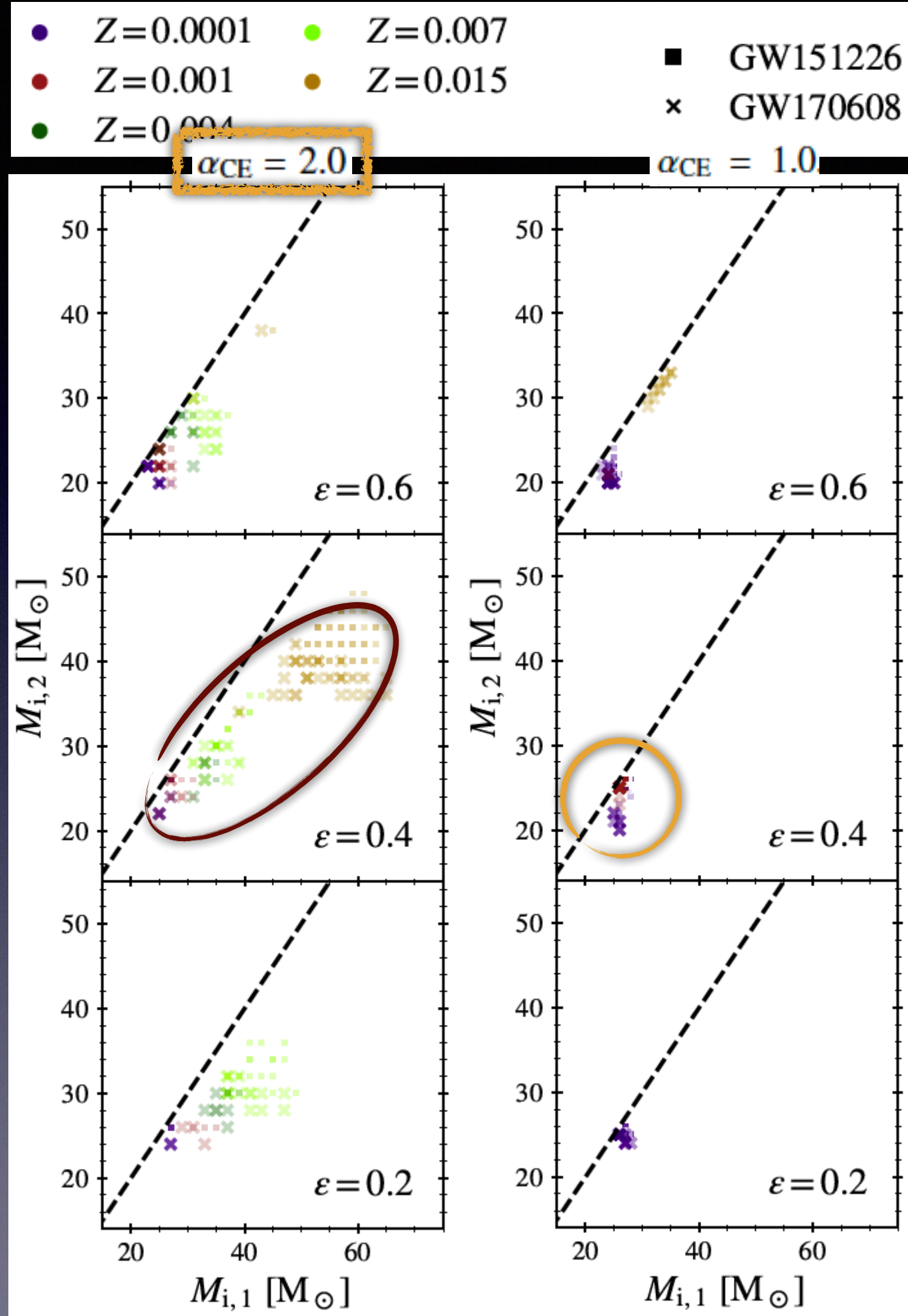
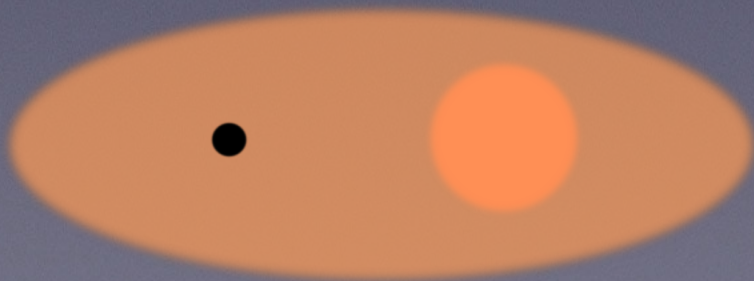
- **CE phase required for all progenitors**, to reduce orbital separation, and merge in  $t < t_{\text{Hubble}}$
- **More progenitors at high CE efficiencies** ( $\alpha_{\text{CE}}=2.0$ ), due to early ejection of envelope, avoiding a *premature merger* during CE





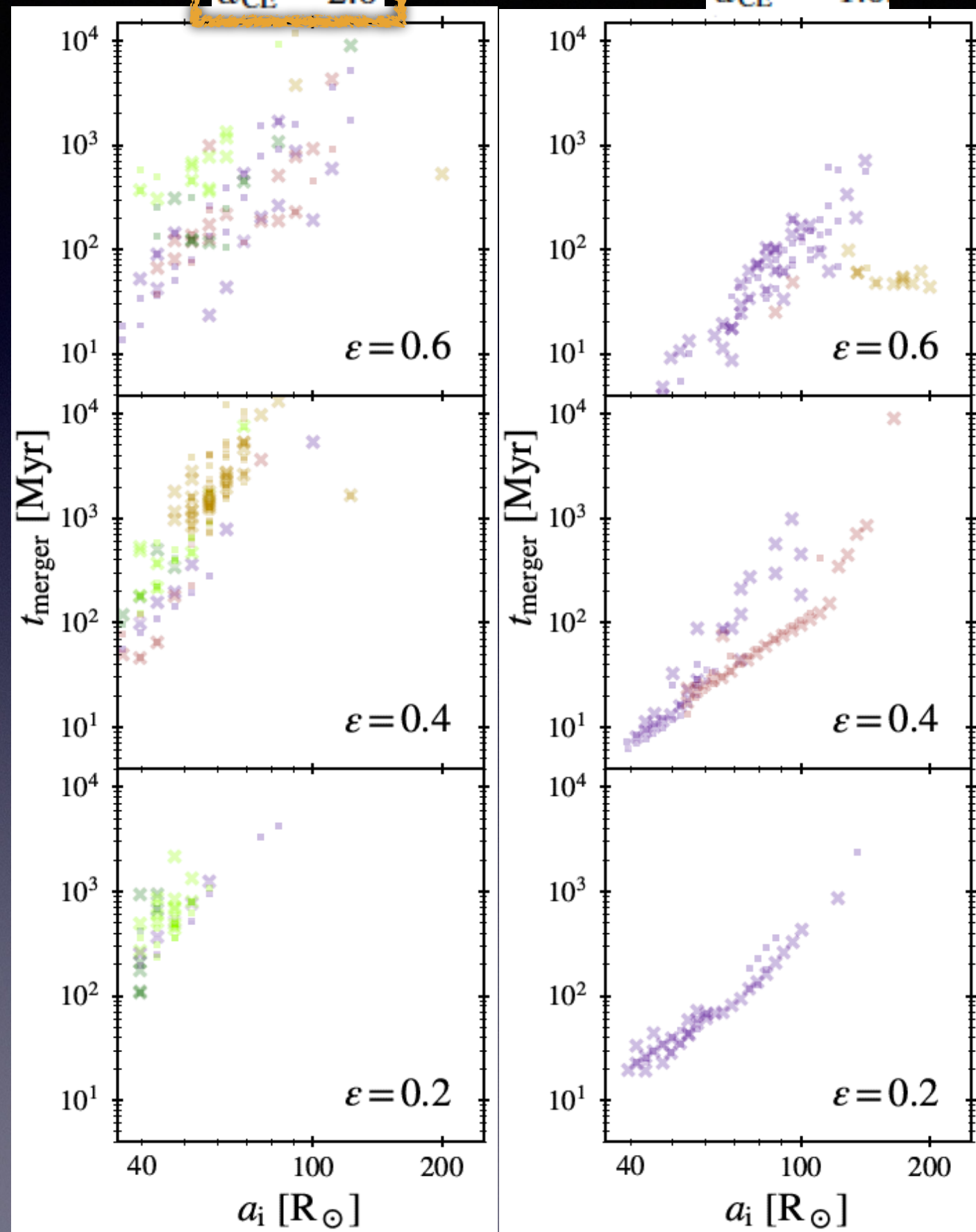
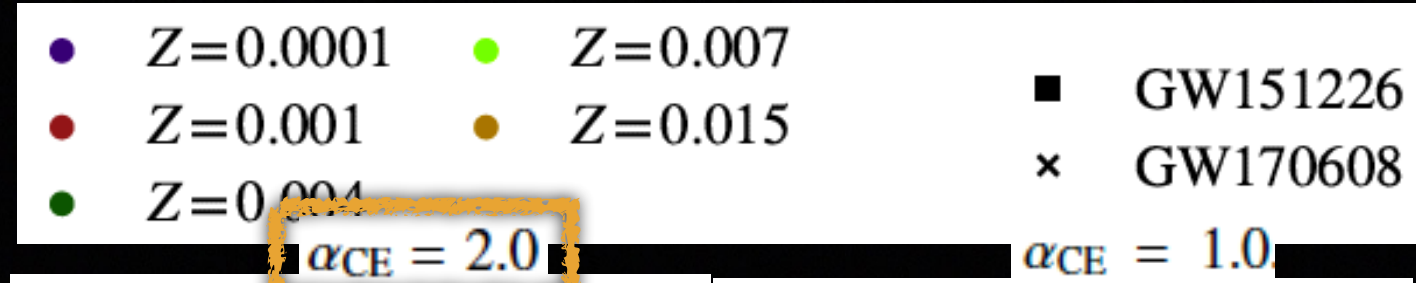
# Properties of binary progenitors ( $M_{i,2}$ vs $M_{i,1}$ )

- **CE phase required for all progenitors**, to reduce orbital separation, and merge in  $t < t_{\text{Hubble}}$
- **More progenitors at high CE efficiencies** ( $\alpha_{\text{CE}}=2.0$ ), due to early ejection of envelope, avoiding a *premature merger* during CE
- **High  $Z$**  => massive progenitors (mass loss — stellar winds)





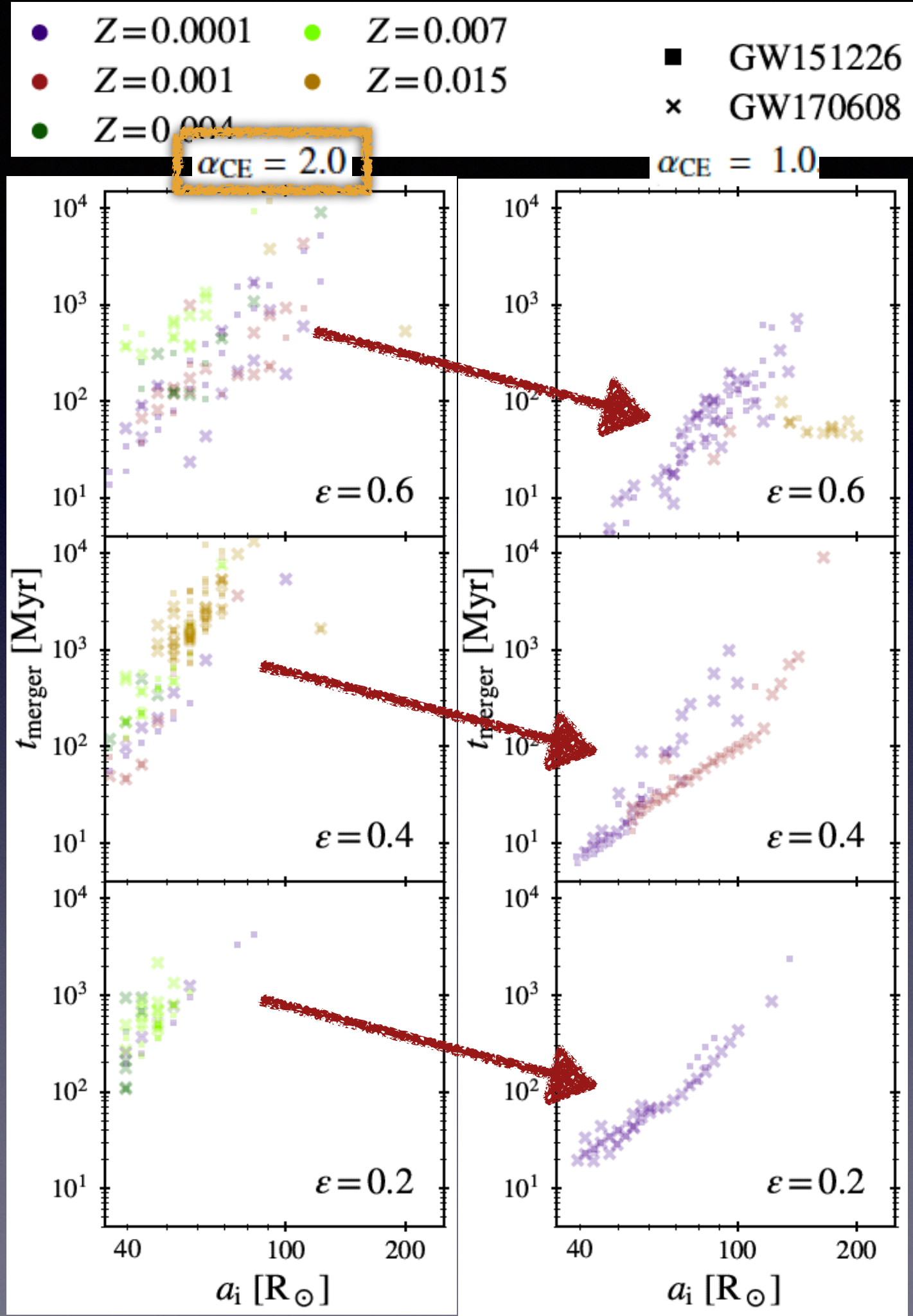
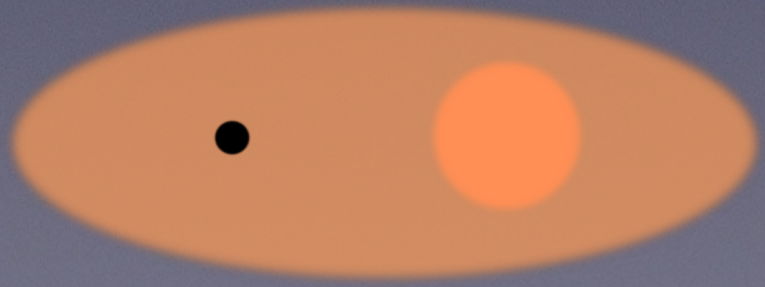
# Properties of binary progenitors ( $t_{\text{merger}}$ vs $a_i$ )





# Properties of binary progenitors ( $t_{\text{merger}}$ vs $a_i$ )

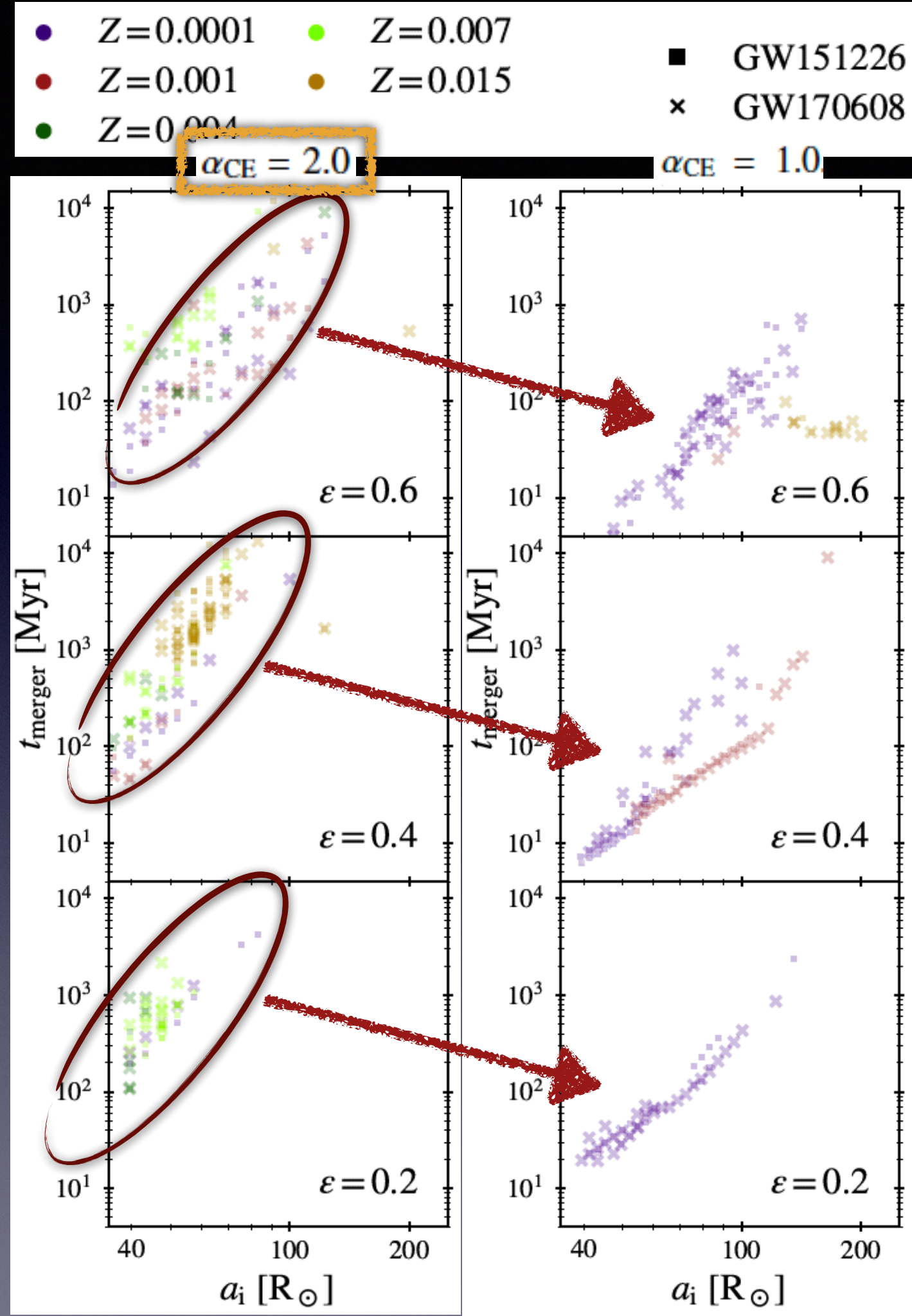
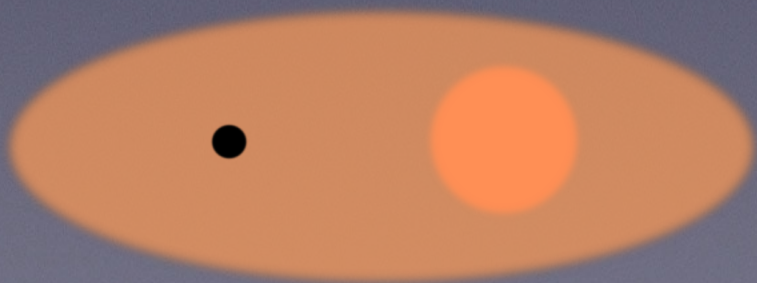
- $t_{\text{merger}}$  correlated with  $a_i$   
**reduced by 10 for  $\alpha_{\text{CE}}=1.0$**   
 (late CE ejection reduces  $a_i$ )





# Properties of binary progenitors ( $t_{\text{merger}}$ vs $a_i$ )

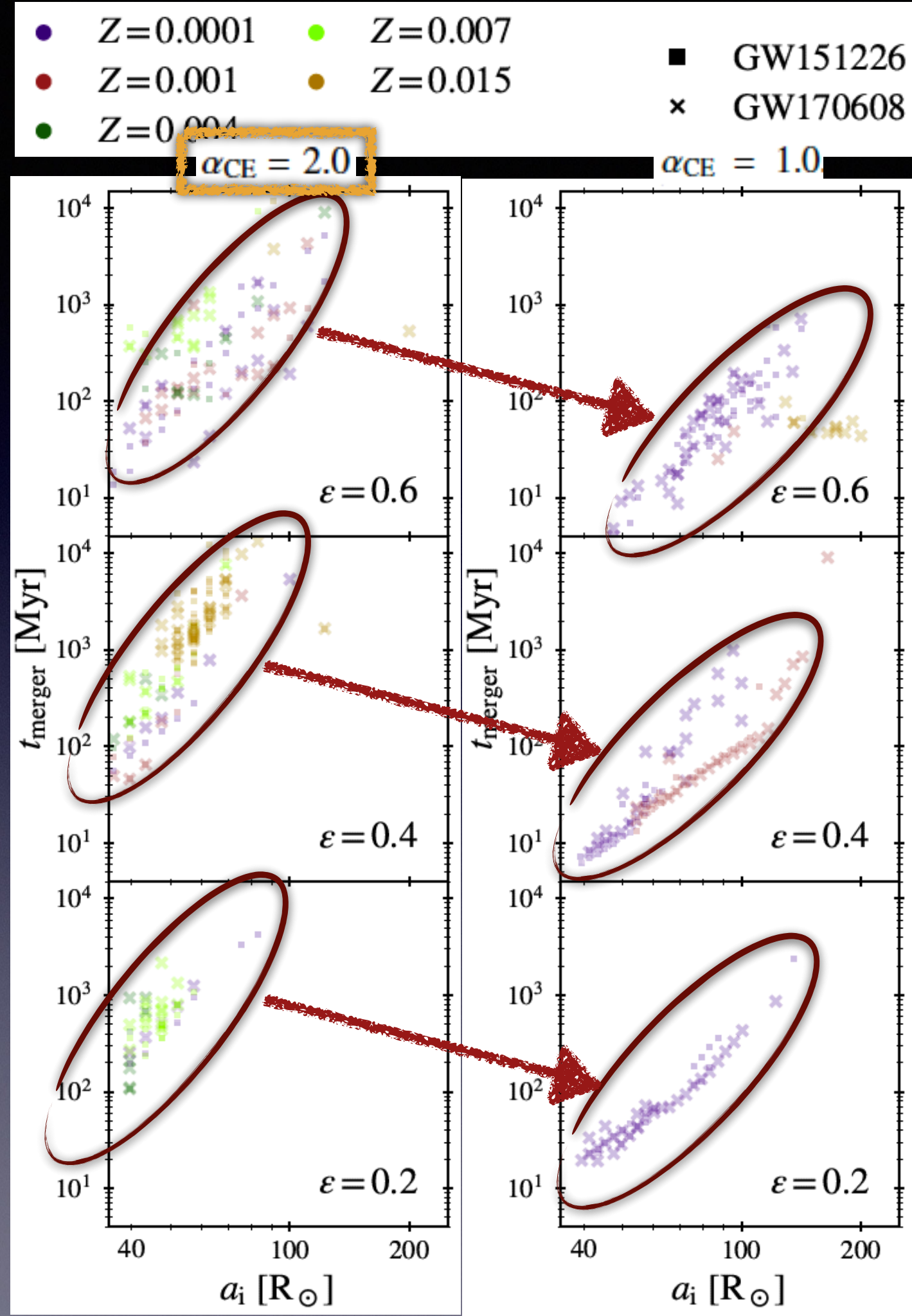
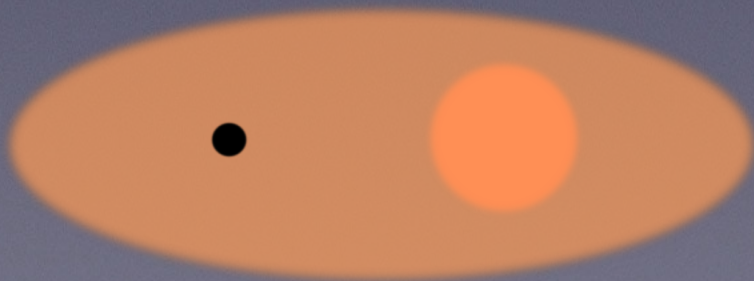
- $t_{\text{merger}}$  correlated with  $a_i$   
reduced by 10 for  $\alpha_{\text{CE}} = 1.0$   
(late CE ejection reduces  $a_i$ )
- $\alpha_{\text{CE}} = 2.0$ : longer  $t_{\text{merger}}$  1 Gyr  
[0.1-8 Gyr] (early CE ejection)  
old & high Z population





# Properties of binary progenitors ( $t_{\text{merger}}$ vs $a_i$ )

- $t_{\text{merger}}$  correlated with  $a_i$   
reduced by 10 for  $\alpha_{\text{CE}} = 1.0$   
(late CE ejection reduces  $a_i$ )
- $\alpha_{\text{CE}} = 2.0$ : longer  $t_{\text{merger}}$  1 Gyr  
[0.1-8 Gyr] (early CE ejection)  
old & high Z population
- $\alpha_{\text{CE}} = 1.0$ : shorter  $t_{\text{merger}}$  100 Myr  
[0.01-1 Gyr] (late CE ejection)  
young & low Z population





# Merger time delay calculation

weak  $e_{\text{BBH}} < 0.25$

small  $a_{\text{BBH}} < 20 R_{\odot}$

$a_{\text{BBH}} \times 10 \Rightarrow t_{\text{merger}} \times 10^4 !$

## Appendix C: Merger time delay calculation

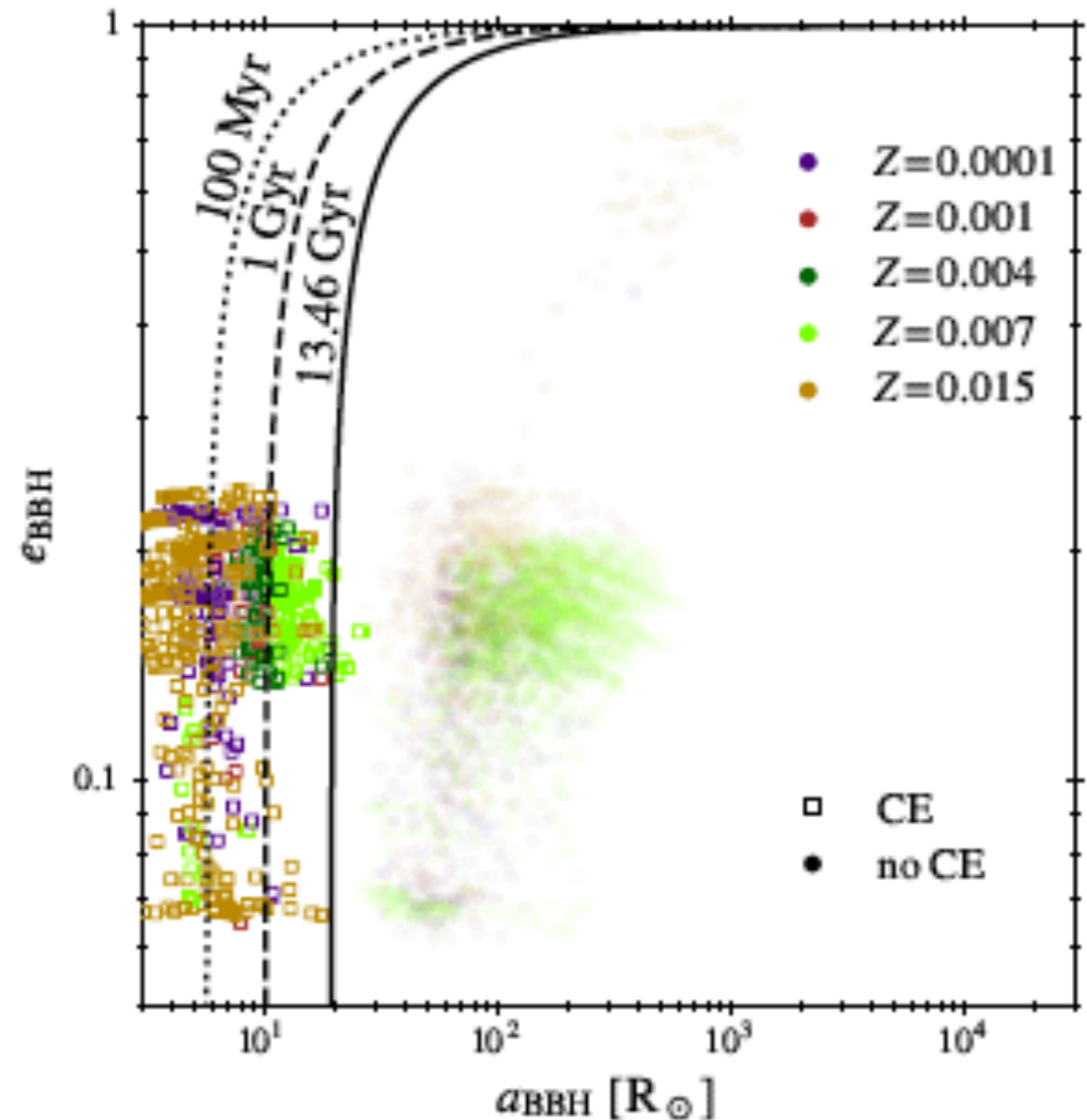


**Fig. C.1.** Final binary parameters for all our BBHs with  $M_{\text{chirp}}$  consistent with GW151226 or GW170608. Colours indicate different metallicities (see legend). Dotted, dashed, and solid black lines correspond to values of constant  $t_{\text{merger}}$ : 100 Myr, 1 Gyr,  $\tau_{\text{Hubble}}$ , respectively, assuming BH masses of 12.3 and 7.65  $M_{\odot}$ .



# Merger time delay calculation

weak  $e_{\text{BBH}} < 0.25$

small  $a_{\text{BBH}} < 20 R_{\odot}$

$a_{\text{BBH}} \times 10 \Rightarrow t_{\text{merger}} \times 10^4 !$

## Appendix C: Merger time delay calculation

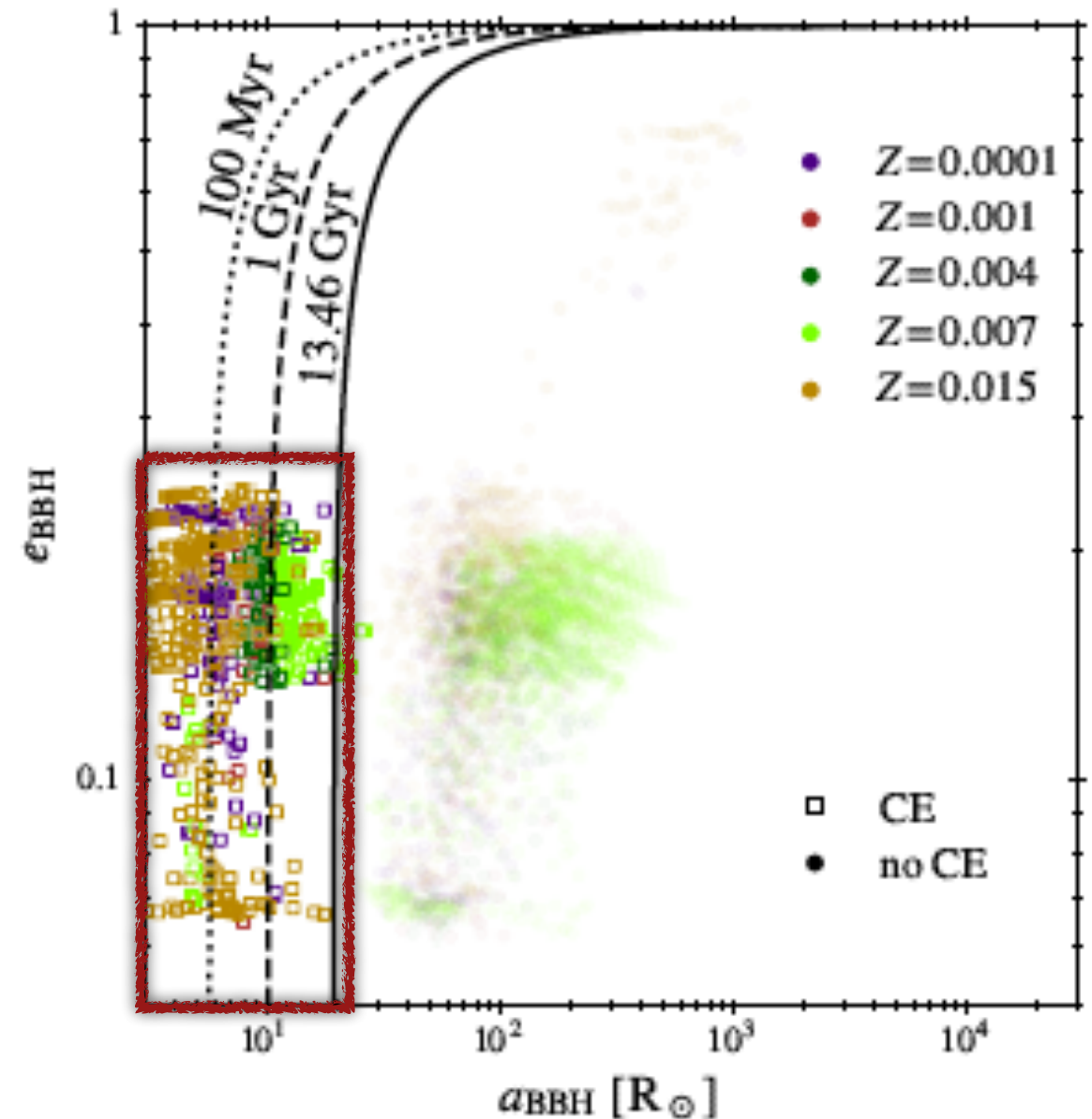


**Fig. C.1.** Final binary parameters for all our BBHs with  $M_{\text{chirp}}$  consistent with GW151226 or GW170608. Colours indicate different metallicities (see legend). Dotted, dashed, and solid black lines correspond to values of constant  $t_{\text{merger}}$ : 100 Myr, 1 Gyr,  $\tau_{\text{Hubble}}$ , respectively, assuming BH masses of 12.3 and 7.65  $M_{\odot}$ .



# Merger time delay calculation

weak  $e_{\text{BBH}} < 0.25$

small  $a_{\text{BBH}} < 20 R_{\odot}$

$a_{\text{BBH}} \times 10 \Rightarrow t_{\text{merger}} \times 10^4 !$

## Appendix C: Merger time delay calculation

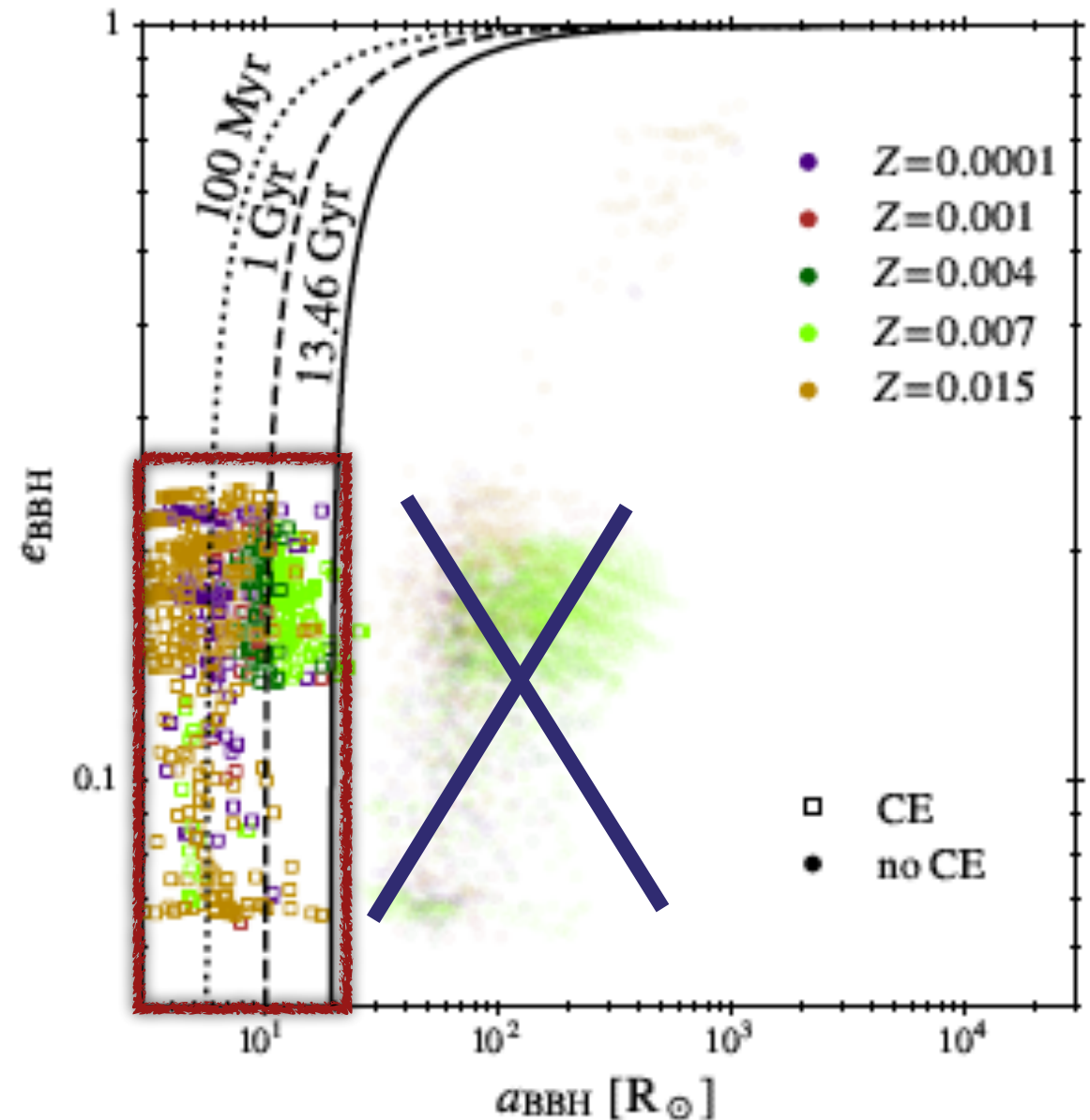
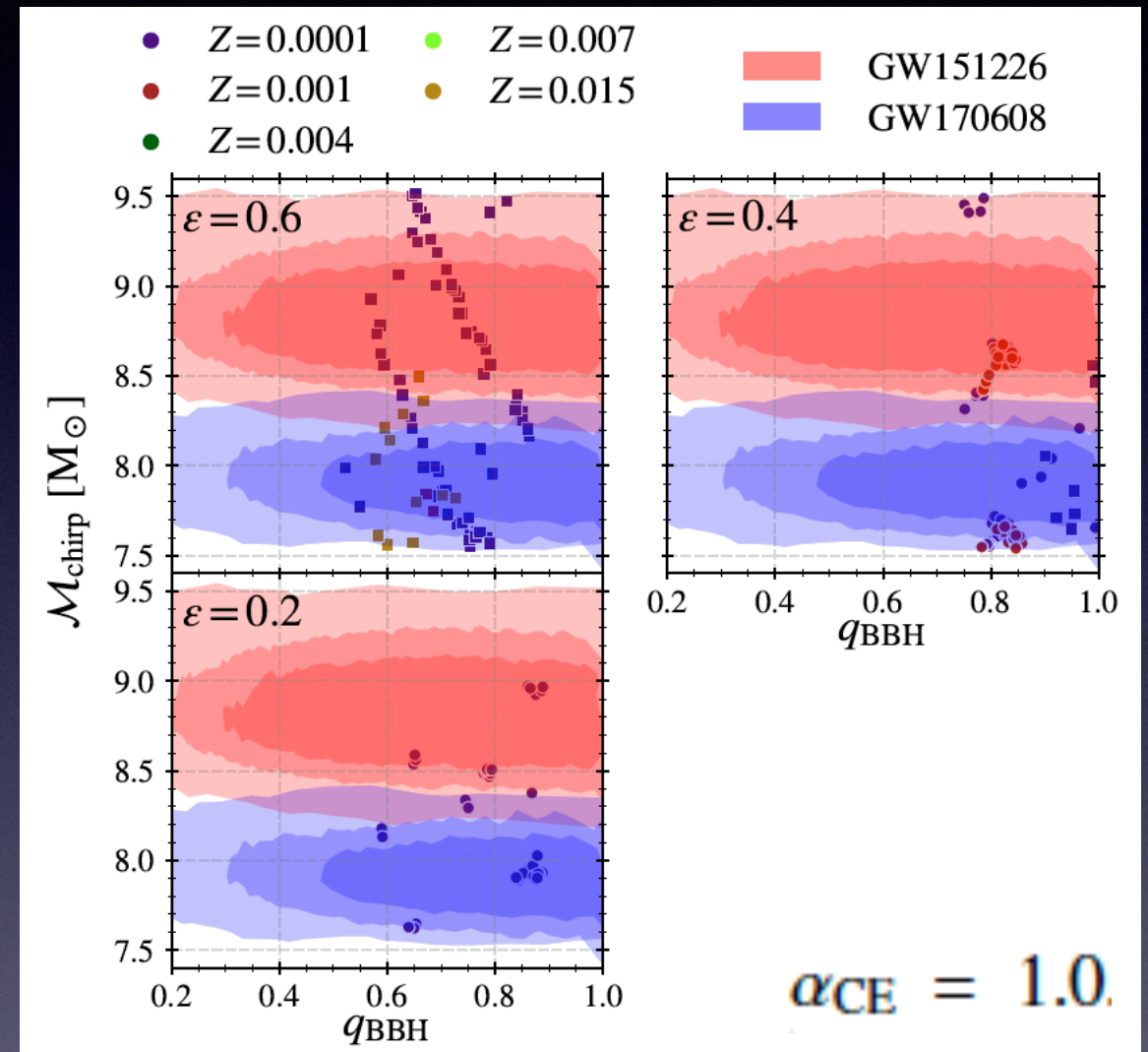
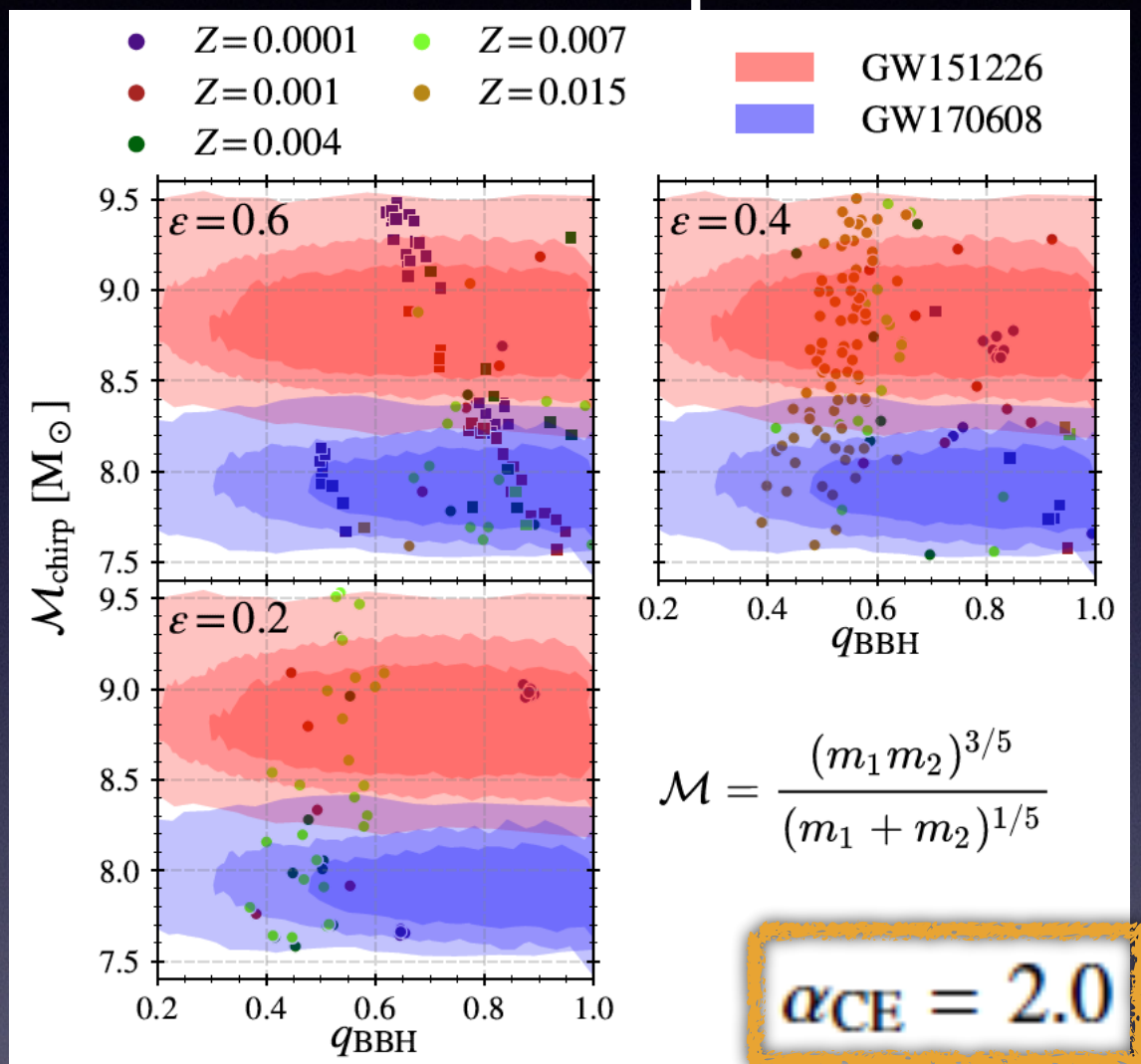


**Fig. C.1.** Final binary parameters for all our BBHs with  $M_{\text{chirp}}$  consistent with GW151226 or GW170608. Colours indicate different metallicities (see legend). Dotted, dashed, and solid black lines correspond to values of constant  $t_{\text{merger}}$ : 100 Myr, 1 Gyr,  $\tau_{\text{Hubble}}$ , respectively, assuming BH masses of 12.3 and 7.65  $M_{\odot}$ .

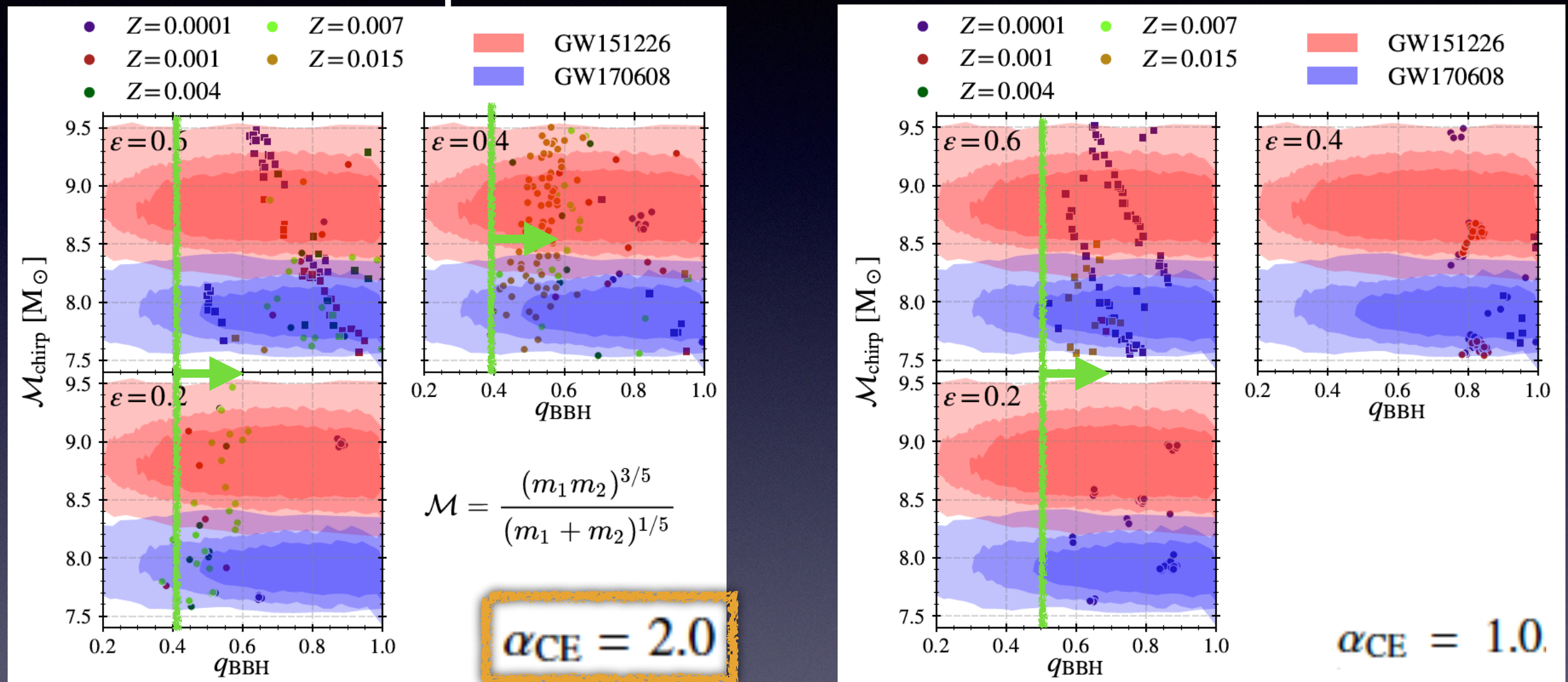


# Properties of formed BBH: chirp mass vs mass ratio





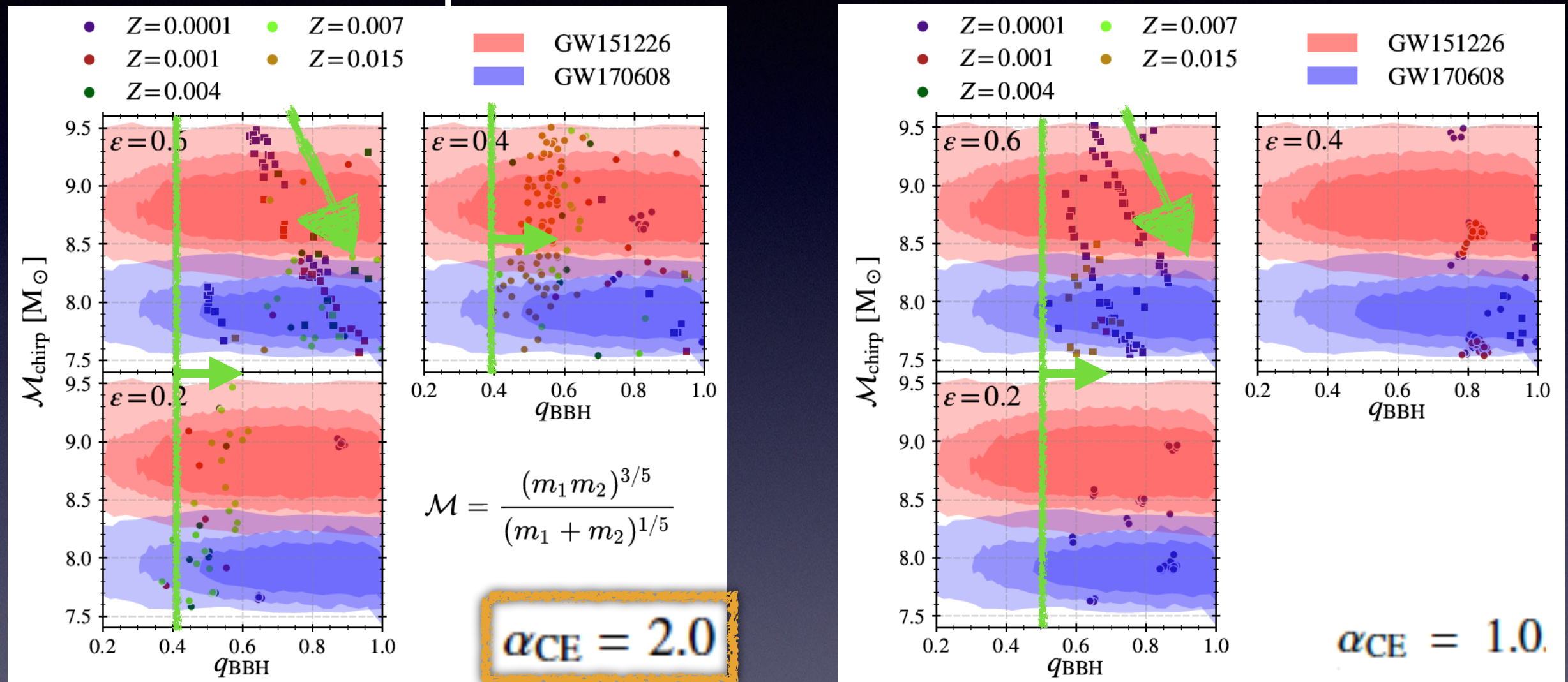
# Properties of formed BBH: chirp mass vs mass ratio



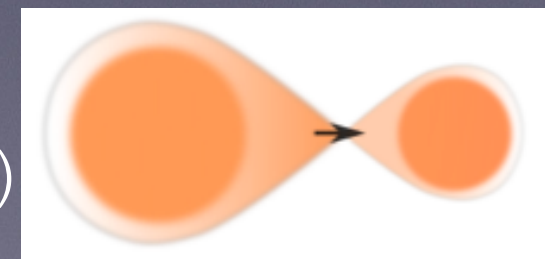
- BBH are formed with symmetric mass ratios  $q$  ( $=M_2/M_1$ )  $> 0.4$



# Properties of formed BBH: chirp mass vs mass ratio



- BBH are formed with symmetric mass ratios  $q$  ( $=M_2/M_1$ )  $> 0.4$
- High  $\epsilon=0.6$  form BBH with  $q$  increasing up to 1: **rejuvenation process** (mass transfer  $\Rightarrow$  2<sup>nd</sup>-formed BH becomes more massive than 1<sup>st</sup> one)

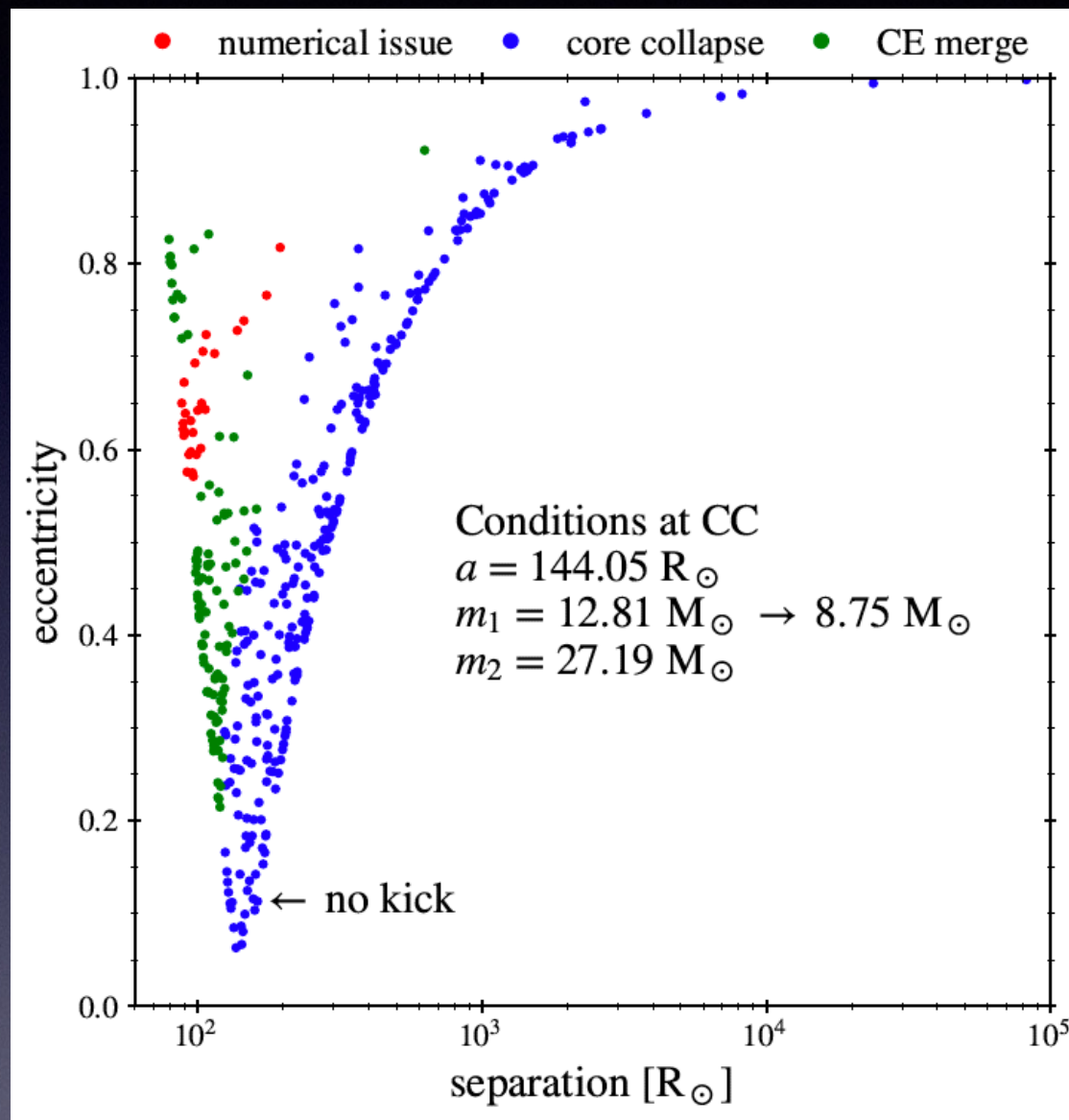




# Black hole kicks



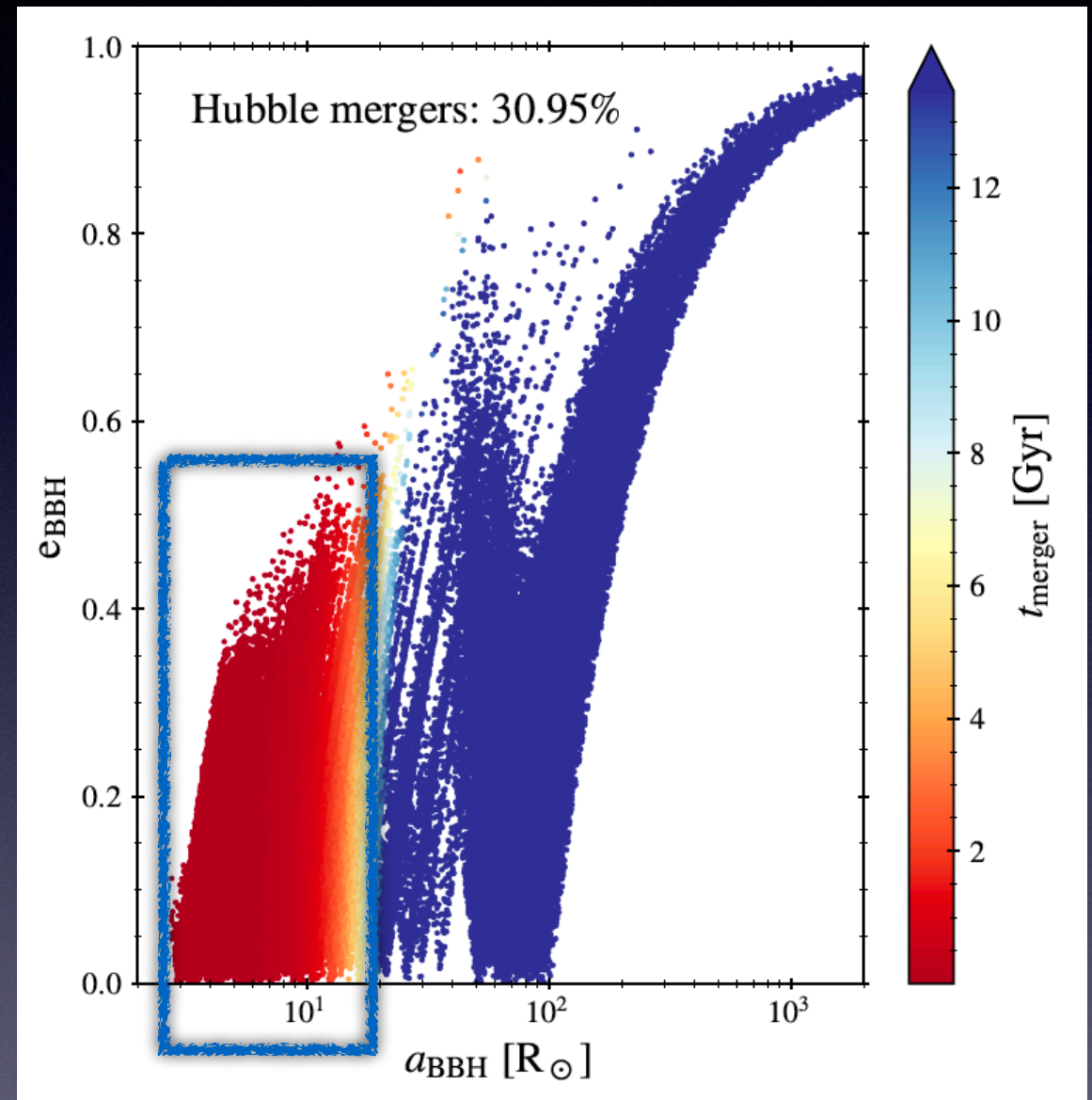
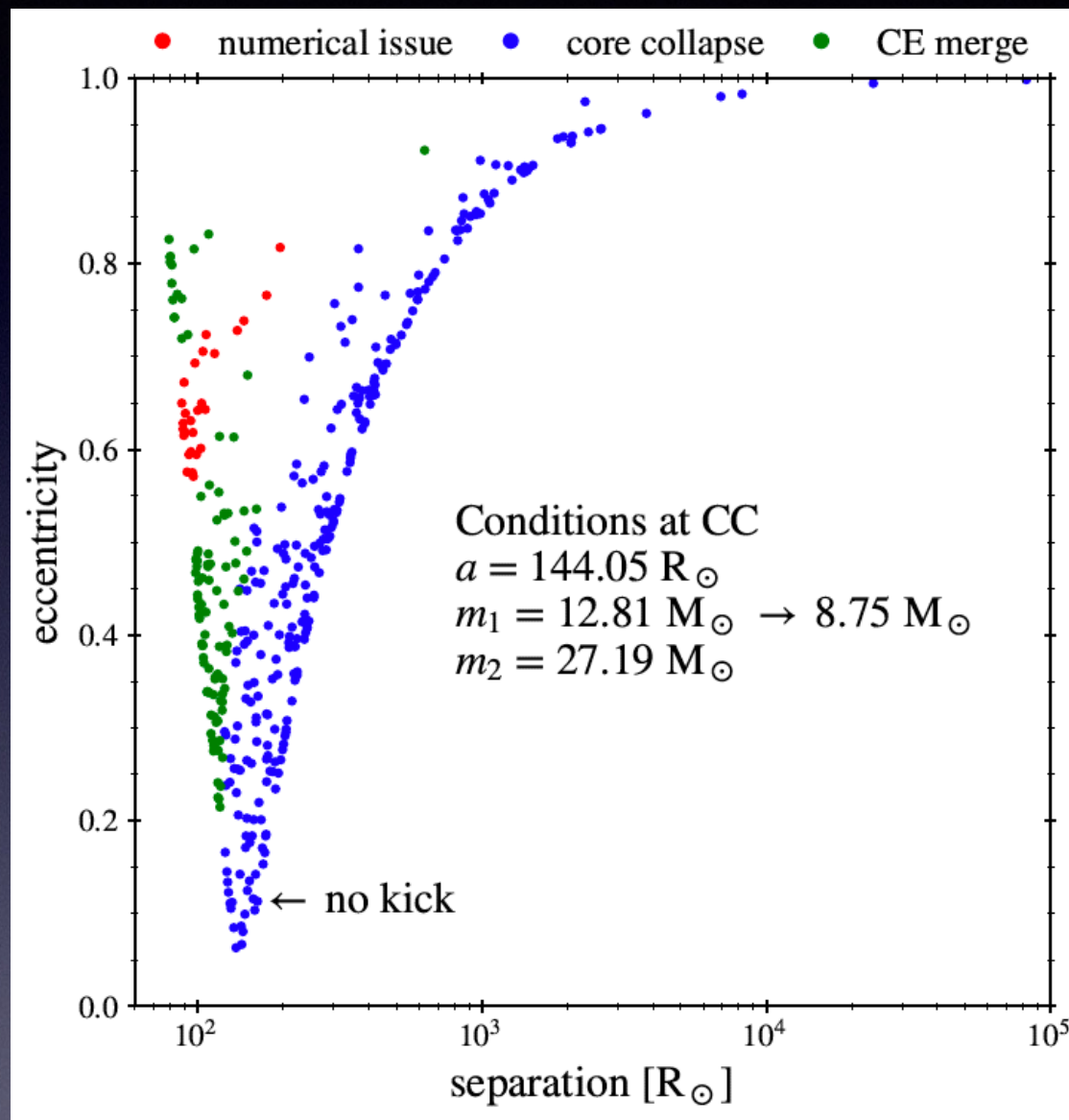
# Black hole kicks



Applying a **natal kick** during the formation of the 1st BH



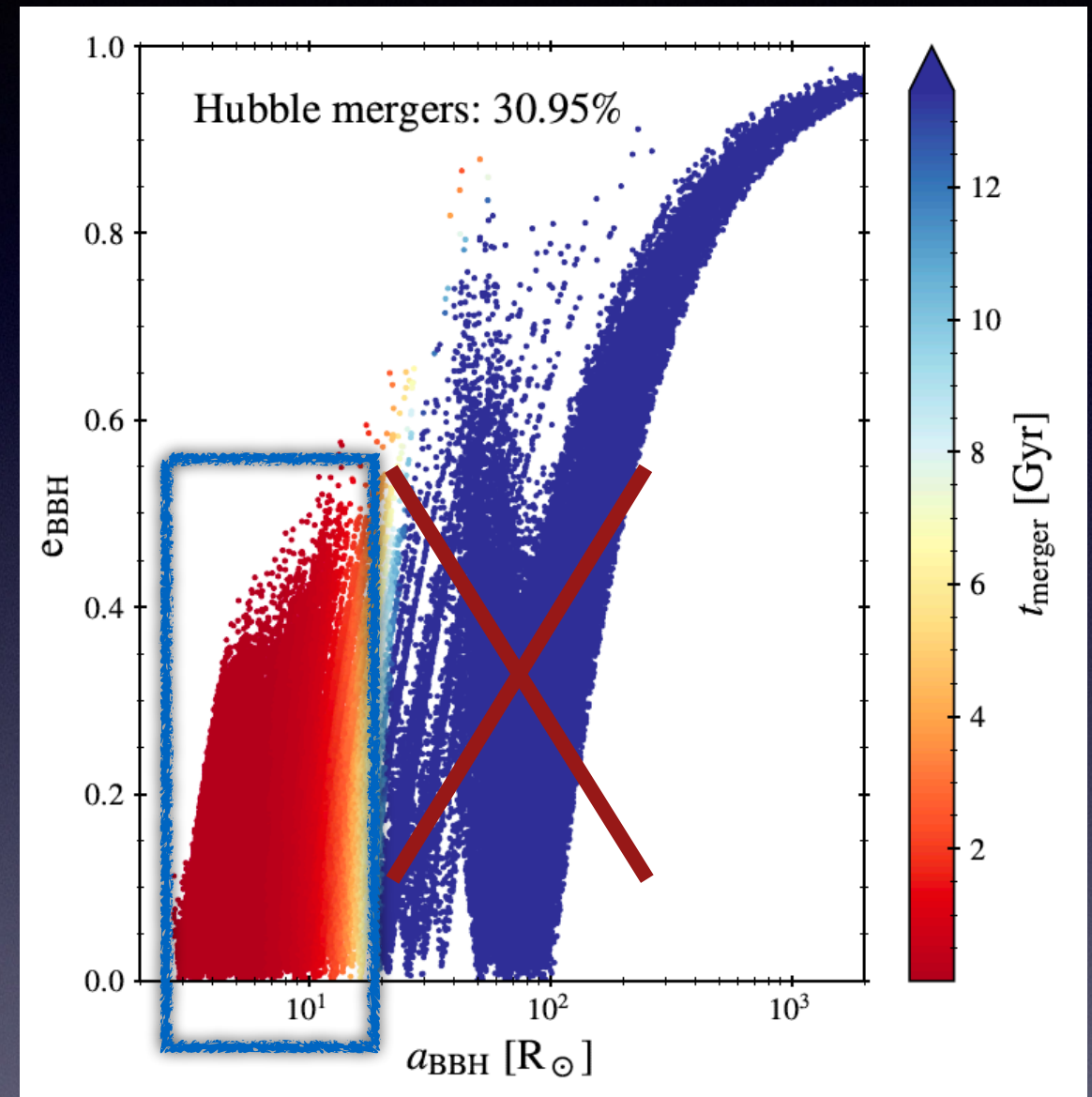
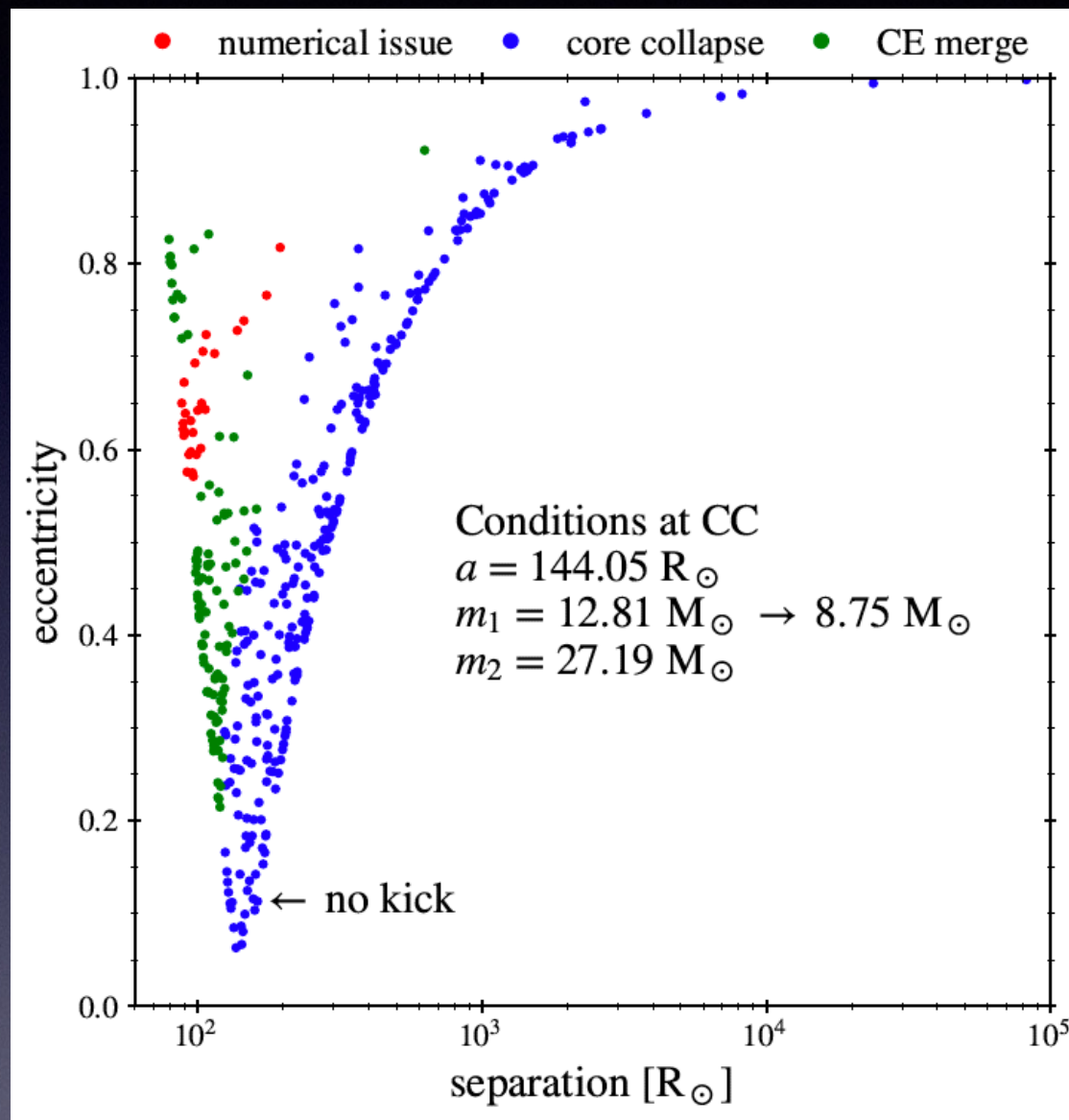
# Black hole kicks



Applying a **natal kick** during the formation of the 1st BH  
After kick: ~30% chance that BH merge within Hubble time



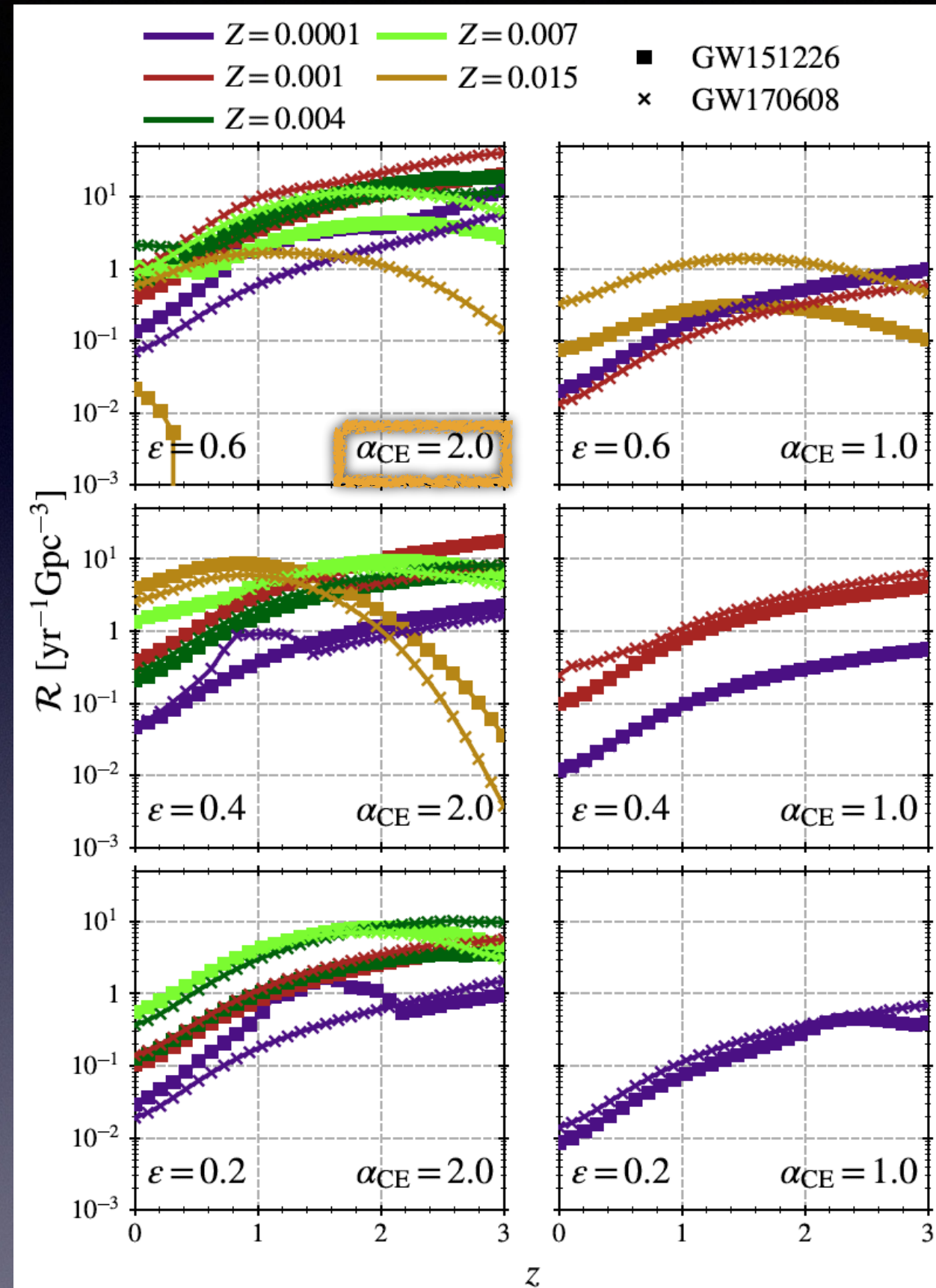
# Black hole kicks



Applying a **natal kick** during the formation of the 1st BH  
After kick: ~30% chance that BH merge within Hubble time



# Merger-rate density estimates



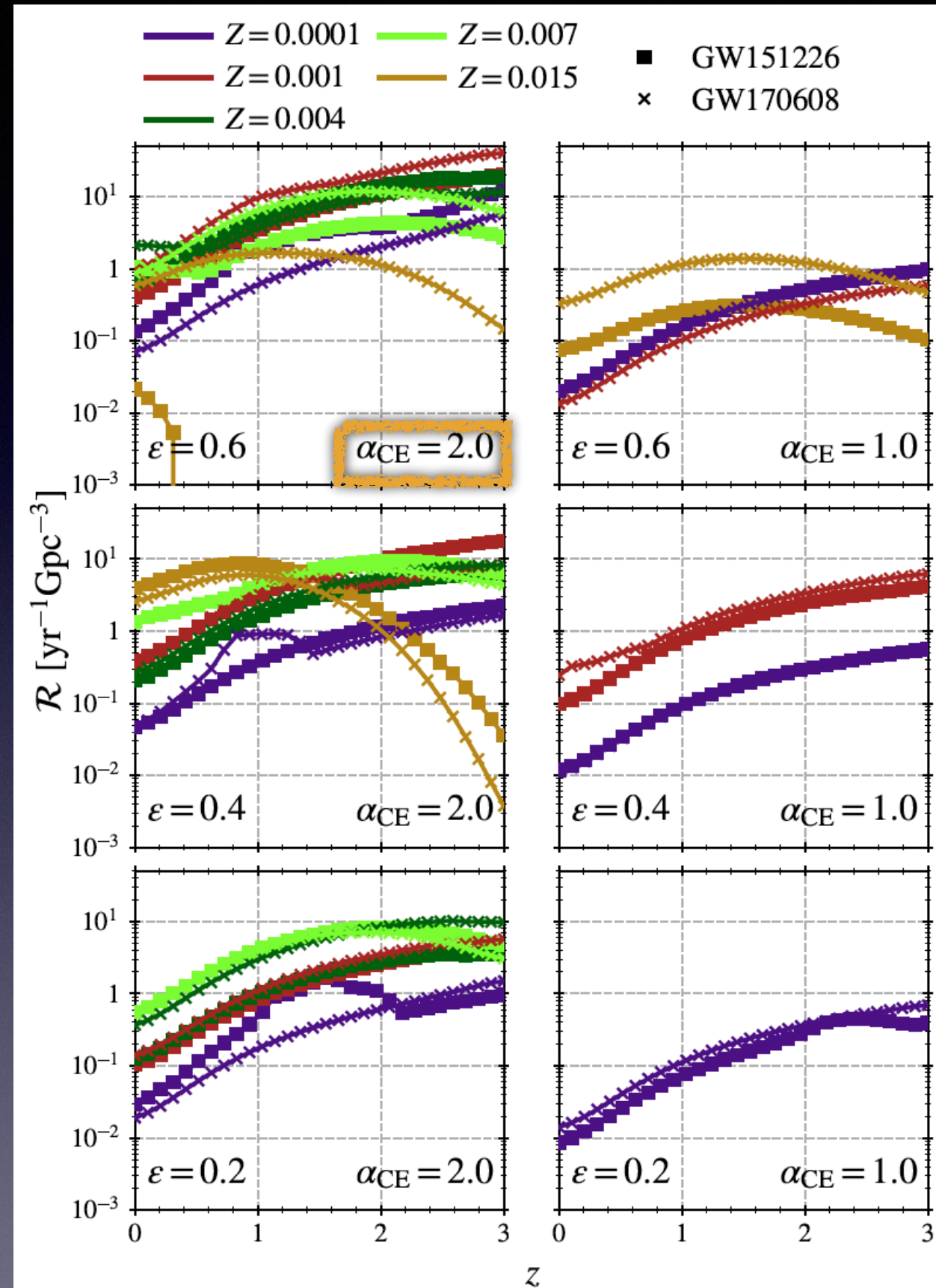


# Merger-rate density estimates

- GW event rate at redshift  $z$  obtained by Monte-Carlo simulation:

$$\mathcal{R}(Z, z(t)) = N_{\text{corr}} \int_0^{t(z)} \int_{M_{i,1}} \int_{M_{i,2}} \int_{a_i} \int_0^{t(z)} \frac{dN}{dM_{i,1} dM_{i,2} da_i dt_m} \widehat{\text{SFR}}(t'; Z) \delta[t(z) - (t_m + t')] dt_m da_i dM_{i,2} dM_{i,1} dt'$$

- SFR: star formation rate (Strolger+2004); metallicity evolution (Langer+2006)



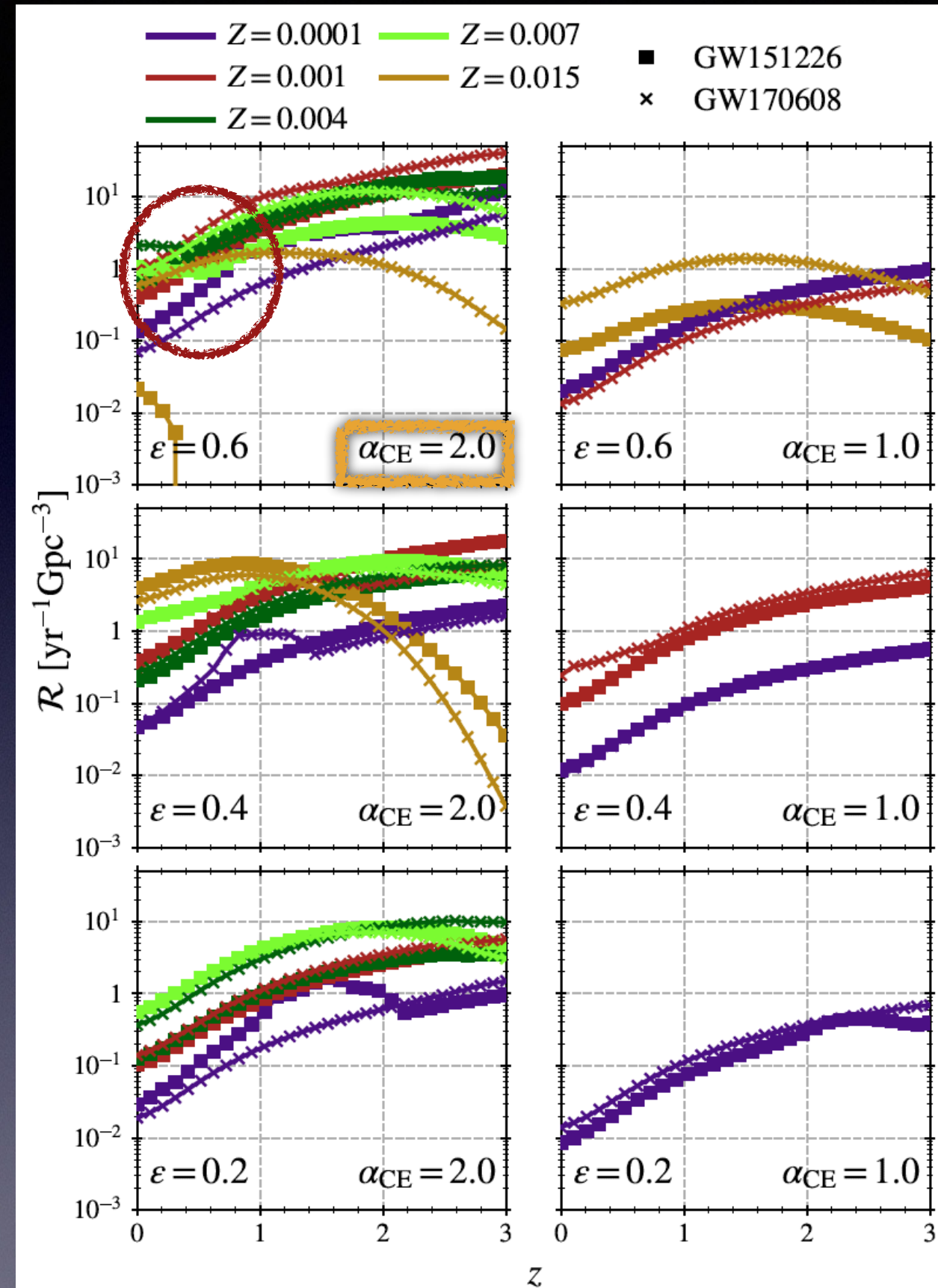


# Merger-rate density estimates

- GW event rate at redshift  $z$  obtained by Monte-Carlo simulation:

$$\mathcal{R}(Z, z(t)) = N_{\text{corr}} \int_0^{t(z)} \int_{M_{i,1}} \int_{M_{i,2}} \int_{a_i} \int_0^{t(z)} \frac{dN}{dM_{i,1} dM_{i,2} da_i dt_m} \widehat{\text{SFR}}(t'; Z) \delta[t(z) - (t_m + t')] dt_m da_i dM_{i,2} dM_{i,1} dt'$$

- SFR: star formation rate (Strolger+2004); metallicity evolution (Langer+2006)
- **Rate evolution shaped by SFR across  $z$ :**  
rapid decay found for  $z < 1$



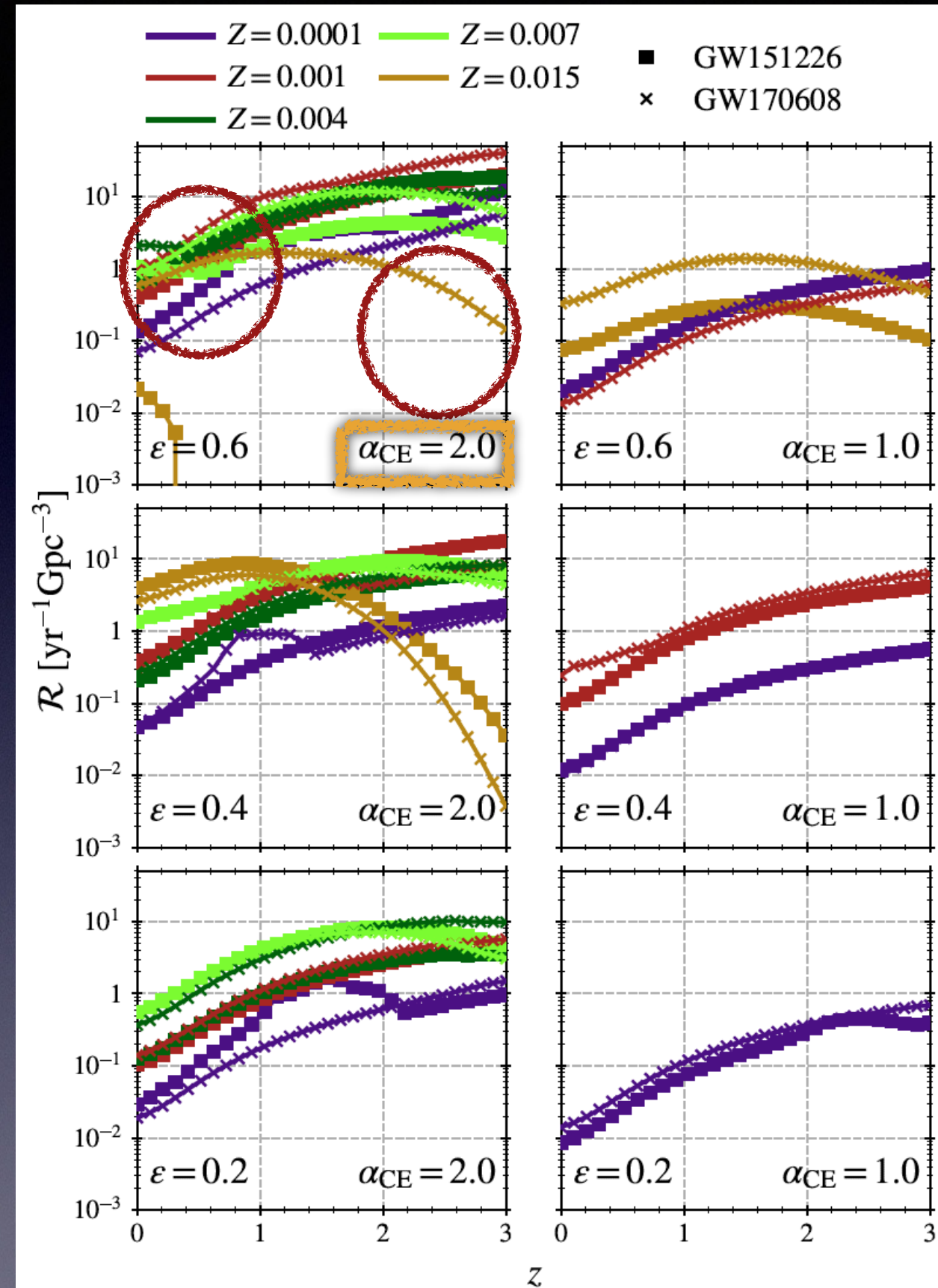


# Merger-rate density estimates

- GW event rate at redshift  $z$  obtained by Monte-Carlo simulation:

$$\mathcal{R}(Z, z(t)) = N_{\text{corr}} \int_0^{t(z)} \int_{M_{i,1}} \int_{M_{i,2}} \int_{a_i} \int_0^{t(z)} \frac{dN}{dM_{i,1} dM_{i,2} da_i dt_m} \widehat{\text{SFR}}(t'; Z) \delta[t(z) - (t_m + t')] dt_m da_i dM_{i,2} dM_{i,1} dt'$$

- SFR: star formation rate (Strolger+2004); metallicity evolution (Langer+2006)
- **Rate evolution shaped by SFR across  $z$ :** rapid decay found for  $z < 1$
- **Impact of chemical evolution on the rates (competition effect):** high  $Z$  progenitors not expected at high  $z$



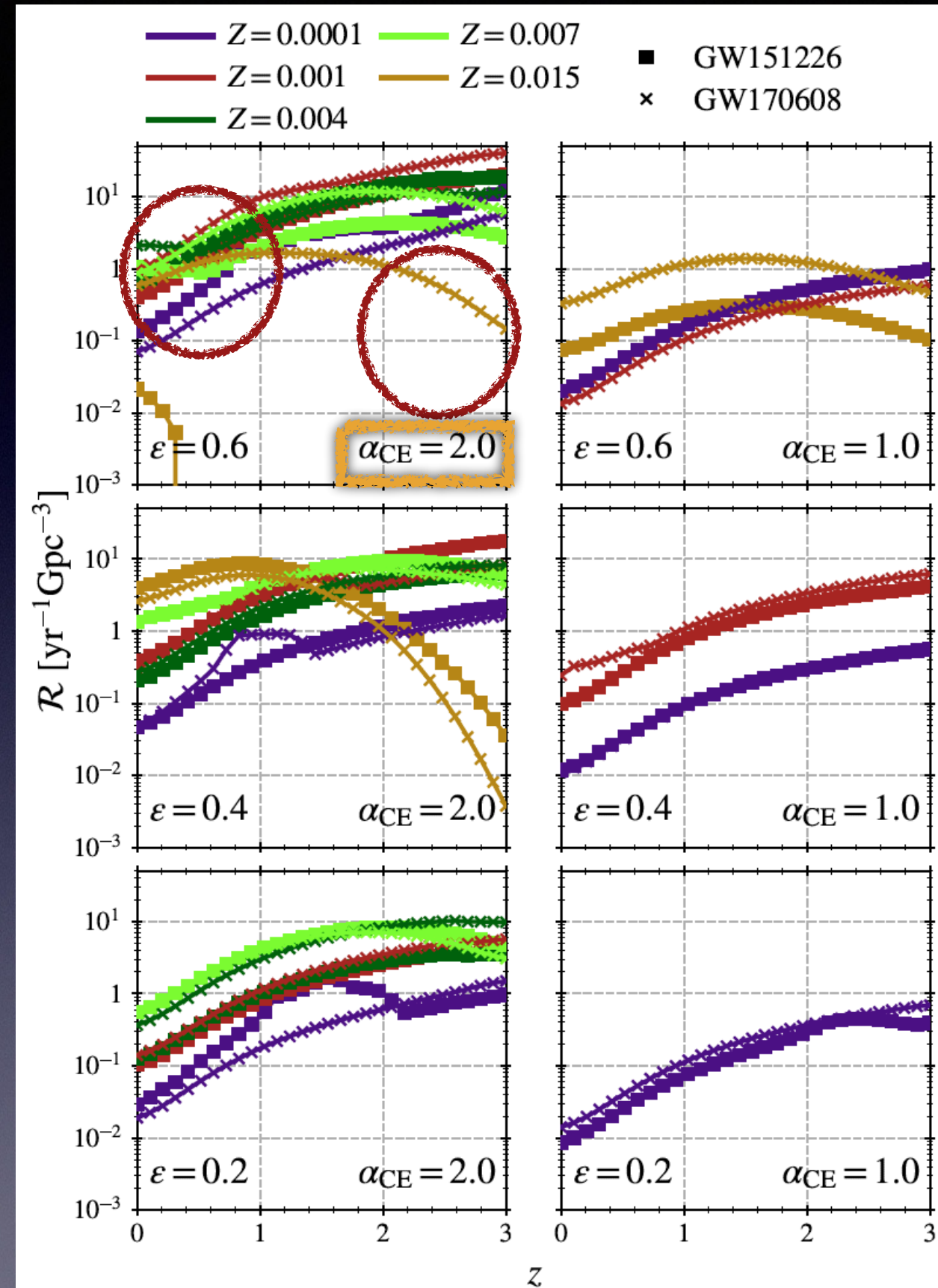


# Merger-rate density estimates

- GW event rate at redshift  $z$  obtained by Monte-Carlo simulation:

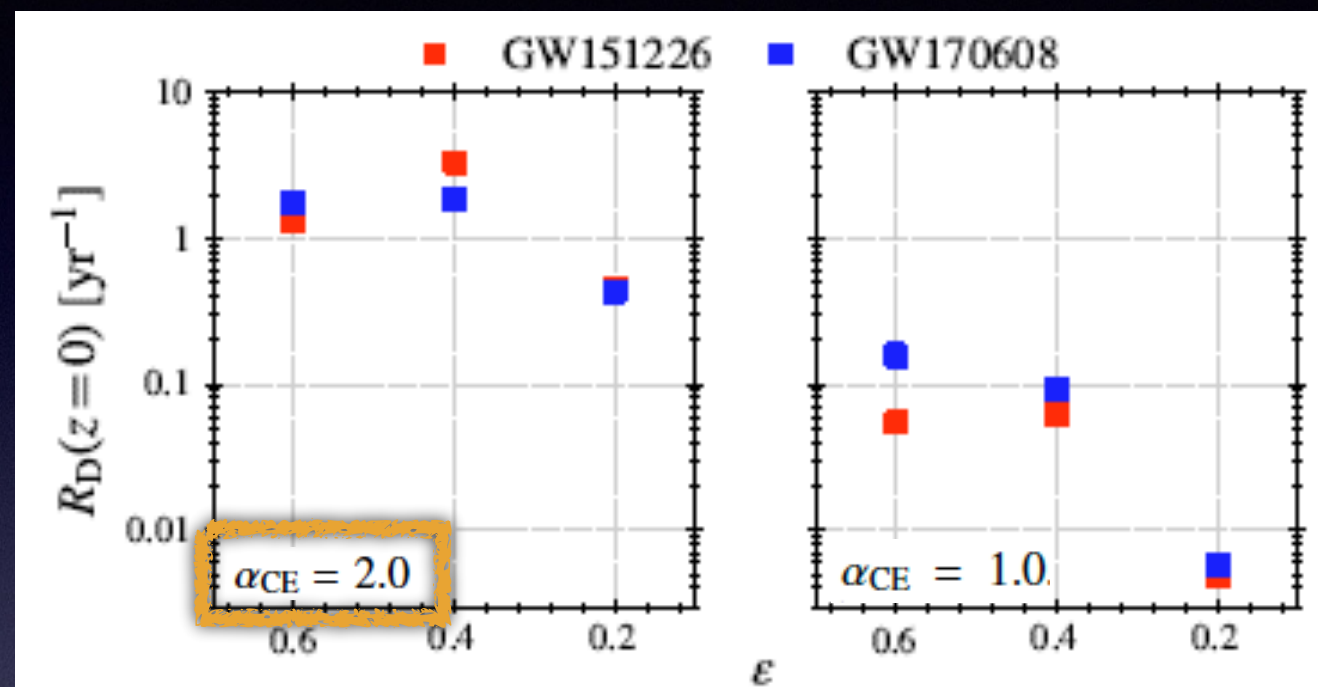
$$\mathcal{R}(Z, z(t)) = N_{\text{corr}} \int_0^{t(z)} \int_{M_{i,1}} \int_{M_{i,2}} \int_{a_i} \int_0^{t(z)} \frac{dN}{dM_{i,1} dM_{i,2} da_i dt_m} \widehat{\text{SFR}}(t'; Z) \delta[t(z) - (t_m + t')] dt_m da_i dM_{i,2} dM_{i,1} dt'$$

- SFR: star formation rate (Strolger+2004); metallicity evolution (Langer+2006)
- **Rate evolution shaped by SFR across  $z$ :** rapid decay found for  $z < 1$
- **Impact of chemical evolution on the rates (competition effect):** high  $Z$  progenitors not expected at high  $z$
- **Local merger rate densities are larger for high MT & high CE efficiency**





# Total merger detection rates for O1/O2 runs

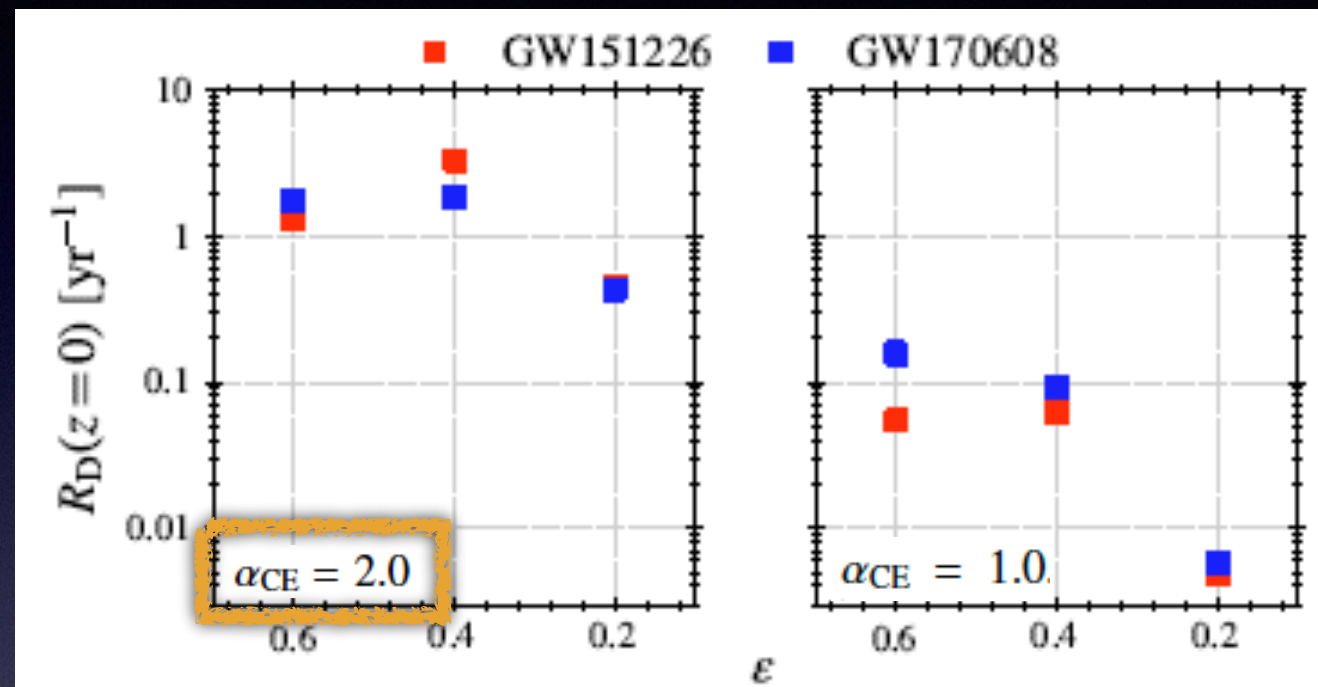


Rate dependence vs MT/CE efficiency

$D_h$ : horizon distance  
 $M_c$ : BBH chirp mass  
 $R$  merger rate density



# Total merger detection rates for O1/O2 runs



Rate dependence vs MT/CE efficiency

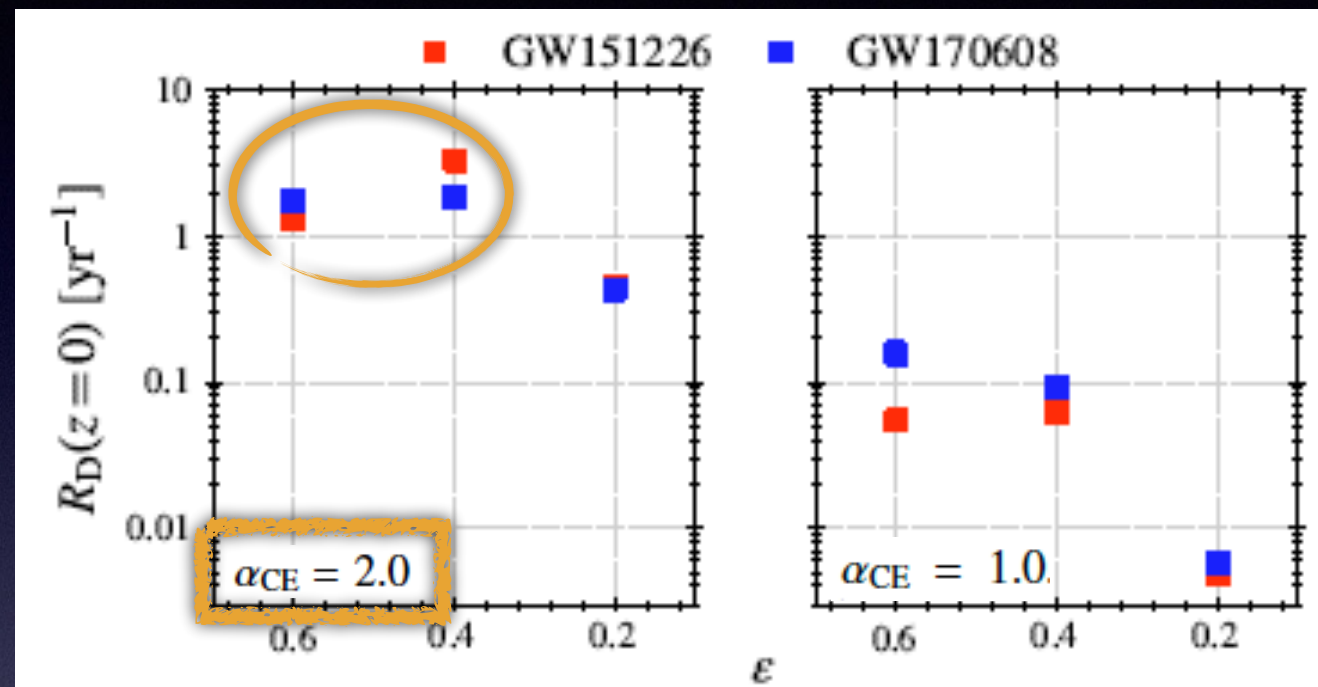
- To estimate the local detection rate, we consider the detector sensitivity of LIGO/Virgo and the local ( $z=0$ ) merger rate densities:

$$R_D = \frac{4\pi}{3} D_h^3 \langle w^3 \rangle \langle (M_c / 1.2 M_\odot)^{15/6} \rangle \mathcal{R}(z=0)$$

$D_h$ : horizon distance  
 $M_c$ : BBH chirp mass  
 $\mathcal{R}$  merger rate density



# Total merger detection rates for O1/O2 runs



Rate dependence vs MT/CE efficiency

- To estimate the local detection rate, we consider the detector sensitivity of LIGO/Virgo and the local ( $z=0$ ) merger rate densities:

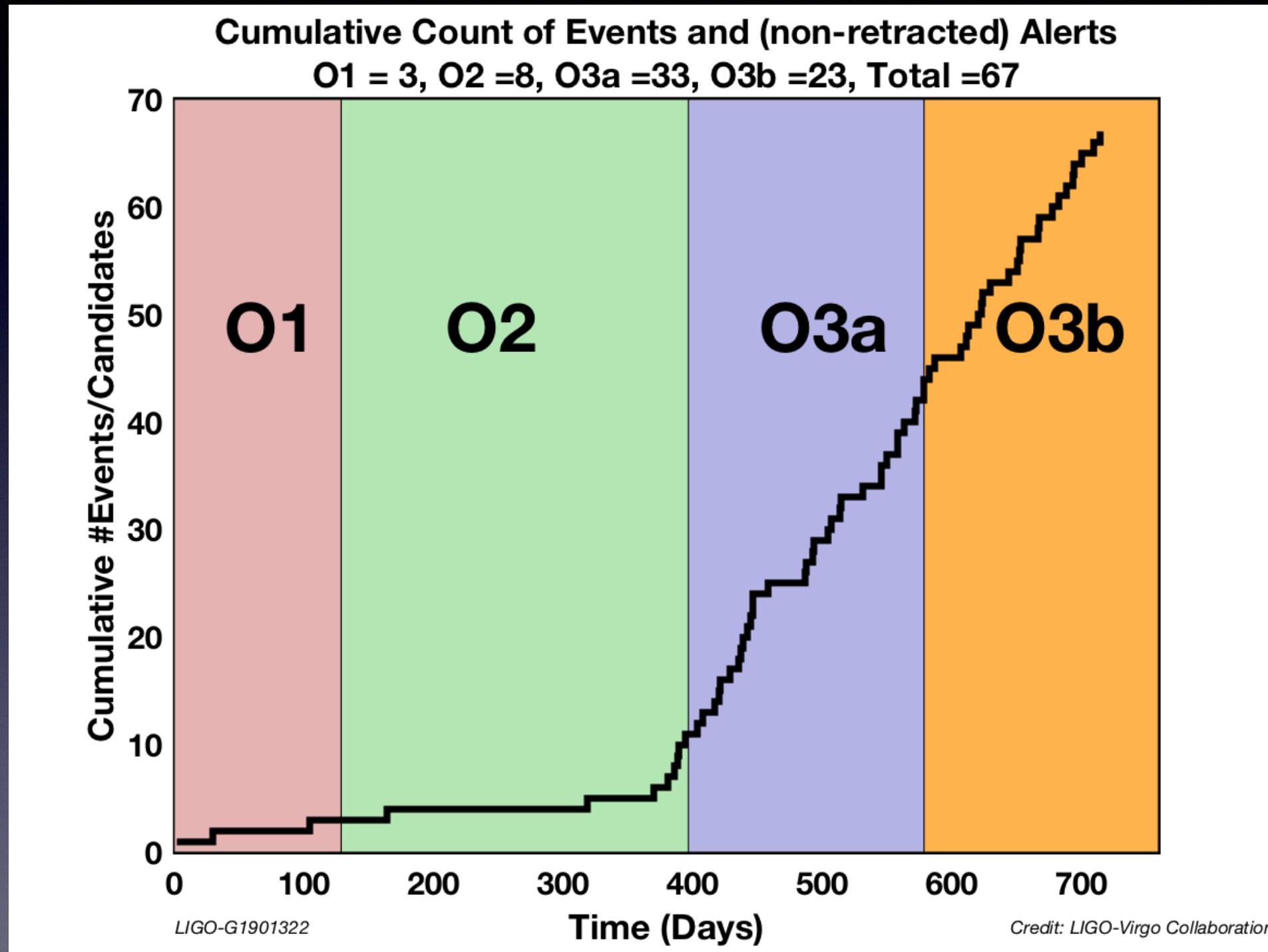
$$R_D = \frac{4\pi}{3} D_h^3 \langle w^3 \rangle \langle (M_c / 1.2 M_\odot)^{15/6} \rangle \mathcal{R}(z=0)$$

$D_h$ : horizon distance  
 $M_c$ : BBH chirp mass  
 $\mathcal{R}$  merger rate density

- => detection rate of low-mass BBH : **0.5 - 3.0 Gpc<sup>-3</sup> yr<sup>-1</sup>** ( $\sim 1.2$ - $3.3$  events/yr)  
 To compare to **10 - 30 Gpc<sup>-3</sup> yr<sup>-1</sup>** for full BBH population (O1—O3, Abbott+2021)

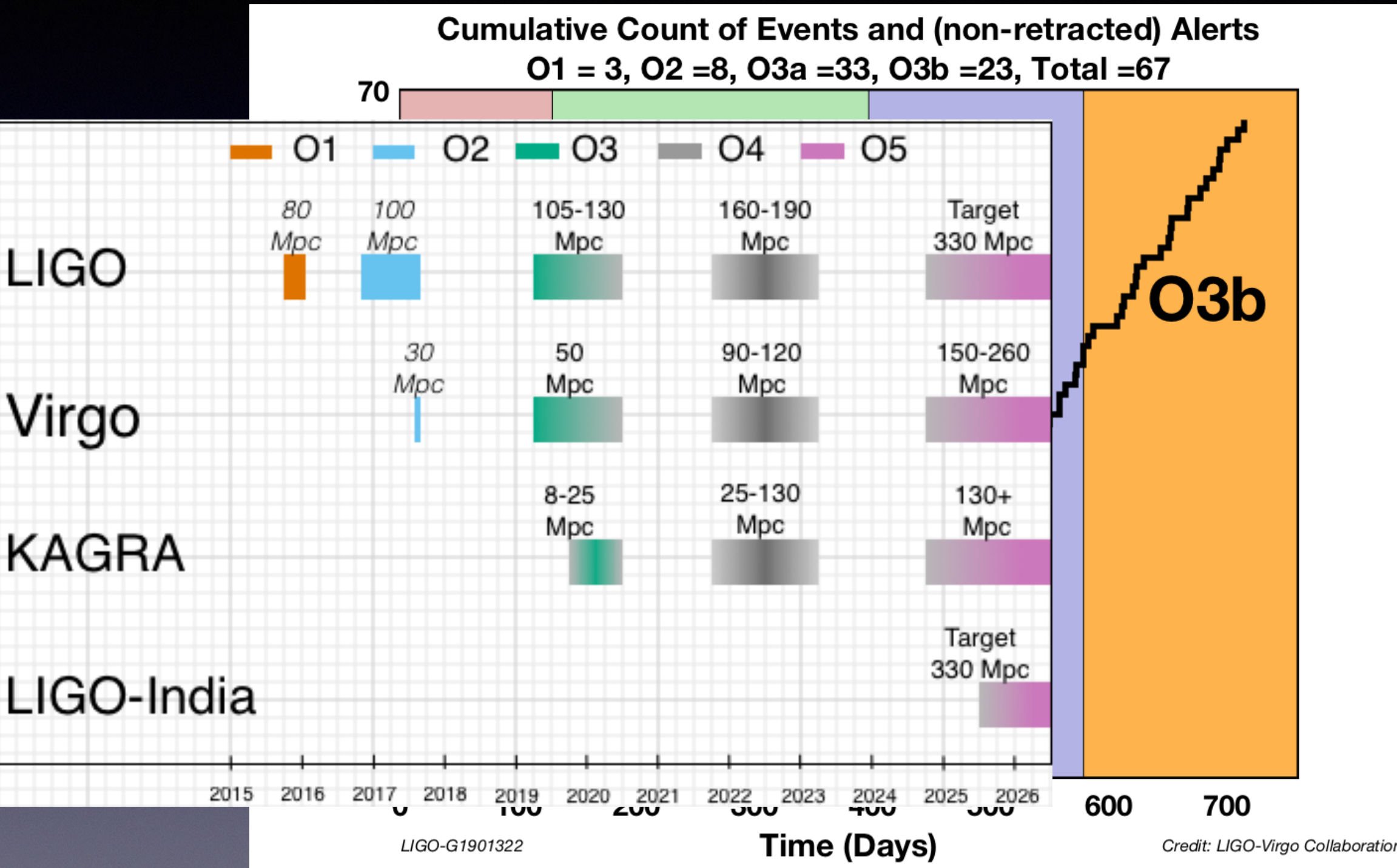


# Gravitational waves (LIGO/Virgo/KAGRA)





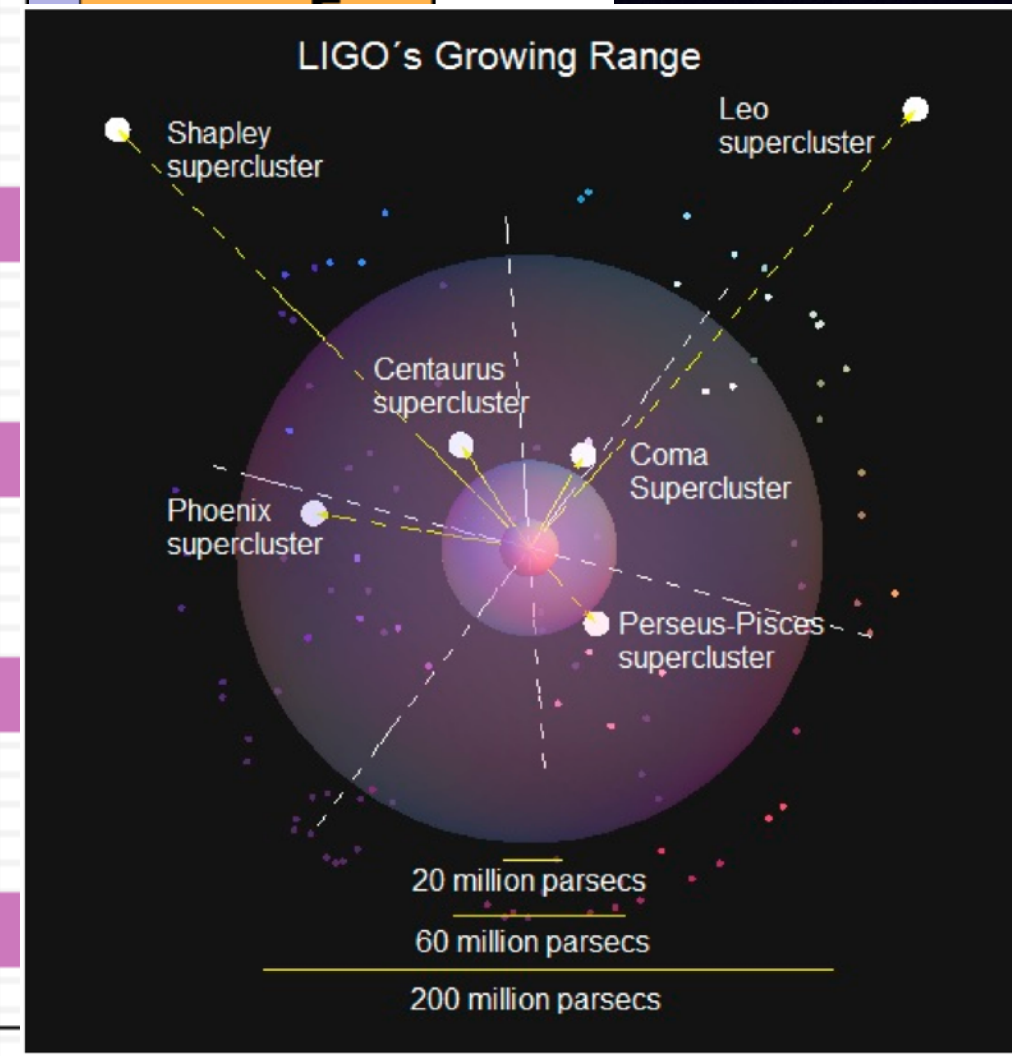
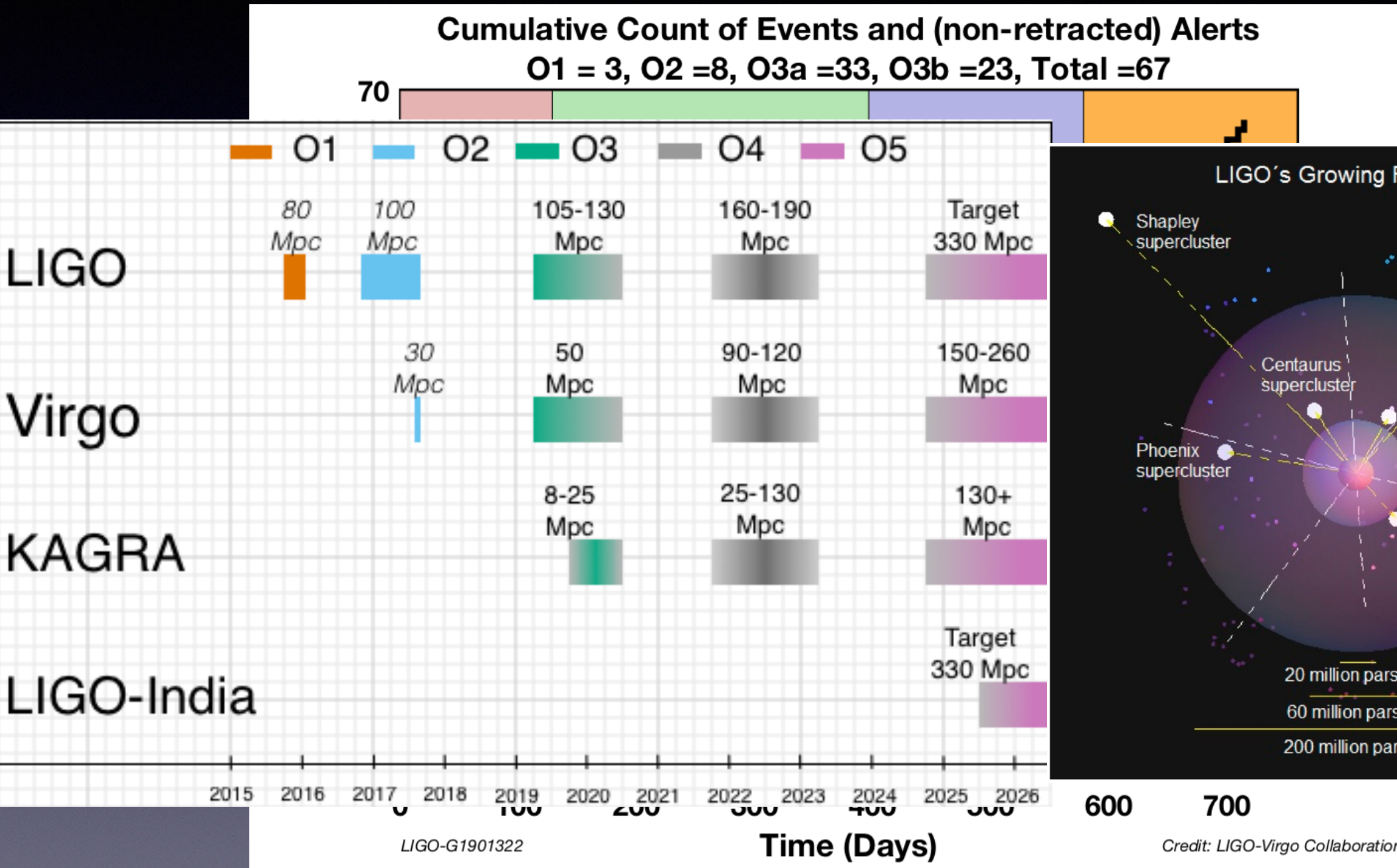
# Gravitational waves (LIGO/Virgo/KAGRA)



- LVK future observations (O4 from 12/2022)



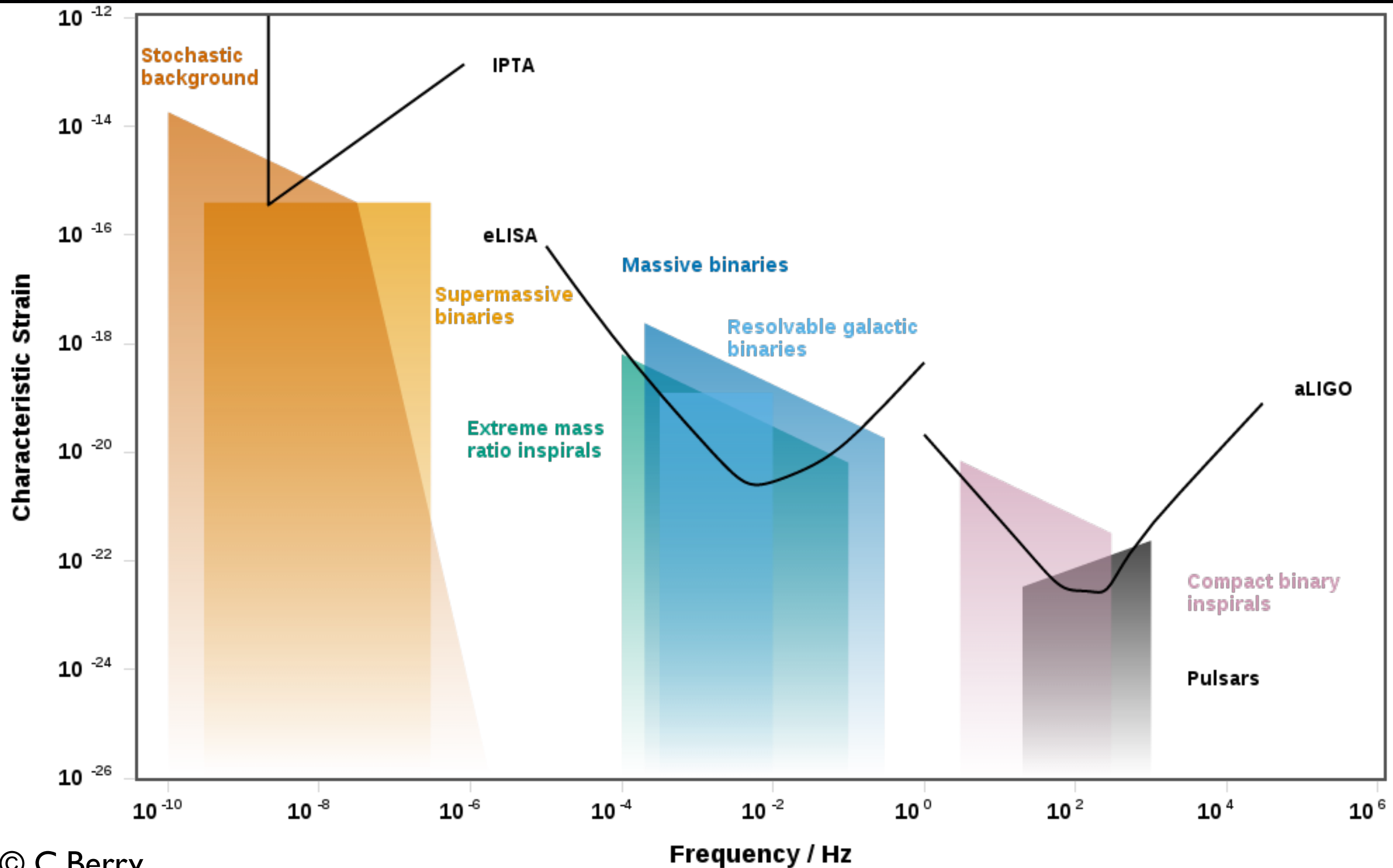
# Gravitational waves (LIGO/Virgo/KAGRA)



- LVK future observations (O4 from 12/2022)

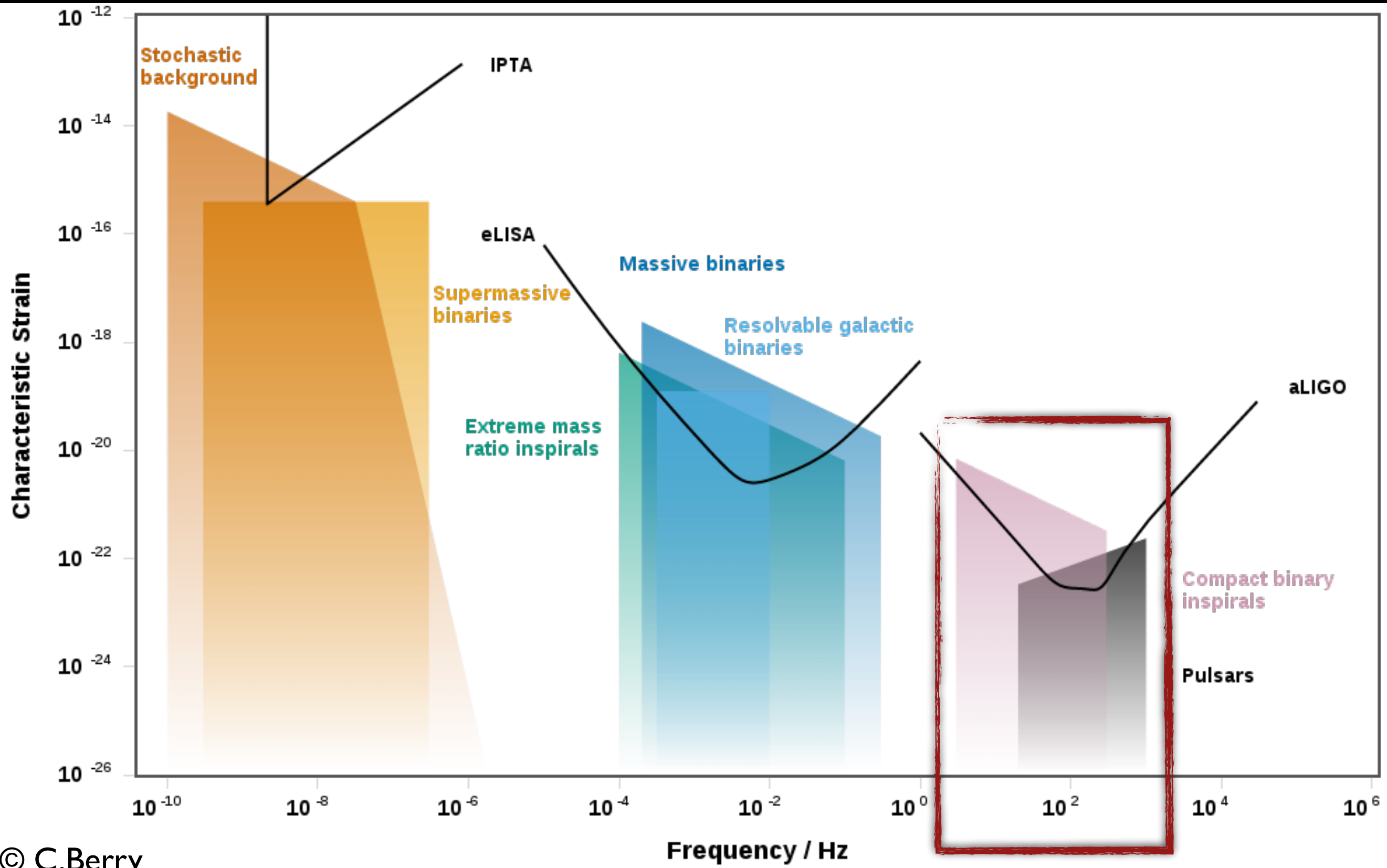


# The future of gravitational waves





# The future of gravitational waves

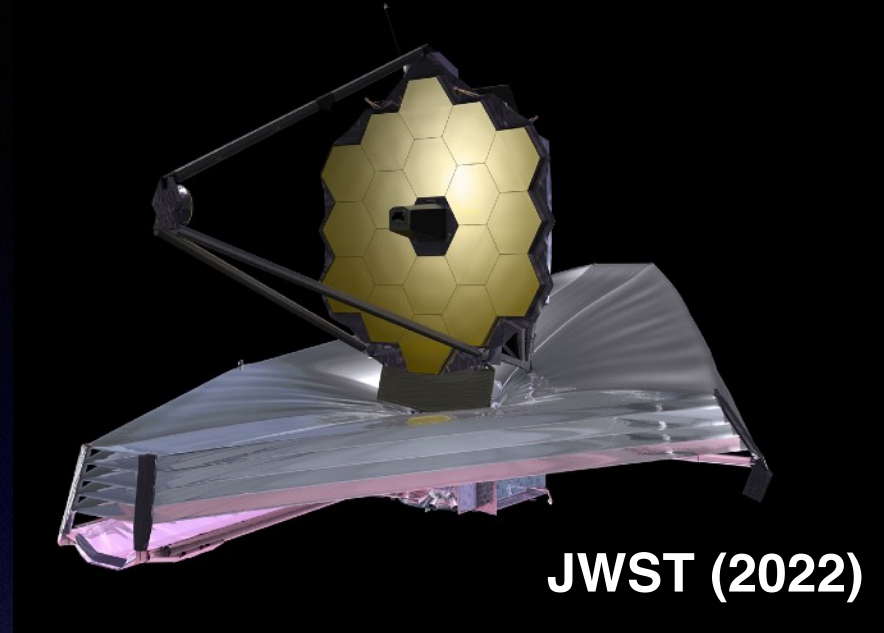




# Multi-wavelength + multi-messenger astrophysics

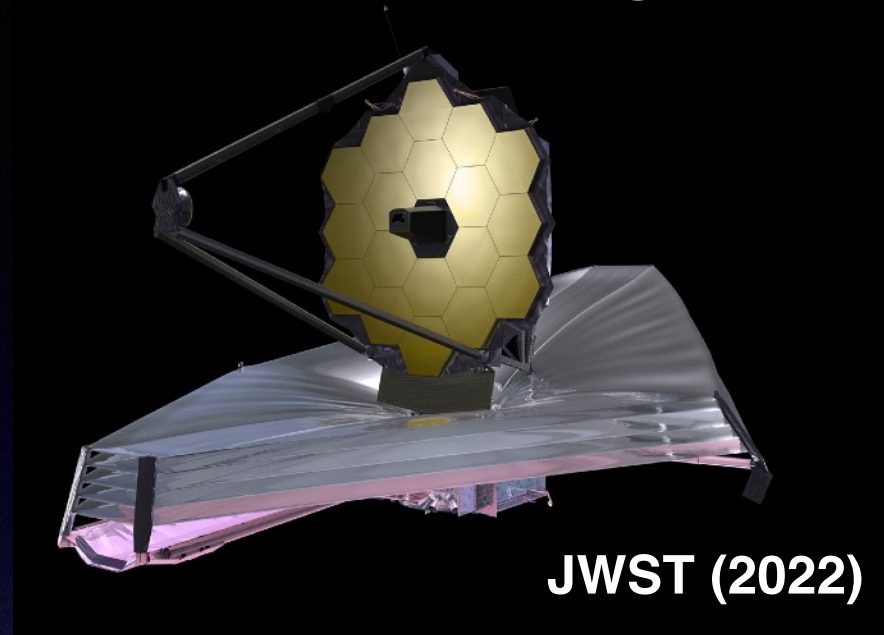


# Multi-wavelength + multi-messenger astrophysics



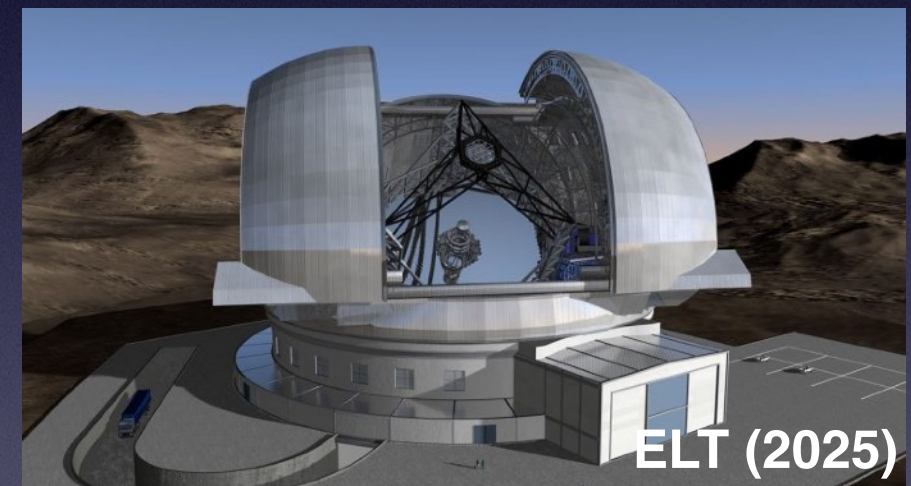
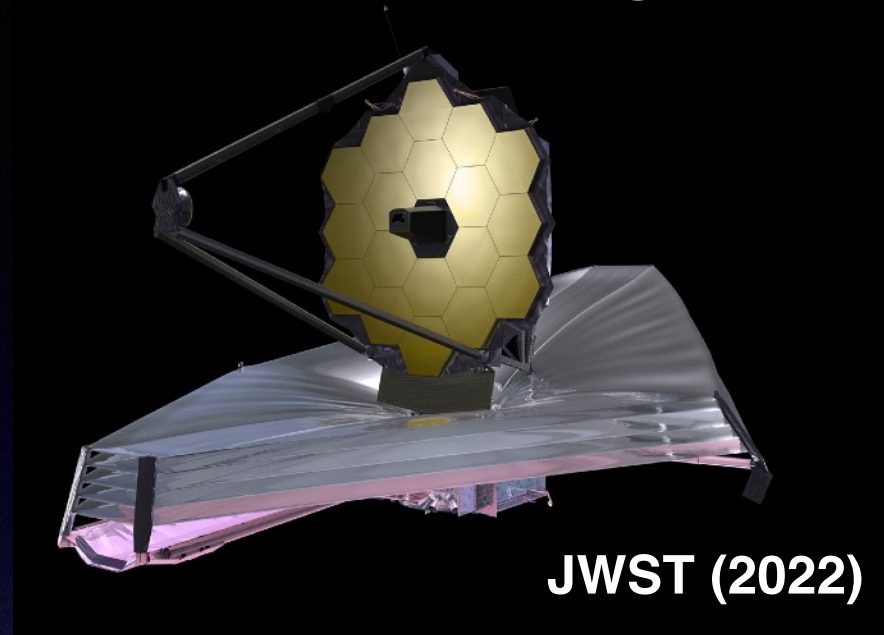


# Multi-wavelength + multi-messenger astrophysics



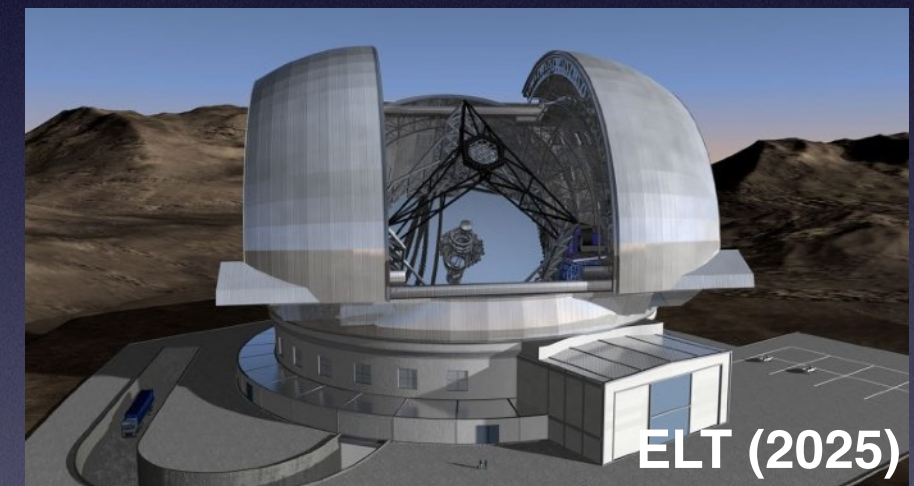
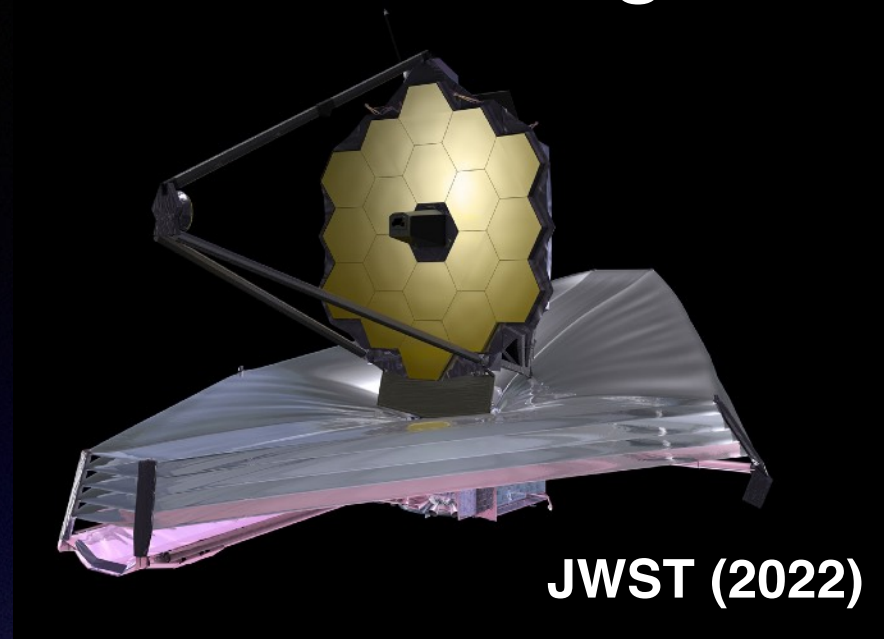


# Multi-wavelength + multi-messenger astrophysics



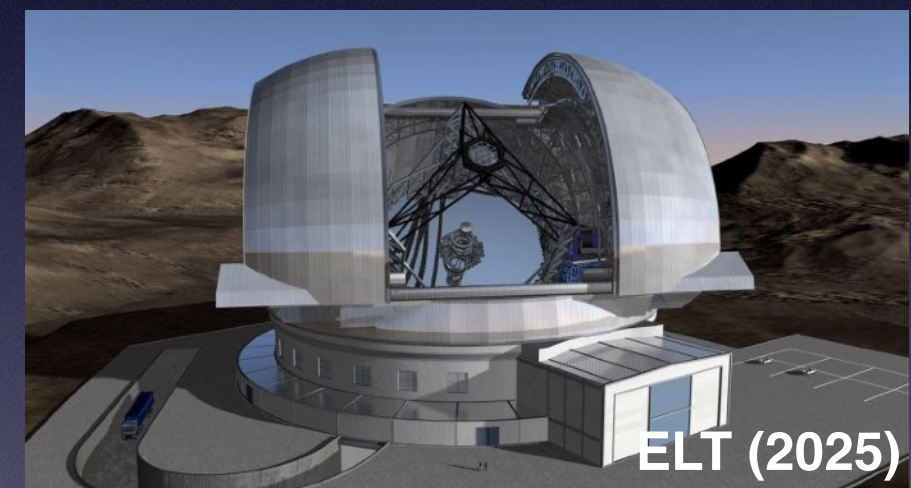
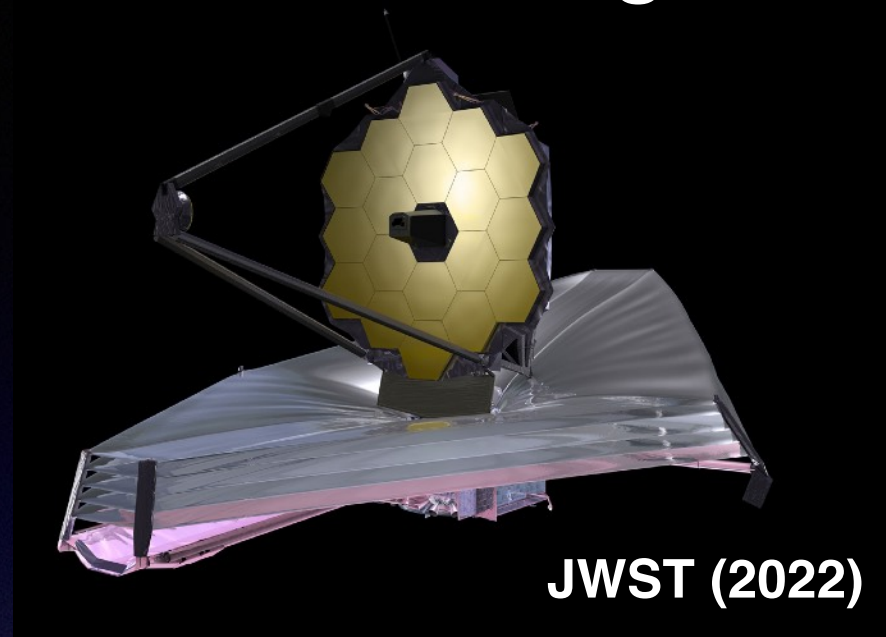


# Multi-wavelength + multi-messenger astrophysics



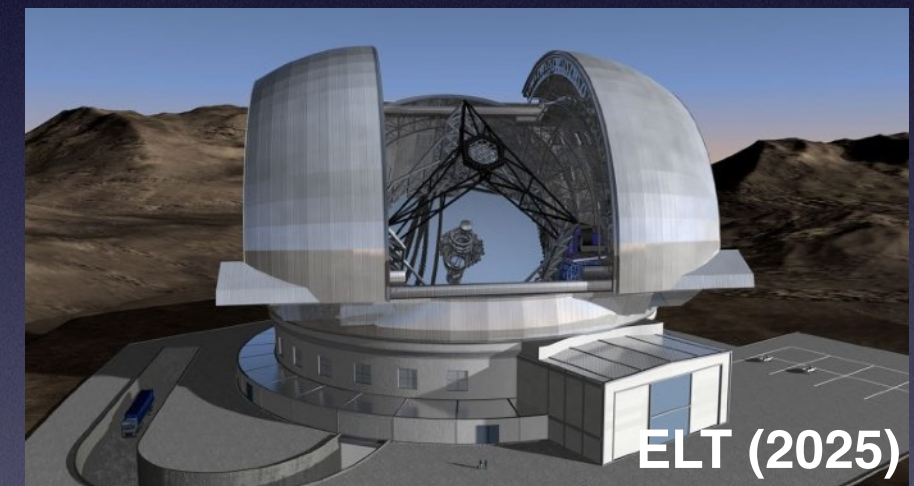
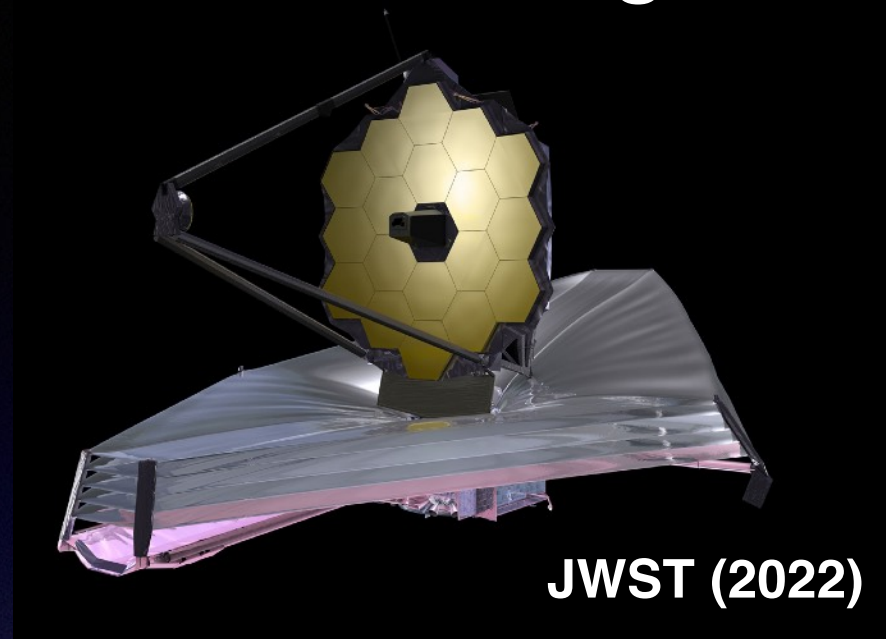


# Multi-wavelength + multi-messenger astrophysics



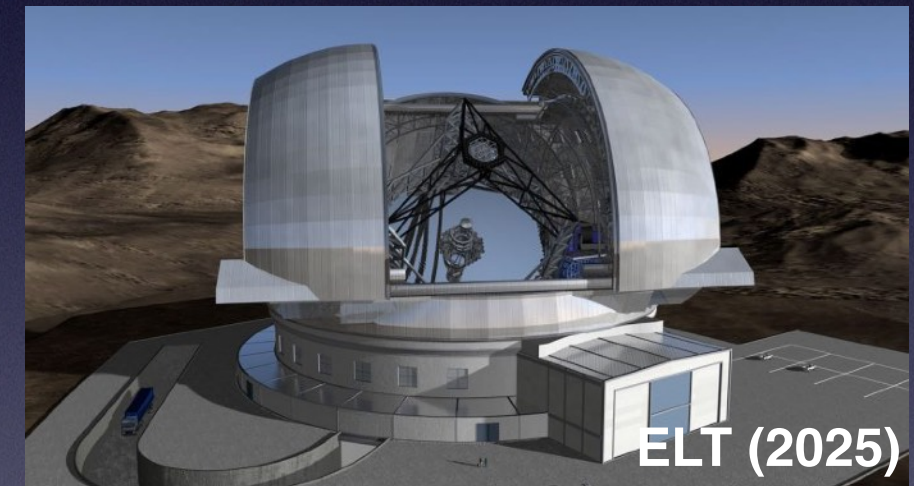
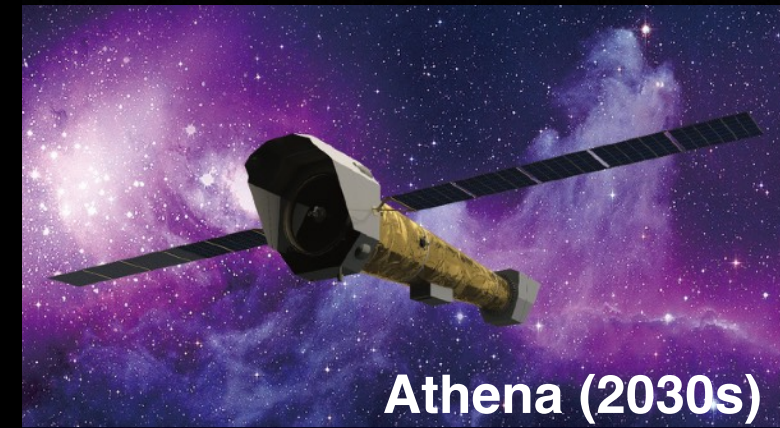
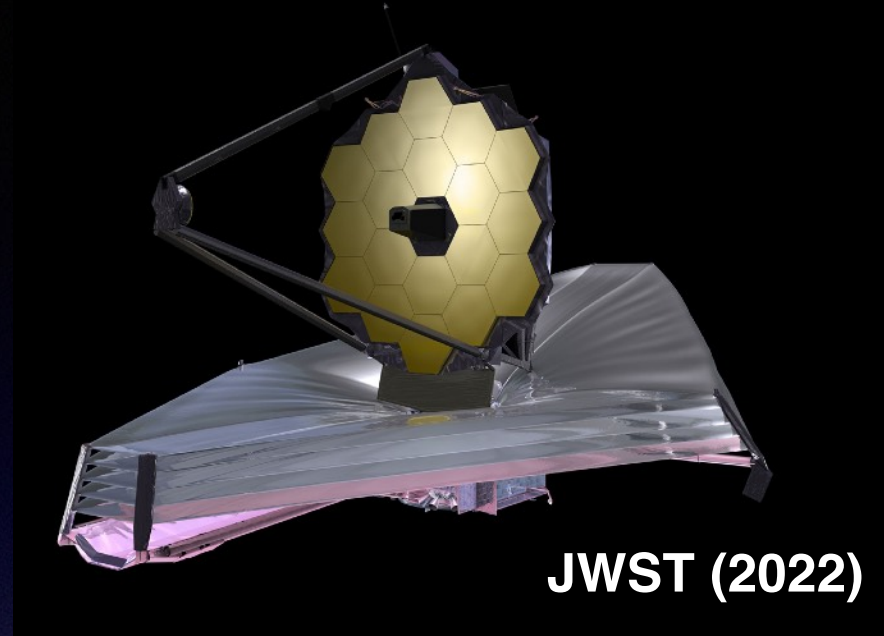
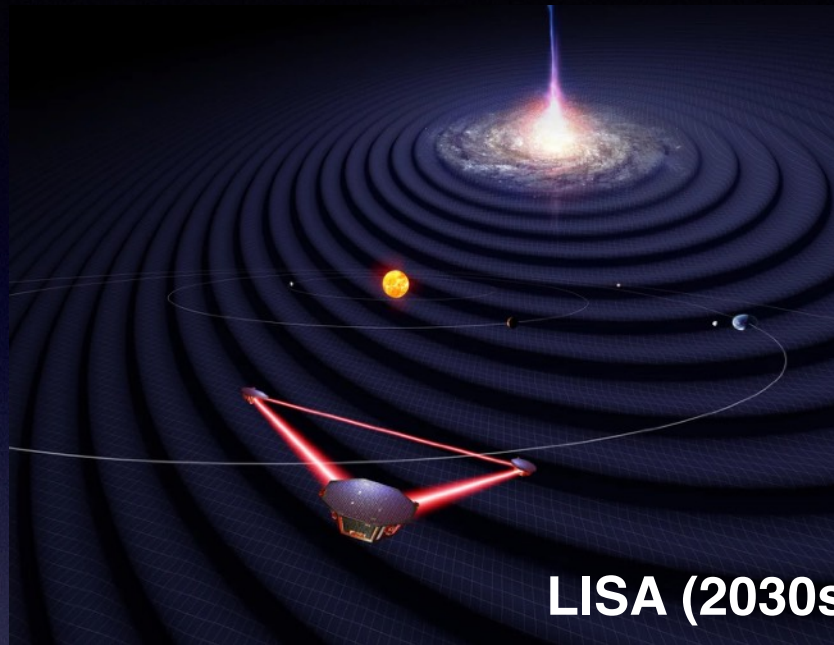


# Multi-wavelength + multi-messenger astrophysics



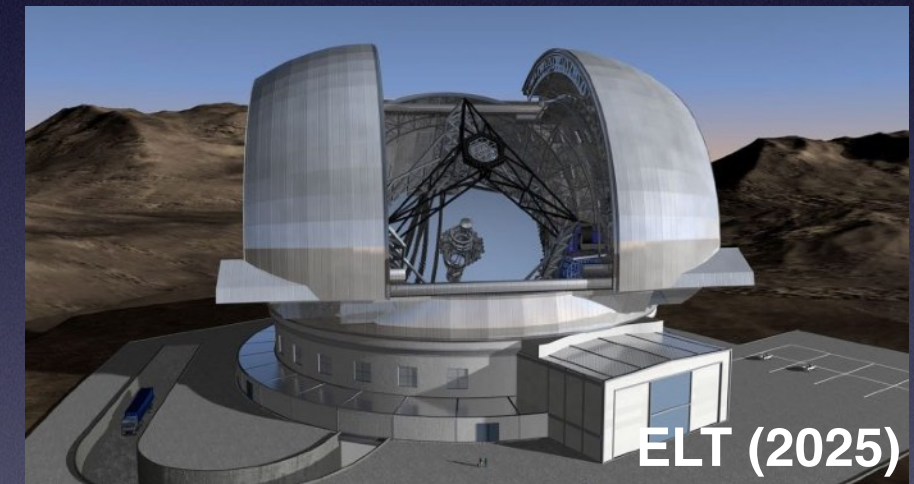
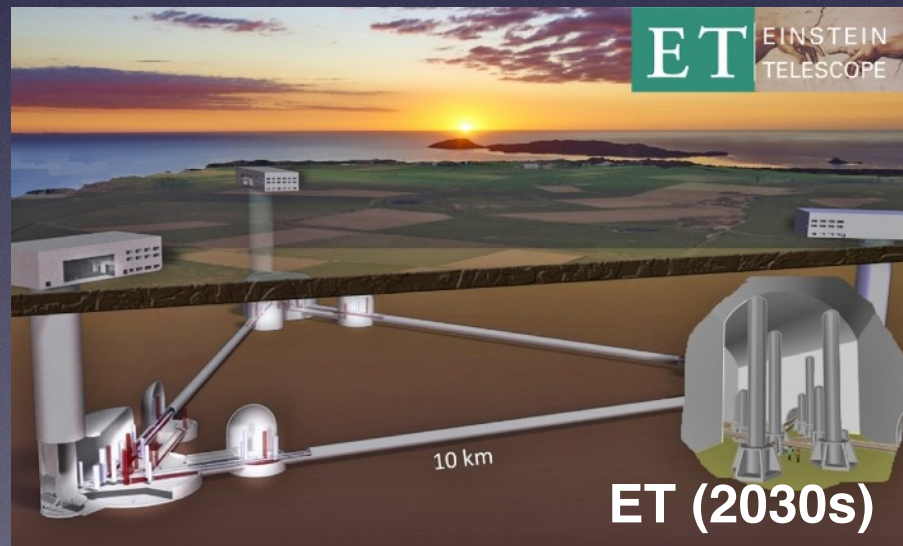
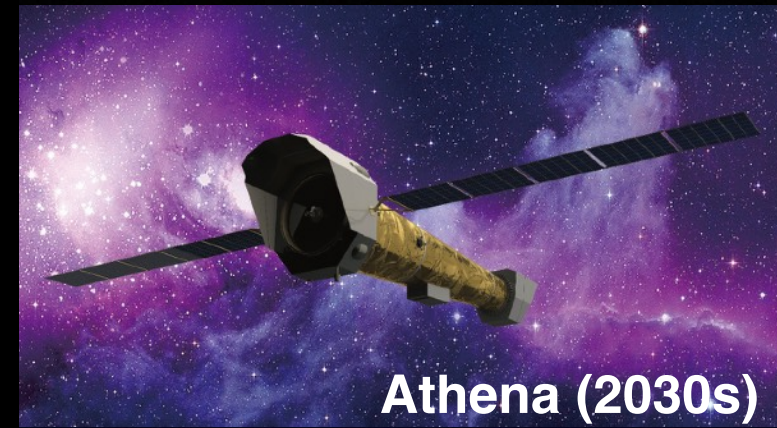
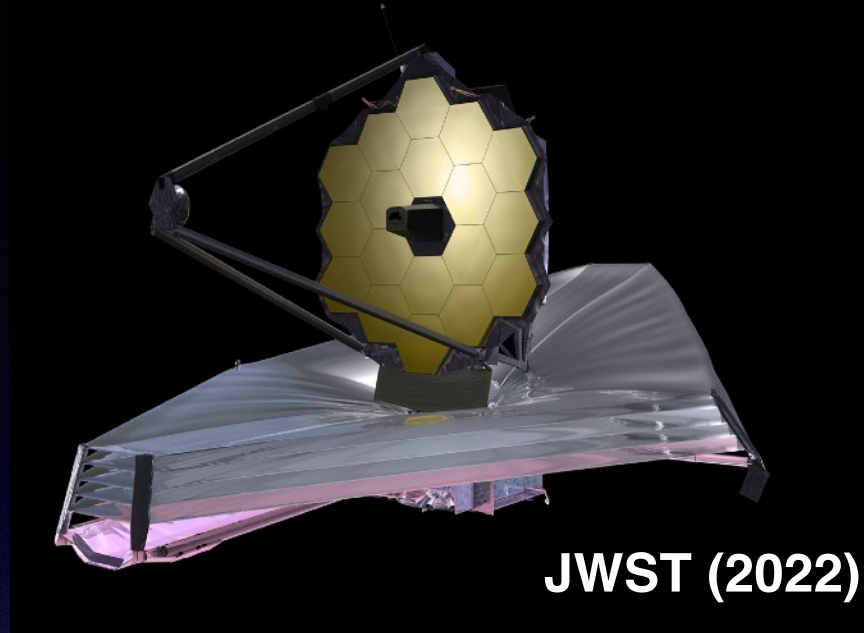
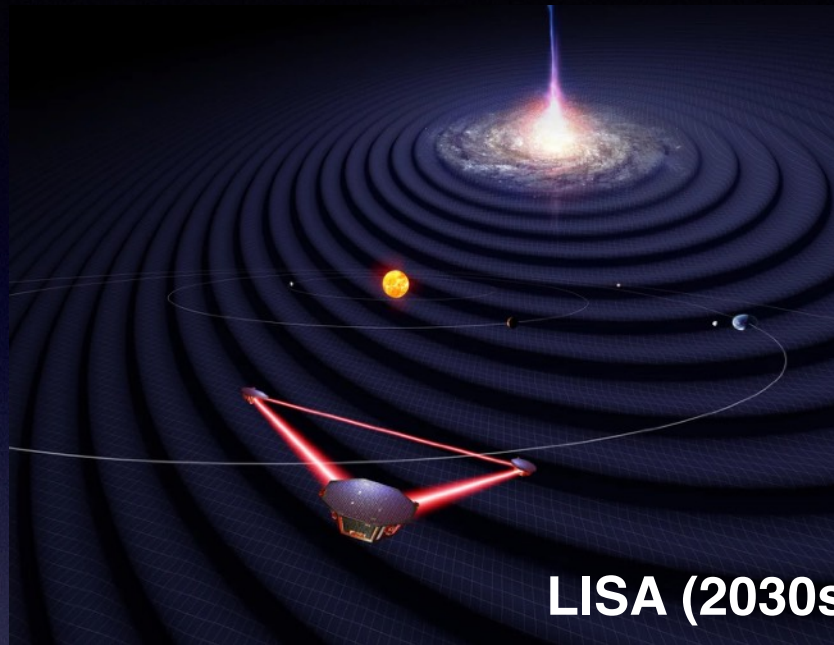


# Multi-wavelength + multi-messenger astrophysics





# Multi-wavelength + multi-messenger astrophysics





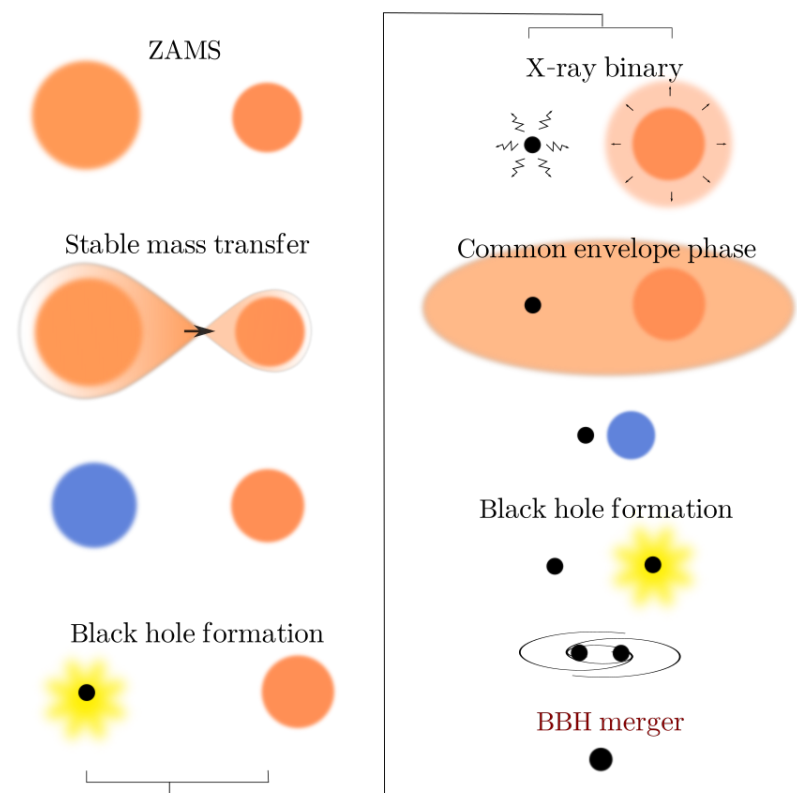
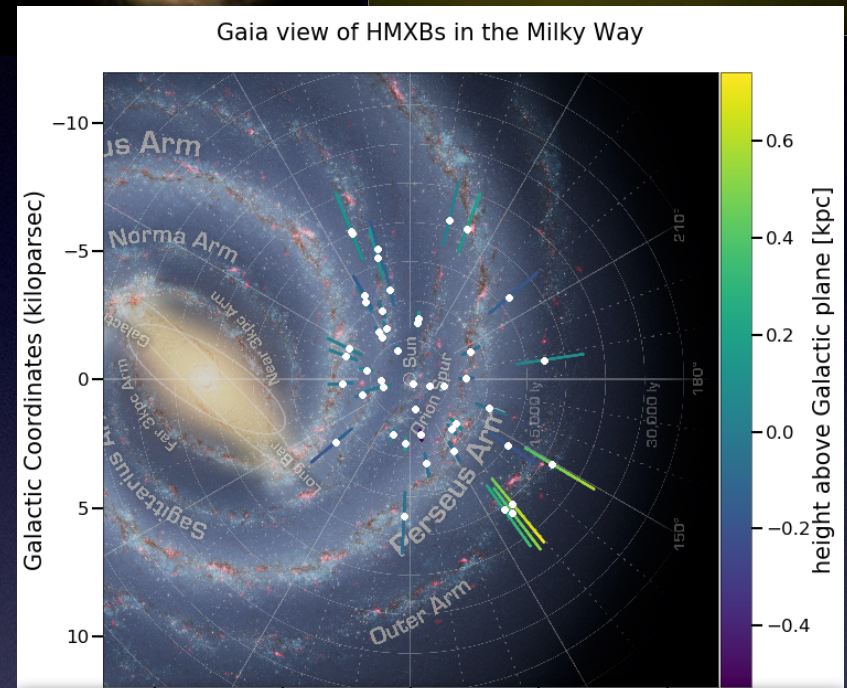
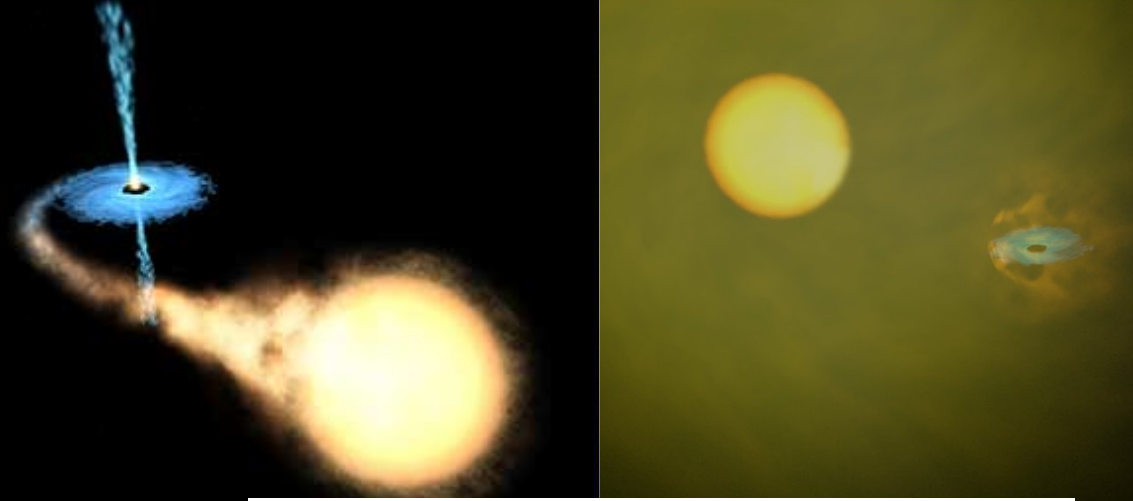
# Conclusions



# Conclusions

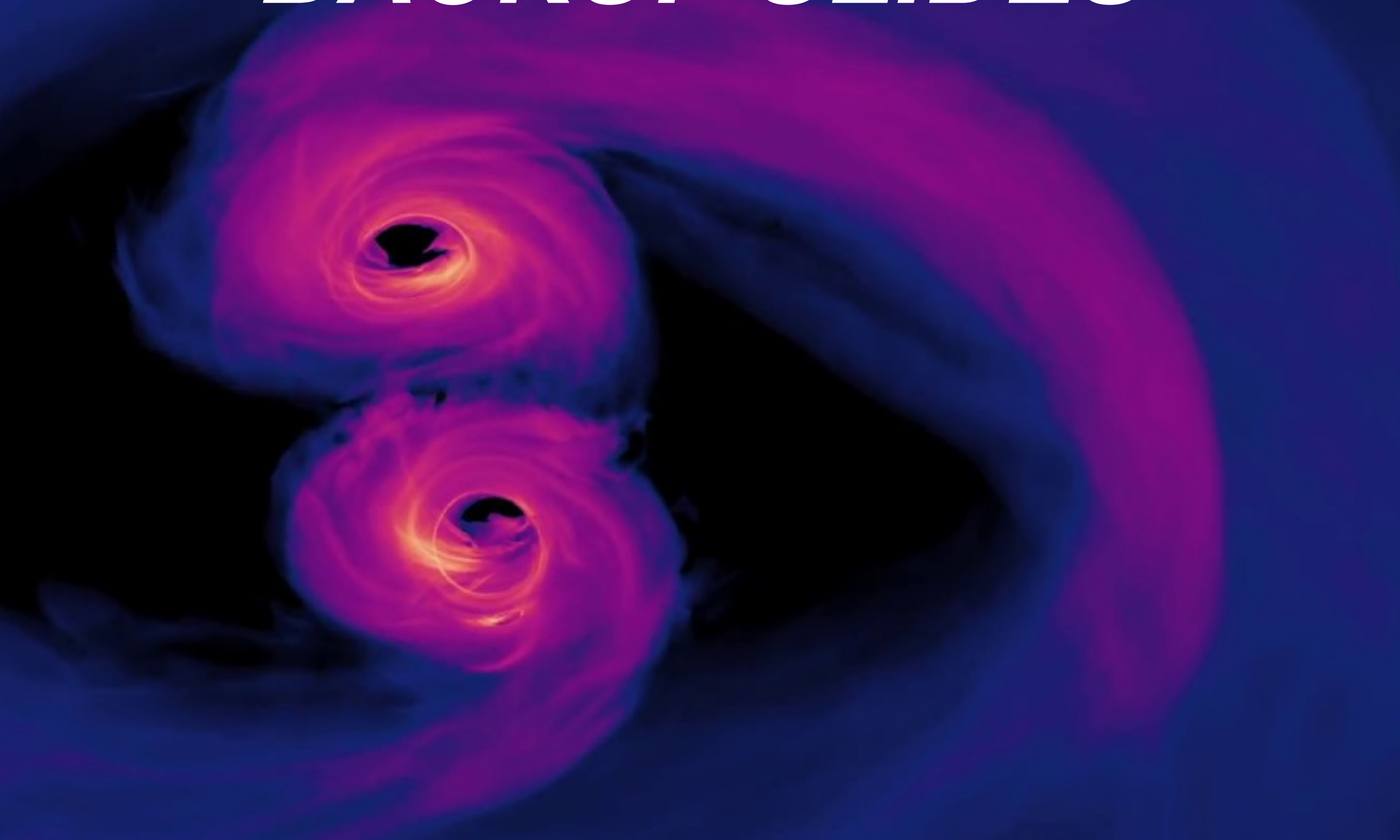
- New era of multi-messenger astronomy
- Evolution of massive compact binaries, progenitors of gravitational wave emission

Thank you for your attention!



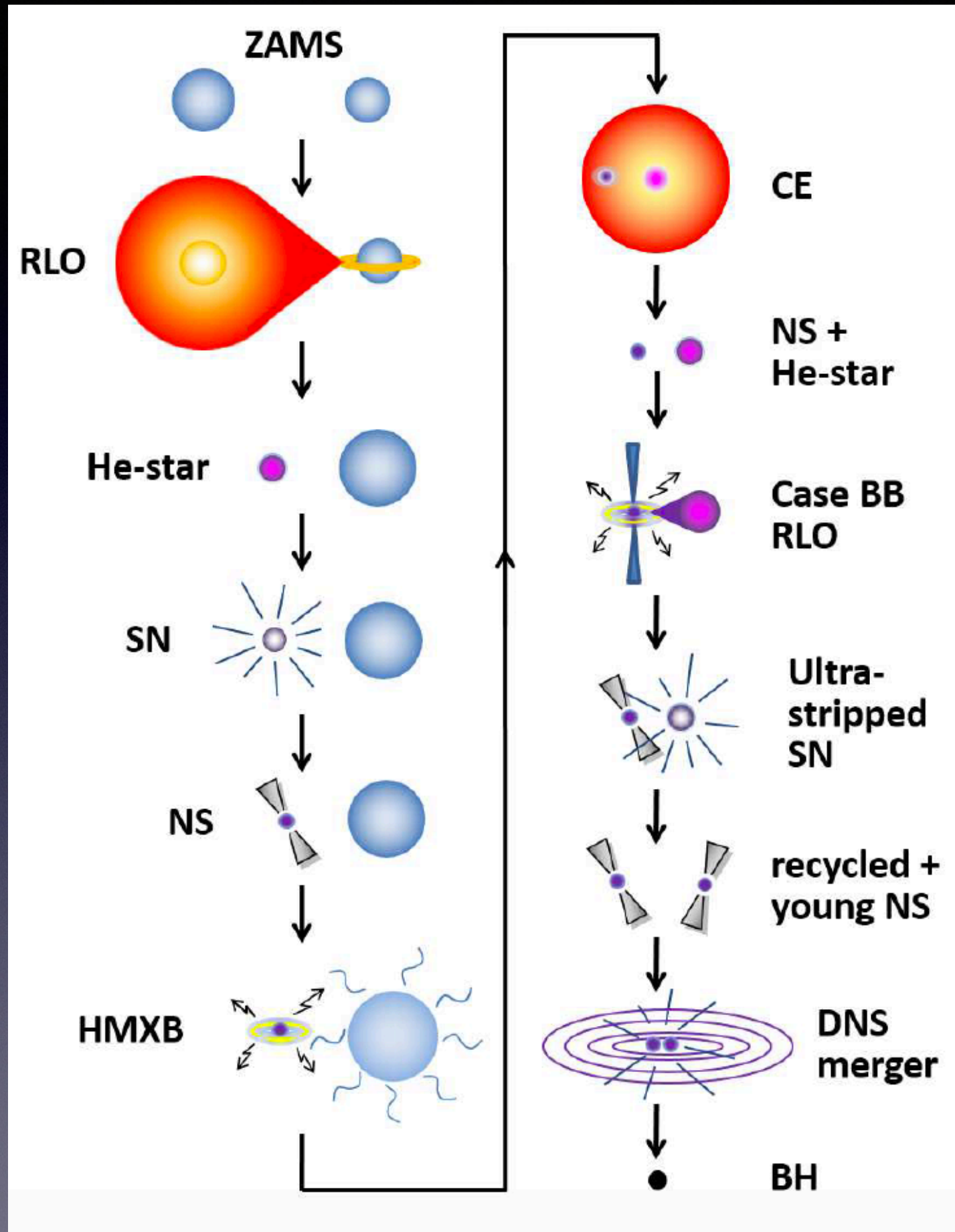


# ***BACKUP SLIDES***



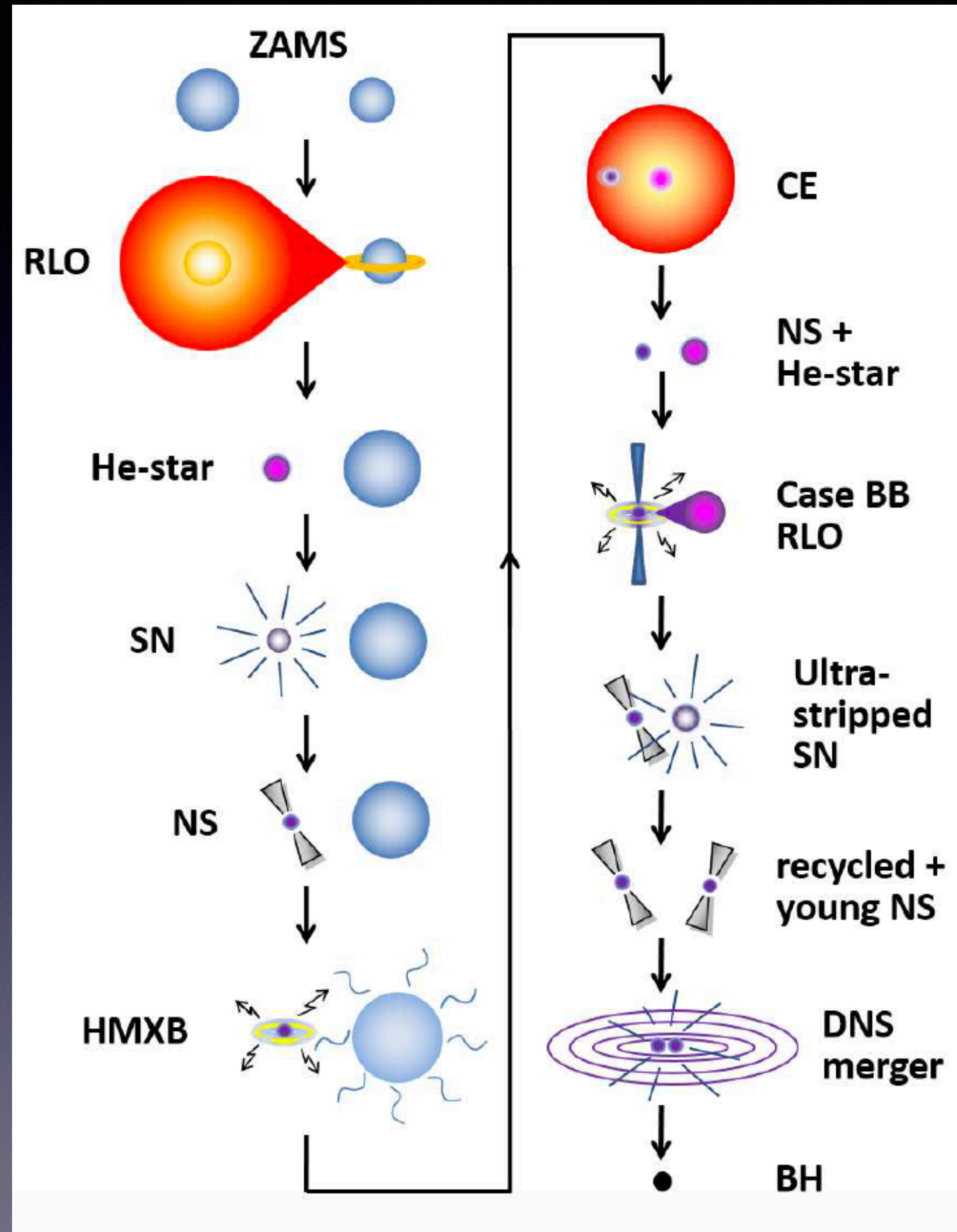


# Evolution





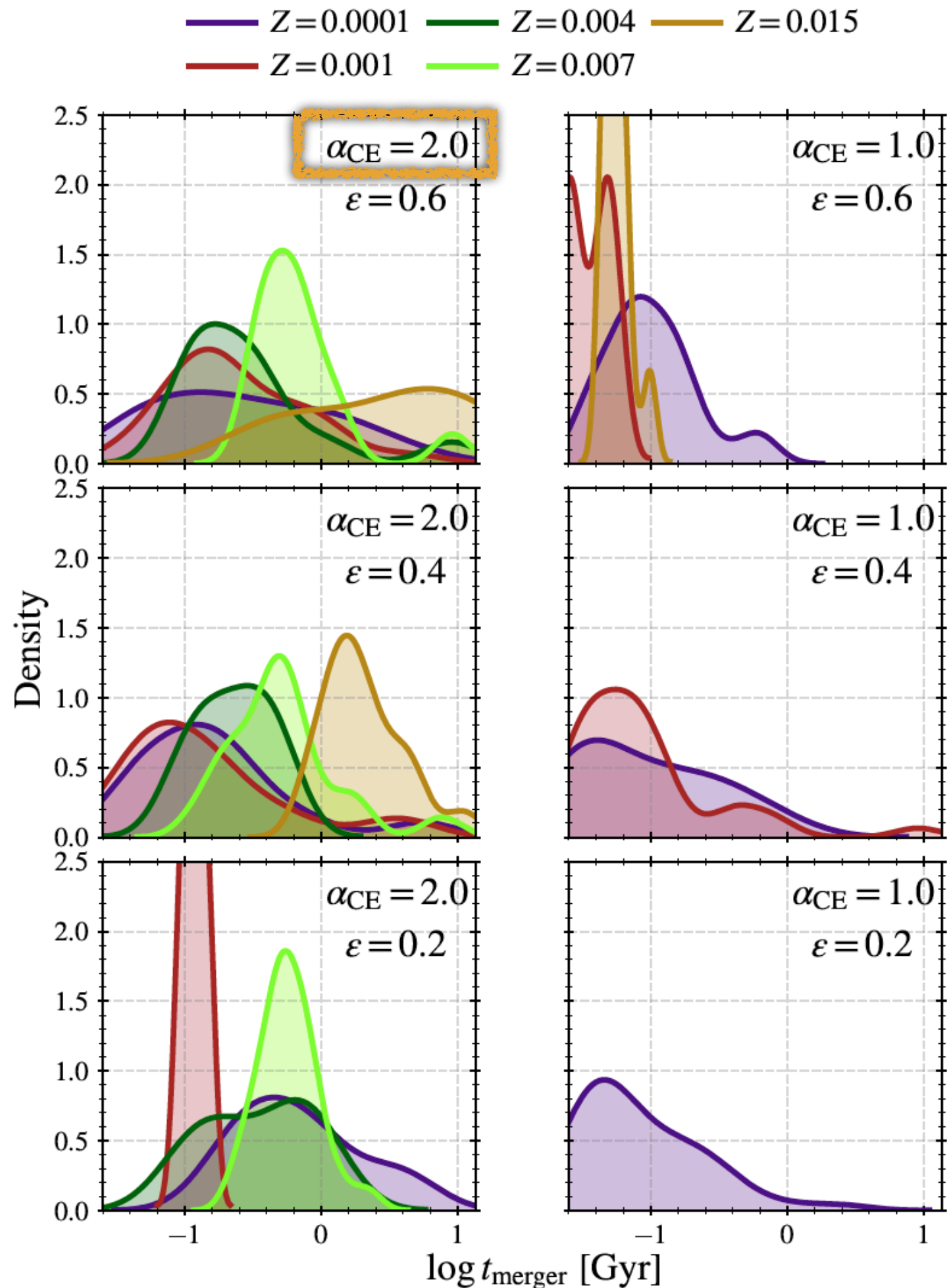
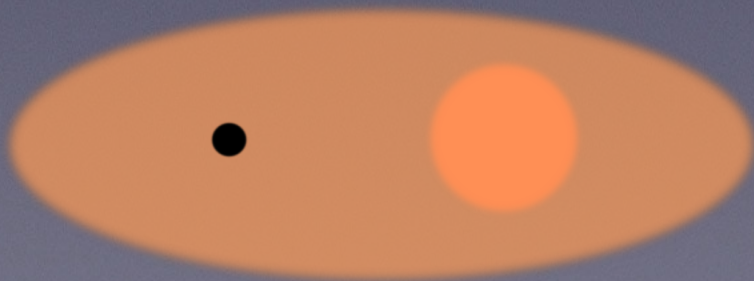
# Evolution





# Population-weighted results: merger time delay

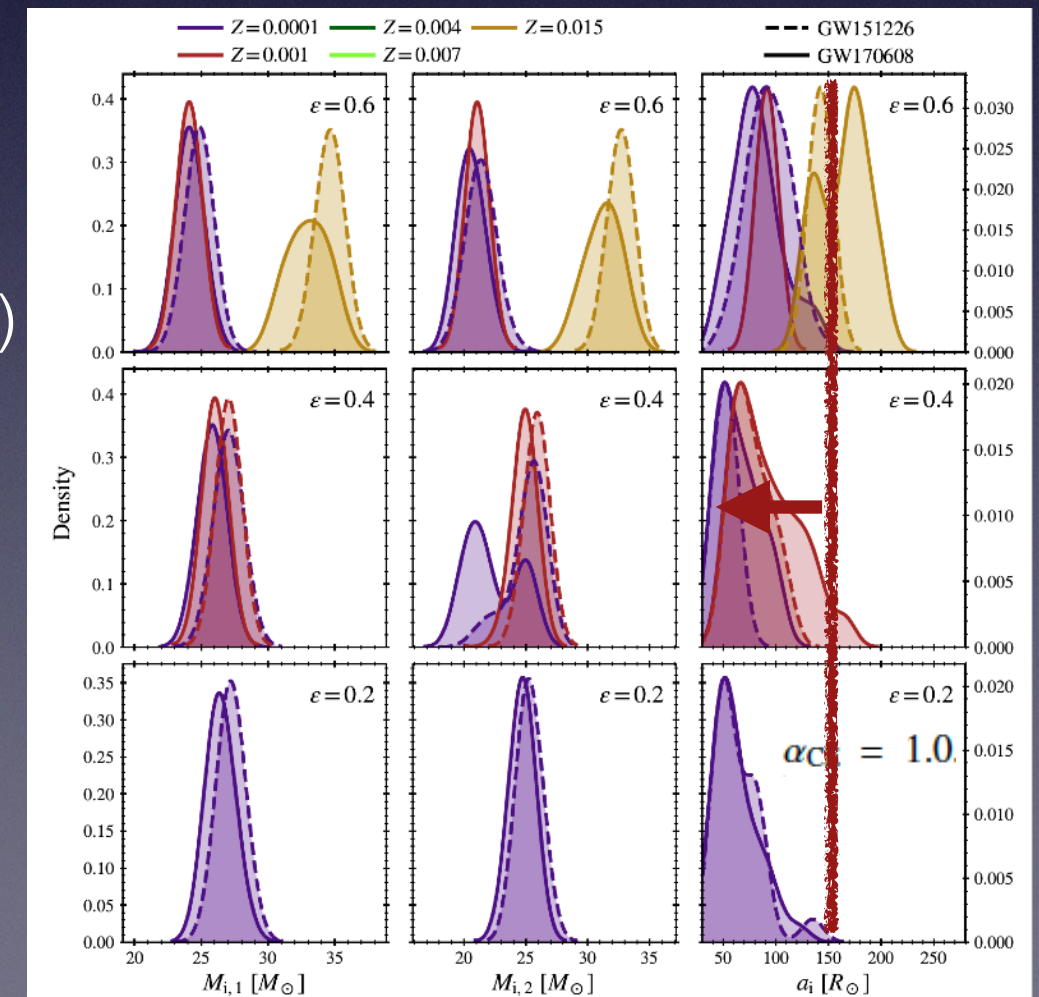
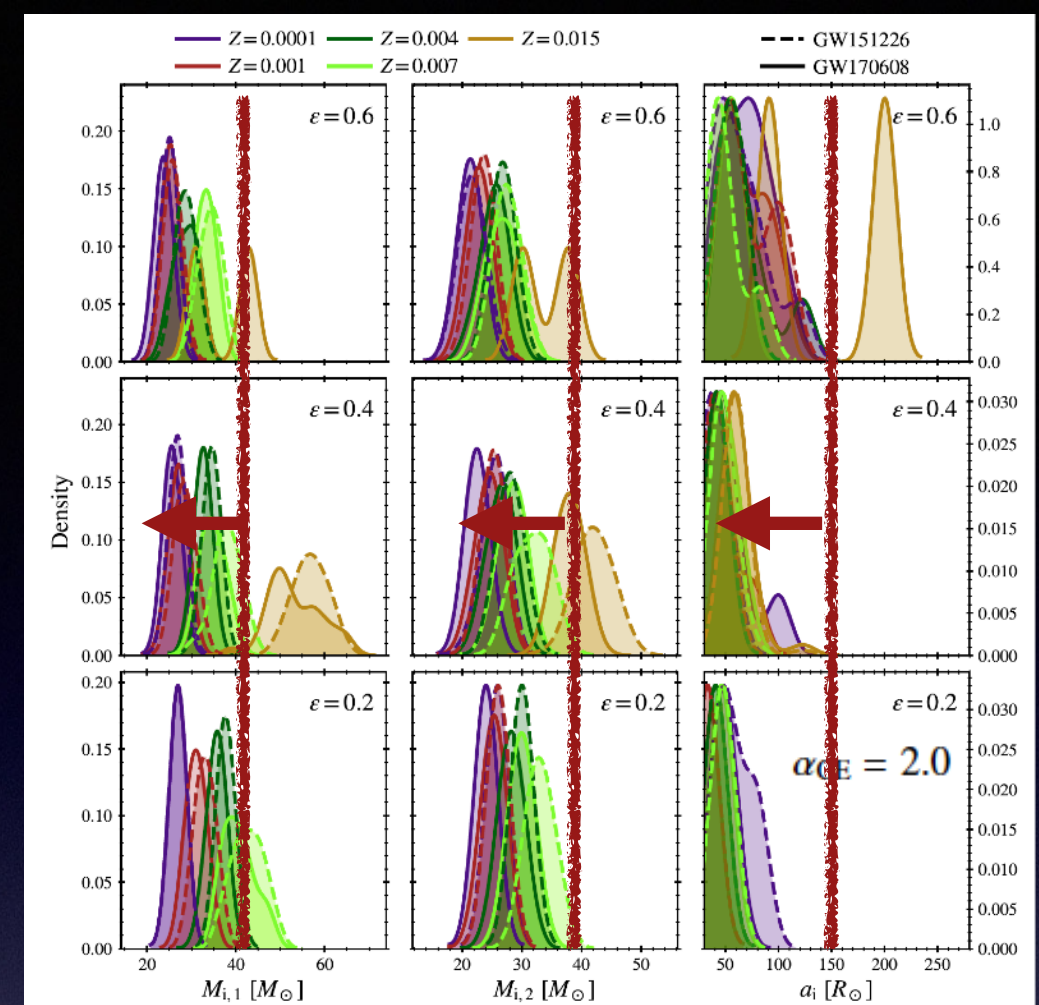
- $t_{\text{merger}}$  correlated with  $a_i$   
reduced by 10 for  $\alpha_{\text{CE}}=1.0$   
(late CE ejection reduces  $a_i$ )
- $\alpha_{\text{CE}} = 2.0$ : longer  $t_{\text{merger}}$  1 Gyr  
[0.1-8 Gyr] (early CE ejection)  
old & high Z population
- $\alpha_{\text{CE}} = 1.0$ : shorter  $t_{\text{merger}}$  100 My  
[0.01-1 Gyr] (late CE ejection)  
young & low Z population





# Population-weighted results: mass and separation

- We use **uniform grids to estimate relative contributions of progenitors**:  
Initial Mass Function [Kroupa+2001]; Mass-ratio [0.1-1.0]; Separation/period [Sana+2012] ( $\log P \propto -0.55$ )
- **Progenitors**:  $M$  [20-40  $M_{\odot}$ ] and  $a_i < 150 R_{\odot}$   
(except for  $\alpha_{CE}=2.0$ /high  $Z$ :  $M \rightarrow 70 M_{\odot}$  /  $a_i \rightarrow 250 R_{\odot}$ )
- **Strong dependence on MT efficiency**:  
interplay between stellar wind mass loss and initial binary separation





# Population-weighted results: mass ratio and chirp mass

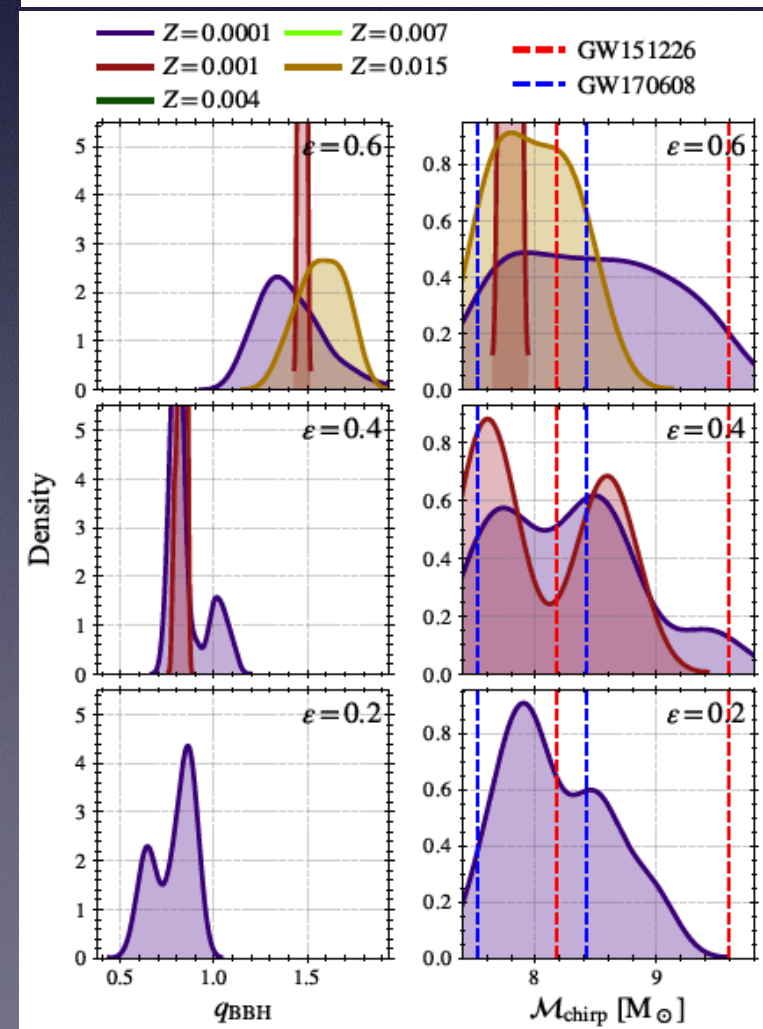
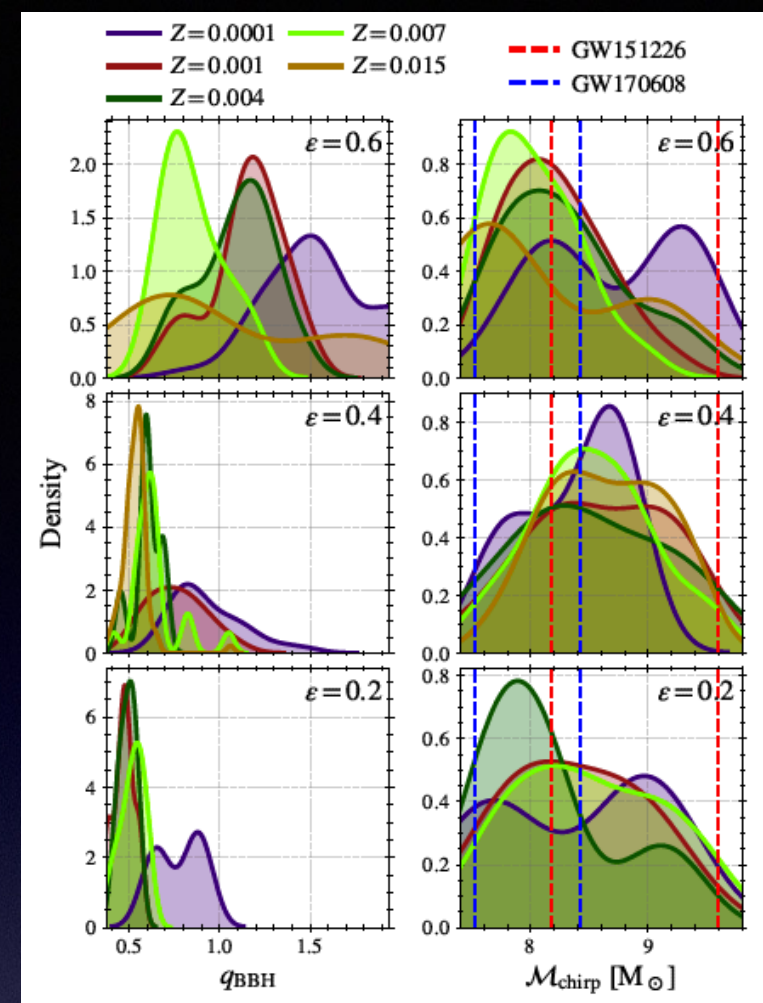
- **Parameter distribution:**

- **For  $\alpha_{CE}=2.0$ :**  $Z$  decreases  $\rightarrow$   $q$  peaks towards 1, chirp mass spans entire CI for both GW events, independent of  $MT$  and  $Z$

- **For  $\alpha_{CE}=1.0$ :** secondary BH is the heaviest, chirp mass decreases for solar  $Z$

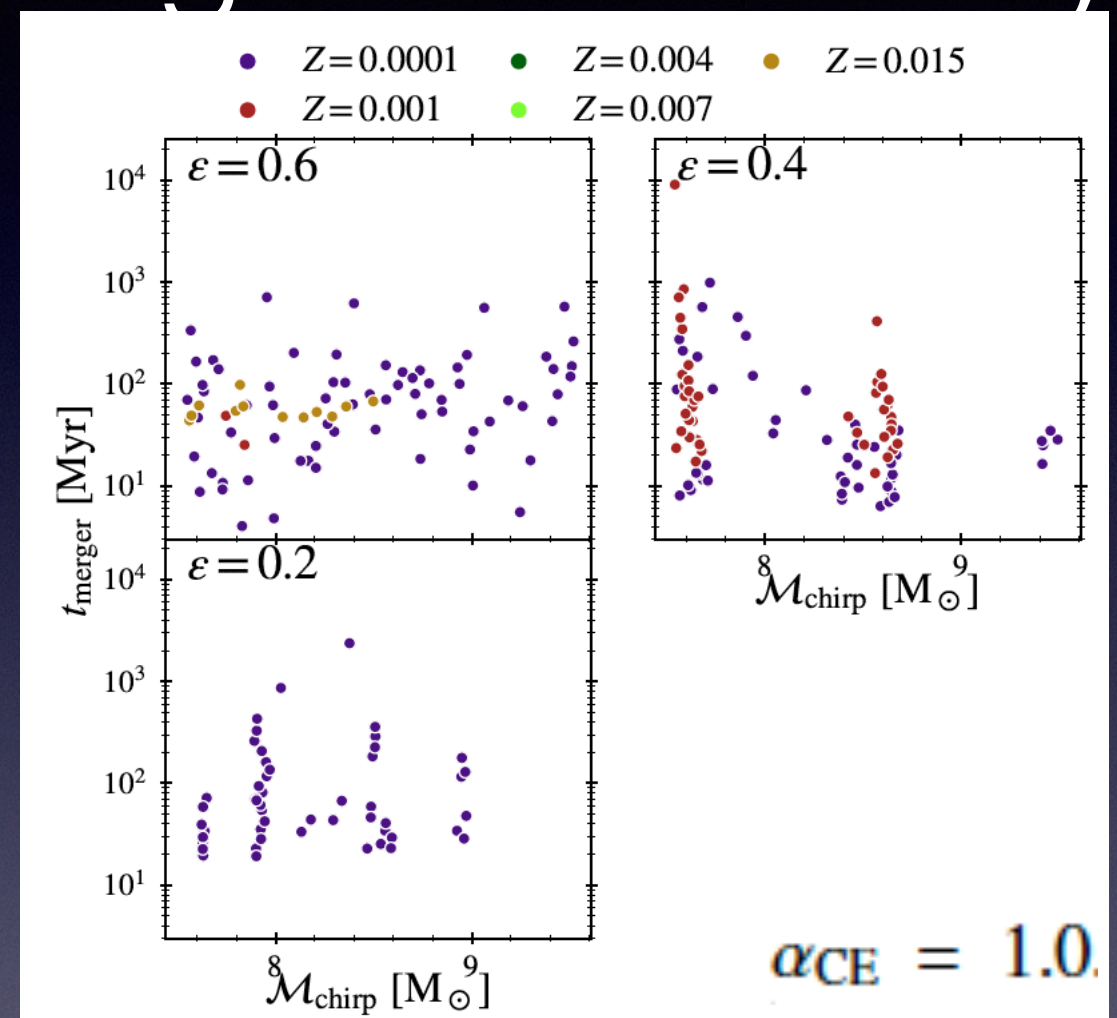
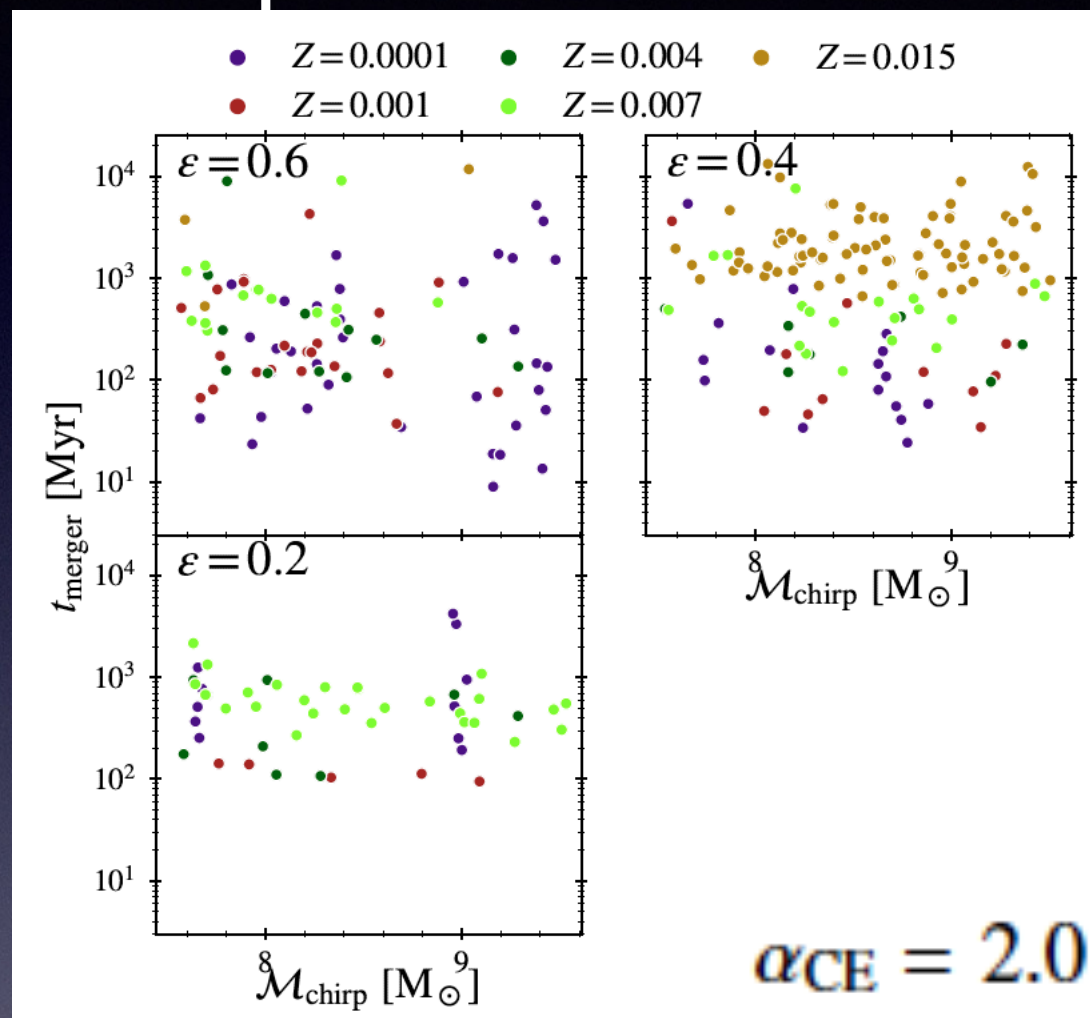
$\alpha_{CE} = 2.0$

$\alpha_{CE} = 1.0$





# Properties of formed BBH: chirp mass and merger time delay





# Multi-wavelength + multi-messenger astrophysics



# Multi-wavelength + multi-messenger astrophysics





# Population de binaires compactes

The next phase...

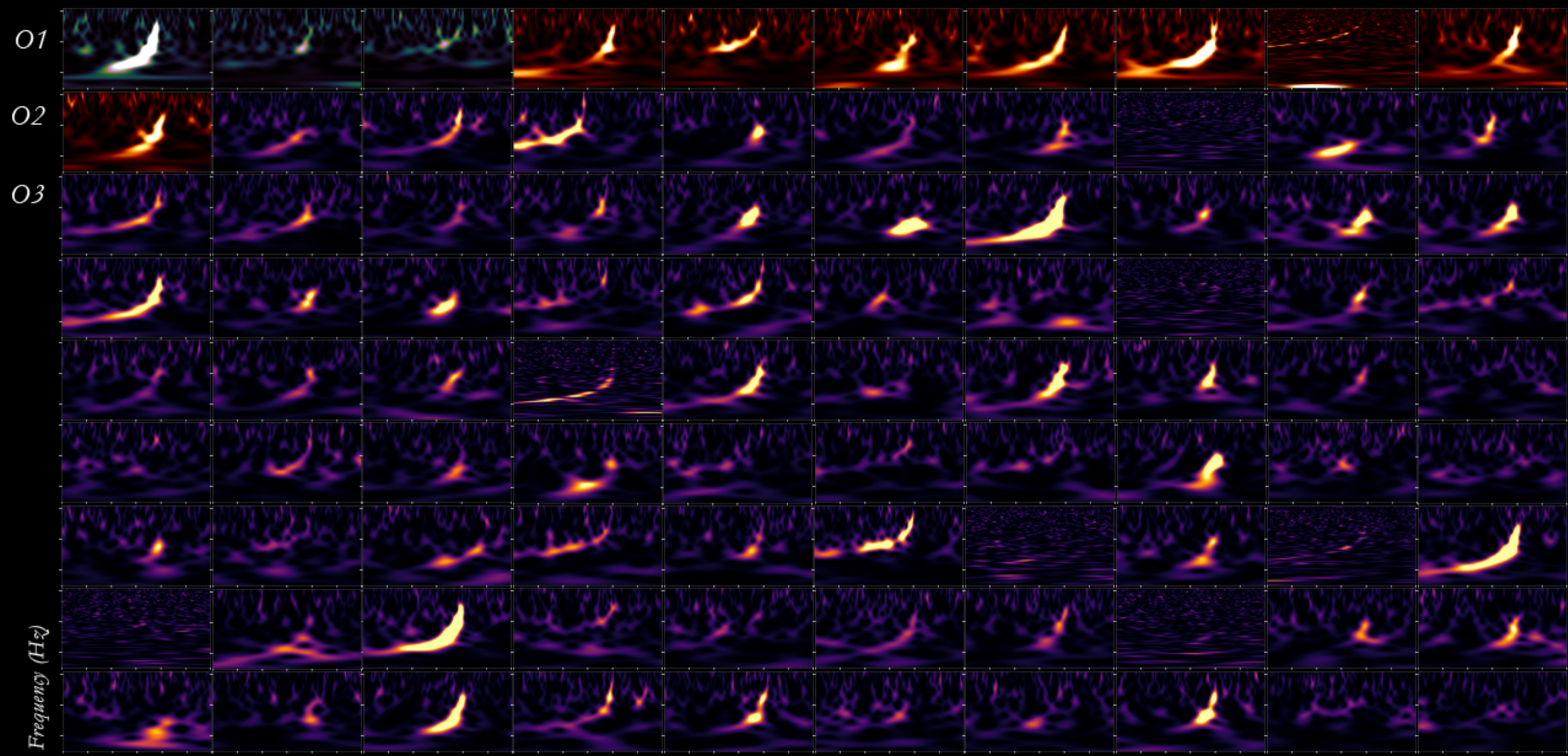


Observation Run	Network	Expected BNS Detections	Expected NSBH Detections	Expected BBH Detections
O3	HLV	$1_{-1}^{+12}$	$0_{-0}^{+19}$	$17_{-11}^{+22}$
O4	HLVK	$10_{-10}^{+52}$	$1_{-1}^{+91}$	$79_{-44}^{+89}$
		Area (deg <sup>2</sup> ) 90% c.r.	Area (deg <sup>2</sup> ) 90% c.r.	Area (deg <sup>2</sup> ) 90% c.r.
O3	HLV	$270_{-20}^{+34}$	$330_{-31}^{+24}$	$280_{-23}^{+30}$
O4	HLVK	$33_{-5}^{+5}$	$50_{-8}^{+8}$	$41_{-6}^{+7}$
		Comoving Volume (10 <sup>3</sup> Mpc <sup>3</sup> ) 90% c.r.	Comoving Volume (10 <sup>3</sup> Mpc <sup>3</sup> ) 90% c.r.	Comoving Volume (10 <sup>3</sup> Mpc <sup>3</sup> ) 90% c.r.
O3	HLV	$120_{-24}^{+19}$	$860_{-150}^{+150}$	$16000_{-2500}^{+2200}$
O4	HLVK	$52_{-9}^{+10}$	$430_{-78}^{+100}$	$7700_{-920}^{+1500}$

*Abbott et al, LRR (2020)*



# O1 — O3 detections (GWTC-1+2+3, 09/2015-03/2020): 90 BBH/BNS/NSBH



Time (s)

Sudarshan Ghonge | Karan Jani

